Enhancing OpenStreetMap for the Assessment of Critical Road Infrastructure in a Disaster Context

Johanna Guth

Doctoral Thesis
Karlsruhe, 2021

Enhancing OpenStreetMap for the Assessment of Critical Road Infrastructure in a Disaster Context

Zur Erlangung des akademischen Grades einer

DOKTOR-INGENIEURIN (Dr.-Ing.)

von der Fakultät für
Bauingenieur-, Geo- und Umweltwissenschaften
des Karlsruher Instituts für Technologie (KIT)

genehmigte

DISSERTATION

von

Johanna Guth

geboren in Singen (Hohentwiel)

Tag der mündlichen Prüfung 12.04.2021

Referent Prof. Dr.-Ing. habil. Stefan Hinz
Institut für Photogrammetrie und Fernerkundung (IPF)
Karlsruher Institut für Technologie (KIT)

Korreferent Prof. Dr.-Ing. habil. Stephan Winter
Department of Infrastructure Engineering
The University of Melbourne

Karlsruhe (2021)

Johanna Guth
Enhancing OpenStreetMap for the Assessment of Critical Road Infrastructure in a Disaster Context
Doctoral Thesis
Date of examination: 12.04.2021
Referees:
Prof. Dr.-Ing. habil. Stefan Hinz
Prof. Dr.-Ing. habil. Stephan Winter

Karlsruhe Institute of Technology (KIT)
Department of Civil Engineering, Geo and Environmental Studies
Institute of Photogrammetry and Remote Sensing (IPF)
Kaiserstr. 12
76131 Karlsruhe

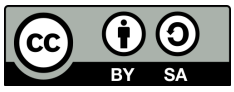

Für Fritz

Abstract

The frequency of natural disasters is increasing all over the world, which can cause immense damage to road infrastructure and its functionality. Therefore, it is crucial to consider the functionality of critical road infrastructure before, during, and after a disaster. For that, global road network data, which is usable for routing applications, is required. OpenStreetMap (OSM) provides global, crowd-sourced road network data that is free and accessible for everyone. However, the usability for routing applications is often an issue. Two main gaps in related studies are identified: the intrinsic improvement of certain aspects of OSM road data for navigational purposes, and missing approaches for the assessment of critical road infrastructure in disaster cases that can handle limited global data availability. Therefore, the aim of this thesis is to develop a generic, multi-scale concept to assess critical road infrastructure in a disaster context using OSM data. For this main objective, two consecutive research goals are identified: (i) improving the routability of OSM data intrinsically, and (ii) assessing critical road infrastructure in a disaster context. Therefore, this thesis and the developed concept are divided into two main parts, each addressing one research goal.

In the first part of this thesis, the OSM road network data is enhanced by improving its routability. The quality of the OSM road network is analyzed in detail, which leads to the identification of two major challenges for the applicability of OSM data in routing applications: missing speed information and road classification errors. To address the first challenge, a Fuzzy Framework for Speed Estimation (Fuzzy-FSE) is developed that employs fuzzy control to estimate average speed based on the parameters road class, road slope, road surface, and link length. The Fuzzy-FSE consists of two parts: a rule and knowledge base, which decides on the output membership functions, and multiple Fuzzy Control Systems, which calculate the output average speeds. Results demonstrate that even using only OSM data, the Fuzzy-FSE performs better than existing methods such as fixed speed profiles. The second challenge of road classification errors is addressed by developing a novel approach to detect road classification errors in OSM by searching for disconnected parts and gaps in different levels of a hierarchical road network. Different parameters are combined in a rating system to obtain an error probability. The rating system can then suggest possible misclassifications to a human user. The results indicate that more classification errors are found at gaps than at disconnected parts. Furthermore, the gap search enables the user to find classification errors quickly using the developed rating system that indicates an error probability. An enhanced OSM road network dataset results from the first part of this thesis.

In the second part of this thesis, the enhanced OSM data is applied to assess critical road infrastructure in a disaster context. The second part of the generic, multi-scale concept is developed, which consists of multiple, interconnected modules. One module implements two accessibility indices, which highlight different aspects of road network accessibility. A basic travel demand model is developed in another module, which estimates daily intercity traffic solely based on OSM data. A third module uses the above-described modules to estimate different natural disaster impacts on the road network. Finally, the vulnerability of the road network towards further disruptions during long-term disasters is analyzed in a fourth module. The generic concept with all modules is applied exemplarily in two different case study regions for two wildfire scenarios. As a result, the concept provides a valuable, flexible, and data-sparse decision aid tool for regional planners and disaster management that can be applied globally and enables country- or region-specific adaptations.

Zusammenfassung

Die Häufigkeit von Naturkatastrophen nimmt weltweit zu, was zu immensen Schäden an kritischer Straßeninfrastruktur und deren Funktionalität führen kann. Daher ist es von entscheidender Bedeutung, die Funktionalität kritischer Straßeninfrastruktur vor, während und nach einer Katastrophe zu beurteilen. Dazu werden globale Straßendaten benötigt, die für die Routenplanung nutzbar sind. OpenStreetMap (OSM) stellt globale Straßennetzdaten zur Verfügung, die kostenlos und frei zugänglich sind. Allerdings ist die Verwendung der OSM Straßendaten für Routenplanungsanwendungen oft eine Herausforderung. Das übergeordnete Ziel dieser Arbeit ist die Entwicklung eines generischen, mehrskaligen Konzepts zur Analyse kritischer Straßeninfrastrukturen im Kontext von Naturgefahren unter Verwendung von OSM Daten. Dafür werden zwei aufeinander folgende Forschungsziele aufgestellt: (i) die Verbesserung der Routingfähigkeit von OSM Daten und (ii) die Bewertung kritischer Straßeninfrastruktur im Kontext von Naturgefahren. Daraus resultiert die Gliederung dieser Arbeit in zwei Hauptteile, die jeweils den Forschungszielen entsprechen.

Im ersten Teil dieser Arbeit wird die Nutzbarkeit von OSM Daten für Routing Anwendungen verbessert. Zunächst wird dafür die Qualität des OSM Straßennetzwerks im Detail analysiert. Dabei werden zwei große Herausforderungen im Bereich der Anwendbarkeit von OSM Daten für die Routenplanung identifiziert: fehlende Geschwindigkeitsangaben und Fehler in der Straßenklassifizierung. Um die erste Herausforderung zu bewältigen, wird ein Fuzzy-Framework zur Geschwindigkeitsschätzung (Fuzzy-FSE) entwickelt, welches eine Fuzzy Regelung zur Schätzung der Durchschnittsgeschwindigkeit einsetzt. Diese Fuzzy Regelung basiert auf den Parametern Straßenklasse, Straßenneigung, Straßenoberfläche und Straßenlänge einsetzt. Das Fuzzy-FSE besteht aus zwei Teilen: einer Regel- und Wissensbasis, die über die Zugehörigkeitsfunktionen für den Ausgangsparameter Geschwindigkeit entscheidet, und mehrere Fuzzy-Regelsysteme, welche die resultierende Durchschnittsgeschwindigkeit berechnen. Die Ergebnisse zeigen, dass das Fuzzy-FSE auch bei ausschließlicher Verwendung von OSM Daten eine bessere Leistung erbringt als bestehende Methoden. Die Herausforderung der fehlerhaften Straßenklassifizierung wird durch die Entwicklung eines neuartigen Ansatzes zur Erkennung von Klassifizierungfehlern in OSM angegangen. Dabei wird sowohl nach nicht verbundenen Netzwerkteilen als auch nach Lücken im Straßennetzwerk gesucht. Verschiedene Parameter werden in einem Bewertungssystem kombiniert, um eine Fehlerwahrscheinlichkeit zu erhalten. Auf Basis der Fehlerwahrscheinlichkeit kann ein menschlicher Nutzer diese Fehler überprüfen und korrigieren. Die Ergebnisse deuten einerseits darauf hin, dass an Lücken mehr Klassifizierungsfehler gefunden werden als an nicht

verbundenen Netzwerkteilen. Andererseits zeigen sie, dass das entwickelte Bewertungssystem bei einer benutzergesteuerten Suche nach Lücken zu einem schnellen Aufdecken von Klassifizierungsfehlern verwendet werden kann. Aus dem ersten Teil dieser Arbeit ergibt sich somit ein erweiterter OSM Datensatz mit verbesserter Routingfähigkeit.

Im zweiten Teil dieser Arbeit werden die erweiterten OSM Daten zur Bewertung der kritischen Straßeninfrastruktur im Katastrophenkontext verwendet. Dazu wird der zweite Teil des generischen, mehrskaligen Konzepts entwickelt, das aus mehreren, miteinander verbundenen Modulen besteht. Ein Modul implementiert zwei Erreichbarkeitsindizes, welche verschiedene Aspekte der Erreichbarkeit im Straßennetzwerk hervorheben. In einem weiteren Modul wird ein grundlegendes Modell der Verkehrsnachfrage entwickelt, welches den täglichen interstädtischen Verkehr ausschließlich auf der Grundlage von OSM Daten schätzt. Ein drittes Modul verwendet die oben beschriebenen Module zur Schätzung verschiedener Arten von Auswirkungen von Naturkatastrophen auf das Straßennetzwerk. Schließlich wird in einem vierten Modul die Vulnerabilität des Straßennetzes gegenüber weiteren Schäden bei Langzeitkatastrophen analysiert. Das generische Konzept mit allen Modulen wird exemplarisch in zwei verschiedenen Regionen für zwei Waldbrandszenarien angewendet. Die Ergebnisse der Fallstudien zeigen, dass das Konzept ein wertvolles, flexibles und global anwendbares Instrument für Regionalplaner und Katastrophenmanagement darstellt, das länder- bzw. regionenspezifische Anpassungen ermöglicht und gleichzeitig wenig Daten benötigt.

Acknowledgement

First of all, I want to thank Prof. Dr. Stefan Hinz for the ongoing supervision and support during my PhD and for the opportunity of working at the IPF. I always felt like I could come to you at any time if I ever encountered any problems. You provided me with so many great opportunities during my time at the IPF, like the reserach stay in Australia, going to conferences, and so much more. Also, you have created a working atmosphere in the institute that is super friendly, uncomplicated and open. I'm very proud to be part of the IPF you created.

Secondly, I want to warmly thank Dr. Sina Keller for being my direct supervisor in every aspect. During my PhD time you have supported me greatly, both professionally and personally. You have accompanied me every step of the way and without you this thesis would not be what it is. I know I can count on you every time of the day, whatever problem there is, to fight and solve it together. I am so grateful that you encouraged me coming up with my own ideas and research directions and then followed me on this path. There are so many moments in these four years I'll remember: long talks about research ideas, papers going back and forth reformulating and restructuring, extensive discussions about figures and style choices, but also personal talks, laughs and walks with the dogs. I thank you so much for everything, Sina! You inspire me, both professionally and personally.

Thirdly, I want to thank my direct office colleagues Philipp Maier, Felix Riese, Chris Michel, and of course Tobi. Our time in the office together was characterized by long discussions and talks about our work, software (Apple vs Windows, Python vs R, QGIS vs ArcGIS, ...) but also everything else (Tobi (!!), food (!!!), dodokay, Game of Thrones, ...). It was so fun working with you and I'm already missing our time together. To you, Felix, a big thanks for reading through the first draft of my entire thesis, chapter by chapter, and for your critical and constructive feedback throughout my PhD. Also, Chris and Philipp, thanks for the final read through this thesis and your valuable comments. To Philipp, especially, thank you for every time you joined our afternoon walk and for always being there to chat.

Thanks also to Sven Wursthorn, first for being the one to bring me to the IPF, and also for the support during my PhD years. Already during my master, your fascination for GIS and spatial databases inspired me and lead me on the path I am today. I could always turn to you to answer database and OSM questions and to discuss new ideas.

Furthermore, I want to thank Prof. Dr. Stephan Winter for the opportunity to go to Melbourne and work with him. The time at the University of Melbourne was very intense. I learned so much in these eight weeks and met great friends who I wish were closer now

(yes, you Ivan and Jelena). I'm very grateful for the time you, Stephan, took to meet with me every week in Melbourne but also afterwards to discuss ideas and point me in the right direction. You really raised my work to another level, thank you!

Next, I want to thank all my colleagues at the IPF for their support during my PhD time. This support was provided in the form of direct supervision but also in the form of so many informal chats, meetings, and, most importantly, lunch and coffee breaks in between. My time at the IPF was wonderful and intense because the entire group at the IPF feels like one big family and I am so lucky to be a part of it. Furthermore, I want to thank CEDIM and especially Dr. James Daniell for the cooperation and insights into the interdisciplinary research.

I am grateful for the unlimited support of my entire family throughout my years of study and also through my years as PhD. To my mother, Ulrike Stötzer: with your extraordinary strength in difficult times and your positive but realistic attitude... you really are my idol and go-to person if I need motivation without sugar-coating. This thesis is dedicated to the memory of my father who teached me to be stubborn and to never give up if I really want something. Fritz, your voice inside my head kept me going through difficult times and I know that you would be even more proud of this thesis than I am.

Finally, to my husband Steffen, thank you for everything: For listening to all my PhD problems, for talking me through "I don't want to"- times, for cooking for me and spoiling me, for so strongly believing in me, never doubting for a moment that I can do this, for keeping up with a pregnant wife during the last months of her PhD (that's almost like two pregnancies at once), and for simply being there every step of the way. Last but not least, my PhD time would not have been half as joyful without our dog Tobi, whose presence in the office was a constant mood-lightener and cause for many laughs. I am very happy to be able to finish this great chapter of our life to start a new, entirely different one as an even bigger family.

Thank you!

Johanna Guth
November 2020

Contents

1 Introduction

> *It wasn't raining when Noah built the ark.*
>
> — **Howard Ruff**
> (Author)

1.1 Motivation

The frequency of natural disasters worldwide has increased almost three-fold in the last four decades from over 1300 events from the years 1975 to 1984, to over 3900 events from the years 2005 to 2014 [1]. Climate-related disasters such as floods, storms, droughts, and wildfires are on the rise, which is most probably caused by climate change [1, 2, 3]. Furthermore, the number of people affected by natural disasters is also continuously rising and many studies find that the poor tend to suffer the worst from natural disasters [4, 5]. Simultaneously, a trend can be observed with disasters featuring lower mortality but much higher economic losses [3].

Natural disasters threaten not only people but also critical infrastructures. These infrastructures include networks functioning together to provide continuous services to network users [6]. Critical infrastructures consist of technical and organizational multi-level structures that are essential for maintaining functions in their social environment [7]. Because of the crucial functions of critical infrastructures for all aspects of human life, a failure can cause severe consequences for humans.

The road infrastructure, as one of the most fundamental parts of the transportation network, is frequently damaged by natural disasters. A damaged road network affects people in many different aspects. On the one hand, the accessibility of everyday needs or emergency facilities is no longer guaranteed for people directly affected by the disaster. On the other hand, emergency management is delayed, or worse, unable to reach disaster-affected regions. Furthermore, a damaged road network may impact an entire country by delaying daily traffic and interrupting transport flows. The road network might remain unserviceable for a long time after an event. Therefore, it is crucial to consider the functionality of critical road infrastructure before, during, and after natural disasters.

In order to assess the functionality of critical road infrastructure, routable road network data is necessary. Commercial and administrative road network datasets exist, but are often only available for a specific region or are expensive or both. If a disaster happens, disaster management first has to search for appropriate data on the respective geographic scale. Furthermore, access limitations might have to be considered, and issues regarding the combination of data from different sources have to be taken into account. These difficulties have to be overcome to obtain road network data and the process can take a lot of time and effort before an actual assessment can be performed. However, time is crucial in disaster events because a response strategy must be developed immediately to provide much-needed help in the right locations. Thus, disaster management can benefit immensely from a worldwide, free and routable road network dataset.

OpenStreetMap (OSM) is such a free, crowdsourced map with global coverage. It contains, among other things, road network data of the entire world that is composed by volunteers and data donations of governments and agencies. The primary benefits of OSM for disaster management are the free and quick accessibility of data and its global coverage. However, as OSM is a crowdsourced dataset and collected by often untrained volunteers, the quality of OSM road data varies a lot between regions [8, 9]. Especially the usability for routing applications, also called routability, is often not directly given [10, 11, 12, 13], because in the beginning of the project the primary purpose of OSM was to only display map data. Now, with the continuously growing and improving road network, the application for navigational purposes is evident. But still, missing attributes, errors in the road topology, and attribute errors are the main reasons why routing applications struggle with OSM data. Therefore, special techniques are required that improve the applicability of OSM for navigational purposes and thus for the analysis of critical road infrastructure.

1.2 Main Objective and Research Goals

The development of techniques to improve the quality of OSM data has become an important research field in the last few years because of the many applications using OSM data. Regarding the routability of OSM road data, many approaches, considering different aspects of routability, have been developed that aim at enhancing OSM data for routing applications. However, many of them (a) require additional data besides the OSM road network [e.g., 14, 15], (b) focus mainly on urban applications [e.g., 14, 16], or (c) consider routability aspects that are not overly significant for the analysis of critical road infrastructure in disaster cases [e.g., 17, 18]. As disasters often also strike in already vulnerable rural regions, developing techniques to enhance the routability of OSM data in these regions is of significant importance but mostly not considered in related studies. Additionally, for the

analysis of critical road infrastructure in disaster cases, a gap in related studies is identified as intrinsically improving the routability of the OSM road network.

The assessment of critical road infrastructure in disaster cases is a broad and interdisciplinary research field with numerous different approaches including complex datasets [e.g., 19, 20], traffic models [e.g., 21, 22], and advanced simulations [e.g., 23, 24, 25]. Many of these approaches focus on one particular case study [e.g., 26, 27, 28], often in a local, urbanized setting [e.g., 29, 30], and are frequently untransferable. However, in reality, complex datasets are rarely available directly after a disaster and thus advanced models or simulations are not applicable. Additionally, the transferability of an approach and its generic applicability, which begins with the essential aspect of global data availability, is commonly overlooked in the scientific community. Hence, a generic concept, which can handle the challenge of limited global data availability and is thus able to analyze disaster impacts on critical road infrastructure directly after an event, is still missing.

To overcome these gaps, the main objective of this thesis is to develop a generic, multi-scale concept to assess critical road infrastructure in a disaster context using OSM data. The resulting concept is herein called **GRIND** (**G**eneric concept for the assessment of critical **R**oad **IN**frastructure in a **D**isaster context). **GRIND** is constructed in a modular way such that single modules can be switched on and off depending on disaster management's requirements. Two consecutive research goals are identified on the basis of the above-identified gaps to develop **GRIND**:

Goal 1: Improving the routability of OSM data with intrinsic methods.

Goal 2: Assessing critical road infrastructure in a disaster context.

The output of the first research goal is an enhanced OSM dataset, which is used to address the second research goal. **GRIND** is, therefore, divided into two distinct parts, according to the research goals, which are visualized in Figure 1.1.

GRIND is realized using only worldwide available, free data sources such that it can be applied globally. It is highly automatized and implemented using a PostgreSQL [31] (version 11.5) database with PostGIS [32] (version 2.5) and pgRouting [33] (version 2.6) extensions.

1.3 Thesis Outline and Contributions

This thesis is organized in three parts. Part I addresses the first research goal of improving the routability of OSM data with intrinsic methods. Following the second research goal, Part II uses the enhanced OSM data generated in Part I to assess critical road infrastructure in a disaster context. The last part, Part III, summarizes the entire thesis in one concluding chapter. Appendix A lists all publications published within the scope of this thesis.

Part I - Improving the Routability of OSM data is subdivided into three chapters: one introductory chapter covering the fundamentals and two chapters developing independent modules of GRIND. It first diagnoses the most relevant shortcomings of OSM road network data for navigational purposes with a quality analysis. Based on the identified shortcomings, methods are developed to improve OSM road network data for routing applications. An enhanced OSM road network dataset results from Part I, which is used in Part II. The methods developed in Part I, can be applied independently of Part II, to improve the routability of OSM data for all kinds of applications. The major contributions of Part I toward the main objective of this thesis can be summarized as follows:

- analyzing the quality of relevant OSM road data in combination with a summary of related work on OSM road data quality (see Chapter 2), and identifying open challenges in the field,
- developing the Fuzzy Framework for Speed Estimation (Fuzzy-FSE), which enables a multi-parameter estimation of average speed in OSM road networks (see Chapter 3),
- designing the Error Search, a novel approach to detect, rate, and categorize road classification errors in OSM (see Chapter 4), and, in summary,
- overcoming the challenge of intrinsically improving the applicability of OSM road data for the assessment of critical infrastructure in a disaster context.

As a result of the first part of GRIND, an enhanced OSM road network dataset with improved routability is obtained. The implementation of the Fuzzy-FSE and Error Search is published freely on GitHub.

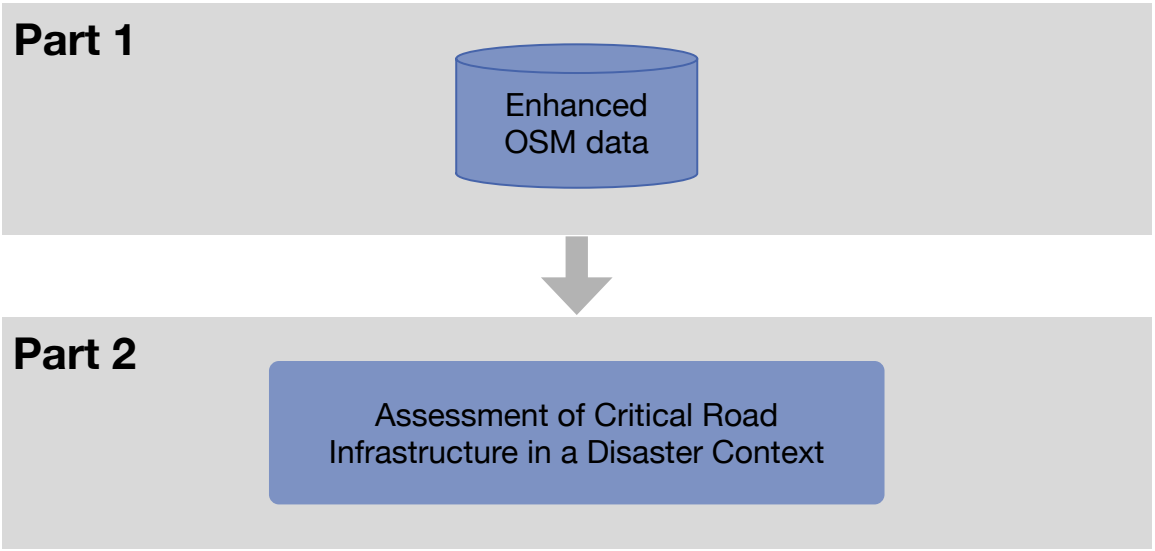

Figure 1.1: Simplified representation of the generic concept for the assessment of critical road infrastructure in a disaster context (GRIND).

Part II - Assessment of Critical Road Infrastructure in a Disaster Context is subdivided into four chapters. In Chapter 5, the fundamentals and the related work essential for the second part of **GRIND** are described, and its prerequisites are lined out. Chapter 6 follows with a detailed description of the methodology used in the critical infrastructure assessment. **GRIND** is applied exemplarily in Chapter 7 in two different case study regions for two wildfire scenarios. Finally, the applicability of the different modules of **GRIND** is discussed in Chapter 8, and its limitations are outlined. Part II advances the main objective with the following five main contributions:

- implementing two accessibility indices which highlight different aspects of accessibility,
- generating a basic travel demand model solely based on OSM and population data,
- estimating different kinds of natural disaster impacts on the road network,
- analyzing the vulnerability of the road network towards further disruptions during long-term disasters, and
- summarizing these contributions in a modular, multi-scale concept to overcome the challenge of limited global data availability.

Part III - Synopsis finishes this thesis with a summary of both **GRIND** parts and concludes the main objective. The conclusion is followed by an outlook presenting possible optimizations and future directions of this work.

Part I

Improving the Routability of OpenStreetMap Data

Part I - Improving the Routability of OSM data develops the first part of **GRIND** and focuses on the quality of OSM road network data and how to improve it for routing applications. A schema of the first part of **GRIND** is visualized in Figure 1.2. Two independent modules, the Fuzzy Framework for Speed Estimation (**Fuzzy-FSE**) and the **Error Search**, are developed to obtain enhanced OSM datasets. The two resulting datasets are then combined into one enhanced OSM dataset. The first part of **GRIND** can be applied independently of the second part to enhance OSM for all kinds of routing applications.

Part I begins with Chapter 2 to introduce OSM and motivate the **Fuzzy-FSE** and **Error Search** modules. Chapter 2 presents the OSM data model, performs a quality analysis of relevant OSM data, and summarizes the related work on OSM quality to conclude how the routability of OSM data can be improved. Chapter 3 follows this conclusion and presents an approach to improve routability by estimating average speed in road networks using Fuzzy Control. The **Error Search**, presented in Chapter 4, develops a method to detect, characterize, and rate road classification errors in road networks. It further enhances the usability of OSM data for routing applications.

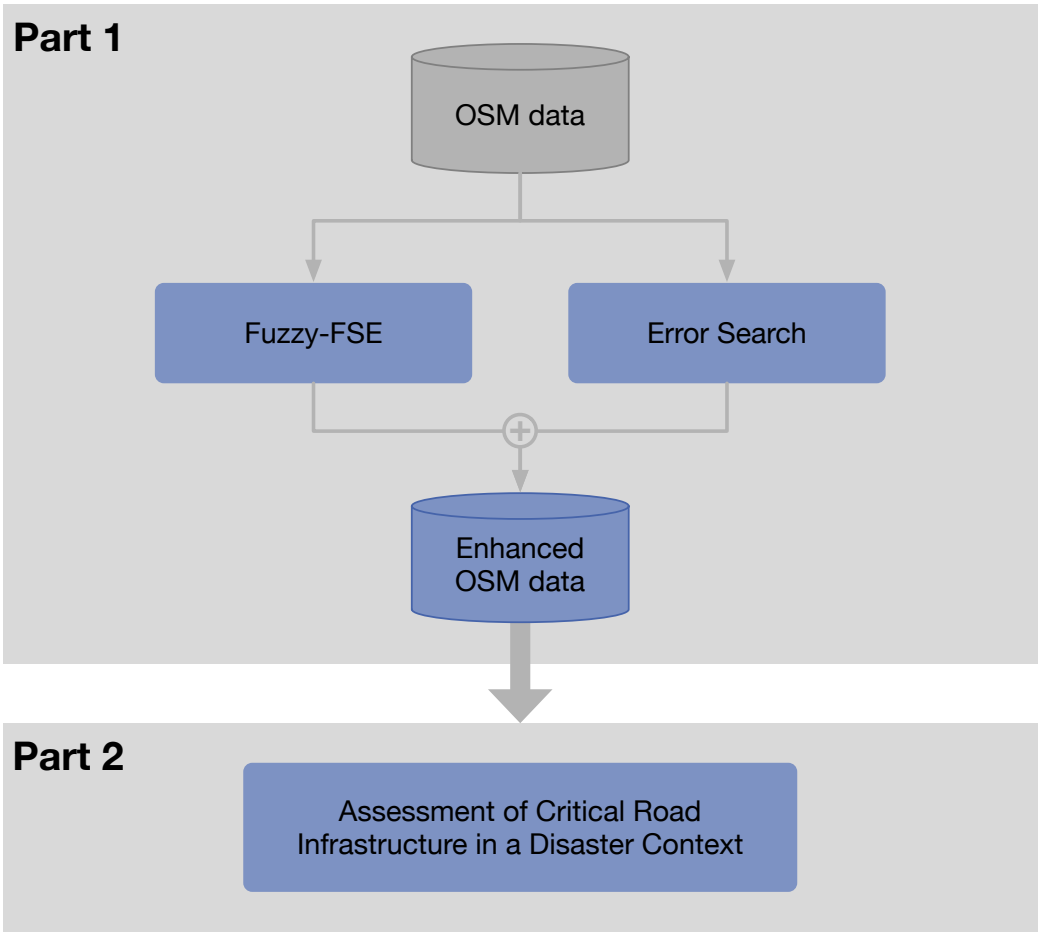

Figure 1.2: Part 1 of the generic concept for the assessment of critical road infrastructure in a disaster context (**GRIND**).

2 Introducing OpenStreetMap

In the past few years, the mapping and spatial data collection activities have radically changed from primarily professional and government agencies to increased involvement of the public [34]. Crowd-sourced Geographic Information can be used as an umbrella term to describe both active (or conscious) and passive (or unconscious) georeferenced information generated by non-experts [34, 35]. One type of Crowd-sourced Geographic Information is Volunteered Geographic Information (VGI), which is spatial data that is contributed by often untrained volunteers. Besides, Crowd-sourced Geographic Information also contains information that may be collected unconsciously or even involuntarily, for example, by using spatial data collected from mobile phones by Google or Facebook. Goodchild [36] shaped the term VGI in the year 2007. Since then, the applications of VGI have increased rapidly: from the development of mapping platforms such as Wikimapia, Google MyMaps, or OSM to text-based georeferenced tweets in Twitter or image-based georeferenced pictures on Instagram.

OSM [37] is the most common and well known VGI mapping project [38]. It is an initiative that started in the year 2004 to create and provide free geographic data to anyone. It is being built by volunteers who collect data using manual surveys, Global Navigation Satellite System (GNSS) devices, aerial photography, and other open sources [39]. Furthermore, agencies, cooperations, and government institutions worldwide donate data to the OSM project. This crowd-sourced data is then made available under the Open Database License [40]. This license intends to allow users to freely share, modify, and use a database while maintaining the same freedom for others. Three main reasons can explain the popularity of OSM: (i) it is completely free and accessible for everyone, (ii) it features millions of registered contributors, and (iii) it features a dynamic and flexible data model [38].

However, the application of OSM data often raises the question of quality. As non-experts from all over the world collect data partly without complying with any quality standards, a quality assessment must be part of every OSM-based application to understand if the information is fit-for-use. Especially the quality of the road network, a primary product of OSM, has become a particular object of interest for many applications. While the completeness and positional accuracy of roads are often the first quality element analyzed, other aspects like attribute completeness and accuracy might be essential for some applications.

This chapter introduces the OSM data model in Section 2.1. In Section 2.2, the OSM road network as the primary focus of this thesis is presented. Furthermore, its attributes are described, and their worldwide availability is analyzed in detail. Other OSM data besides

the road network, which are used in this thesis, are described in Section 2.3. Section 2.4 addresses the topic of the quality of OSM data. This chapter finishes with a synthesis on the OSM road network and its applicability for routing applications (Section 2.5).

2.1 The OSM Data Model

Generally, in all Geographic Information Systems (GIS), a feature represents a real-world object on a map [41]. Unlike other conventional GIS data models, the OSM data model does not use the simple feature model with points, lines, polygons, and their attributes in form of an attribute table. The OSM project has developed its unique data model, which allows for many kinds of attributes for features. These attributes can also be added later to an existing feature and can be unknown when the feature is created. Especially for a crowd-sourced and dynamic project like OSM, this proves to be essential.

The basic components of the OSM data model are elements (Figure 2.1). Elements consist of nodes, ways, relations and tags. A node represents a specific point on the Earth's surface defined by its latitude and longitude. Each node has at least an identification number and a pair of coordinates. A node can define a standalone point or the shape of a way. Ways are ordered lists of nodes that define a polyline. They are used to represent linear features like roads and rivers. Areas are represented as closed ways, meaning ways that have the same start and end node. Additionally, a tag indicating an area like `area=yes` or `building=yes` has to be used to define a polygon. A relation is an ordered list of nodes, ways, or other relations known as the relation's members. Relations document a relationship between two or more data elements, for example, a route relation that lists the ways that form a major highway or a bus route [39].

Nodes, ways, and relations can have tags containing the attributes of an element. A tag has two free format text fields: a key used to describe a topic, a category, or a type of feature and a value containing details to the specific form of the key-specified feature. Conventions are agreed on the meaning and use of tags, which are described in the OSM Wiki [39]. An example of a `key=value` pair is `highway=residential`, which defines the type of a road. A node, way, or relation can have an indefinite number of tags. An element can not have two tags with the same key [39].

A significant advantage of this unique data model is that new features and attributes, which may be unknown at the time the OSM database is created, can always be added. However, this freedom of creating new tags and values renders general consistency checks when entering new data unfeasible. Therefore, OSM data will always be susceptible to errors made by contributors.

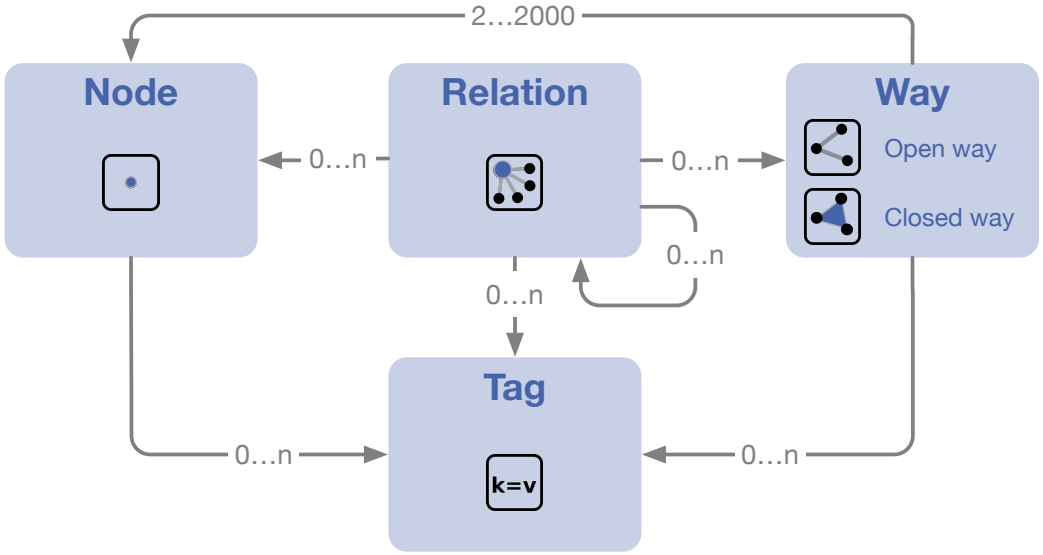

Figure 2.1: OSM data model with the elements node, way, relation and tag.

2.2 The OSM Road Network

The OSM road network is identified with the key `highway`. It includes a hierarchical classification that is described in Table 2.1. In this thesis, hierarchy levels are defined, which are also described in Table 2.1. These road classes and their respective link roads (`motorway_link`, `trunk_link`, `primary_link`, `secondary_link`, `tertiary_link`) form the road network. The definition of every class in the OSM road network is given in the OSM Wiki [39]. In general, a country's main road network is formed by a union of the levels L1 to L5 (see Table 2.1).

For this thesis, the OSM dataset of October 2019 is used. Figure 2.2 shows the distribution of road classes in six different countries and globally. This selection of countries will be analyzed throughout this section. The countries are chosen to represent each continent and demonstrate the quality of OSM data in regions that differ in their development state. For example, the OSM road network of Germany is considered to have a very high-quality road network [9]. In contrast, many African countries like Namibia feature a lower quality of the OSM road network [9].

Figure 2.2 illustrates that Germany has the second-longest road network of these six countries and features the smallest land area, which results in an average of 5749 km road network per km^2. In contrast, the United States of America (USA) has only an average of 1274 km road network per km^2. Less developed countries like Chile (293 km/km^2) and Namibia (157 km/km^2) feature a significantly shorter OSM road network especially in relation to their size. The road network per the area of a country is sometimes considered as an approximation for its completeness however, the population density of the respective country has to be taken into account. In Australia, over 85 % of the population lives within 50 km of

Table 2.1: Road classes and hierarchy level in the OSM road network. The levels range from L1 (top level) to L7 (bottom level).

OSM key	Description (cited from [39])	Level
`motorway`	Restricted access, major divided highway.	L1
`trunk`	Most important roads in a country's system that are not `motorway`.	L1
`primary`	Major highways, linking large towns.	L2
`secondary`	Highways, not part of a major route, form a link in the national route network, often link towns.	L3
`tertiary`	Connect smaller settlements and minor streets to more major roads.	L4
`unclassified`	Minor public roads, lowest level of the network, often link villages and hamlets.	L5
`residential`	Access roads to housing, without function of connecting settlements.	L6
`living_street`	Residential street, pedestrians have legal priority over cars.	L6
`service`	Access roads to or within an industrial estate, camp site, business park etc.	L6
`services`	Roads in service areas, rest areas.	L6
`road`	Road of unknown type, temporary.	L7
`track`	Mostly agricultural or forestry use.	L7

the coast. There, the low value of 159 km/km^2 reflects the low population density in vast areas in the middle of the continent rather than an incomplete road network.

The distribution of road classes for each of the six countries and globally is also shown in Figure 2.2. Other road classes in Figure 2.2 include the OSM tags `highway=living_street`, `highway=service`, `highway=services`, and `highway=road`. It is noticeable that the main road network (gray and blue in Figure 2.2) builds up less than half of the total road network in most countries and globally. This makes sense as, generally in road networks, the length of roads per road class increases with decreasing importance of the road class. The global statistic per road class reflects that phenomenon well. Especially in countries with long road networks such as Germany and the USA, residential roads, tracks, and other roads (orange in Figure 2.2) make up more than 70 % of the road network. This high percentage hints at a very densely mapped road network. Barrington-Leigh and Millard-Ball [9] find that OSM contributors map the most essential road classes first and the less important roads are filled in later. This phenomenon can be observed in Namibia as `primary`, `secondary`, and `tertiary` roads are of approximately equal length and not increasing with decreasing importance of the road class. Also, contributors map very few residential roads in this country.

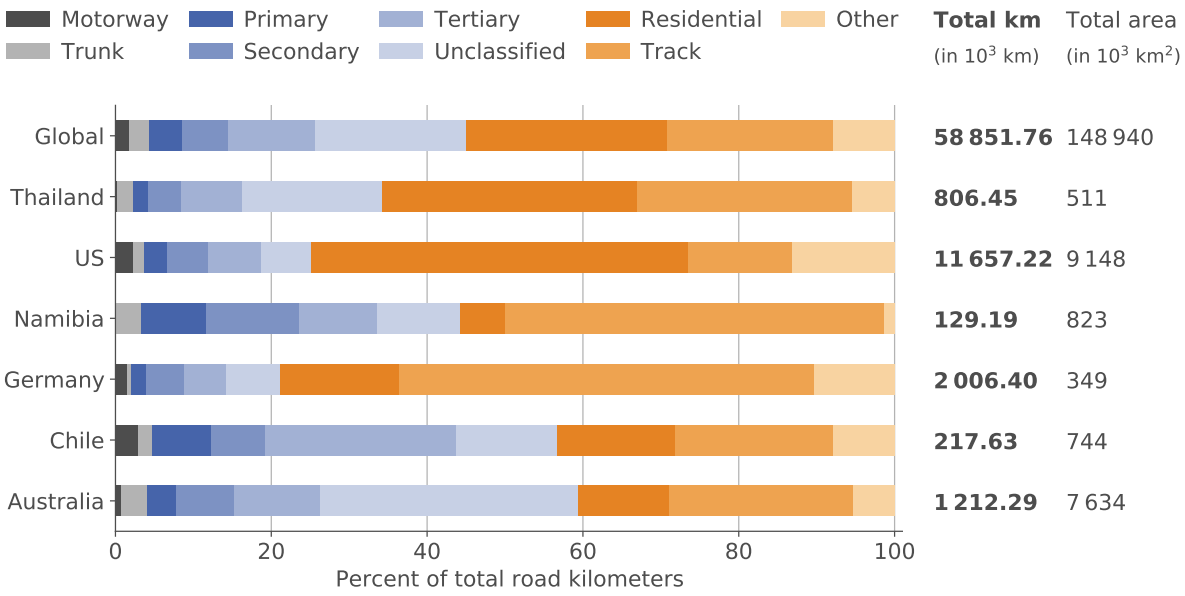

Figure 2.2: OSM key `highway` and its values for six countries worldwide and globally. For better reference, the total road kilometers and the land area of each country or region is given. A country's main network is displayed in gray and blue, further road classes are illustrated in orange.

The OSM data model uses additional tags to add attributes to each road element. The most common keys of the road network, which are also relevant for routing are `surface`, `oneway`, `maxspeed`, `lanes`, `maxwidth`, `maxheight`, and `maxweight`. In the following, these keys and their availability worldwide are described and analyzed. The description of the tags is cited from the OSM Wiki [39] as of August 2020.

Surface Tag

OSM uses the key `surface` to provide additional information about the physical surface of a road or footpath. The tags may contain general values like `surface=paved` for a road covered, for example, with paving stones, concrete or bitumen or `surface=unpaved` for a predominantly unsealed road. Ideally, values contain more precise information such as `asphalt`, `concrete`, or `paving_stones` for paved roads and `compacted`, `gravel`, or `ground` for unpaved roads. [39]

Globally, 24.9 % of all road kilometers have surface information (see Figure 2.3). The most common values are `unpaved`, `asphalt`, `paved`, `ground`, and `gravel`. Paved roads (illustrated in blue in Figure 2.3) build up 9.7 % of the global road network, unpaved roads 13.2 % (displayed in orange in Figure 2.3). 2.1 % of the global road network features other values and consist of both paved and unpaved surfaces. In total, 3359 different values for the key `surface` exist globally. These values include descriptions of various additional surfaces like `dirt`, `grass`, `sand` or `paving_stones`. But also invalid surface

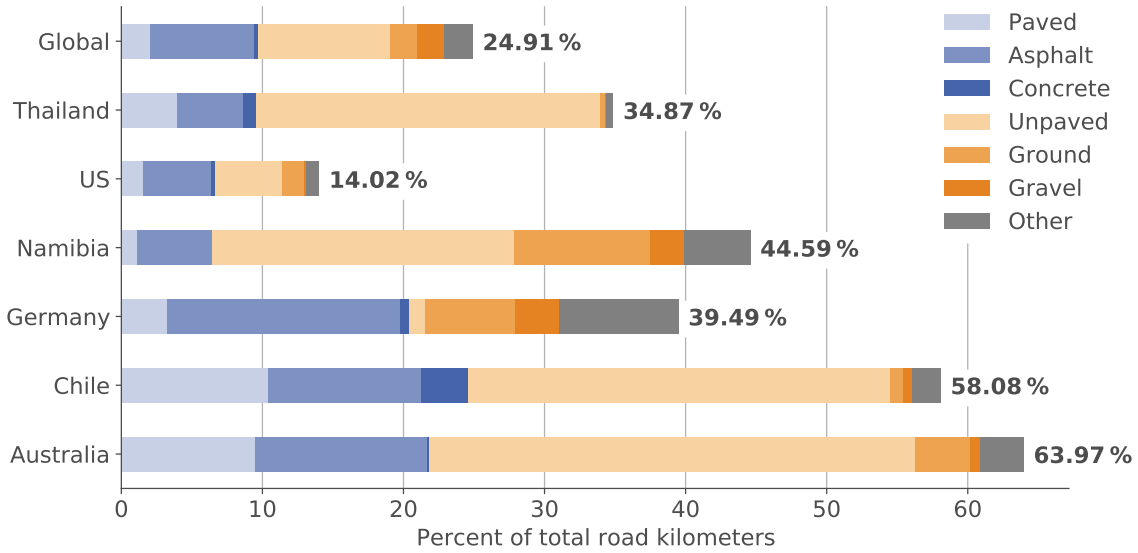

Figure 2.3: OSM key `surface` and some of the values for six countries and globally. The total percentage of all road kilometers with the `surface=*` tag per country is also given.

values are included like words in other languages than English (e.g. `Holzsteg`, `pierre`, `Calcestruzzo-Ghiaia-Asfalto`), spelling errors (e.g. `compcted`, `ssand`, `groumd`) or words without apparent sense (e.g. `Blenheim Heights`, `cobbi2`, `not_very_good`).

Figure 2.4 shows the distribution of the occurrence of the key `surface` worldwide. It can be observed that only a few countries have more than 60 % of road kilometers with surface information. However, both in Latin America and Africa, the percentage of roads with surface information is relatively high, considering many less developed countries in that region. In Europe and the USA, less than 40 % of all roads have surface information.

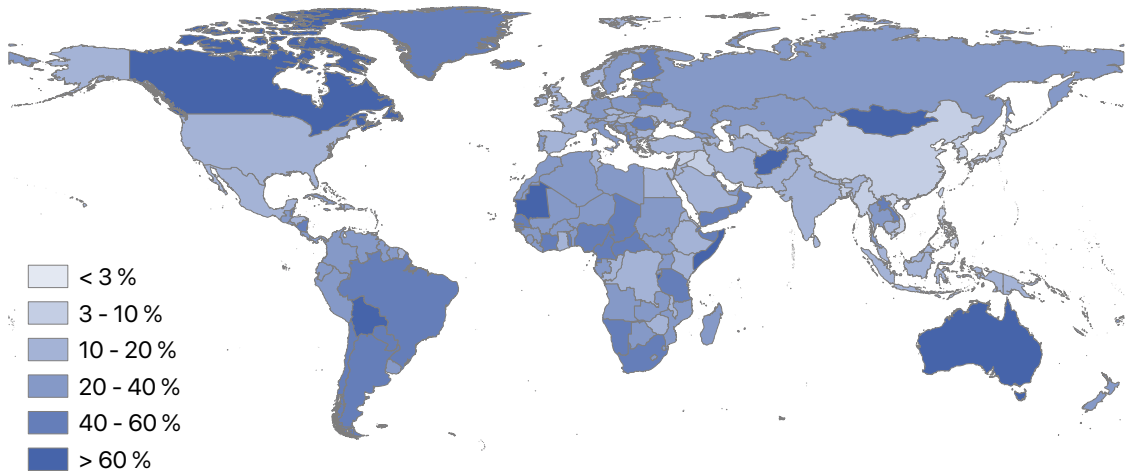

Figure 2.4: Percentage of the total length of all roads with the OSM key `surface` per country for all roads accessible by car. Adapted from [42].

Considering the distribution of values in Figure 2.3, in all analyzed regions except the USA and Germany, there are more unpaved than paved roads in OSM. In Thailand, Australia, Chile, and Namibia, many unpaved roads exist where the surface is often not specified in detail as `unpaved` is the most common surface value. These countries also have many more unpaved roads in total than paved roads. This is especially notable for Namibia as only 6.5 % of all road kilometers are paved and 38.1 % are unpaved. Both Germany and Namibia also feature a significant amount of other values. In Germany, the most common other values with over 10 000 km in the country's road network are `grass`, `compacted`, `dirt`, `concrete`, `paving_stones`, and `fine_gravel`. In Namibia, other common values include, for example, `sand`, `dirt`, `compacted`, and `tar`.

Oneway Tag

`oneway` is attributed to roads to indicate if a road can only be used in one direction. Access restrictions on `motorway` lanes as well as other one-way streets are indicated by `oneway`. The key is generally used in combination with the values `oneway=yes` or `oneway=no`. However, the tag `oneway=no` should only be used to avoid confusion, for example, where one-way streets are common or to override defaults. Other supported values are `-1`, `reversible`, and `alternating`. [39]

The key `oneway` is present for 9.0 % of all road kilometers worldwide (see Figure 2.5). Globally, 5.8 % have `oneway=yes`, and 3.2 % feature `oneway=no`. Only 0.03 % of all road kilometers have other values. Figure 2.6 illustrates the occurrence of the tag worldwide. By definition, the tag does not apply to all roads, but only to one-way roads or special cases. Therefore, the overall percentage of values is low. In most countries, less than 10 % of all road kilometers have a `oneway=*` tag. Notably, South America, Northern Africa, and Southern Europe seem to have more `oneway=*` tags than other countries. In contrast, Central Africa features less than 2 % of road kilometers with one-way information.

Figure 2.5 display the values of the `oneway=*` tag for different countries and worldwide. More `oneway=yes` than `oneway=no` exist in most countries, which is in line with the guidelines in the OSM Wiki [39] as only explicit one-way streets should be tagged. Contributors in Australia and Namibia may not follow these guidelines as there, `oneway=no` occurs significantly more frequently than `oneway=yes`. Of all examined countries, Chile features the highest percentage of one-way streets (`oneway=yes`), followed by the USA. In the analyzed countries, other values occur even less frequently than in the global dataset.

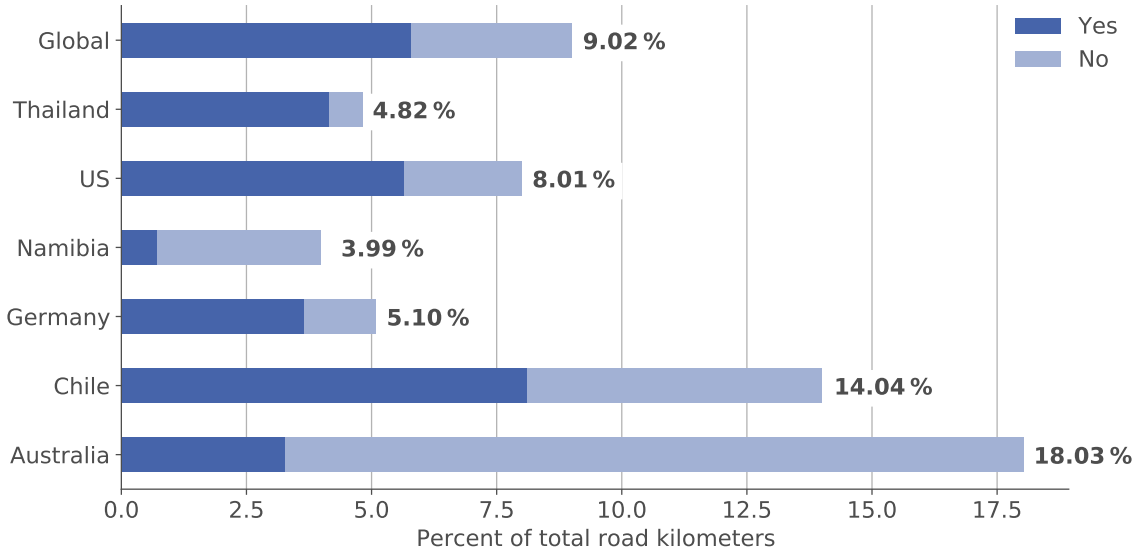

Figure 2.5: OSM key `oneway` and a breakdown of its values `yes` and `no` for six countries and globally. The total percentage of all road kilometers with the `oneway=*` tag per country is also given.

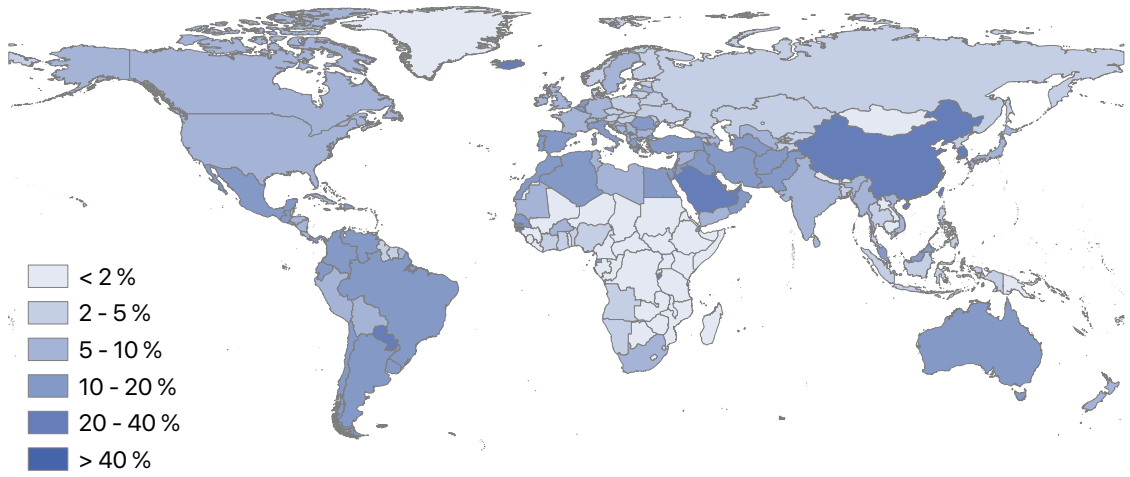

Figure 2.6: Percentage of the total length of all roads with the OSM key `oneway` per country for all roads accessible by car.

Maximum Speed Tag

`maxspeed` defines the maximum legal speed limit for general traffic on a particular road. By default, values are interpreted as kilometers per hour; different units can be added to the end of the value, separated by a space. The most common values are numeric speed limits such as `maxspeed=60` or `maxspeed=50 mph`. Other values like `maxspeed=variable` and `maxspeed=none` are used if there is a variable speed limit or no speed limit. When a road does not feature an explicit speed limit, the corresponding implicit values can (and should) be specified. Contributors can, for example, use `maxspeed=50` in combination

with the tag `source:maxspeed=DE:urban`. The key `maxspeed:conditional` can be used to tag time of day or seasonal changes of speed limits. [39]

Globally, 7.8 % of all road kilometers have maximum speed information. This value is mostly given in km/h (5.9 %) and less frequently in mph (1.8 %). The tag `maxspeed=none` is applied to 0.03 % of the global road network, `maxspeed=variable` is only present for 9.6 km of the global road network. 0.2 % of all road kilometers have other values like for example country specific declarations (e.g. `maxspeed=RO:urban`, `maxspeed=RU:living_street`) or various other values (e.g. `maxspeed=signals`, `maxspeed=100; 80`, `maxspeed=practical:60`).

Considering the global occurrence of the `maxspeed` key, it is apparent that very few countries have more than 40 % of road kilometers with maximum speed information (see Figure 2.7). Especially for most of Africa, the tag occurs in less than 2 % of all road kilometers. But also in well-developed regions with a high-quality road network like Europe or the USA, maximum speed information is available for less than 20 % of all roads. No country reaches the ideal goal with near 100 % of roads with maximum speed information. The countries with the highest percentage values of maximum speed information are Sri Lanka (64.1 %), the Netherlands (51.3 %), Romania (48.5 %), and few city states or island states.

Figure 2.8 illustrates the different values of the `maxspeed=*` tag in the six chosen countries. All countries except the USA provide the maximum speed information in km/h, which is also the default value in OSM. Germany is the only country where the `maxspeed=none` tag occurs (0.95 % of the German road kilometers), which is due to the German Autobahn sometimes having no speed limit. Other values rarely occur with 0.11 % in Germany and <0.01 % in the other analyzed countries in Figure 2.8.

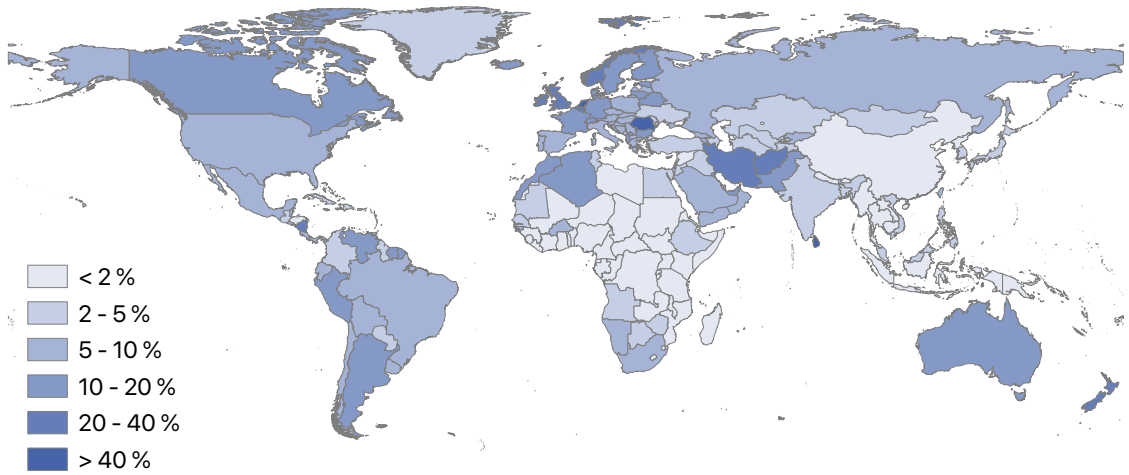

Figure 2.7: Percentage of the total length of all roads with the OSM key `maxspeed` per country for all roads accessible by car.

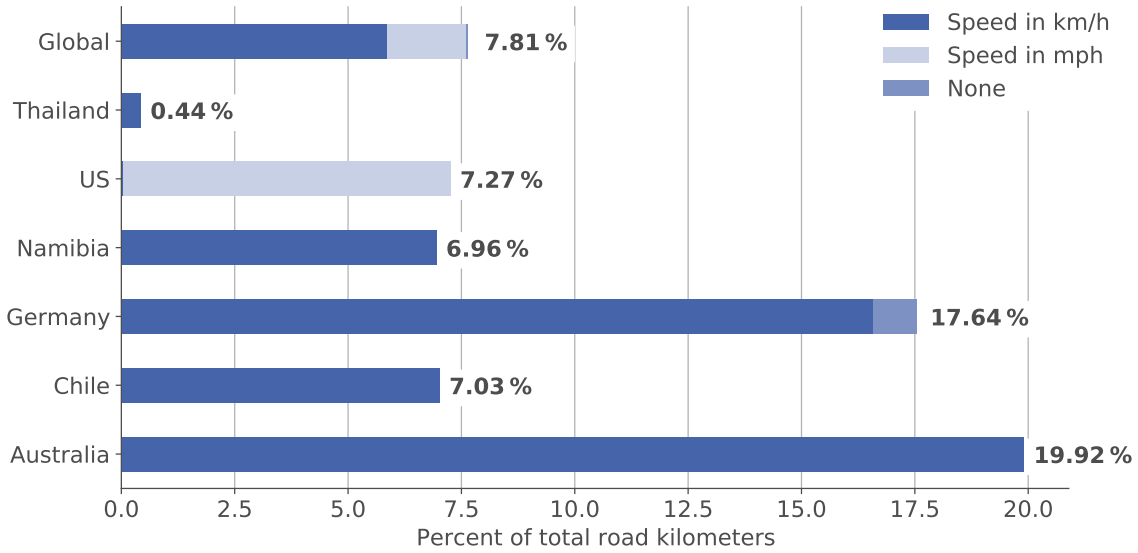

Figure 2.8: OSM key `maxspeed` and a breakdown of its most common values for six countries and globally. The total percentage of all road kilometers with the `maxspeed=*` tag per country is also given.

Lanes Tag

OSM uses the key `lanes` to count the number of traffic lanes on the road. The count excludes cycle lanes and motorcycle lanes that do not permit a motor vehicle. `lanes` should only be used in combination with a numerical value but can be specified with lane type like `lanes:forward=2` or `lanes:bus=1`. However, all cases where the key is not pure "`lanes`" are treated as different keys and are not included in this analysis. [39]

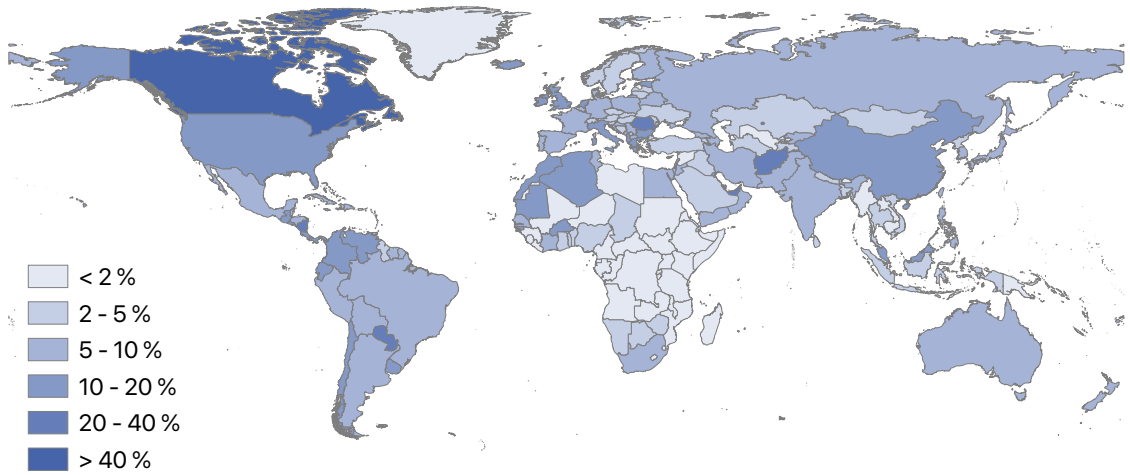

Figure 2.9: Percentage of the total length of all roads with the OSM key `lanes` per country for all roads accessible by car.

Figure 2.9 illustrates the occurrence of the lanes key in a global map. In the global OSM road network, 9.26 % of all road kilometers have the tag lanes=*. South and North America, as well as most of Europe and Asia, have more than 10 % of all road kilometers with information about the number of lanes. Few countries exist with more than 20 % lanes information. The countries with most lanes=* tags, and the only ones over 40 %, are Canada (72.37 %) and Singapore (59.82 %).

The most common values for the lanes key are the numbers 1 to 6 with decreasing frequency, the higher the number of lanes. The most common tag is lanes=2 (7.4 %) followed by lanes=1 (1.08 %), lanes=3 (0.52 %) and lanes=4 (0.24 %). Other values are only present for 5000 km in the global road network, which resembles only 0.01 %.

Maximum Width, Height, and Weight Tags

maxwidth specifies a legal restriction on the maximum permissible width of a vehicle to use that road. Similarly, maxheight can be used to specify a height limit, and maxweight is attributed to roads with a maximum weight. The values are interpreted as meters unless explicitly stated otherwise (e.g. maxwidth=16'3"). These tags should only be attributed to the section of a road it applies to. The value default can be combined with all these keys and can be very useful for truck routing to imply no explicit restriction. [39]

Table 2.2: Occurence of the keys maxwidth, maxheight and maxweight in the OSM road network for six exemplary countries and for the global road network. Both the total kilometers of roads with the respective tag and the percentage of all road kilometers with the respective tag in respect to the total road network in that country are listed.

	maxwidth		maxheight		maxweight	
	km	**% km**	**km**	**% km**	**km**	**% km**
Australia	63	0.01	429	0.04	810	0.07
Chile	5	< 0.01	240	0.11	27	0.01
Germany	9	< 0.01	4040	0.20	13 933	0.69
Namibia	0	-	3	< 0.01	< 1	< 0.01
USA	1234	0.01	2295	0.02	1347	0.01
Thailand	1	< 0.01	91	0.01	105	0.01
Global	5742	0.01	44 165	0.08	63 064	0.11

Table 2.2 shows the total kilometers and the percentage of total kilometers with the keys maxwidth, maxheight, and maxweight for the six chosen countries and globally. Of these three keys, maxweight is the most common but still occurs rarely. All three keys are very rare in the analyzed countries. Germany is the country with most height and weight restrictions,

Namibia and Thailand have almost no information about restrictions. Generally, it has to be considered that `maxwidth`, `maxheight`, and `maxweight` often only refer to small sections of a road like a bridge or a tunnel, which might only be a few meters long. However, the value `default` can be attributed to all roads without restrictions, which would benefit truck routing. Currently, there are only 4693 km with `maxheight=default`, 0.087 km with `maxwidth=default`, and none with `maxweight=default` in the global road network.

2.3 Further Relevant OSM Data

Besides the road network, OSM contains a variety of suitable data for all kinds of applications. Due to the project's open and dynamic character, new map features with new tags can easily be created. The OSM topics are diverse and feature, for example, transport (air, land, and sea), amenities (like toilets, banks, and parking), boundaries, buildings, settlements, shops, tourism, or land use. In this thesis and especially in Part II, three other keys besides the road network are used.

Place

OSM uses the key `place` to provide details about settlements. Places can be mapped as both points and areas. For this thesis, the tags `place=city`, `place=town`, and `place=village` are used. The tag `place=city` is used to identify the largest settlement or settlements within a territory and includes national, state, and provincial capitals as well as other major conurbations [39]. The tag `place=town` is attributed to important urban centers, which usually have a good range of shops and facilities [39]. A town in OSM is larger than a `place=village` but smaller than a `place=city`. A small distinct settlement with few facilities available with people traveling to nearby towns to access facilities is tagged `place=village` [39]. Their population varies by country but typically ranges between 500 and 10 000 inhabitants. Tags for smaller settlements like `place=hamlet` or `place=isolated_dwelling` are not used in this thesis.

Amenity

The key `amenity` can contain a variety of values and describes facilities used by visitors and residents. In this thesis, it is used to locate the emergency facilities police, hospital, and fire station. The tag `amenity=hospital` is used for hospitals, meaning institutions for health care providing treatment by specialized staff and equipment, and typically providing nursing care for longer-term patient stays [39]. Other tags for healthcare like `amenity=clinic` or `amenity=doctors` are not applied in this thesis. A fire station, a facility

from which a fire brigade operates to fight fires, is tagged `amenity=fire_station` [39]. Similarly, a police station is a facility where police officers patrol from and the first point of contact for civilians. It is tagged `amenity=police` [39].

Boundary

Finally, the tag `boundary=administrative` indicates administrative boundaries. Contributors use it in combination with the key `admin_level`, which contains different values corresponding to different admin levels. The admin-level codes vary by country (except `admin_level=2`, which is always used for country borders) and can be found in the OSM Wiki [39]. For example, the tag `boundary=administrative` in combination with `admin_level=4` is used for state or territory borders in Australia.

2.4 Quality of the OSM Road Network

The quality of the OSM road network worldwide is a broad and constantly-evolving research field. Users of OSM data need to be aware of possible quality issues with OSM data before using the data in their applications. Therefore, many studies on the quality of the OSM road network exist which analyze different aspects of data quality.

In this section, data quality elements for geographic data are defined as described by the International Organization for Standardization (ISO) in Section 2.4.1. Then, the related work on the quality of the OSM road network is presented in Section 2.4.2.

2.4.1 Data Quality Elements for Geographic Data

The principles of the ISO can be applied to assess the quality of geographic data. The ISO 19157:2013 [43] defines six data quality elements that each describe certain aspects of geographic data quality. In the following, all six data quality elements mentioned in ISO 19157:2013 are described generally and in the OSM context.

Completeness evaluates the presence or absence of features, their attributes, and relationships. Both errors of omission (data that is missing from a dataset) and errors of commission (excess data present in a dataset) are considered. In the context of OSM, completeness can be evaluated for features, for example, *Is a road element present in the OSM dataset?*, and for attributes, for instance, *Does a road element have a tag `maxspeed=*`?*.

Positional accuracy is the accuracy of the position of features within a spatial reference system. It can be further divided into three categories: absolute or external accuracy (the

closeness of true coordinate values), relative or internal accuracy (closeness of the relative positions of features in a dataset), and gridded data positional accuracy. Positional accuracy in OSM refers to the accuracy of the coordinate values of nodes or ways, for example, of roads. An example of low absolute accuracy but good relative accuracy is if two roads that are supposed to be 100 m apart are at coordinates 1 km west of the true coordinate values but still 100 m apart.

Thematic accuracy is defined as the accuracy of quantitative attributes and the correctness of non-quantitative attributes. It consists of three sub-categories. First, classification correctness, which asks the question if the feature is assigned to the right class(es). Then, non-quantitative attribute correctness, a measure of whether a non-quantitative attribute is correct or incorrect. Finally, the quantitative attribute accuracy, the closeness of a quantitative attribute's value to the true value. In OSM, this concerns the tags associated with a feature. For example, this can be the accuracy of the road class of a road element (classification correctness) or the accuracy of the maximum speed value (quantitative attribute accuracy).

Temporal quality refers to the quality of temporal attributes. It concerns the accuracy of a time measurement, the temporal consistency as the correctness of the order of events, and the temporal validity, also referred to as currency. In OSM, this is especially important in regards to currency as the currency of VGI is expected to surpass authoritative data [44].

Logical consistency is defined as the degree of adherence to logical rules of data structure, attribution, and relationships. These rules should ideally be described in a data product specification. Logical consistency consists of four types: conceptual consistency, domain consistency, format consistency, and topological consistency. In OSM, logical consistency errors can occur in the form of, for example, roads in permanent water bodies. One example of a topological inconsistencies are *almost connections* of two roads where there should be a connection.

Usability, also referred to as fitness-for-use, is based on external user requirements. All five data quality elements can be aggregated to describe the usability of a dataset for a particular application. An example of the OSM datasets usability is the usability for routing applications. Routing applications require different road data than, for example, applications that display road maps.

2.4.2 Related Work on Quality of OSM

With the above-defined data quality elements, the quality of OSM road data can be assessed. In the OSM road network, features are the road elements themselves with their characteristic shape and geographic coordinates. Attributes are the corresponding tags of the road elements. This section evaluates the related work on the quality of the OSM

road network regarding the data quality elements feature completeness, attribute completeness, positional accuracy, thematic accuracy, temporal quality, logical consistency and usability. Table 2.3 lists the most relevant studies on the quality of the OSM road network and the analyzed data quality elements.

Table 2.3: Relevant studies on the quality of OSM data.

Authors	Year	Region	Quality elements	Methodology
Cipeluch et al. [8]	2010	Ireland	Feature completeness, positional accuracy, thematic accuracy, temporal accuracy	Comparison with Google Maps and Bing Maps
Girres and Touya [45]	2010	France	Feature completeness, positional accuracy, attribute accuracy, temporal accuracy, logical consistency, usability	Comparison with authoritative data
Haklay [46]	2010	England	Feature completeness, positional accuracy, temporal accuracy	Comparison with ordnance survey data
Ludwig et al. [47]	2011	Germany	Feature completeness, logical consistency, usability	Comparison with TomTom commercial data
Mondzech and Sester [10]	2011	Germany	Usability (pedestrian navigation)	Comparison with authoritative data
Neis et al. [48]	2011	Germany	Feature completeness, attribute completeness, positional accuracy, thematic accuracy, logical consistency, usability (navigation)	Comparison with Navteq commercial data
Wang et al. [49]	2013	China	Feature completeness, attribute completeness, positional accuracy, thematic accuracy	Comparison with authoritative data
Zielstra et al. [50]	2013	USA	Feature completeness, temporal accuracy	Comparison with TIGER/Line data

Table 2.3: Related studies on the quality of OSM data – continued from previous page

Authors	Year	Region	Quality elements	Methodology
Barron et al. [51]	2014	Multiple	Feature completeness, positional accuracy	Several intrinsic methods
Graser et al. [52]	2014	Austria	Feature completeness, attribute completeness, positional accuracy, usability (navigation)	Comparison with authoritative data
Camboim et al. [53]	2015	Brazil	Feature completeness, attribute completeness, temporal accuracy	Comparison with authoritative data
Sehra et al. [11]	2016	India	Logical consistency, usability (navigation)	Applying topology rules
Davidovic et al. [54]	2016	Global	Thematic accuracy	Statistical analysis
Demetriou [55]	2016	Greece	Feature completeness, positional accuracy, thematic accuracy	Comparison with authoritative data
Barrington-Leigh and Millard-Ball [9]	2017	Global	Feature completeness	Visual assessment against satellite imagery and intrinsic method
Brovelli et al. [56]	2017	Italy	Feature completeness	Comparison with authoritative data
Mahabir et al. [57]	2017	Kenya	Feature completeness	Comparison with authoritative data
Sehra et al. [12]	2017	India	Feature completeness, attribute completeness, thematic accuracy, logical consistency	Intrinsic methods
Almendros-Jiménez and Becerra-Terón [13]	2018	Spain	Attribute completeness, thematic accuracy, logical consistency, usability (navigation)	Statistical analyses

Table 2.3: Related studies on the quality of OSM data – continued from previous page

Authors	Year	Region	Quality elements	Methodology
Zhang and Malczewski [58]	2018	Canada	Feature completeness, positional accuracy, thematic accuracy	Comparison with commercial data
Jacobs and Mitchell [59]	2020	Canada	Feature completeness, temporal accuracy	Unsupervised machine learning
Goldblatt et al. [60]	2020	Small island states	Feature completeness	Comparison with remote sensing data

Feature Completeness

Most studies on the quality of the OSM road network, especially in the early years, assess feature completeness as the primary data quality element. Barrington-Leigh and Millard-Ball [9] assess the global completeness of OSM road data in the year 2017. They reach two major conclusions regarding completeness. On the one hand, OSM is circa 83 % complete, globally, with over 40 % of countries having an almost complete street network. On the other hand, well-governed countries with good internet access tend to be more complete, and completeness has a U-shaped relationship with population density (sparsely populated and dense urban areas are the most complete). It can generally be observed that completeness is higher in densely populated areas and lower in rural areas. This observation is supported by studies in Brazil [53], Canada [58], China [49], Ireland [8], England [46], Germany [47, 48], Ireland [8], Italy [56], Kenya [57], and USA [50, 51]. Feature completeness also varies between road classes, with high-level roads such as `motorway` and `primary` (see Table 2.1) having higher completeness than low-level roads like residential roads [47, 49, 51].

Following the related work on feature completeness from the year 2011 until now, the quality is generally improving. In urban regions, it often surpasses authoritative datasets in completeness, a phenomenon that can first be observed in countries with a very active community like Germany [48], England [46] and Austria [52] and later also in less active communities like in Brazil [53]. Barrington-Leigh and Millard-Ball [9] find that the Gross Domestic Product (GDP) has no apparent impact on the completeness, except at the lowest densities, and that small countries tend to be more complete.

Attribute Completeness

As feature completeness is becoming adequate in most countries, attribute completeness is gaining attention. Especially for navigation, additional attributes for road elements are required. However, due to the open and voluntary tagging system, road elements often have no tags besides the mandatory one (`highway=*`). Camboim et al. [53] find that in their urban study region in Brazil in 2015, 30 % of roads have no additional tags. Generally, the number of tags linearly increases with the number of contributors [45]. In the context of attribute completeness, the keys `name`, `oneway`, and `maxspeed` are often considered.

The most commonly analyzed tag regarding attribute completeness is `name=*`, which contains the road name and is essential for the display of maps and finding addresses. Ludwig et al. [47] state that in the year 2011, in their study region in Germany, the percentage of missing names increases from inhabited areas (5.6 %) to uninhabited ones (17.5 %) and from important (4.7 %) to less important streets (13.8 %). Another study by Neis et al. [48] in the same year and also in Germany finds that 16 % of all roads have neither a name nor a route number. In an urban environment in 2014 in Vienna, 78 % of all roads have names, and the name attribute completeness is relatively equal for all road categories [52]. In 2016, Demetriou [55] finds a road name completeness of around 100 % for high-level roads and circa 40 % for low-level roads in Crete, Greece. In Spain in the year 2018, the name tag is present in 73 % of urban roads [13], and in Canada, in the year 2017, circa 60 % of all roads (urban and rural) have names [58]. Wang et al. [49] find that only 36 % of roads in Wuhan, China have names. In conclusion, the name's tag completeness varies by region but is, on average, reasonably complete.

The second most frequently analyzed tag regarding attribute completeness is `oneway=*`. In Germany, in the year 2011, the attribute oneway is more often missing in uninhabited areas (48.8 %) than in inhabited ones (28.1 %) [47]. In Vienna (2014), 87.8 % of the one-way streets in the reference dataset matched OSM `oneway` [52]. The completeness of the `oneway=*` tag in cities in Spain (2018) (70.1 %) is similar to the completeness of the name tag in the same study (73 %) [13]. The information about one-way streets is crucial for routing algorithms in urban regions where travel times can vary significantly when one-way streets are considered.

The completeness analyses for the key `maxspeed` show dramatic results. Ludwig et al. [47] state that it is missing for 81 % of the objects in inhabited areas and 93 % of the objects in uninhabited areas in 2011 in Germany. Later in 2014, Graser et al. [52] find that only 43 % of roads in Vienna, a city with a very active OSM community, and only 30 % of roads in a low-level road category contain a maxspeed value. In Spain in the year 2018, Almendros-Jiménez and Becerra-Terón [13] find that an average of 73 % of roads in cities is missing maximum speed information. In the same study, they compare Spanish cities with other European cities and find that more than 90 % of roads have maximum speed information in Berlin, London,

Rome, and Vienna. This high percentage indicates that since 2011 [47] and 2014 [52], the attribute completeness for the tag `maxspeed` has increased considerably for cities with active OSM communities. In contrast, Sehra et al. [12] finds that in Punjab, India, in the year 2017, only 5 % of features have maximum speed information. In conclusion, the maxspeed attribute's completeness varies a lot by region and by OSM contributor activity and is generally higher in urban than in rural regions [47, 52, 13]. In general, it has to be improved as the maximum speed is important information, especially for navigation [47, 13, 12].

Positional Accuracy

The positional accuracy of the OSM road network can generally be considered very high. Studies find average positional accuracies of between 5 m to 10 m (France, 2010) [45], 6 m (England, 2010) [46], circa 6 m (Germany, 2011) [47], circa 15 m (Madrid - Spain, 2014) [51], circa 6 m (Cyprus - Greece, 2016) [55] and circa 7 m (Canada, 2017) [58]. Zhang and Malczewski [58] find that `primary` and `secondary` roads have relatively low positional accuracy, whereas local roads are the most accurate ones. Haklay [46] also observes this phenomenon and justifies it by local roads receiving more attention. Moreover, high-level roads are usually wider than local roads, so errors are more likely to occur if the highways are traced by road lanes instead of center lines [58]. Wang et al. [49] observe the opposite in Wuhan, China, in 2013, where the positional accuracy of high-level roads is higher than of low-level roads.

Thematic Accuracy

The thematic accuracy of tags is often a challenge to estimate because of the frequently low attribute completeness [58], incompatible classification schema, or classification ambiguity [58, 49, 54]. As the road class (tag `highway=*`) is a mandatory tag for every road element, it is often considered in thematic accuracy analyses.

Girres and Touya [45] find that in 2010 in France, the main roads `motorway` and `primary` have a 100 % correct classification. However, only 49 % of `secondary` roads are correct compared to the applied reference dataset. The road importance is mainly underestimated as `secondary` roads are classified as `residential` or `tertiary` [45]. In Wuhan (China) in 2013, Wang et al. [49] find a classification accuracy of only 32.2 %. But, they also argue that this is mainly due to incompatible classification schemas of OSM and their applied reference data. The same can be said for the study of Zhang and Malczewski [58] in Canada (2018) as they find that 40 % of all roads are misclassified. However, their research has a design error as they count the OSM class `unclassified` as misclassified roads [58]. The definition of the class in [39] states clearly that these are not unclassified roads but minor public roads. The name `unclassified` is a historical artifact of the UK road system.

The road name is a frequent tag of road elements. Davidovic et al. [54] find excellent compliance for the name tag in residential roads and good compliance for `primary` roads in their global analysis of cities in the year 2016. Similarly, the road name's attribute accuracy is 100 % for `motorway` in Crete, Greece, in 2016 and exceeds 86 % for lower road classes [55].

Davidovic et al. [54] analyze the compliance or usage of suggested tags, and tag values from the OSM map features Wiki [39] and conclude that it is disappointingly low. Often this results from confusion about how to apply tags correctly. One example is `highway=unclassified`, which is intuitively used by contributors for roads, which are not yet classified. Other examples exist like for the tag `oneway=*` where Davidovic et al. [54] find poor compliance in all cities they analyzed. The suggestions of tag usage in the OSM wiki are either not considered before mapping or may sometimes be confusing or counter-intuitive. However, a change of guidelines is often thought impossible with such an active global community that will adhere to the old guidelines [39].

Temporal quality

The temporal quality of OSM data often surpasses authoritative data, especially in regions with many active contributors [44]. Girres and Touya [45] conclude that the more contributors there are in a region, the more recent the objects are. In Brazil, in 2015, Camboim et al. [53] analyze the temporal quality of the OSM road network and find an average of 20 contributors per municipality and, on average, 120 days since the last edition in urban regions. Considering that administrative data is often only updated yearly or less frequent, OSM can be the more recent data source. Furthermore, as each OSM feature's history is preserved, it provides a timeline of changes that may be valuable for some applications.

Logical consistency

The logical consistency of the OSM road network is mostly analyzed by considering topological errors. Girres and Touya [45] discover that in the year 2010 in France, the connectivity of roads is ensured in about 95 % of cases. They state that the model's structure is not ideal as a good model should finish a line at each intersection, which is rarely the case in OSM. Also, in Germany, it can be seen that in the year 2011, the number of *almost connections* has decreased over the years and remains high only for cyclist or pedestrian routes [48]. They also find that duplicate streets have decreased over the years. Sehra et al. [11] analyze the road network of Punjab, India, in 2016 and identify 8492 logical errors such as undershoot, overshoot, and mismatches within a tolerance of 3 m. Furthermore, 44 036 errors are found with other rules, most of them being *almost connections* [11].

Usability

In the beginning, the objective of the OSM project was to collect geographical information to display map data. The developers and contributors mostly have this initial purpose in mind when creating new content. However, the data has become so good that it is nowadays used in a variety of applications. Considering the road network, it is reasonable to try to apply the data for navigational purposes. While Cipeluch et al. [8] state that in 2010 the OSM quality necessary for routing and navigation applications is not sufficient, the improving quality over the years has caused others to evaluate the usability of OSM data for navigation in more detail. Neis et al. [48] find in the year 2011 that the commercial dataset TomTom has five times more turn restrictions available for Germany than OSM. In 2014, already 60.6 % of the turn restrictions in a reference dataset in Vienna matched the OSM turn restrictions. Despite the clear improvement of the OSM data for routing applications over the years most studies conclude that OSM data requires thorough preprocessing before being used for navigational purposes [10, 11, 12, 13]. Mostly attribute completeness and accuracy needs to be improved [13].

2.5 Synthesis on the OSM Road Network Quality

In conclusion, the OSM road network can nowadays be considered relatively complete and reasonably accurate as feature completeness and positional accuracy are relatively high in most regions. The unique OSM data model and the growing number of OSM contributors advance the dataset to develop further according to the needs of the users. The various tags covering all kinds of topics allow for many applications. The dataset's biggest advantage is its worldwide free availability, which allows for global analyses and applications. The alternative to search for data in every country worldwide is very time consuming and often not feasible due to data incompatibility. Thus, OSM data is often the only option for generic approaches.

However, especially considering OSM data in routing applications, the attribute completeness and accuracy are still lacking. This becomes apparent in Section 2.2 with the low percentages of attribute occurrence in all regions and in the related studies presented in Section 2.4. For routing applications and especially for the analysis of critical road infrastructure, two major challenges are identified.

Challenges and Consequences for this Work

The first challenge is the often missing speed information. To calculate fastest paths in a network, a routing application requires the travel time of a road segment as a cost factor. As this is rarely given in OSM, routing applications have to consider alternative

ways to obtain the travel time. For this reason, we develop the **Fuzzy-FSE**, which is presented in the next chapter (Chapter 3).

The second challenge is the attribute accuracy, especially regarding the road classification. On the one hand, the road class is often used as an approximation for the average speed where speed information is missing. On the other hand, some road classes imply access limitations, which hinders routing. Moreover, a correctly classified road network is usually connected on each level. This connectedness enables the user to remove lower-level road classes while still maintaining the road network's functionality. In studies on post-disaster assessment of critical road infrastructure this is a common practice as it drastically reduces computing time. To address this challenge, an **Error Search** is developed that detects, characterizes, and rates potential classification errors. This **Error Search** is presented in Chapter 4.

3 Multi-Parameter Estimation of Average Speed in Road Networks Using Fuzzy Control

This chapter includes material from the journal article

Johanna Guth, Sven Wursthorn, and Sina Keller. "Multi-Parameter Estimation of Average Speed in Road Networks Using Fuzzy Control". In: *ISPRS International Journal of Geo-Information* 9.1 (2020), pp. 1–18. It is cited as [42] and marked with an orange line.

and from the conference paper which is a pre-study to the above-quoted study

Johanna Stötzer, Sven Wursthorn, and Sina Keller. "Fuzzy Estimation of Link Travel Time from a Digital Elevation Model and Road Hierarchy Level:" in: *Proceedings of the 5th International Conference on Geographical Information Systems Theory, Applications and Management*. Heraklion, Crete, Greece: SCITEPRESS - Science and Technology Publications, 2019, pp. 15–25. It is cited as [61] and marked with a red line.

3.1 Introduction

Applications like route planning, disaster risk management or transportation depend on finding the fastest path in a road network. For the computation of the fastest path, average speed values are assigned to every edge in the road network to calculate link travel times. The link travel time is the average time a vehicle spends traveling along a network edge [14]. In studies on critical road infrastructure and accessibility, the link travel time often serves as a cost factor for the road network [62, 63, 64, 65].

Many of these approaches use OSM data. However, as stated in Section 2.2, the maximum speed is only present in 7.4 % of all road elements in the worldwide OSM dataset released in October 2019 (see Figure 2.8). To compute link travel times and fastest paths, maximum speed information for every edge in the road network is crucial.

Influencing factors on average speed in urban and in rural areas differ for many reasons. While traffic, turn restrictions, one way streets and traffic signals have a noticeable impact on average speed in the city, other factors dominate in rural areas. For example the road quality has a considerable impact on the average speed: asphalted roads e.g. allow for a higher speed than unsealed gravel or mud roads. The road width and number of lanes also have an impact on speed, as well as the topography [66]. The slope of a road limits the driving speed, both by increasing sinuosity and by the slope itself.

Many studies and routing applications rely on fixed speed profiles for every road class defined by various input parameters. To avoid jumps at these class borders, a Fuzzy Control System (FCS) can be used. Such a FCS is able to fuzzify these input parameters and provides a more continuous, nonlinear output. Furthermore, it is based on expert knowledge and does not rely on reference data to learn its behavior.

In this chapter, we develop a Fuzzy Framework for Speed Estimation (**Fuzzy-FSE**) to estimate the average speed on rural roads in the network. The speed is derived from multiple input parameters: road hierarchy level, surface, slope and link length. The OSM road network and Shuttle Radar Topography Mission (SRTM) data serve as input data for the **Fuzzy-FSE**. Two different approaches are presented: the first approach relies solely on OSM data. It uses the number of support points of the vector shape of a road as an approximation for the slope (see Section 3.4.1). The second approach calculates road slope from a SRTM digital elevation model. The Google Directions API (GD-API) is used as reference data and as input for a baseline calculation. The **Fuzzy-FSE** contains multiple FCSs which are employed to obtain a continuous speed output. The FCSs are set up with the Membership Function (MF) for the input parameters slope and link length and different MFs for the output parameter speed. Two exemplary case studies are performed: One in the BioBío and Maule (BM) region in Chile and the other in North New South Wales (NNSW) in Australia.
The main contributions of this chapter are summarized as follows:

- development of a multi-parameter **Fuzzy-FSE** containing a combination of multiple FCSs;
- a detailed analysis and discussion of the performance of the **Fuzzy-FSE** in comparison to an existing method;
- usage of only open source and worldwide available data (OSM, SRTM);
- transferability of the presented method to other regions;
- possibility to use the **Fuzzy-FSE** only with OSM data as input;
- exemplary case studies in the BM region in Chile and in New South Wales (NSW) in Australia;
- the datasets and the implementation of the **Fuzzy-FSE** are published on GitHub [67].

In this chapter, we first provide an overview of the related work on average speed and link travel time in OSM in Section 3.2 and introduce the concept of Fuzzy Control in Section 3.3. The OSM, SRTM and GD-API datasets are described in Section 3.4. Then, the developed **Fuzzy-FSE** with the FCSs is explained in Section 3.5. A description of both case studies (Section 3.6), the results (Section 3.7) and a detailed discussion (Section 3.8) are presented. Finally, a conclusion and an outlook are given in Section 3.9.

3.2 Related Work on Link Travel Time in OSM

Many routing applications exist that compute fastest paths, and consequently link travel time, and base on OSM data. Popular examples are the OpenRouteService [68], the Open Source Routing Machine (OSRM) [69], the OpenTripPlanner [70] and YOURS [71]. The latter three are open source applications and use the maximum speed information in OSM to calculate link travel time if available. If not, the OSM Wiki [39] contains default speed limits for some countries (24 countries worldwide) which are processed and applied by these routing applications. The applications also include other attributes like the road type and the number of lanes (if available) to derive fixed speed profiles for every road class. The algorithm for the OpenRouteService is not accessible by public. But it seems more complex than the other routing applications as it provides additional information like the slope and type of a route. However, like many commercial routing applications such as Google Maps or Bing Maps the exact calculation is not transparent.

Few studies address the issue to derive link travel time from the OSM road network. Stanojevic et al. [14] present a methodology to calculate link travel times based on origin-destination and timestamp information generated by a taxi fleet and OSM data. They estimate travel times in urban regions with 60 % lower errors than OSRM. A lot of related work concentrates on urban regions and how to improve the estimation of travel time in networks with a lot of traffic. Steiger et al. [15] include real-time traffic data into the OpenRouteService application.

As mentioned in Section 3.1, the important factors for routing in urban and rural areas differ considerably. In the design standards of Asian highway routes, the assigned maximum speed of a road in a rural region is directly dependent on the slope of the terrain [72]. Brabyn and Skelly [73] model access to public hospitals and calculate shortest and fastest paths. To estimate the link travel time, they consider if the road is inside or outside an urban area, the number of lanes and the sinuosity of a road. The sinuosity of a road is calculated with a sinuosity index. They categorize the roads by these factors and assign fixed velocities for every combination.

This study aims at filling some of the existent gaps in the related work. Most routing applications with OSM focus more on the city than the rural areas and only include country wide speed limits in their travel time calculation. Few studies focus on the calculation of link travel time. The ones that do, rely on self-collected or commercial datasets. To our knowledge, a fuzzy control system has never been applied to estimate link travel time with different parameters.

3.3 An Introduction into Fuzzy Control Systems

The idea of Fuzzy Control was first introduced by [74] for a steam engine and boiler combination. FCSs work on linguistic terms and partial memberships which are able to express fuzziness. A FCS takes crisp input values and fuzzifies them with the help of membership functions. In a second step, a rule base provides the basis for the inference mechanism. A defuzzification generates crisp and continuous output values.

The main advantages of Fuzzy Control are its flexibility and its simple construction. It involves human reasoning and decision making such that it is useful in providing solutions to complex problems in different kinds of applications. Furthermore, it is able to include imprecise input information. Figure 3.1 shows an exemplary FCS. In the following, the different parts of a FCS are introduced.

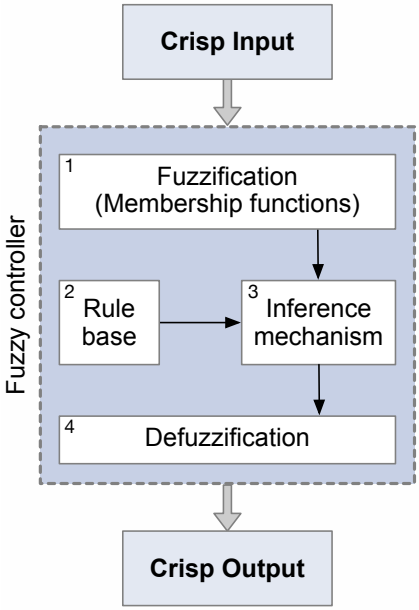

Figure 3.1: Schema of a Fuzzy Control System.

Fuzzy logic introduces the idea of partial membership. In classical or crisp sets, each individual in the universal set is assigned a value of either 1 or 0, where 1 signifies that the

individual is in the set and 0 means that it is not. This divides the individuals into members and nonmembers of the crisp set. A fuzzy set however, contains elements that have varying degrees of membership. It allows a member to belong to a set to some partial degree, the boundaries between subsets become vague or smooth. The partial degree membership of a fuzzy set can be mapped into a function, the so-called Membership Function (MF). [75]

MFs are defined of an interval of 0 (not a member) to 1 (full member) and convert crisp input values into fuzzy sets (Figure 3.1, Step 1). The MFs are the central feature of a FCS as they need to be representative of the input and output space of the system. Determining the shape of the MFs of a FCS is an important task that directly affects the modeling accuracy and system performance of the FCS. Usually designers choose MFs that are convenient to be described mathematically and adopt regular shapes of known parameterized MFs. Piecewise linear MFs are the simplest and most widely used MFs. They include triangular (Figure 3.2, a) and trapezoidal (Figure 3.2, b) MFs and can be either symmetric or asymmetric. Their popularity stems from their simple formulae and computational efficiency that renders them valuable especially for real-time applications. When piecewise linear MFs are not suitable for an application, nonlinear smooth MFs are often used. They include for example Gaussian (Figure 3.2, c), bell-shaped (Figure 3.2, d), and sigmoidal functions (Figure 3.2, e). [75]

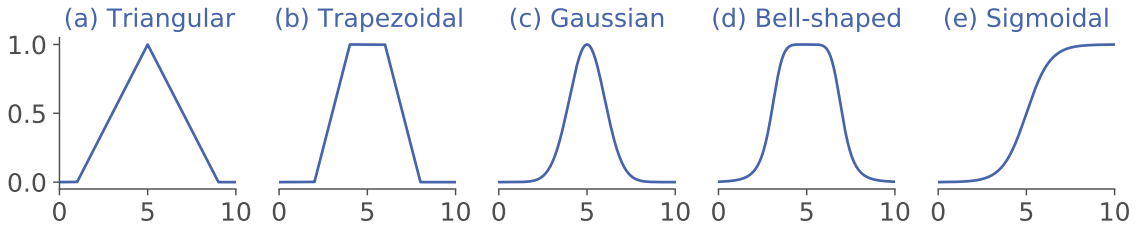

Figure 3.2: Exemplary fuzzy membership functions defined on an interval of 0 to 10.

The fuzzification includes two processes; the design of the MFs for input and output variables and their representation with linguistic variables [75]. Each MF is assigned linguistic terms that represent ranges of values. As an example the room temperature can be considered: Temperatures between 10 °C to 16 °C can be considered low, temperatures between 16 °C to 23 °C are described as medium and temperatures between 23 °C to 30 °C are felt as high. The temperature value 20 °C, depending on the exact definition of the MF, belongs to both low and medium to certain degrees.

After the MFs are defined, the rule base of the FCS has to be formed. The rules are derived by human experts who apply rules of physical laws and experience [75]. A Mamdani fuzzy inference system [74], which is commonly applied, features a rule base where every rule has an antecedent (IF) part and a consequent (THEN) part (Figure 3.1, Step 2). Both antecedents and consequents can be aggregated using an AND-operator. As an example, a heating system can be considered with the input parameters room temperature and heater

temperature (both low, medium or high) and the output parameter aperture of the valve for hot water (small, medium, wide). Two exemplary rules for this FCS could be formulated as:

- IF room temperature is low AND heater temperature is low THEN aperture is wide.
- IF room temperature is high AND heater temperature is high THEN aperture is small.

The last step of a FCS is the defuzzification (Figure 3.1, Step 4) which converts the fuzzy output generated by the Inference mechanism to crisp output. Different defuzzification methods exist. The Mean of Maximum method, the Center of Gravity method and the Height method are the most commonly used. The Mean of Maximum method takes the average of all values where the fuzzy sets are maximal. A shortcoming of this method is that it does not take into account the entire shape of the output function but only its maximum values. The Center of Gravity method, which is the most popular method, calculates the centroid of the fuzzy set to obtain a crisp output value. Finally, the Height method's advantage is its simplicity: it takes the maximum value of the height of the output function. [75]

Since the development of Fuzzy Control, it has been applied successfully in various research areas: in the environmental research e.g. for flood simulation [76], in remote sensing e.g. for classification of multispectral data [77], in GIS applications [78] or in analytic chemistry [79]. Das and Winter [80] employ fuzzy logic to detect the transport mode in an urban environment.

Fuzzy Control allows for many input and many output parameters. Such parameters can be combined in an if-then rule [81]. The two greatest strengths of fuzzy control are the ability to reason with uncertainty and its utilization in complex ill-defined processes without much knowledge of their underlying dynamics [75].

3.4 Datasets

The two datasets OSM and SRTM serve as input for the **Fuzzy-FSE**. The OSM dataset provides the parameters road class, road surface, link length and support points per kilometer. The road slope is calculated from SRTM data. Data from the GD-API is applied as reference data and is used as input for the speed profile. In this section, the different datasets and parameters are described.

3.4.1 OSM Data

OpenStreetMap road data includes a hierarchic classification of the road network that is described in Table 2.1. These road classes and their respective link roads (`motorway_link`,

trunk_link, primary_link, secondary_link, tertiary_link) form the road network. For the Fuzzy-FSE, only road classes with a hierarchy level lower or equal to five are used.

An analysis of the available attributes of roads in OSM is performed in Section 2.2. As stated in Section 2.2, the road surface is the most prominent of all parameters, globally. The distribution of the key surface per country is shown in Figure 2.4.

We include only the most frequent tag surface=* as an input parameter in our Fuzzy-FSE. It contains different values: general information such as paved or unpaved, and detailed description of the surface (e.g. asphalt, concrete, gravel). Most roads only feature general information, few have exact surface descriptions. For this study the surface values are classified according to the two main groups: paved and unpaved [39].

The link length serves as an additional input parameter for the Fuzzy-FSE. The road network is represented as a graph with nodes and links. All links have a start node and an end node, but no nodes in between. In this graph, every intersection and every change of parameter in the road network represents a node. Thus, links in a sparse network are longer than in a dense network with many intersections. If there are many intersections on a road and therefore shorter links in the graph, average speed decreases.

The number of support points per kilometer is used as an approximation for slope as it can be calculated from the shape of the road in OSM. The curvier a road is, the more support points are needed to form the road and the more the average speed decreases. In OSM, the distribution of support points per road segment is not uniform. Some mappers create curves with more support points and other mappers model similar curves with much less support points. In our study, to obtain a uniform number of support points, the vector data of the road is simplified using the Douglas-Peucker algorithm [82] with a tolerance of one meter. This algorithm is applied to simplify the number of support points of the road network without an effect on the accuracy of the network in this study. Note that the overall accuracy of the OSM road network is worse than one meter. Finally, the number of support points per kilometer is calculated.

3.4.2 SRTM Data

The Shuttle Radar Topography Mission was a joint mission by National Imagery and Mapping Agency and the National Aeronautics and Space Administration (NASA) to collect an open source global elevation dataset. We use the SRTM void-filled, 1 arc-second global data [83] with a resolution of approximately 30 m.

Due to this resolution, it has to be taken into account that one pixel of the SRTM raster may be the average of the road itself as well as possible hills beside that road. Therefore, we

consider the slope of the surrounding terrain, which is, in most cases, higher than the actual road slope. With this in mind we refer to the results as road slope in the following.

To calculate road slope, a slope percentage raster is created from the original Digital Elevation Model (DEM) by applying the Horn algorithm [84]. Then, the OSM road network is overlaid with the slope raster. Every road segment intersects multiple pixels of the slope raster. The average of all intersecting pixels is assigned as road slope value to the road segment. In [61] we introduced a second approach to calculate road slope. However, the results in [61] show that the method described above better fits the problem which is why we dismiss the other approach in this study.

3.4.3 Google Directions API Data

Google Directions API (GD-API) is a service that calculates routing directions and travel times between locations. The GD-API data includes the distance in meter, the travel time in seconds at a given time and the coordinates of the points on a road closest to the input point coordinates. The speed values are calculated using the travel time and distance output.

The GD-API relies on Google Maps and its underlying road and traffic data. The quality of Google Maps data is difficult to assess, especially in developing countries. During our studies, both roads that exist in OSM and are non-existent in Google Maps and vice versa have been detected. In [8] the accuracy of Bing Maps, OSM data and Google Maps data in Ireland is compared and the results support our observations. The authors find that although some areas are better served by one data source than by the others, no single data source proves to have better overall coverage. As for the speed and traffic data, there is no data available to evaluate the quality of Google Maps. We employ GD-API speed values as reference data while keeping in mind that this might, in some cases, be untrue.

Therefore, obstacles arise when comparing the output of the **Fuzzy-FSE** to the GD-API output. Both the Google data and the OSM data may contain errors. As the GD-API always takes the shortest path, it may take a different path between the two input coordinates than the road from which we want to compare the velocity. Also, the travel time output of the GD-API is whole seconds. Therefore, the calculated speed of short road segments with a travel time of only few seconds may be less accurate due to rounding. An exemplary output from the GD-API of 4 s for a 100 m road segment can signify a speed of 81 km/h (for 4.4 s) or 102 km/h (for 3.5 s).

For this study, four types of possible errors or large inaccuracies are captured automatically and are excluded of the comparison:

- the distance between either the start or the end points on the road in OSM and in Google is larger than 50 m;

- the lengths of the road in OSM and in Google differ in more than 20 %;
- the road is shorter than 200 m;
- the request to the GD-API returns an error or an empty result set.

To evaluate the performance of the **Fuzzy-FSE**, we compare it to a fixed speed profile. The speed profile assigns different speed values for each road class. Within a road class all roads obtain the same speed value. For this study, the speed profile is derived from the average speed of the GD-API for every road class.

3.5 Methods

This section presents the architecture of the **Fuzzy-FSE** (see Figure 3.3). It consists of two parts: The first part is the MF rule base with the knowledge base which form different MFs for speed. From this, multiple FCSs are built which calculate speed from the input parameters road slope and link length. One FCS is built for every MF speed, depending on the road class and surface.

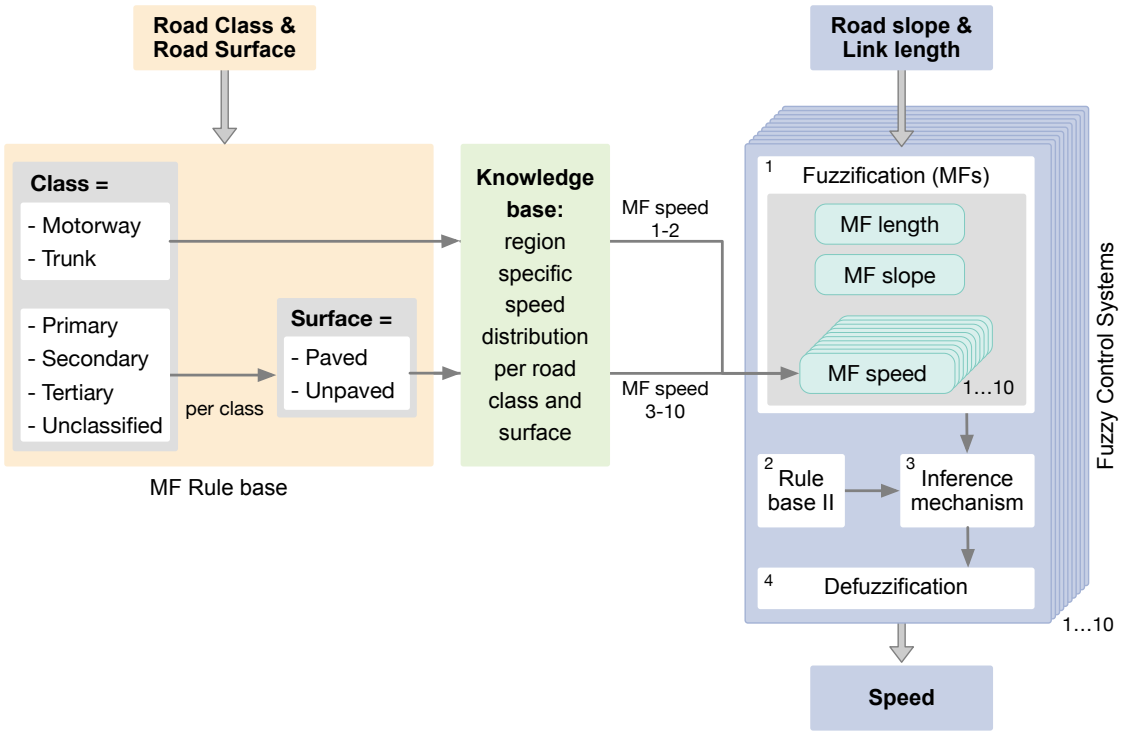

Figure 3.3: Schema of the **Fuzzy-FSE** with four input parameters: road class, road surface, road slope and link length. Combined with the knowledge base, the MF rule base forms ten different MFs for the output parameter speed. Adapted from [42].

Road slope and link length serve as input parameters for the FCSs to calculate the average speed. As mentioned in Section 3.4.1, the parameter road slope can either be calculated from the SRTM data or can be approximated by using the number of support points per kilometer of the road. In this study, both are implemented.

For our **Fuzzy-FSE**, we define triangular and trapezoidal MFs for slope and for link length which are illustrated in Figure 3.4. The MFs are represented with linguistic variables. Linguistic terms for slope include level, rolling, mountainous and steep. The linguistic terms for link length range from very short to very long. The output parameter speed varies between slow, medium and fast. In pre-studies, we have analyzed the impact of different shapes of MFs on the results. Then, we combine that with expert knowledge from literature [72, 85] to obtain the presented MFs. Each FCS uses the same MF for link length and slope but different MFs for speed.

According to the MF rule base, different MFs speed are defined. Depending on the input parameters road class and road surface, 10 different MF speed are designed:

- MF speed 1: Class = `motorway`
- MF speed 2: Class = `trunk`
- MF speed 3: Class = `primary` & Surface = `paved`
- MF speed 4: Class = `primary` & Surface = `unpaved`
- MF speed 5: Class = `secondary` & Surface = `paved`

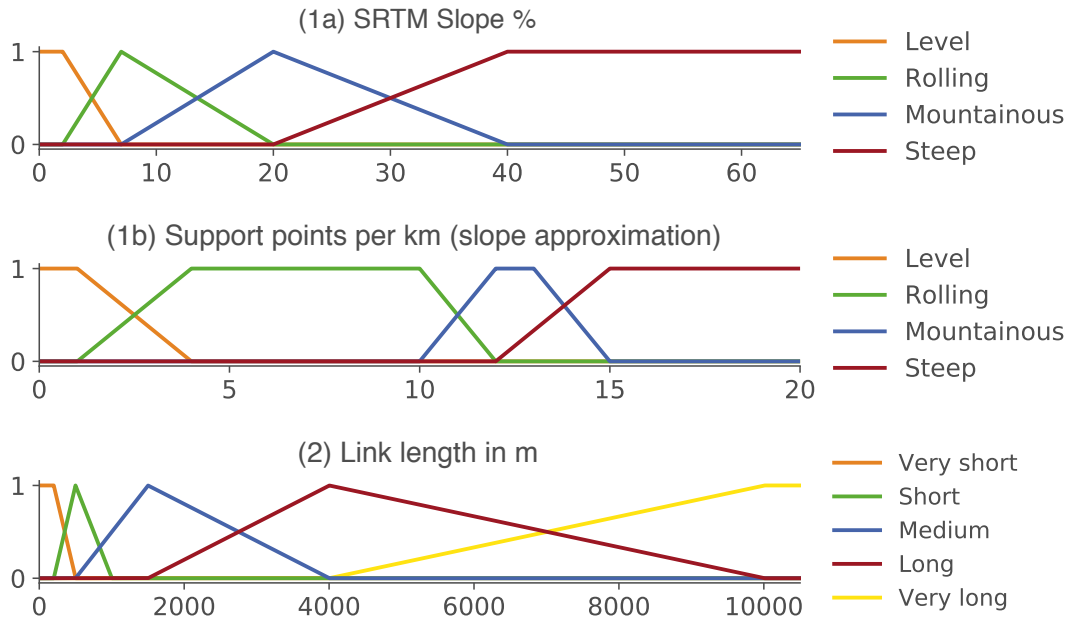

Figure 3.4: MFs of the parameters (1a) SRTM slope %, (1b) support points per kilometer, and (2) link length. Adapted from [42].

- MF speed 6: Class = `secondary` & Surface = `unpaved`
- MF speed 7: Class = `tertiary` & Surface = `paved`
- MF speed 8: Class = `tertiary` & Surface = `unpaved`
- MF speed 9: Class = `unclassified` & Surface = `paved`
- MF speed 10: Class = `unclassified` & Surface = `unpaved`

For the classes `motorway` and `trunk` a paved surface is assumed. In other regions even less MF speed might be necessary as less unpaved roads exist. The ten MFs speed are designed using region specific expert knowledge about the speed distribution per road class and surface. For roads without surface information, the surface is assumed `paved` for the road classes `primary` and `secondary`, and `unpaved` for the road classes `tertiary` and `unclassified`. Specific MFs speed depending on the case study region are generated (see Section 5).

20 rules have been developed with two antecedents (slope and link length) and one consequent (speed) each. Two exemplary rules are:

- IF slope is level AND link length is very long THEN speed is fast.
- IF slope is rolling AND link length is very short THEN velocity is medium AND slow.

We provide all applied rules in the form of a Python notebook via GitHub [67].

The last step of every FCS is the defuzzification (Figure 3.3, Step 4) which converts fuzzy output to crisp output. In our study, we tested different defuzzification methods like centroid, bisector and mean-, minimum- and maximum- of maximum. A centroid-based defuzzification fits our estimation best, as it results in a continuous distribution.

Note, the MFs for length and slope as well as the MF rule base and the rule base of the FCSs remain the same for every study region. Only the ten different MF speed per road class and road surface have to be adapted with expert knowledge for different regions.

3.6 Case Study Regions

The **Fuzzy-FSE** is applied exemplary for the BM regions in central Chile and for a part of northern NSW in Australia. In New South Wales, the study region consists of the statistical divisions Mid-North Coast, Richmond-Tweed and Northern. The study regions in Chile and in Australia are comparable in size but are at different stages of development.

In Chile, the road infrastructure is typical of a developing country. Even in populated regions, many unpaved roads exist and paved roads are often not maintained so the average speed is low compared to the same road classes in more developed countries. Australia is a developed country with a well maintained road infrastructure. There are more high level roads in the

more densely populated parts in NNSW than in comparable parts of the BM regions. This also leads to higher average speeds in all road classes which can be seen in Figure 3.5. Also, the OSM dataset for NNSW is more complete and contains more additional information than the OSM dataset for the BM regions. The tag `maxspeed` is filled out for 22.5 % of all road kilometers in NNSW but only for 7.2 % of all road kilometers in the BM regions.

The BM regions have a characteristic topography with the coastal mountain range in the west and the Andes in the east. That leads to a wide range of road slopes in the Chile dataset. Australia is less mountainous and has fewer roads with a high road slope. Both study regions feature large rural areas which are not densely populated. Both study regions feature more unpaved than paved roads (see Table 3.1) and many more low level roads than high level roads. The combination of all mentioned characteristics makes both regions ideal candidates to apply the developed **Fuzzy-FSE**. The transferability of the method to different rural regions is demonstrated by applying the **Fuzzy-FSE** to these two regions which differ in many aspects mentioned above.

Table 3.1 gives an overview of the OSM data for both study regions. The largest road class in Chile is `tertiary` which makes up more than 50 % of the road network. In Australia, most roads are in the class `unclassified`. Another notable difference is the road class `trunk` which is almost nonexistent in Chile but is used a lot in Australia. In both countries most roads have surface information. The surface information is classified into two main categories `paved` and `unpaved` as more detailed surface information is rare. The tags `paved`, `unpaved`

Table 3.1: Overview of the OSM data in the BM regions in Chile and NNSW in Australia. Reprinted from [42].

	BM (Chile)		NNSW (Australia)	
	km	**% km**	**km**	**% km**
All roads	30 349.84	100	38 956.41	100
`motorway`	1 624.79	5.56	882.21	2.27
`trunk`	142.47	0.47	901.06	2.32
`primary`	4 246.53	13.99	1 998.80	5.13
`secondary`	3 281.87	10.82	4 372.52	11.23
`tertiary`	15 643.31	51.55	8 821.94	22.65
`unclassified`	5 410.94	17.83	21 979.86	56.42
Surface information	25 211.83	83.07	30 606.80	78.57
`paved`	7 945.20	26.18	12 406.64	31.84
`unpaved`	17 266.63	56.89	18 200.16	46.72
`maxspeed`	2 176.42	7.17	8 756.55	22.48

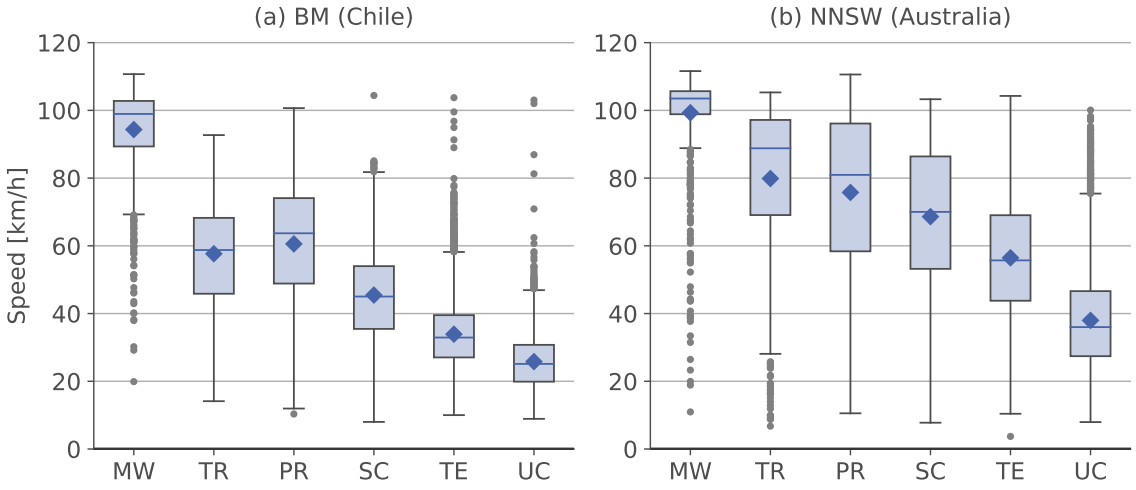

Figure 3.5: Boxplots of the speed distribution per road class of the reference data (GD-API) for the BM (Chile) and NNSW regions (Australia). Road classes: MW - `motorway`, TR - `trunk`, PR - `primary`, SC - `secondary`, TE - `tertiary`, UC - `unclassified`. The blue diamonds in the boxes symbolize the respective median, the blue lines the respective mean value. The lower limit of each box is the 25th percentile (Q1), the upper limit the 75th percentile (Q3) so that the difference builds the Interquartile Range (IQR). Whiskers extend to Q1 – 1.5 ∗ IQR and Q3 + 1.5 ∗ IQR. Any points beyond the whiskers are outliers and are plotted as circles. Adapted from [42].

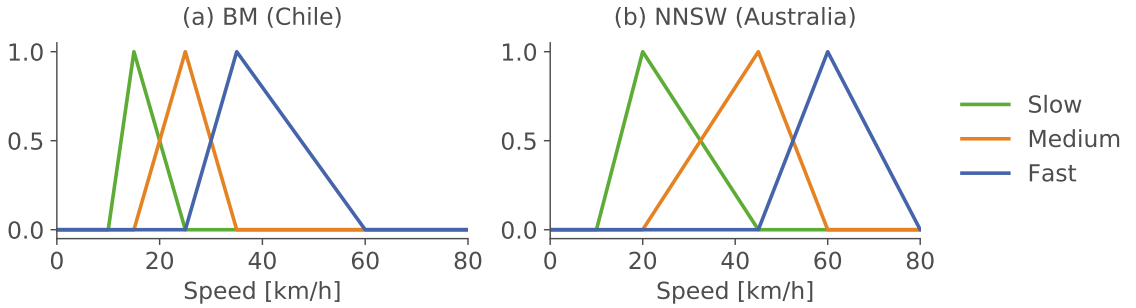

Figure 3.6: Exemplary MFs speed for (a) the BM (Chile) regions and (b) NNSW (Australia) for class = `tertiary` and surface = `unpaved`. Adapted from [42]. See all MFs speed in [67].

and `asphalt` make up 97.6 % (BM) and 82.1 % (NNSW) of the surface information. However few roads in Australia and very few roads in Chile feature speed information which underlines the need for a speed calculation. A spatial analysis shows that many roads that feature speed information are either `motorway` or are located in urban regions in both study regions. In [61] we demonstrate that it is valid to exclude roads shorter than 200 m from the validation.

Figure 3.5 shows the distribution of the GD-API speed data of both study regions and for the different road classes. Average speeds per class are calculated from the GD-API to compare against the estimations of the **Fuzzy-FSE**. In the GD-API dataset for the BM regions the average speeds are: 94 km/h (`motorway`), 58 km/h (`trunk`), 61 km/h (`primary`), 45 km/h (`secondary`), 34 km/h (`tertiary`) and 26 km/h (`unclassified`). In the NNSW dataset

average speeds are: 99 km/h (motorway), 80 km/h (trunk), 76 km/h (primary), 68 km/h (secondary), 56 km/h (tertiary) and 38 km/h (unclassified).

As described in Section 3.5, ten MFs for speed are defined for every study region. The MFs speed are defined manually using expert knowledge about the regions road conditions and speed distribution. In this case, the expert knowledge is taken from the distribution of the GD-API speed data. Two exemplary MFs speed, one for the BM region and one for NNSW, for the class tertiary and for an unpaved surface are shown in Figure 3.6. The definition of all MFs speed for both study regions is provided via GitHub [67].

Of the 17809 (BM)/ 21977 (NNSW) roads considered for the evaluation, approximately 12 % (BM) / 4 % (NNSW) are excluded due to the errors described in Section 3.4.3. The errors occur when the road distance between the OSM and the GD-API data differ in more than 20 % (50 % (BM) / 28 % (NNSW) of the errors) and when the start or endpoints differ in more than 50 m (46 % (BM) / 69 % (NNSW) of the errors). In 60 (BM) / 20 (NNSW) cases the GD-API respond with an error.

3.7 Results

We apply the Fuzzy-FSE on both study regions in two modes: Once with only OSM data, using the support points per kilometer as an approximation for road slope. The other mode calculates road slope percentages with SRTM data and uses OSM for the rest of the input parameters. Both applications are tested once with all roads included and once with only the roads having a surface information. As described in Section 3.5, when all roads are

Table 3.2: Comparison of the Coefficient of Determination (R^2) and Root Mean Squared Error (RMSE) of the BM regions (Chile) for all links over 200 m, 400 m and 600 m, respectively. Reprinted from [42].

		Google	**OSM**		**OSM + SRTM**	
		Baseline	All roads	Roads with surface	All roads	Roads with surface
> 200 m	R^2 [%]	66.66	**67.90**	61.31	**67.73**	61.00
	RMSE [km/h]	12.74	**13.29**	13.60	**12.92**	13.12
> 400 m	R^2 [%]	72.09	**73.00**	67.16	**73.48**	67.55
	RMSE [km/h]	11.79	**12.49**	12.83	**11.69**	11.95
> 600 m	R^2 [%]	73.64	**75.12**	70.04	**75.66**	70.53
	RMSE [km/h]	11.48	**12.00**	12.13	**11.08**	11.28

Table 3.3: Comparison of the R^2 and RMSE of NNSW (Australia) for all links over 200 m, 400 m and 600 m, respectively. Reprinted from [42].

	Google	OSM		OSM + SRTM	
	Baseline	All roads	Roads with surface	All roads	Roads with surface
> 200 m R^2 [%]	51.10	57.67	**61.73**	57.56	**61.56**
RMSE [km/h]	16.83	16.81	**15.92**	16.45	**15.77**
> 400 m R^2 [%]	57.68	64.90	**69.04**	65.12	**69.28**
RMSE [km/h]	16.00	15.62	**14.51**	14.92	**13.99**
> 600 m R^2 [%]	58.35	66.22	**70.29**	66.50	**70.57**
RMSE [km/h]	16.02	15.35	**14.21**	14.58	**13.61**

included the ones without surface information are assigned a default surface depending on the road class. Additionally, the influence of link length on the results is analyzed by testing the effect of including first all roads longer than 200 m, then all roads longer than 400 m and finally all roads longer than 600 m. A fixed speed profile that consists of the average speed for each class of the GD-API speed data is calculated as a baseline.

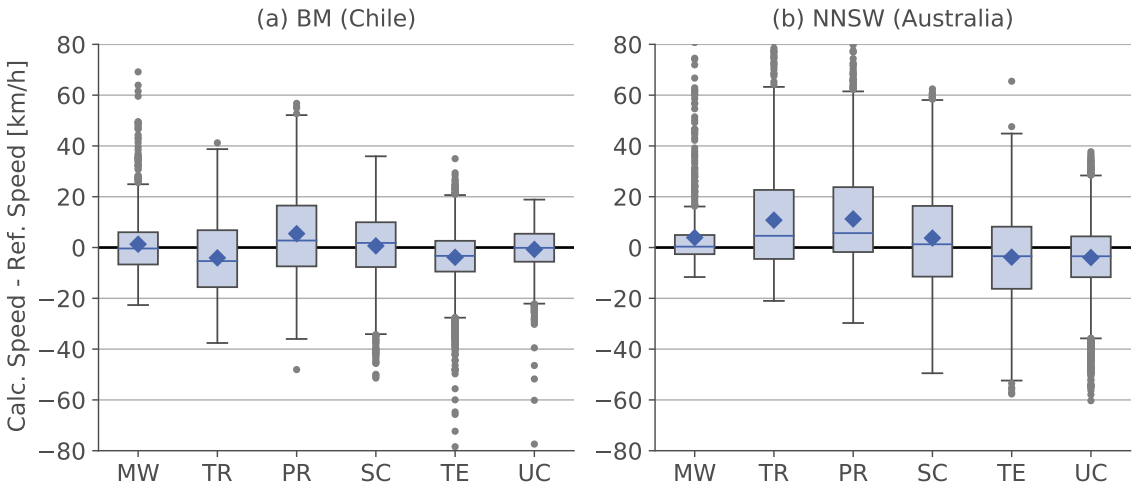

Figure 3.7: Boxplots of the distribution of the difference between estimated speeds and the GD-API reference speed data per road class. Both OSM and SRTM are used as input data. Negative values signify lower estimated speed values than reference speed values. Road classes: MW - `motorway`, TR - `trunk`, PR - `primary`, SC - `secondary`, TE - `tertiary`, UC - `unclassified`. The blue diamonds in the boxes symbolize the respective median, the blue lines the respective mean value. The lower limit of each box is the 25^{th} percentile (Q1), the upper limit the 75^{th} percentile (Q3) so that the difference builds the Interquartile Range (IQR). Whiskers extend to Q1 – 1.5 ∗ IQR and Q3 + 1.5 ∗ IQR. Any points beyond the whiskers are outliers and are plotted as circles. Adapted from [42].

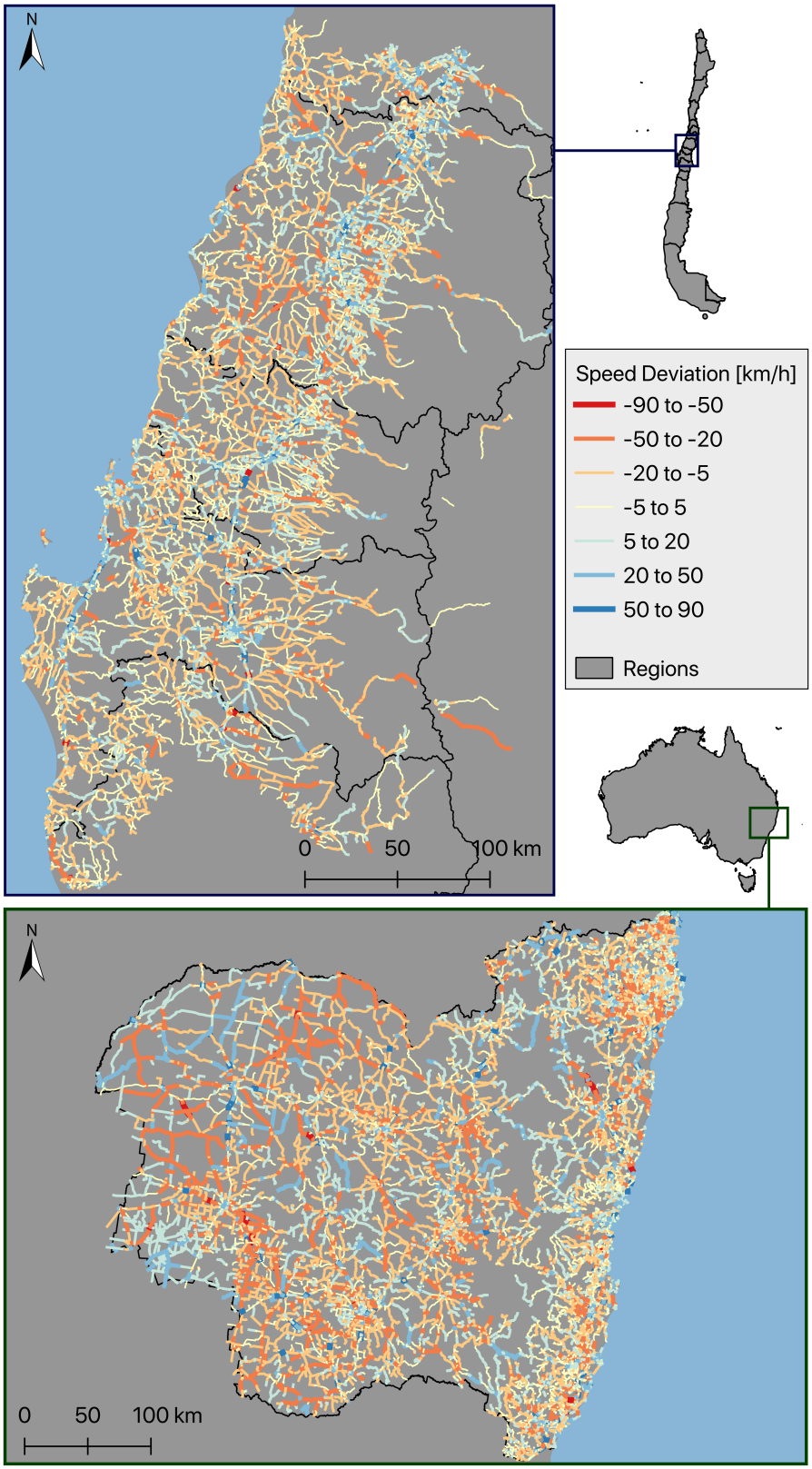

Figure 3.8: Map of the difference between calculated speeds and the GD-API reference speed in the BM regions in Chile (above) and in NNSW in Australia (below). Negative values (red and orange) signify lower estimated speed values than reference speed values. Reprinted from [42].

Table 3.2 shows the results for the BM regions for all tested modes. Both applications of the Fuzzy-FSE perform better than the baseline. The performance increases with the length of the links. The results of the Fuzzy-FSE for the BM regions are much better when all roads are included, instead of only the roads with surface information. The performance of the Fuzzy-FSE with the input from both OSM and SRTM data is approximately equal to the Fuzzy-FSE using only OSM data. The best result for the BM regions (R^2: 75.66 %, RMSE: 11.08 km/h) is achieved by taking both OSM and SRTM data as input and only considering all roads longer than 600 m.

The results for NNSW in Australia are presented in Table 3.3. The Fuzzy-FSE performs significantly better than the baseline with an R^2 which is between 6 % to 12 % higher than the one of the baseline. Similar to the results of the BM regions, the performance of both Fuzzy-FSE modes is approximately the same. Contrary to the BM regions, the results are better if only the roads with surface information are considered. Using both OSM and SRTM data as input and only evaluating the links with surface information and over 600 m length leads to the best result with an R^2 of 70.57 % and a RMSE of 13.61 km/h.

Figure 3.7 shows the distribution of the difference between the calculated speed and the reference speed per road class for both study regions. The speed values include all links longer than 200 m and are calculated with both OSM and SRTM as input data. In NNSW the differences between the calculated and the reference speed is generally higher than in the BM regions. In the BM regions the classes `motorway`, `tertiary` and `unclassified` perform best. The classes `motorway` and `unclassified` feature the best results in NNSW.

A map of the speed deviation with all roads over 200 m and both OSM and SRTM data as input is illustrated in Figure 3.8. Generally, the geographic distribution of the speed deviation is consistent in both study regions. However in the west of the study region in Australia, some roads exist, that are both significantly under- and overestimated. Within the urban centers, the Fuzzy-FSE mostly calculates higher speed values than the GD-API.

3.8 Discussion

Our developed Fuzzy-FSE is applied for both study regions in various modes. This allows for a detailed analysis of the different results. In this section we discuss and interpret the results shown in Section 3.7. We concentrate on the performance of the Fuzzy-FSE rather than detailed regional analyses. In the discussion we focus on the performance of: the Fuzzy-FSE versus the baseline, including only OSM data versus adding also SRTM data, analyzing all roads or only the ones with surface information and evaluating different link lengths.

The calculated baseline represents the current state of art. As explained in Section 3.2, most routing applications use fixed speed values per road class to calculate the cost factor travel

time. The baseline we calculate is most likely more adapted to the regions characteristics than other speed profiles as it uses the average speed of the GD-API, which is an information most routing engines lack. In comparison to the baseline, the developed **Fuzzy-FSE** performs better for both study regions. For NNSW, the improvement is much more significant than for the BM regions. This may be caused from the differences in the datasets. According to the range of the GD-API speed data (see Figure 3.5), the speed range in NNSW is considerably larger than in the BM regions. The smaller the range of the speed values, the better it can be approximated by an average speed value. In NNSW, the large speed range can be estimated significantly better with the **Fuzzy-FSE** than with the baseline as it is able to provide a continuous range of speed values. On the other hand, the overall performance of all estimations presented in this study is better in the BM regions. This is also caused by the large speed range in NNSW as even the **Fuzzy-FSE** cannot cover the entire speed range.

We analyze two modes to calculate speed which differ in the input data for road slope. The first mode uses only OSM data, while the second mode adds SRTM data. Although the R^2 are more or less equal for both modes, the RMSE is smaller when SRTM data are included. The road slope approximated by calculating support points per kilometer is less accurate as a curvier road does not always signify higher slopes. Also, the vector shapes in OSM may often be more straight than the actual road as contributors map imprecisely. Still, the results show that accurate speed estimations can be calculated by the **Fuzzy-FSE** using only OSM data with no additional data source.

The effect of road surface information in OSM is also analyzed. We compare the performance of the **Fuzzy-FSE** with all roads to the results which include only the roads which feature surface information in OSM. The results in both study regions are contrary. The initial expectation was that including only the roads with surface information should be better than considering all roads. This expectation is confirmed in NNSW. However in the BM regions, taking all roads and thus including the default surface values per road class (see Section 3.5), results in significantly better performance of the **Fuzzy-FSE**. We assume that this might stem from a possible bad quality of the road surface data in the BM regions. Considering the study region NNSW, the **Fuzzy-FSE** performs worse without surface information but still are at least 6 % better than the baseline.

Furthermore, we evaluate the effect of link length on the performance of the **Fuzzy-FSE**. The resulting speed values are less accurate for shorter links than for longer links. A large part of this is due to the insecurities of the GD-API speed data which are described in Section 3.4.3. Additionally, a false speed value has a smaller effect for a shorter road than for a longer one as it is later multiplied by the distance to obtain travel time. Therefor it is valid to only consider longer roads for an evaluation of the **Fuzzy-FSE**.

The **Fuzzy-FSE** estimates some road classes better than others. Comparing the ranges of the speed values per road class (Figure 3.5) with the difference between calculated speeds

and reference speeds (Figure 3.7), a correlation can be seen. The larger the range of speed values, the larger is the distribution of the speed difference. Considering the real world, a `motorway` features a mostly homogeneous speed, generally at least two lanes and little slope variation. `primary` roads however represent a very inhomogeneous class with some roads having two lanes and others that may not even be asphalted. The `unclassified` roads are again more homogeneous with mostly unpaved roads where faster speeds are not possible.

The presented **Fuzzy-FSE** is designed for rural application. In urban and suburban regions traffic, number of turns or local speed limits play a much bigger role for the speed estimation than surface, link length, slope and road class. Especially traffic is a very big factor in the urban environment that cannot be estimated from OSM data, only. Traffic estimations require data on road capacity and volume of vehicles per day or hour. Furthermore, traffic is a factor that is highly variable in time with peak hours in the morning and evening and almost no traffic at nighttime. Thus, the inclusion of traffic in the **Fuzzy-FSE** is not possible with the available data and therefore not the objective of this study. Also, speed limits in urban regions are not considered in the definition of the MFs speed. The **Fuzzy-FSE** is not able to differentiate between urban and rural regions, because the OSM dataset contains no information on population density. Therefore, estimated speed values in urban centers should be treated with caution. Furthermore, roads in urban regions often already feature speed information as in the OSM datasets the tag `maxspeed` is filled out more often in urban centers than in rural regions. This reduces the need to calculate average speeds for the urban road infrastructure.

In comparison to our previous study [61] we analyze the speed values instead of travel times. As it turns out, the evaluation of travel time provides little information about the quality of the estimation. There are very few high values which make up the upper three quarters of the range. This leads to misleading high R^2-values. The FCS developed in [61] performs worse or equal to the baseline, both analyzing speed values and travel times.

The GD-API data is applied as reference data for the **Fuzzy-FSE**. As mentioned in Section 3.4.3 some inconsistencies exist between the Google Maps data and the OSM data. The error statistics in Section 3.6 emphasize this issue. Some errors cannot be caught and are treated as reference data which falsifies the results. Thus, the GD-API data is only suitable to some extend as valid reference data. However, other reference datasets that are readily available and feature worldwide coverage do not exist.

Finally, if the developed **Fuzzy-FSE** is supposed to be applied to a different region, its limitations have to be considered. The **Fuzzy-FSE** does not consider traffic or other temporal factors like visibility or wildlife activity at certain times of the day. Therefore, the calculated speed values have to be considered as rough estimates rather than exact values. However, better estimates would need more input data than just OSM data. As discussed above it is also not applicable to urban regions as on the one hand the factors in urban environments are different and cannot be taken from OSM data. On the other hand, different MFs speed

would be needed for each road class inside the cities as speed limits are much lower than outside the cities. Thus, the **Fuzzy-FSE** is applicable to regions where the road network mainly consists of rural streets or as part of a tool that has a different calculation method for urban average speed values. One major limitation stems from the nature of fuzzy control and is the dependence of the **Fuzzy-FSE** on the expert knowledge. It is very sensitive towards false knowledge but that can be detected by comparing the results to adequate ground truth data. Generally, the **Fuzzy-FSE** is able to include more parameters but a FCS does not scale well as the number of required rules rises approximately as the product of number of categories of the input parameters.

In a later study we apply Machine Learning models to perform the same task as the **Fuzzy-FSE** with the same data in the same study regions [86]. The Machine Learning models train on the GD-API data to learn the estimation of average speed in rural road networks from the parameters road class, surface, support points per kilometer, start- and end coordinates, slope calculated from the SRTM in two different ways, sinuosity, road length, and region. All applied Machine Learning Models find that the road class is the most important feature, most use the surface and the support points per kilometer as second or third important feature. This is comparable to the **Fuzzy-FSE**, as it bases on the same input parameters. Almost all Machine Learning models outperform the **Fuzzy-FSE**, the best model (Extra Trees) reaches an R^2 of 80.43 % for all roads longer than 600 m with a combined dataset for both study regions. However, it has to be considered that Machine Learning Models require reference data to train, which in this case is from the GD-API. This reference data is often difficult and expensive to obtain. In contrast, the **Fuzzy-FSE** is based on expert knowledge and requires no other input data than OSM. If enough reference data is available, the machine learning approach should be used as it provides a more accurate estimation. But, if reference data is unavailable, the **Fuzzy-FSE** provides a valuable and data-sparse alternative with acceptable accuracy.

3.9 Conclusion and Outlook

We develop a **Fuzzy-FSE** that employs multiple FCSs to estimate average speed from the parameters road class, road slope, road surface and link length. These parameters can all be extracted or calculated from the open source and worldwide available dataset OSM. The inclusion of SRTM data to estimate road slope is tested but improves the results only slightly. The GD-API data serves as reference data and as foundation for the baseline calculation. Exemplary applications on case studies in the BioBío and Maule regions in Chile and north New South Wales in Australia demonstrate the applicability in two distinct regions which differ in their state of development and in their quality of OSM data. Average speed values are estimated better compared to existing methods and compared to our previous study in [61].

The developed Fuzzy-FSE offers the advantages of Fuzzy Control. It includes fuzzy input parameters and a reasoning process of a human operator. In contrast to machine learning approaches, training data is not needed as it is based on expert knowledge. However, it has to be considered that the ability of a FCS to perform well, highly depends on its design. Thus, the Fuzzy-FSE is much more susceptible to false assumptions than for example a machine learning model would be.

A major advantage of the developed Fuzzy-FSE is the worldwide transferability for the average speed estimation in rural regions. When applying the Fuzzy-FSE to a different region it has to be considered, that the Fuzzy-FSE is not designed to estimate average speed in urban regions. A region that contains both rural and urban regions would need a different methodology for the urban part of the region in addition to the Fuzzy-FSE. To estimate average speed values for a different region, only the MFs speed have to be adapted using expert knowledge about the new study region. Furthermore, the Fuzzy-FSE is able to estimate average speed only with OSM data itself. This enables a very quick application without much preprocessing. Both the fixed speed limit baseline and the Fuzzy-FSE perform best in regions where the speed distribution per road class is relatively uniform. However, another advantage of the Fuzzy-FSE is that it is still able to obtain good results even if the range of speed values per road class is large. This is where, in comparison, fixed speed limits fail.

The findings of this study can be used in many different applications. Most routing engines could include the Fuzzy-FSE rather than using fixed speed profiles for every road class. Many studies on critical road infrastructure rely on commercial travel time data as a cost factor in the road network. They could benefit very much from estimated average speed values in rural regions.

In future research we aim at combining the Fuzzy-FSE developed in this study with Machine Learning methods applied in Keller et al. [86]. Also, a least squares optimization could find the optimal membership functions as well as the rule set to best fit the FCS to the ground truth. The performance of these methods can then be compared to the results of the Fuzzy-FSE. The Fuzzy-FSE itself is extendable as data from additional data sources could introduce parameters with a temporal variability like visibility or traffic. Other methods to approximate road slope like using the relationship between the driving speed and the turning radius can also be implemented. Furthermore, it could be investigated if it is possible to adapt the Fuzzy-FSE to urban circumstances with different MFs speed and possibly different input parameters. The result would then consist of two different Fuzzy-FSE: one for urban and the other for rural environments. Also, more analyses could be performed including different study regions with different qualities of OSM data. Especially, including more densely populated countries like Germany could be interesting. The application in more and different study regions would enable a detailed sensitivity analysis towards the input parameters.

As a result of this chapter, the **Fuzzy-FSE** enhances the OSM road network data with average speed, and therefore also travel time, for each road segment. With this information, the routability of the OSM data is improved significantly, as routing applications are now able to calculate fastest paths. However the second challenge, identified in Section 2.5, of road classification errors in the OSM data, still prevails. The following chapter addresses this challenge.

4 Towards Detecting, Characterizing, and Rating of Road Class Errors in Crowd-sourced Road Network Databases

This chapter includes material from the journal article

Johanna Guth, Sina Keller, Stefan Hinz, and Stephan Winter. "Towards detecting, characterizing, and rating of road classification errors in crowd-sourced road network databases". In: *Journal of Spatial Information Science* 22 (2020), pp. 1–30. It is cited as [87] and marked with a green line.

4.1 Introduction

Road networks worldwide contain an inherent hierarchy of road classes that is linked to the movement needs of vehicles. High-capacity roads such as freeways and highways form the highest level in the road classification hierarchy and are designed to satisfy the highest traffic needs. They are followed by distributor or arterial roads with medium traffic, and then collectors and local access routes, which are lowest in the hierarchy and generally feature a low traffic volume [88].

Therefore, the class of a road is crucial in determining its purpose for the road network. Particularly routing applications often rely on the road class for information about the road network like maximum speed, capacity, or access limitations. Thus, errors in the road class can hinder routing applications and may lead to detours because of false assumptions about travel time or access limitations. These errors may also become obstructive for hierarchical route planning which uses the level of detail appropriate for the task to solve the task with the least amount of effort [89]. Finer levels of detail are not considered [89]. Hierarchical routing algorithms can result in large detours when there is a classification error in a high-level road. Furthermore, as high-level roads are generally more important

and sparser than lower-ranked roads, class allocation errors for high-level roads have a larger impact on route planning. The frequency of classification errors in a road network is dependent on the quality of the underlying road data.

As established in Section 2.4, the OSM road network is susceptible to road classification errors because of its crowd-sourced nature. These frequent road classification errors in OSM are identified as a major challenge for routing applications, especially if only a high-level road network is considered for routing (see Section 2.5).

This study aims at finding potential classification errors automatically. Human experts can then check if the detected potential error is an error and, if necessary, correct it. The presented methodology is based on an extension of the definition by Liu [90]. He states that in a hierarchical road network, one can observe that major roads form a network themselves. This subnetwork of major roads is more sparse than the complete network, and while it may not form a connected network in a city, it may form a connected major road network in a state or country [90]. We define a subnetwork as a union of all roads with a level equal or higher to the subnetwork's level. As a result, multiple subnetworks for one road network are obtained with increasing level of detail, the more levels are included. We expand the assumption of Liu [90] and suggest that each subnetwork should (a) be connected and (b) have no gap of the sort that for any pair of origin and destination (OD) in a subnetwork, the shortest route in the subnetwork is significantly longer than in the complete network.

Under these assumptions, we formulate our hypothesis: *Both disconnected parts and gaps of subnetworks in the OSM road network are indicators for road classification errors if the disconnection or the gap can be resolved in the complete network.* In order to test the hypothesis, we formulate two main research questions:

1. Is an approach by searching for disconnected parts or gaps in subnetworks able to find potential road classification errors? Is this approach able to provide information about the likelihood that the result is an error?

2. Which parameters (such as lengths of detours on a subnetwork compared to the complete network) or combination of parameters indicate gaps in road networks best?

To answer the first research questions, we develop a novel approach to detect road classification errors in OSM by searching independently for (a) disconnected parts and (b) gaps in subnetworks. It demonstrates – against expectations – that the **Error Search** at disconnected parts leads to fewer results than at gaps. The **Error Search** at gaps in subnetworks identifies different parameters that indicate gaps in road networks and combines them in a rating system to obtain an error probability. An efficient implementation of the **Error Search** is published on GitHub [91]. To answer the second research question, we provide a detailed analysis of parameters and combination of parameters that indicate gaps and their influence on the error probability. We test our **Error Search** with an exemplary case study on the

OSM dataset of NSW in Australia. A reference dataset of identified OSM classification errors compared to authoritative PSMA data is also published on GitHub [91].

We argue that, instead of finding all classification errors, the presented **Error Search** only finds the most important classification errors for routing applications and aims to improve the navigability. Identified errors have to be checked by a human expert because our assumption of connected subnetworks without gaps is an ideal that is not met in resource-strapped road infrastructures in all cases. Furthermore, this approach is not able to identify which errors cannot be detected by this method. The errors that can be found by the **Error Search** can cause routing applications to take large detours because they might imply that some road classes cannot be passed with all vehicles. Furthermore, classification errors at gaps and disconnected network components can lead to wrong travel time calculations because of the assumed low road class.

In this chapter, we first provide a short overview of the related work on error detection in OSM data in Section 4.2. In Section 4.3, we elaborate on the theoretical foundation of the presented methodology and identify parameters that we suspect to indicate gaps. The **Error Search** contains two main parts, which are described in Section 4.4. First, the search for disconnected network components (Section 4.4.1) is presented, and then the different steps of the implementation for the **Error Search** at gaps (Section 4.4.2) are described. The collection of the reference data set is described in Section 4.4.3. The results are presented in Section 4.5 and discussed in detail in Section 4.6. Finally, a conclusion and an outlook are given in Section 4.7.

4.2 Related Work

In Section 2.4 the related work on the quality of the OSM road network is analyzed in detail. As a result, the challenge of the often low attribute accuracy, especially regarding the road classification, is identified. In this section the related work regarding error detection in the OSM road network is presented (see Section 4.2.1). Then, the gaps of existing approaches are summarized, and the novelty of the approach presented in this study is highlighted (see Section 4.2.2).

4.2.1 Detection of Errors in the OSM Road Network

To reduce the number of errors in OSM, tools have been developed by the OSM community that help the user while mapping OSM data to find the right tags. OSMRec [92] is an application that recommends categories such as road or building for spatial entities in OSM based on a Support Vector Machine classification. OSMantic is a similar tag recommender system that

relies on relationships between tags based on semantic similarity [93]. Undocumented keys can be considered errors because they are missing a definition. To reduce the number of undocumented keys, Majic et al. [94] propose an unsupervised approach to identify equivalent documented keys to the used undocumented keys. They evaluate semantic similarity of keys based on the extensional definitions through their values, co-occurring keys, and geometries of the features they annotate. In a further study, they concentrate on the discovery of bridges by topological relations [95]. This approach enables detecting errors in the *bridge* tag, as a bridge in OSM must be defined with the tag *bridge=yes*. An algorithmic approach to error detection flags errors in names and speed limits is presented in [96] and bases on the comparison of two data sets. Londögård and Lindblad [97] employ deep learning to find spelling errors in tags and correct them. Sehra et al. [12] use a number of basic topological error detection methods available in the desktop GIS Openjump. They find many basic topological errors and conclude that the OSM data in the metropolitan area in Punjab (India) needs preprocessing before using it for navigation. These basic methods include checking minimum segment length, identifying duplicate lines, or finding nodes that almost touch a line. Keller [18] proposes the software ReMAPTCHA, a map-based anti-spam method that can correct *almost connections* in OSM. However, it is not able to detect these *almost connections*.

Few studies have addressed the issue of road classification errors in the OSM road network. Within this field, two general approaches can be distinguished: An approach by machine learning and a rule-based approach.

In their master thesis, Stypa and Sandberg [98] use machine learning techniques to classify roads in OSM with intrinsic methods. The authors identify major challenges due to the incompleteness of OSM. To address these challenges, they use rule-based data imputation, for example, for the tags *oneway*, *maxspeed*, and *lanes*. Furthermore, they employ feature engineering and create synthetic attributes like node count, element length, and mean density. They achieve an overall accuracy of around 40 % with the original dataset and around 79 % using their data imputation and feature engineering methods. However, they test their model on a small dataset in Sweden and do not validate their model against reference data. Similarly, machine learning has been used to learn the road class in OSM networks in a series of studies [99, 100, 101]. The authors first develop a representation of the street network, which combines primal and dual graphs, called multi-granular street network representation [99]. Then, they propose an intrinsic machine learning model that learns the geometrical and topological characteristics of different semantic classes of streets [100]. They test the data set with the London OSM street network and conclude that the model's accuracy varies with the road class because some road classes are geometrically and topologically similar. In a similar study, the model of [101] achieves precision and recall values of 68 % and 65 %, respectively.

Rule-based approaches to error detection have mostly been proposed by the OSM community. Several tools exist to find various types of errors, such as Keep Right, Osmose,

JOSM/Validator, OSM Inspector, Maproulette, and many others [39]. The error types they detect range from the validity of spatial objects like non-closed areas to topology related issues like dead-ended one-ways and attribute incompleteness like POIs without names. Osmose [102] includes two issue types for possible road classification errors: the issue *sudden highway type change* and *broken highway continuity*. The issue *sudden highway type change* is detected when a road connects directly to a road with a much lower level like a *primary* road connecting with a *residential* road. The issue *broken highway continuity* is raised when the classification of a highway is not consistent along a path, for example, if there is a *secondary* road that connects to a *residential* road and again to a *secondary* road. However, it is only detected if the misclassified part is shorter than 1000 m and if at least one end of the high-level road does not connect to another road besides the low-level road. These issues are presented together on a map and can be corrected by contributors.

4.2.2 Gaps in Existing Approaches

In summary, existing machine learning approaches such as [100, 101, 98] either need sufficient reference data or suffer from the incompleteness of OSM attributes. The presented studies classify roads with passable accuracy for many applications but create many false positives in the process. These false positives then have to be checked by humans manually, which is time-consuming. Furthermore, the presented machine learning approaches such as [100] are good for low-level road classes but worse for higher-level road classes, which are more important for routing. Rule-based approaches, like those in the Osmosis tool, can detect very specific classification issues. However, due to static rules, Osmosis detects only errors that are specifically described in the rule. Slight variations of the same type of error are not discovered. Also, it produces a large number of false positives. Additionally, the presented machine learning and rule-based methods cannot provide the error probability or select the most important errors for navigability.

Compared to existing approaches, the **Error Search** presented in this paper aims at finding only misclassifications that can cause large detours for routing algorithms. Using the detours, it can provide the user with an importance-based ranking of the errors. This reduces the number of false positives the user has to check to obtain a network with improved navigability. Furthermore, it can prioritize the search for classification errors in high-level road classes that are more important for routing. Because the presented approach does not rely on static rules but dynamic thresholds, it does not suffer from the limitations of a rule-based approach.

4.3 Theoretical Background of the Error Search

A road network can be formally represented as a graph. G is a non-empty set of n nodes N connected by a set of m links L. The elements of $N \equiv n_1, n_2, ..., n_n$ and the elements of $L \equiv l_1, l_2, ..., l_m$. In a graph, each link is defined by two nodes i and j and denoted as l_{ij}. An alternating progression of adjacent nodes with no node visited more than once is called a path [103]. For this study, the graph G is an undirected graph. We use an undirected graph to avoid issues with the *oneway* tag in OSM.

The OSM road network graph is a multi-class graph with each link l_{ij} belonging to one of the classes in Table 2.1. Values of the tag highway beside the road classes and their link roads in Table 2.1 are not included in this study. For this study, OSM road classes are also categorized into different hierarchy levels (Table 2.1, right column). The levels range from L1 (top-level) to L7 (bottom level). Link roads are categorized into the respective level (e.g., *motorway_link* in L1 and *primary_link* in L2). We combine the classes *motorway* and *trunk* in one hierarchy level because in our study region in NSW in Australia, few *motorways* exist. The classification might have to be adapted for different study regions with a more dense *motorway* network. A road network graph may contain a union of multiple levels: A graph that contains, for example, *motorways* (L1), *trunks* (L1), and *primary* roads (L2) contains the union of L1 and L2.

Accordingly, we will refer to seven networks in total: Six subnetworks and the complete road network. The most sparse subnetwork S1 consists only of L1 (*motorway*, *trunk*). The next subnetwork, S2, contains all L1 roads (*motorway*, *trunk*) and all L2 roads (*primary*). It is, therefore, less sparse than S1. The subnetworks S3 to S6 are formed correspondingly, as unions of all roads with a level smaller or equal to the subnetwork's level. The complete road network graph is formed as the union of all levels, $L1 \cup ... \cup L7$, equivalent to S7. These networks are illustrated in Figure 4.1 for a part of the study region in NSW. In each subnetwork (S1-S6) of the OSM road network, we search for (a) disconnected network components and (b) gaps to find potential road classification errors.

Focusing first on the disconnected components, we search for disconnected network components in all subnetworks, respectively. Disconnected components are individual graphs that are not connected by any link with each other. Examples of disconnected network components are visualized in Figure 4.2. Often, a road network graph of a subnetwork in OSM consists of one large connected graph with many vertices and links that can be considered the main road network. Additionally, it may contain disconnected components that are not connected by any link to the main road network.

With the assumption that subnetworks are typically connected, disconnected network components can indicate four types of errors: *Connection error*, *Self error*, *Disconnected*, and

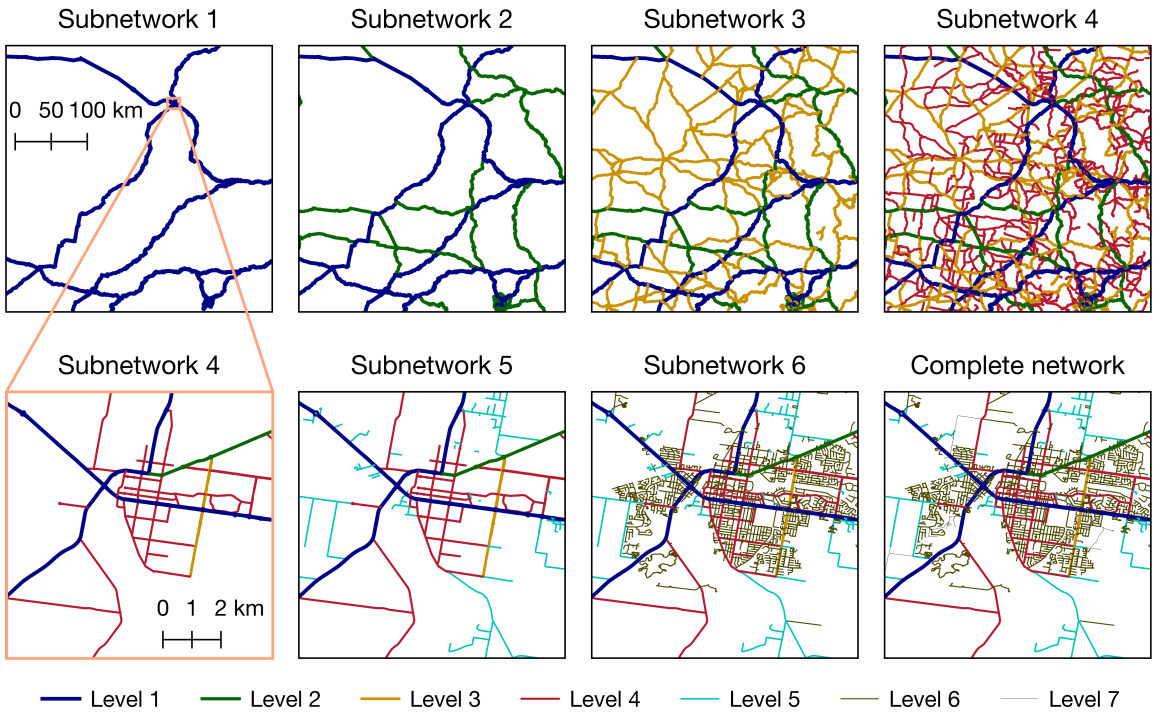

Figure 4.1: An example of subnetworks in the OSM road network in New South Wales (Australia). Reprinted from [87].

Border error. If a disconnected network component is a *Connection error*, the connection(s) to the disconnected network component is wrongly classified (see Figure 4.2 for an example). *Self error* is assigned if the roads of the disconnected network component itself are in the wrong class (see Figure 4.2 for an example). Network components that are disconnected both on the subnetwork and on the complete network are called *Disconnected*. These disconnections might happen because of missing roads in OSM but also

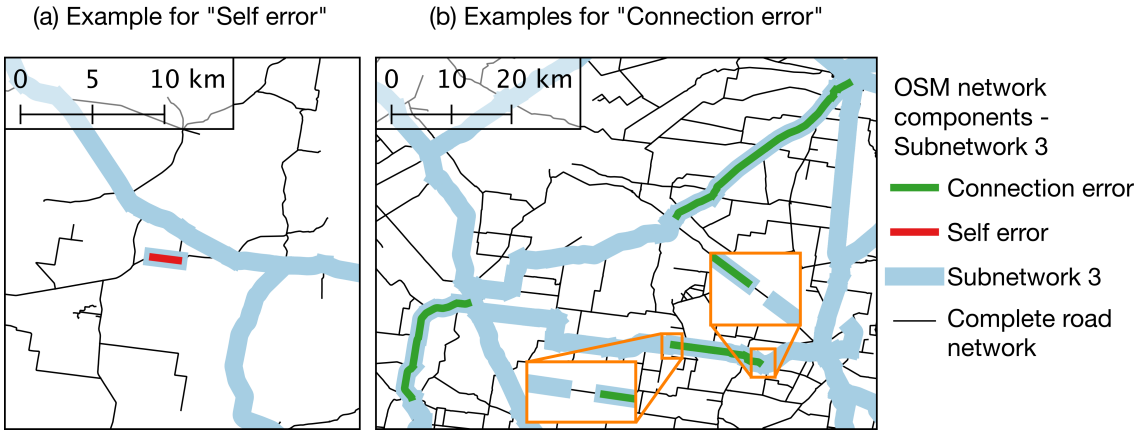

Figure 4.2: Examples of two types of errors in disconnected network components. In (a), the red network component itself is the wrong class. In (b), the green disconnected networks are not connected to subnetwork S3 because the connection is the wrong class. Reprinted from [87].

because of real-world disconnections like islands. Due to cuts at the region borders, disconnected network components can be generated, which are connected in the bordering region. These network components are called *Border error*.

Secondly, regarding the gaps, we search for gaps in the otherwise connected OSM road network graph. The gap search is the more challenging task because the identification of gaps is an unsolved problem. The challenge starts with a clear definition of a gap, which turns out to be context-dependent. We identify a gap between an origin O and a destination D in any connected subnetwork if the shortest path from O to D is substantially longer than on the complete network. The exact limit of how much longer it has to be cannot be determined universally because it varies by many factors such as the level of the subnetwork (S1-S6), the geography of the region, or the population density. Therefore, indicators have to be identified that point at possible gaps.

A combination of an origin O and a destination D suspected to be a gap is herein called a gap candidate. Three distance measures are identified to find gap candidates: the shortest path distance on the subnetwork from O to D (Pd), the Euclidean distance from O to D (Ed), and the shortest path distance on the complete network from O to D (cPd). We analyze five different parameters (G1-G5) which might indicate a gap:

- G1 = Pd/Ed.
- G2 = Pd – Ed.
- G3 = number of destinations on the same spot (only gap candidates where G1 is highest per origin).
- G4 = Pd/cPd.
- G5 = Pd – cPd.

We are aware that some correlations may exist between the parameters G1 and G2, as well as G4 and G5. Figure 4.3 is an exemplary road network that helps to visualize these parameters. Calculations of G1, G2, G4, and G5 in the exemplary road network in Figure 4.3 are given in Table 4.1.

The parameter G3 is calculated by first selecting only the gap candidates where G1 is highest per origin. As a result, we obtain only gap candidates with distinct origins, but the destinations can still intersect. G3 is calculated as the number of gap candidates that have the same destination. This calculation is based on the observation that the more gap candidates with a high G1 per origin map to the same destination, the more likely this destination is located at a gap.

We distinguish the errors at gap candidates between *No error*, *Near error*, and *Error*. *Near error* is assigned if either O or D is not the start or end of the road connection on the complete network. If both O or D are not the start or end of the road connection on the

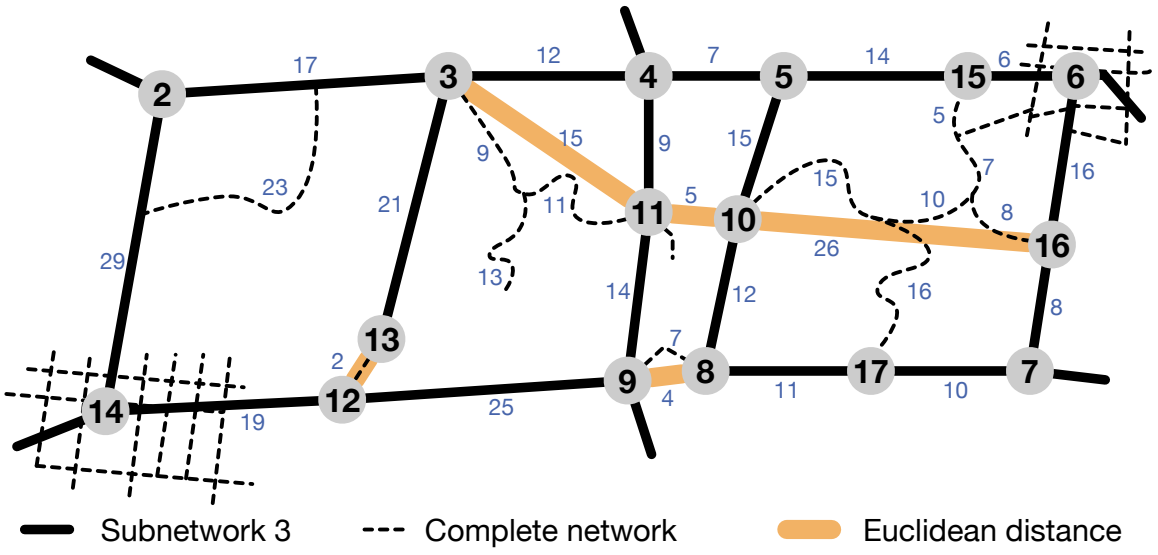

Figure 4.3: Exemplary road network with nodes 1-14 (gray) and links (thick black lines) of the subnetwork S3. The complete network is represented by dotted thin black lines. The Euclidean distance is shown exemplary for four gap candidates. The relevant links are labeled with their cost factor (blue). The figure is not drawn to scale. Reprinted from [87].

Table 4.1: Exemplary G1, G2, G4 and G5 calculations for gap candidates in Figure 4.3. Reprinted from [87].

Gap candidate	Ed	Pd	cPd	G1	G2	G4	G5	Is gap?
3-11	15	21	20	1.4	6	1.1	1	No
8-9	4	57	7	14.3	53	8.1	50	Yes
10-11	5	31	31	6.2	26	1	0	No
10-16	26	41	33	1.6	15	1.2	8	No
12-13	2	81	2	40.5	79	40.5	79	Yes

complete network, *No error* is assigned. *Errors* are detected if both O and D are the start or end of the road connection on the complete network.

Multiple gap candidates often indicate a single class error as multiple OD pairs near a gap feature high ratings. Also, multiple connection possibilities for a gap might exist leading to multiple gap candidates labeled *Error* or *Near error*. We assign the same error id for every gap candidate that indicates the same class error. As a result, we obtain a count of *Unique errors* where all unique error ids are counted.

4.4 Implementation of the Error Search

As described in Section 4.3, the developed **Error Search** consists of two independent parts: (a) the search for disconnected network components and (b) the gap search. The search for disconnected network components is presented in Section 4.4.1. Part (b) of the **Error Search** is the gap search presented in Section 4.4.2. The results of both parts are compared against reference data and are described in Section 4.4.3. The implementation is realized in a PostgreSQL (version 11.5) database with PostGIS (version 2.5) and pgRouting (version 2.6) extensions. We apply the command-line tool *osm2pgrouting* (version 2.3) [104] to import the OSM road network into a pgRouting graph in the PostGIS database.

4.4.1 Search for Disconnected Network Components

Disconnected network components are identified by using a depth-first search algorithm. This algorithm begins at a certain node and notes all connected vertices along each branch before backtracking such that each node in a connected network is visited. Then, it selects a node not yet visited and does the same with this network component until all nodes in the network have been visited. We run this algorithm on each subnetwork to identify disconnected network components for every subnetwork. As described in Section 4.3, these components likely indicate errors in the road classification. The identified disconnected network components can be checked and corrected by a human user if they indicate errors.

4.4.2 Gap Search

This section describes the different steps of implementing the gap search, also illustrated in Figure 4.4. To prepare the networks for the gap search, meshes in all subnetworks are identified in Section 4.4.2. In the core module, the gap search is performed for each identified mesh (Section 4.4.2), and finally, a rating system is employed that rates gap candidates according to their likelihood of being an error (Section 4.4.2).

Mesh Identification

In order to find gaps in the road network, the shortest paths have to be calculated between OD pairs. All pairs shortest paths are computationally expensive, especially in large networks such as the one for the state of NSW in Australia. However, to solve the problem of gap identification, only the shortest paths between specific OD pairs are required. To find these specific OD pairs, the theory of planar graphs has been considered.

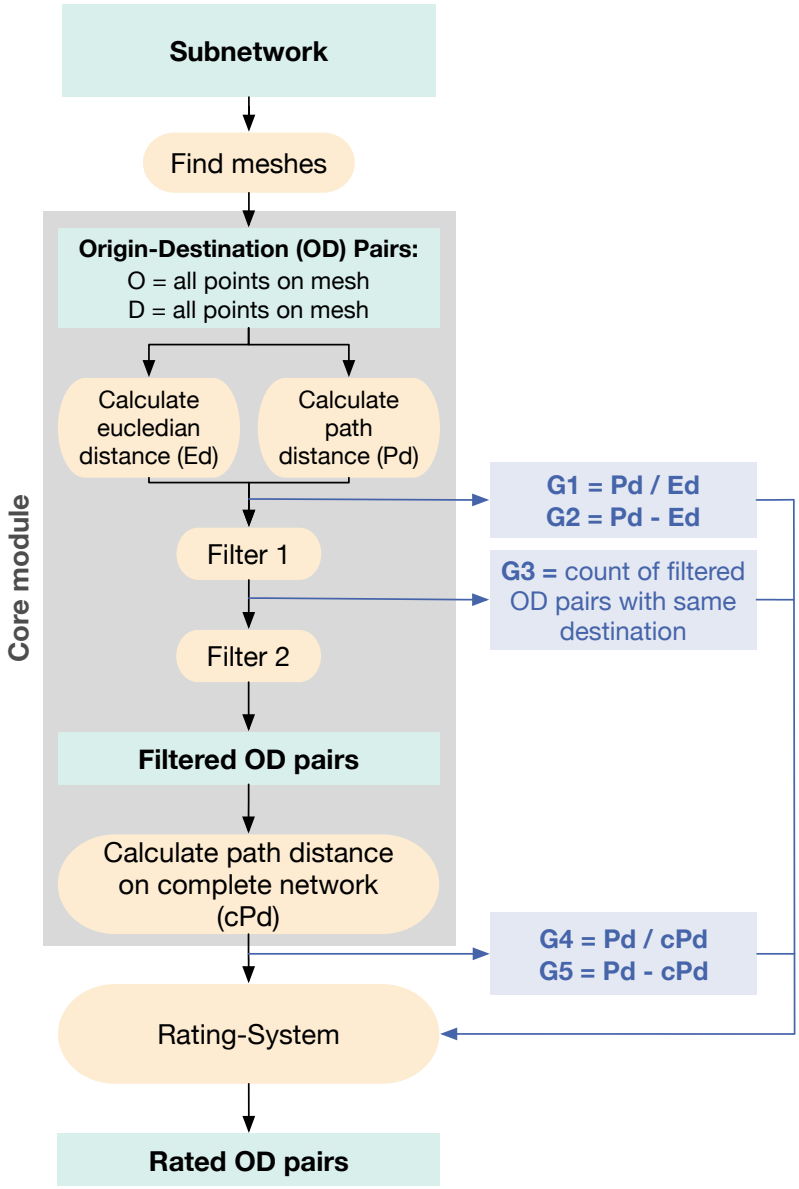

Figure 4.4: Overview of the implementation for the gap search. Reprinted from [87].

The planar representation of a graph divides the pane into regions, called faces. One of these faces – the exterior one – is unbound and is called the infinite face. Faces are the maximal open, two-dimensional regions that are not further divided into sub-areas. Each face is bounded by a closed walk we herein call a mesh. Every link of the network belongs to one or at most two meshes, one mesh in each direction. Figure 4.5 is an exemplary planar representation of a graph.

In this example, five faces exist: the inner faces f_1-f_4 and the infinite outer face f_5. The face f_1 with its corresponding mesh m_1 (highlighted in blue in Figure 4.5) and the face f_3 with its corresponding m_3 (highlighted in orange in Figure 4.5) are illustrated exemplarily. The link

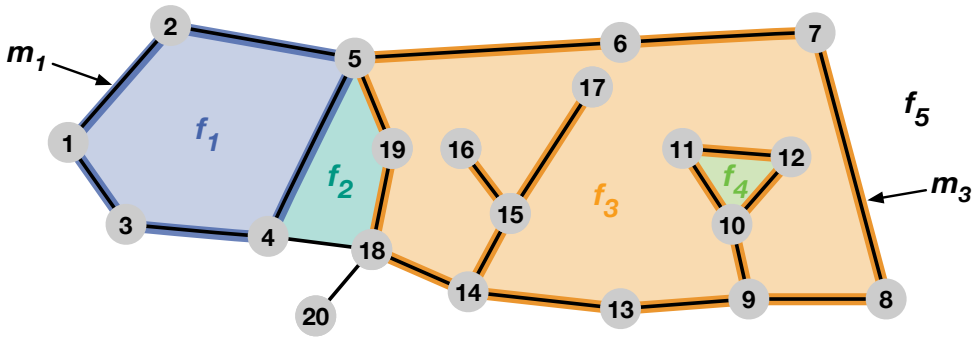

Mesh	Corresponding links
m_1	1-2, 2-5, 5-4, 4-3, 3-1
m_3	5-6, 6-7, 7-8, 8-9, 9-10, 10-12, 12-11, 11-10, 10-9, 9-13, 13-14, 14-15, 15-17, 17-15, 15-16, 16-15, 15-14, 14-18, 18-19, 19-5

Figure 4.5: Planar graph with nodes 1-20 (gray) and links between nodes (black). The graph has five faces, the inner faces f_1-f_4 and the infinite outer face f_5. The faces are bounded by meshes. Two meshes are illustrated exemplarily: the mesh m_1 is drawn with thick blue lines, the mesh m_3 is illustrated with thick orange lines. For illustration purposes, m_2, m_4 and m_5 are not colored. Reprinted from [87].

$l_{4,5}$ belongs to two meshes: In direction 5-4 it belongs to m_1, and in direction 4-5, it belongs to m_2. Similarly, the link $l_{9,10}$ belongs to m_3 in both the direction 9-10 and in direction 10-9.

As stated above, to solve the problem of gap identification, only the shortest path between specific OD pairs, namely between OD pairs, where O and D are located on the same mesh, are required. To illustrate this, Figure 4.5 can be considered. A gap might exist between nodes n_{16} and n_{19} or any other pair of points corresponding to the mesh m_3 because a connection is possible. However, gaps between nodes located on different meshes, for example, nodes n_{16} and n_4, are already covered by calculating the shortest path between nodes n_{16} and n_{18} or n_{19}, both located in the same mesh as node n_{16}. Thus, instead of calculating all pairs of shortest paths, we reduce computing time radically by only calculating the shortest paths between OD pairs located on the same mesh.

The road network itself is not a planar graph because links like bridges or tunnels exist which cross other links without a node at their intersection. Thus, to create a planar representation of the road network, we create artificial nodes where two links intersect. Then, meshes in the road network can be identified, reducing computing time for the gap search. We can now limit the search for gaps to all pairs of shortest paths within one mesh instead of all possible OD pairs in the entire graph. Scenarios exist where gaps occur across meshes, for example, if a bridge over a road is missing. This special case can not be detected by this methodology. However, the radical reduction of computation time justifies the discharge of these rare scenarios.

With the planar representation of the road network graph, an algorithm to find meshes is then implemented based on maze solving algorithms. Algorithm 1 finds meshes by following a link from a starting node to the counterclockwise next link and continues to do so until the start node is reached again. For illustration we show our implementation of Algorithm 1 in PL/Python procedural language in a PostGIS database with a road network graph created by the pgRouting extension (see [91]).

Algorithm 1 Finds all meshes in a planar road network graph. Reprinted from [87].

```
node_id list = all node ids in road network graph
mesh id = 0
for each node id in node id list do
    link id list = all links with start = node id or end = node id
    for each link id in link id list that has mesh id = NaN in this direction do
        set mesh id of link with link id = mesh id
        next node = id of the node at the other end of the link link id
        link = link id
        while next node ≠ node id do
            next link = the id of the counterclockwise from link next link where the source
            or the target is next node
            link = next link
            set mesh id of link = mesh id
            next node = node id of the next node following the trail of link
        end while
        mesh id = mesh id + 1
    end for
end for
```

Core Module of the Gap Search

After the identification of meshes, the gap search begins in the core module for each subnetwork individually. Although the meshes are identified for the network with artificial nodes, the gap search uses the original road network but calculates the shortest paths only for OD pairs located on the same mesh (see Section 4.4.2). First, the shortest paths on the respective subnetwork from all nodes of a mesh to all nodes of a mesh are calculated. Then, the Euclidean distance is calculated for these OD pairs. This is done for all meshes in a subnetwork. The parameters G1 and G2 are calculated from the resulting path distance and Euclidean distance. Figure 4.5 can be considered an example of the first step of the gap search in the core module. In this example, the methodology will calculate the shortest paths between all nodes in m_1, m_2, m_3, m_4, and m_5, respectively. Within m_3 all shortest path combinations and the Euclidean distance between all nodes five to nineteen are calculated. In this example, both resulting parameters G1 and G2 are highest for the OD pair 17-6.

Table 4.2: Effect of filtering on the OD pair dataset for New South Wales (Australia). Reprinted from [87].

	S2	S3	S4	S5	Total
OD pairs (million)	5.7	7.6	7.9	6.4	27.7
OD pairs after filter 1	15275	39584	71762	78793	205414
OD pairs after filter 2	803	5906	15482	19046	41237
G1 threshold	6.39	4.09	4.21	5.07	4.56
G2 threshold [m]	757	852	645	565	645

Even though all-pairs shortest paths only have to be calculated within meshes on subnetworks, this still results in a high number of OD pairs. Shortest path calculations on the complete network are computationally more expensive than on subnetworks because of the higher level of detail. Thus, the number of OD pairs for the shortest path calculation on the complete network has to be reduced. Most of the resulting OD pairs are not gap candidates. The parameter that indicates gap candidates best at this stage is G1 such that OD pairs with a low G1 can probably be filtered out (for a detailed discussion, see Section 4.6).

We employ two filters on the data. In a first filter, for each start point S_n, only the OD pair with the highest value of G1 is kept. However, many OD pairs still exist, which are not gap candidates as many start points are not at gaps. The second filter reduces the data such that only those OD pairs above the 70 % quantile of G1 and above the 25 % quantile of G2 are kept. These values are chosen, so that much unnecessary information is filtered out, and at the same time, possible gap candidates are kept. The selection and the impact of the filters on the **Error Search** is also discussed in Section 4.6. Table 4.2 provides values for the number of OD pairs before and after filtering in the study region and exact values for the 70 % quantile of G1 and 25 % quantile of G2.

The parameter G3, the number of endpoints of gap candidates on one spot, is calculated after the first and before the second filter. If G3 is calculated before the first filter, it contains no information because the data set contains all possible OD pairs, so G3 is the same for every point in one mesh. If G3 is calculated after the second filter, the number of endpoints on one spot is much lower, and much of the information which makes G3 valuable for gap identification has been filtered out. Because of this, G3 is calculated after filtering only the OD pairs with the highest G1 per start point and before deleting all OD pairs under a certain threshold of G1 and G2.

Finally, the path distance on the complete network is calculated only for the filtered OD pairs. The parameters G4 and G5 result from the relation of the path distance on the complete road network to the path distance on the subnetwork. The workflow for the gap search is also illustrated in Figure 4.4 in the gray box.

Rating System

We employ a rating system to rate the parameters G1, G2, G3, G4, and G5. The rating system assigns points from 1 to 10 to the parameters mentioned above.

The parameter G3 contains discrete numbers with many low values and very few high values. To assign points, the distribution of the values has to be evaluated, and points are assigned according to how high the value is. The point rating is constructed with expert knowledge (for a more detailed evaluation, see Section 4.6) and is given in Table 4.3. It might have to be adapted for different study regions. A classification of the sorted data by deciles as for the parameters G1, G2, G4, and G5 (see below) is not applicable for G3 because of the discrete values.

Table 4.3: Exemplary parameter rating for G3. Reprinted from [87].

$G3_R$	1	2	3	4	5	6	7	8	9	10
G3	1	2	3	4	5-6	7-8	9-10	11-12	13-15	> 15

We calculate ten deciles for each parameter G1, G2, G4, and G5 (see Table 4.4), which divide the sorted data into ten equal parts so that each decile represents one-tenth of the data. Then, each value is assigned the point rating of the decile is located in. For example, if a value of G1 lies between the 0 % and 10 % quantile, the point rating 1 is assigned. Ten points are assigned if the value is above 90 %.

Table 4.4: Deciles for parameter rating for GX_R where $X = 1, 2, 4, 5$. Reprinted from [87].

GX_R	1	2	3	4	5	6	7	8	9	10
%	< 10	10-20	20-30	30-40	40-50	50-60	60-70	70-80	80-90	90-100

The resulting point ratings are noted as $G1_R$ for all G1 ratings, and similarly for G2, G3, G4, and G5 as $G2_R$, $G3_R$, $G4_R$, and $G5_R$ (see Table 4.3 and Table 4.4). The combination of point ratings serves as an indicator of how likely a gap candidate is a classification error. In this study, both the importance of each point rating individually and the influence of different combinations of point ratings on the result are evaluated.

4.4.3 Reference Data

We employ the authoritative PSMA Street Network data [105] as reference data, especially the road network data of the state of NSW. This dataset is also chosen because it is independent of the OSM road network data: Unlike other official road data, PSMA data has not been integrated into the OSM database.

The description of the road classes in the PSMA dataset can be found in [105]. The road classes in the PSMA dataset do not match the OSM road classes. For example, *secondary* roads in OSM are mostly (around 60 %) classified as Sub-arterial roads in PSMA. However, many cases also exist where they are categorized as Arterial roads or Collector roads. Similarly, Sub-arterial roads in PSMA include OSM *primary*, *secondary* and *tertiary* roads. Therefore, a direct comparison of road classes to detect errors is not possible. We manually check both the resulting disconnected network components and gap candidates and decide if there is a classification error.

To facilitate the generation of reference data, we aim at applying some general rules. These rules are based on the assumption that even though the classification schemes do not match, the continuity of a road class in the PSMA dataset still contains some useful information. If both O and D of a gap candidate are located on roads with the same PSMA road class, the connection must be a road of the same or higher PSMA class to be an error. In this case, if the connection is a lower PSMA road class, the gap candidate is not marked as an error. Similarly, suppose O and D are located on roads with different PSMA road classes. In that case, the gap is an error if the connection is a road of the same or higher PSMA road class as the lower one of both PSMA road classes of O and D. This is illustrated exemplarily in Figure 4.6. However, in some cases, these rules do not apply because of the incompatible classification schemes. Then, we decided with expert knowledge and by comparison with additional data sources like Google Maps.

Since it is not feasible to analyze every gap candidate manually, all gap candidates with high ratings are checked. Furthermore, many gap candidates with medium ratings and

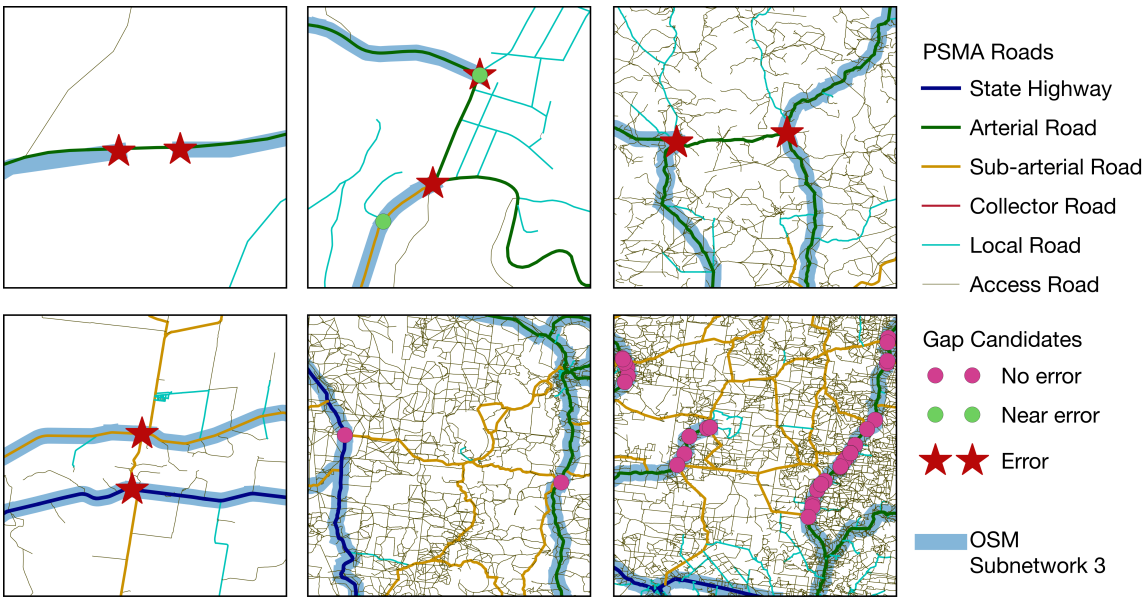

Figure 4.6: Examples of the collection of reference error data for gap candidates. Note that a gap candidate is always illustrated as two points, an origin and a destination. Reprinted from [87].

few gap candidates with low ratings are checked. The lower the ratings, the fewer *Errors* are found, which supports this methodology (see Section 4.6).

4.5 Results

In this section, we show the results of applying the presented **Error Search** on the OSM road network for the study region of NSW. The region is chosen because it is large enough so that all subnetworks form a network themselves and because of the availability of the PSMA data as ground truth. Generally, the population density is much higher on the coast in the east of the region than in the Outback in the west.

In this chapter, the results of applying the presented **Error Search** in the study region in NSW are presented. First, we present the results of the **Error Search** at disconnected components, then we focus on the results of the gap search. For the gap search, we calculate the presented point ratings and present the results; first each of the point ratings separately, then in combination with each other. The error types per subnetwork for all disconnected network components and gap candidates are presented in Table 4.5. We find 1991 disconnected network components on all levels, with 94.48 % of them in subnetwork S5. Most disconnected network components are *Self errors* (95.13 %), and few are *Connection errors* (3.37 %). Subnetworks S1-S4 feature a total of 110 disconnected network components with 22.73 % *Connection errors* and 59.09 % *Self errors*.

In total, 11.06 % of all analyzed gap candidates are *Errors*, 8.47 % are *Near errors*. The lower the level, the more errors occur: 64.10 % of all *Unique errors* are in subnetwork S5, and only 1.80 % of all *Unique errors* are in subnetwork S2. No *Errors* or *Near errors* are found in subnetwork S1. In subnetworks S1-S4, there are many more unique errors (279) than disconnected

Table 4.5: Error types per subnetwork both at disconnected components and at gap candidates. Reprinted from [87].

	Disconnected components				**Gap candidates**			
	Con. error	Self error	Dis-con.	Border error	Error	Near error	Unique error	No error
Subnetwork S1	0	3	0	1	0	0	0	151
Subnetwork S2	0	2	1	0	14	13	14	362
Subnetwork S3	13	12	0	4	66	110	51	1857
Subnetwork S4	22	48	0	4	304	444	214	3362
Subnetwork S5	32	1829	17	3	871	394	498	3514
Sum	**67**	**1894**	**18**	**12**	**1255**	**961**	**777**	**9131**

network components (110). 69.23 % of all *Connection errors* in subnetwork S3 and 27.27 % of all *Connection errors* in subnetwork S4 are also identified by gap candidates. Figure 4.7 shows a map of all detected *Errors* and *Near errors* in gap candidates per subnetwork in NSW.

Figure 4.8 shows the distribution of the error types over the ratings 1-10 for all analyzed gap candidates. Most *Errors* and *Near errors* feature a high $G1_R$ and $G4_R$. On the other hand, $G1_R$ and $G4_R$ values indicate *No error* more often than *Error* or *Near error*. Regarding $G2_R$ and $G3_R$, *Errors* and *Near errors* are distributed approximately uniformly over the ratings 1-10, with slightly more *Errors* for the higher ratings of $G2_R$. $G3_R$ is the only point rating that has many *No errors* in the lower ratings, especially for the rating 1 (3603 *No errors*). $G5_R$ features more *Errors* and *Near errors* for medium and high ratings than for low ratings. Also, the number of *No errors* is high for high ratings for $G5_R$.

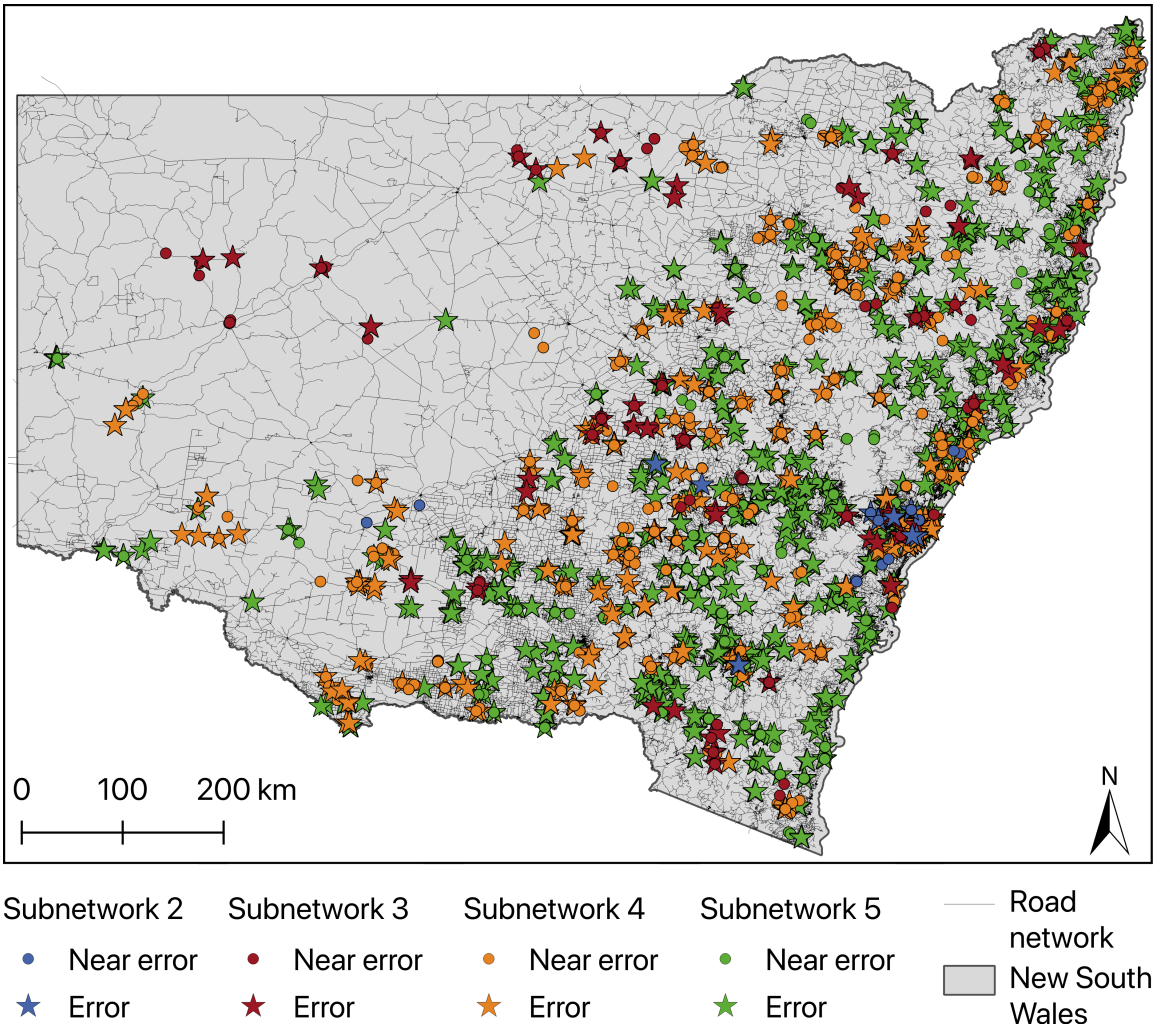

Figure 4.7: All *Errors* and *Near errors* in New South Wales (Australia) per subnetwork. Reprinted from [87].

In Figure 4.9, $G1_R$ is combined with the other point ratings, respectively. The highest number of *Errors* in the high ratings can be observed by adding $G1_R + G4_R$. There, 88 % of all *Errors* and 41 % of *No errors* have a rating higher or equal to 16. This results in a rate of 88/41 = 2.14 of *Errors* versus *No errors* for all ratings higher or equal to 16. The y-axis on the right of Figure 4.9 shows the rate of all *Errors* and *No errors* equal or higher to the current rating. Note that the scale of the rate is different in each plot in Figure 4.9. The sum of $G1_R + G2_R$ and $G1_R + G5_R$ has fewer *Errors* and a lower rate in high ratings than $G1_R + G4_R$. However, $G1_R + G5_R$ has slightly higher ratings, and more *Errors* in high ratings than $G1_R + G2_R$. $G1_R + G3_R$ has a low absolute number of *Errors* in high ratings, but at the same time also a low absolute number of *No errors* in high ratings. This leads to a high rate of 2.65 for all ratings higher or equal to 12, where 78 % of all *Errors* and 29 % of all *No errors* are analyzed.

Figure 4.10 shows different combinations of point ratings. In Figure 4.10 (a), the point ratings $G1_R$, $G3_R$, and $G4_R$ are added up, resulting in a maximum of 30. Figure 4.10 (b) shows the combination of the point ratings $G1_R$, $G3_R$, $G4_R$, and $G5_R$, ranging from 0 to 40. The absolute numbers of gap candidates per rating are displayed in the upper plots of Figure 4.10. The middle plots illustrate the percentage of *Errors*, *Near errors*, *No errors*,

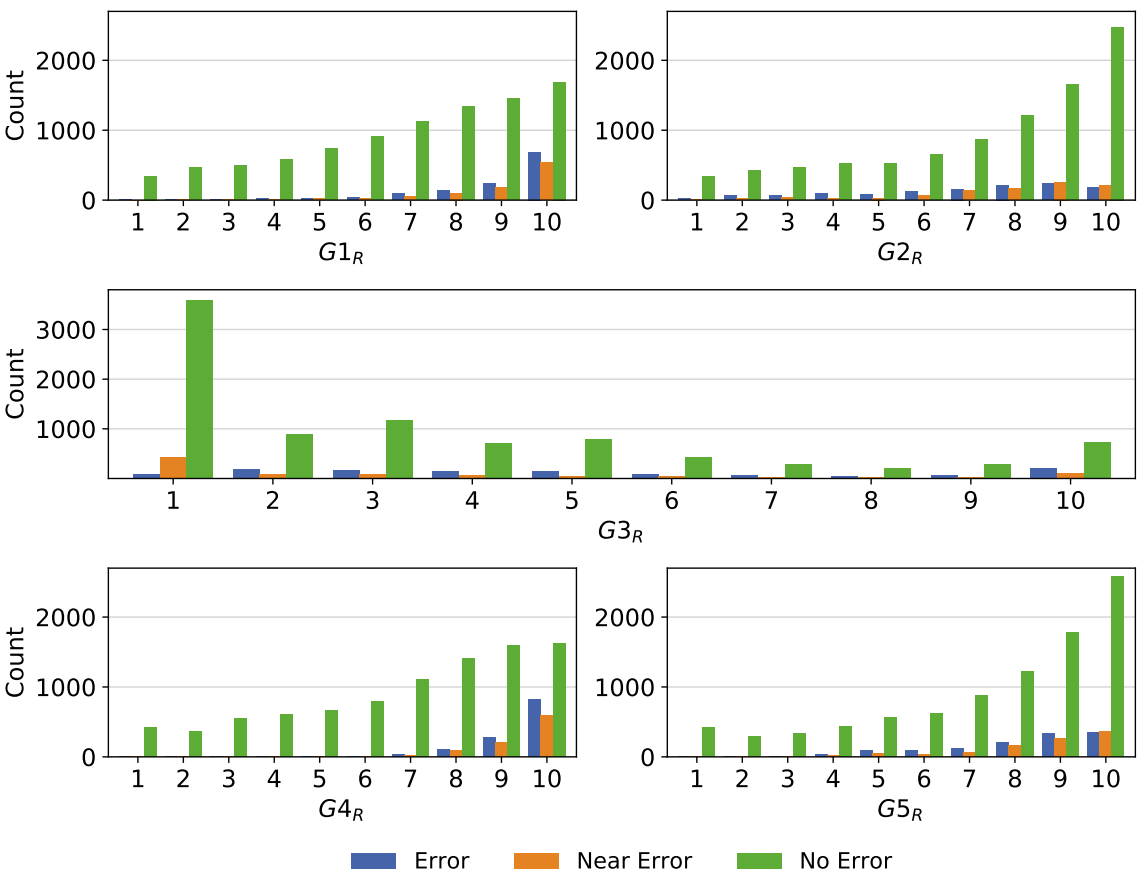

Figure 4.8: Error types per rating for all point ratings. Reprinted from [87].

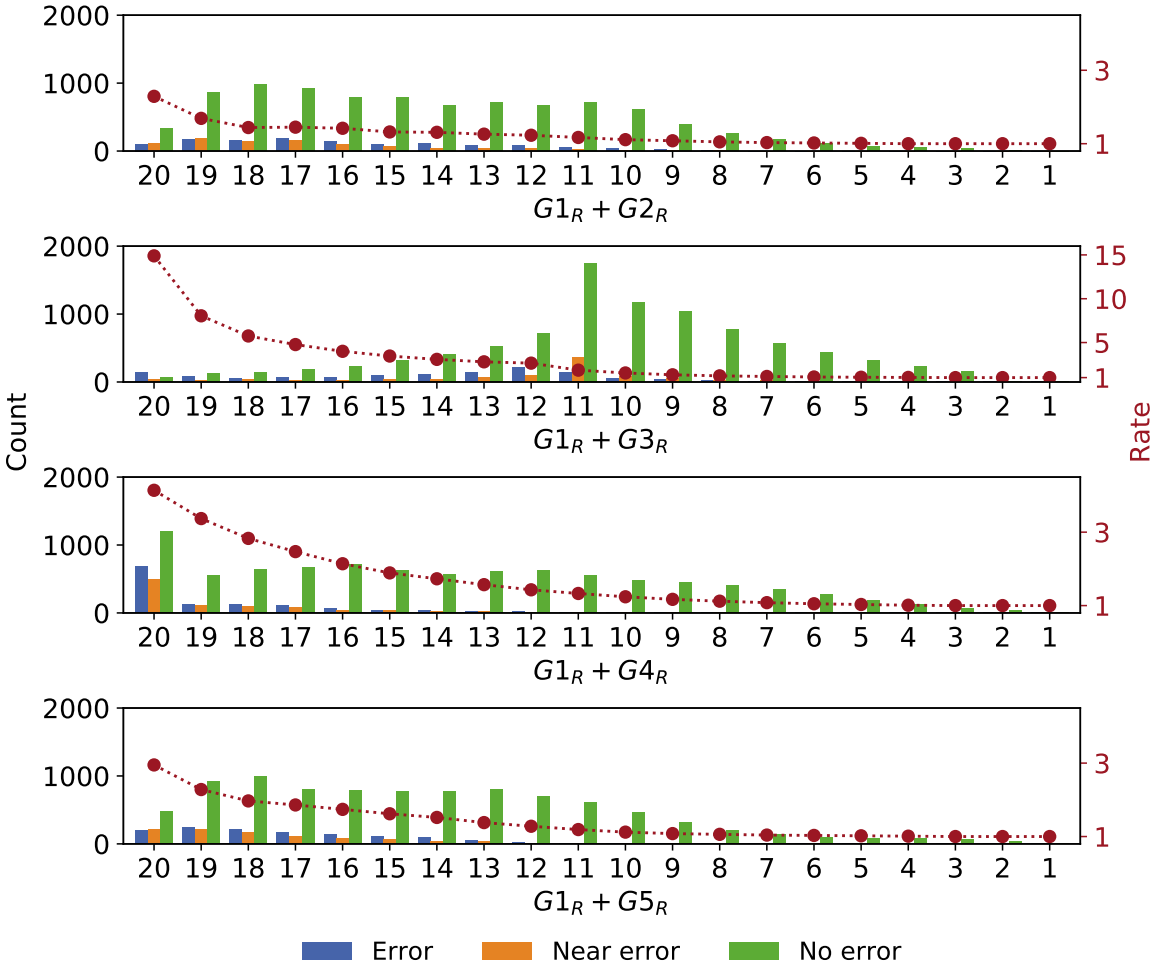

Figure 4.9: Combinations of $G1_R$ with all other point ratings, respectively. The y-axis on the right displays the rate of all *Errors* versus *No errors* equal or higher to the current rating. Note the different scale of the rate in the second plot. Reprinted from [87].

and *NaN* per rating. *NaN* signifies gap candidates where it is unknown if they are *Errors*, *Near errors*, or *No errors*. The lower plots of Figure 4.10 show the cumulative percentage of different values per rating, beginning with high ratings.

For the combination $G1_R$, $G3_R$ and $G4_R$, 91 % of all gap candidates with rating 30 are *Errors* or *Near errors*. This declines to 83 % for 29, 71 % for 28 and 63 % for 27. The trend continues until the percentage of *Errors* and *Near errors* is next to zero for ratings lower or equal than 18. Furthermore, 75 % of all data has a rating lower or equal to 18. Simultaneously, 94 % of all unique errors have a rating above or equal to 18. 50 % of all unique errors can be found by searching 1.73 % of all data. The combination $G1_R$, $G3_R$, $G4_R$, and $G5_R$ shows the same trend, but slightly more data has to be searched to obtain the same amount of unique errors. To obtain 50 % of all unique errors, 1.99 % of all data has to be searched in the combination $G1_R$, $G3_R$, $G4_R$, and $G5_R$. Figure 4.11 compares all presented combinations concerning the percentage of *Errors* and unique errors found against the percentage of all data searched.

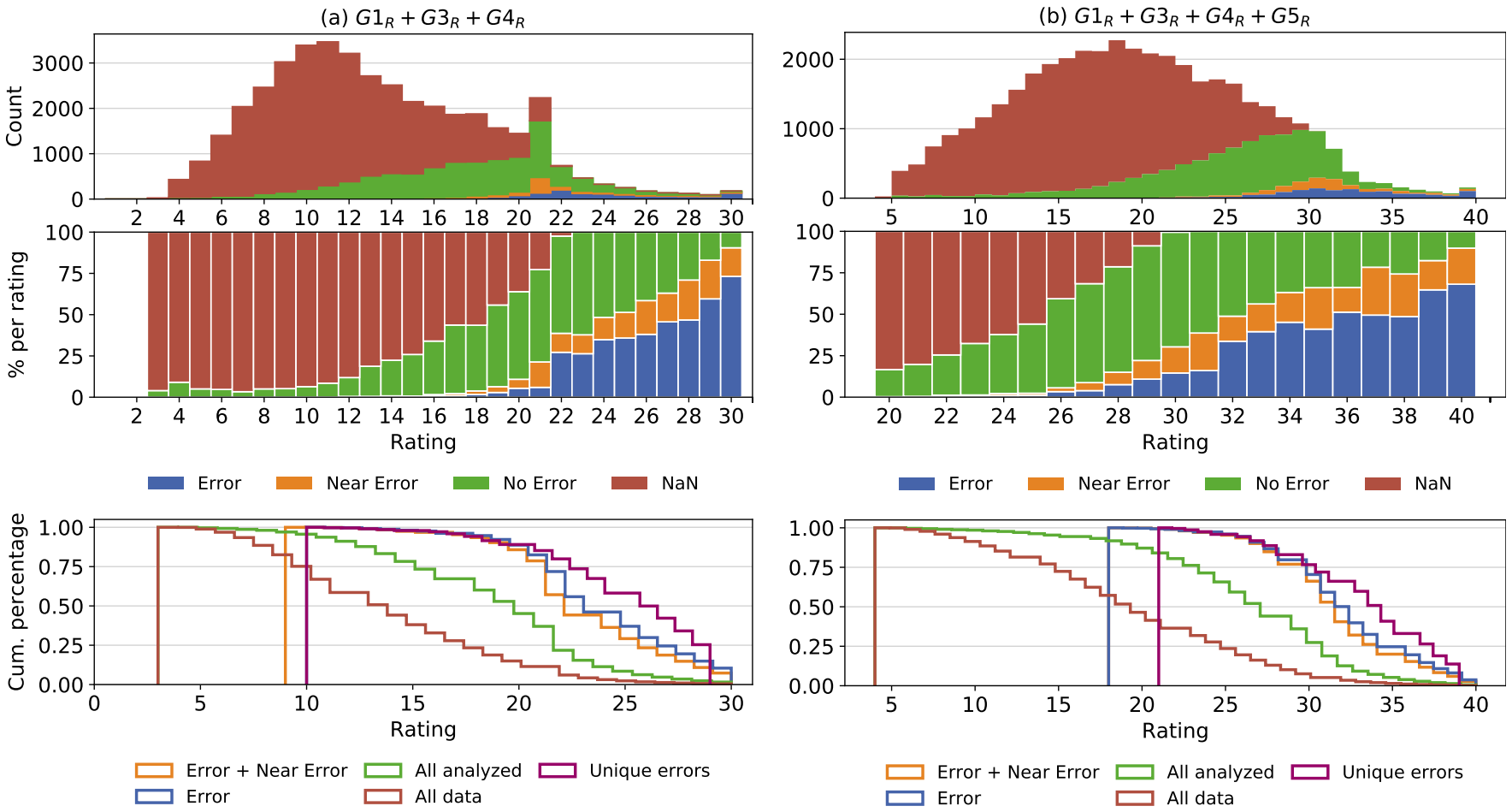

Figure 4.10: Combinations of the point ratings $G1_R$, $G3_R$ and $G4_R$ (left) and $G1_R$, $G3_R$, $G4_R$ and $G5_R$ (right). The absolute numbers of gap candidates per rating (stacked) are displayed in the upper plots. The plots in the middle illustrate the percentage of error types per rating. The lower plots show the cumulative percentage of error types per rating. Reprinted from [87].

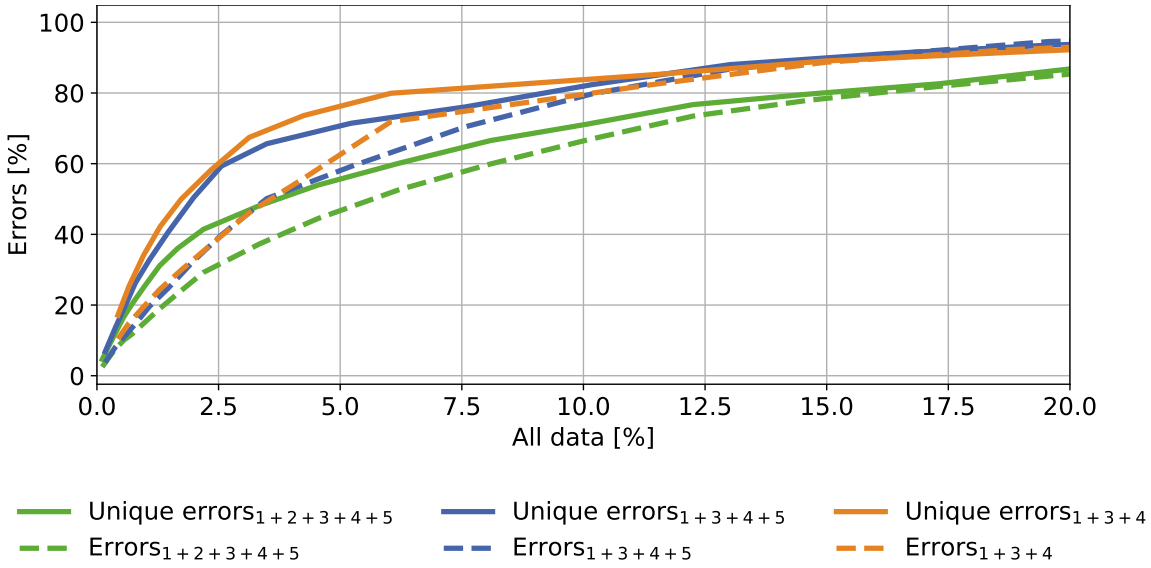

Figure 4.11: Percentage of *Errors* and *Unique errors* found in respect to the percentage of all data searched for different combinations of ratings. Reprinted from [87].

4.6 Analysis and Discussion

In this section, we discuss and interpret the results shown in Section 4.5. We focus on the applied filters, the distribution of errors over the network levels and their spatial distribution in Section 4.6.1. In Section 4.6.2, we evaluate the parameters and the performance of different parameter combinations. Finally, we discuss the research hypothesis, the limitations and sources of errors, and the transferability to other regions in Section 4.6.3.

4.6.1 Analysis and Discussion of Resulting Error Types

Two filters are applied (see Section 4.4.2) to reduce the number of gap candidates prior to the path calculations on the complete network. The parameters G1, G2, and G3, can be calculated before the path calculations on the complete network. As shown in Figure 4.8, the point ratings $G1_R$, which results out of G1, is the most significant for the **Error Search** because *Errors* generally have a high $G1_R$. The lower the rating, the fewer *Errors* are found. *No errors* are found in the ratings 1, 2, or 3 of $G1_R$. It can be assumed that if *No errors* occur in the lowest ratings of $G1_R$, *No errors* will appear with even lower G1 values that are filtered out with the second filter. Furthermore, the first filter only keeps the gap candidate with the highest G1 per start node. This filter can be justified with the

same argument that a high G1 has a higher probability for an *Error*. However, this filter also discharges *Errors* in some rare cases. By analyzing the highest G1 values of the gap candidates discharged by this filter, we find that for discharged *Errors* there are in almost all cases *Near errors* that are found by the methodology. The second filter also removes all gap candidates below the 25 % quantile of G2. In Figure 4.8, it seems that $G2_R$ and with that G2 are insignificant for error detection. However, in the definition of a gap, we state that the detour has to be significant for a gap candidate to be considered a gap. Table 4.2 shows that the 25 % quantile of G2 is between 565 m to 852 m. Any potential *Error* lower than this range is deemed not significant because the detour is too small.

Because the parameters G1 and G2, as well as G4 and G5, are calculated from the same values, a correlation might be expected. However, the Pearson correlation coefficient does not suggest a correlation in both cases: for G1 and G2 it is 0.039, and for G4 and G5 it is 0.048.

The **Error Search** finds both errors at disconnected components and at gaps. As we argue in Section 4.1, the important errors are the ones that can potentially cause large detours for routing applications. While *Self errors* are indeed classification errors, they are not important for routing as they do not cause detours. *Connection errors* are usually more important for routing because, like *Errors* at gaps, they can cause large detours (as visible in Figure 4.2). It can be seen in Table 4.5 that at disconnected network components, many more *Self errors* than *Connection errors* are found. In comparison to *Errors* at gap candidates, the *Connection errors* are few. This leads to the conclusion that the gap search finds more and also more important errors than the search for disconnected network components. Furthermore, some of the *Connection errors* in the subnetworks S3 and S4 are also identified with a gap search.

A hierarchical road network is constructed so that the importance of a road decreases from a high hierarchy level (e.g., *motorways*) to a low hierarchy level (e.g., *tracks*). Considering subnetworks, as a union of levels, the sum of road network kilometers in subnetworks is much lower in high-level subnetworks like S1 than in low-level subnetworks like S6. Furthermore, L5 of the road network are *unclassified* roads, which are technically defined as minor public roads and the lowest level of the network (see Table 2.1). However, mappers might often intuitively tag roads with unknown classification with *highway=unclassified*, such that there might be many classification errors in the L5 network. For these reasons, there are many more *Errors* (see Table 4.5) in low-level subnetworks than in high-level subnetworks. However, the *Errors* in high-level roads are more significant for a country's transportation network because high-level roads carry more traffic than low-level roads. Thus, more vehicles are affected by *Errors* in high-level roads than by *Errors* in low-level roads. We do not search for errors on S6 because we find that level L6 and L7 are often not distinguishable.

Regarding the spatial distribution of *Errors* at gap candidates, most *Errors* of S5 are in the east of the region where the population density is high. We often find *Errors* in S5 inside a city's road network where major roads in cities are classified as *residential*. *Errors* in S3 and

S4 are also often located in rural regions. A significant amount of *Errors* in rural areas is also due to bridges that are classified in a different road class than the connecting roads.

4.6.2 Analysis and Discussion of the Rating System

Considering the point ratings $G1_R$ – $G5_R$ separately in Figure 4.8 provides some information on how significant the parameters are for the **Error Search** at gap candidates. This suggests that the point ratings $G1_R$ and $G4_R$ might be the most significant point ratings for the **Error Search**. Looking only at the absolute number of *Errors* in high ratings, the point ratings can be ranked in the following order of significance: $G4_R > G1_R > G5_R > G2_R > G3_R$. This indicates that the calculated ratio of distance is much more significant for the **Error Search** than the mathematical difference of distance. However, the absolute number of *Errors* in high ratings is just one aspect. If the number of *No errors* is also high, many potential gap candidates have to be searched to find *Errors*. This is the reason why the point rating $G3_R$ is essential even if the number of errors in high ratings is low. Compared to the other point ratings, it features significantly more *No errors* in low ratings.

The significance of $G3_R$ becomes apparent when looking at the combinations of point rating $G1_R$ with all others in Figure 4.9. The rate of *Errors* and *No errors* is crucial because it is an indicator of how many *No errors* have to be searched in relation to the numbers of *Errors* that are found. Ideally, this rate is high such that most gap candidates that are searched are *Errors* and *Near errors*, and very few are *No errors*. Figure 4.9 demonstrates that the rate of *Errors* and *No errors* in high ratings is highest for the sum of the point ratings $G1_R$ and $G3_R$. The second-highest rate for high ratings can be seen in $G1_R + G4_R$. However, there are fewer *Errors* in high ratings in $G1_R + G3_R$ than in all other combinations. As can be expected by looking at the ratings of $G1_R$ and $G4_R$ individually, the sum $G1_R + G4_R$ features the highest number of absolute *Errors* in high ratings. We conclude that, out of the point ratings analyzed in this study, $G1_R$, $G3_R$, and $G4_R$ are the most significant indicators of *Errors* at gaps.

Therefore, we establish a rating system with the combination of $G1_R$, $G3_R$, and $G4_R$ and then compare it to the combination of $G1_R$, $G3_R$, $G4_R$, and$G5_R$ and to the combination of all point ratings. All three combinations show the desired result where many *Errors* occur in high ratings. As it turns out, the combination $G1_R$, $G3_R$, and $G4_R$ performs best as the rate of both *Errors* and unique errors versus analyzed data is highest. Adding $G5_R$ lowers this rate slightly, and further adding $G2_R$ lowers it significantly.

The underlying problem with the different input parameters is basically a multi-criteria decision problem. Our developed rating system implements a basic multi-criteria decision system with the parameters G1 – G5 as criteria. This basic decision system can still be improved. A weighting of the criteria could potentially enhance the rating system's performance, but finding the appropriate weights for a study region requires additional

studies. Furthermore, outranking methods like ELECTRE or PROMETHEE could reduce the number of gap candidates before applying the rating system. However, because of the high number of potential gap candidates (41 237 for NSW, see Table 4.2), a pairwise comparison of gap candidates for the determination of the concordance and discordance matrix (ELECTRE) and for the determination of deviation (PROMETHEE) would probably result in huge matrices, and hence, remains the subject of future investigations.

The results of the combination $G1_R, G3_R$, and $G4_R$ suggest that the error probability is decreasing with the rating: All gap candidates of rating 30 have a 91 % probability of being an error, all gap candidates with a rating of 29 an error probability of 83 %, etc. This supports a methodology by gap detection where a human user can prioritize the **Error Search** by first checking the gap candidates with the highest ratings and then eventually continuing to the lower-rated gap candidates. When checking all gap candidates equal or higher than 22, 80 % of all errors can be detected by either an *Error* or a *Near error*. At the same time, 51 % of gap candidates with a rating equal or higher than 22 are *Errors* or *Near errors*. Moreover, the errors that significantly impact the accuracy of routing are the ones with the highest ratings as the possible detour is the largest for high ratings. Thus, a human user can quickly detect influential errors for routing applications by prioritizing high ratings in gap candidates.

4.6.3 Limitations and Implications for Practical Use

The **Error Search** is based on the hypothesis that both disconnected parts and gaps of subnetworks in the OSM road network are indicators for road classification errors if the disconnection or the gap can be resolved in the complete network. Our results prove this hypothesis. Disconnected parts and gaps of subnetworks in the OSM road network prove reliable indicators for road classification errors. However, they are not guaranteed classification errors. In the real world, a *primary* road may turns into a lower quality road for a certain distance and then back into a *primary* road. This can have numerous reasons like different jurisdictions, traffic, or missing funding. For example, the US interstate highway system has some well-known true gaps [106]. These gaps occur mostly because the connecting roads fail to conform to interstate standards fully, and for some of these gaps plans to close them already exist. Therefore, a human expert has to check the results of the **Error Search** to confirm them.

When applying the **Error Search**, its limitations have to be considered as well. First and foremost, the method is not able, but also not designed to find all classification errors in a road network. It is only designed to find the errors which lead to detours when considering only a subnetwork. We can not clearly state how many *Errors* are missed to be detected because it is not feasible to analyze the entire network manually. We argue that the *Errors* missed are few and less influential on the accuracy of routing applications because of the

distribution of *Errors* in Section 4.5. Roads that are wrongly classified as a higher class than they actually are can not be detected with this method. Also, using an undirected graph might cause the **Error Search** to miss gaps that would otherwise be detected. But, a directed graph makes use of the OSM tag *oneway*. The accuracy and completeness of this tag are often low [13, 54, 107], and its enhancement is not in the scope of this study. Some missing roads are found by the search for disconnected network components and gap search, but this is also not the scope of this study.

Generally, we observe two categories of false positive gap candidates, meaning gap candidates with high ratings, which are *No errors*. Both categories are visualized in Figure 4.12. On the one hand, the high number of *No errors* with high ratings is often due to gap candidates in a broader range along *Errors* that cause a large detour. While they are not classified as *Near error*, because they do not start or end at the gap, the point ratings are often high due to the gap in the vicinity. This phenomenon also leads to *Errors* near other *Errors* getting a high rating even though the detour caused by the fist *Error* is very small. The combination of both *Errors* then leads to large detours, resulting in a misleading high rating for this *Error*. On the other hand, false-positive gap candidates sometimes occur because the hypothesis does not apply. As mentioned above, this can have numerous reasons. We observe is that the most frequent reason is that there is no need for a high-level connecting road because it is not used frequently. Especially in the rural parts of NSW, the population is concentrated in towns, and large areas are uninhabited. Thus, these uninhabited parts of the country do not require good accessibility. Furthermore, sometimes a high-level connecting road is impossible because of difficult terrain, for example, in mountain ranges. The methodology cannot separate these cases, so a human user is required to confirm the result.

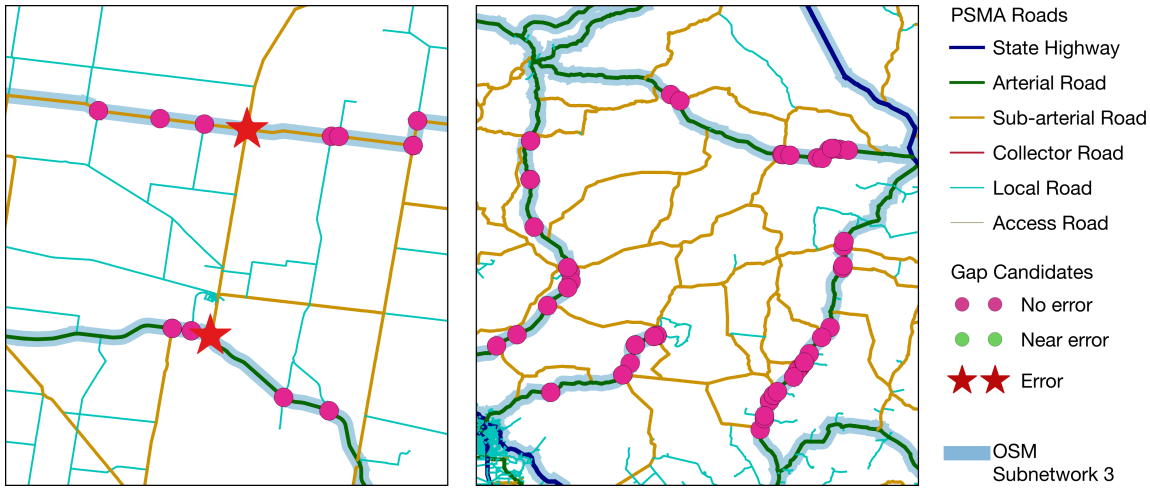

Figure 4.12: Examples of false positive gap candidates. On the left, *No errors* in the vicinity of an *Error* are visualized. The *Error* causes the high rating of the *No errors* which are not marked as *Errors* because they do not start or end at a gap candidate. On the right, *No errors* are visualized where there is no need for a high-level connecting road. Reprinted from [87].

Table 4.6: Summary of strengths and limitations of the **Error Search**. Reprinted from [87].

Strengths	Limitations
• Intrinsic methodology • Finds road class errors at disconnected components and gaps • Based on basic graph theory • Includes a probability-based ranking of identified gap candidates • Errors which might lead to large detours are found first because of the rating system • Applicable to road network databases worldwide • Expendable by the community because the implementation is freely available	• Does not find all road class errors • No information about missed errors available • Requires human user to check potential errors • Can not detect roads wrongly classified in higher class • Some errors might be missed because of the use of an undirected graph • A gap leading to a large detour can cause false positives in the surrounding area • Adaptation to different regions required

Generally, the presented **Error Search** can be applied for all road networks. However, it has to be considered that some values have to be adapted to fit the characteristics of a different region. The classification of the road network into hierarchy levels might have to be adapted to the country's circumstances. Especially the thresholds for Filter 2 have to be analyzed in detail and may be higher for regions with overall lower quality of the road network. Furthermore, as the rating system is based on relative thresholds, there is the underlying assumption that there are classification errors in every road network. For road networks with higher or lower quality of road classification, the resulting probability of error distribution will be different. To apply the **Error Search**, a region's road network has to be more or less complete such that there are few missing roads because this might hinder the **Error Search**.

The strengths and limitations of the **Error Search** are summarized in Table 4.6.

4.7 Conclusion and Outlook

Errors in road classification that occur in crowd-sourced geographic data such as OSM can hinder routing applications because of false assumptions about travel time or access limitations. We develop a novel approach to detect these road classification errors by searching for disconnected parts and gaps in subnetworks. A detailed and efficient implementation of the developed methodology is provided in this study. The methodology is successfully applied in an exemplary case study on the OSM road network dataset of NSW in Australia.

In the introduction to this chapter, we formulated two main research questions:

1. Is an approach by searching for disconnected parts or gaps in subnetworks able to find potential road classification errors? Is this approach able to provide information about the likelihood that the result is an error?

2. Which parameters (thresholds such as lengths of detours on a subnetwork compared to the complete network) or combination of parameters indicate gaps in road networks best?

To answer our first research questions, we conclude that a search for disconnected parts finds fewer potential road classification errors than a search for gaps. A gap search can find a significant number of misclassifications together with an error probability that results from a multi-parameter rating system. As an answer to our second research question, our study has shown that three parameters are most relevant for the estimation of the error probability: G1 – the ratio of the shortest path distance on the subnetwork network divided by the Euclidean distance, G4 – the shortest path distance on the subnetwork network divided by the shortest path distance on the complete network, and G3 – the number of filtered destinations on the same spot. A combination of these parameters performs best as the rate of errors versus analyzed data is highest, meaning few data has to be checked by a human user to obtain many classification errors. In our case study, only 6 % of gap candidates have to be checked by a human user to find 80 % of identified road classification errors using the multi-parameter rating system.

A major advantage of this methodology is the worldwide transferability to all regions of the world, which have an almost complete road network in OSM. When a different region is analyzed, some values might have to be adapted to fit the characteristics of the new region. Furthermore, it can also be applied for road network data from other sources, as long as it is represented as a graph. The **Error Search** is intrinsic such that no additional data besides the road network is required to find misclassifications. The source code of the implementation is published on GitHub [91], such that the study can be easily repeated or applied to other datasets.

The findings of this study can be used in many different applications. On the one hand, it can generally improve OSM data quality by detecting and correcting the errors. On the other hand, it is also a valuable tool for routing algorithms to improve their underlying data and search for potential errors. In research on critical road infrastructure, often, only higher road network levels are analyzed because lower-level roads are less relevant and increase computing time [65, 108]. In these studies, a gap on a high-level subnetwork can cause false results. The presented search for misclassifications can be introduced to these studies as a data preprocessing step. Furthermore, the presented methodology can be applied to assess the quality of OSM by checking for navigability, an important quality aspect of road network data.

In future research, the methodology can be extended. As disconnected components might appear more often in other countries, a methodology to rate the error probability at discon-

nected network components could also ease the job of manually checking these disconnected network components for errors. Available tags of gap candidates and their connecting roads can be analyzed for continuity, such as the name, surface, or maximum speed of the road and could be included as additional parameters. Also, strokes [109] could be computed to observe their behavior at gap candidates. The information if a connection between gap candidates consists of a single or multiple strokes could, for example, be considered as a parameter for the rating system. These parameters could provide additional information on the error probability. Regarding the rating system as a multi-criteria decision system, it could still be extended, for example, by adding weights to the parameters or by implementing outranking methods to reduce the number of gap candidates. Furthermore, remote sensing can be applied to check if the shape of a road changes at gap candidates, indicating a class change. More case studies can be performed, including different study regions with different qualities of OSM data. These case studies would enable a detailed sensitivity analysis. Ideally, a reference dataset could be used where an automated matching of roads is possible. Then, it would also be possible to identify which types of classification errors can not be found by this methodology. It could also be interesting to apply the **Error Search** and test the human correction with real OSM contributors to check the applicability of the **Error Search**.

4.8 Synthesis on the First Part of GRIND

In Part I of this thesis, two independent modules of **GRIND**, the **Fuzzy-FSE** and the **Error Search**, are developed. The modules aim at improving the routability of OSM data for routing applications by addressing the two challenges identified in Section 2.5. The **Fuzzy-FSE** targets the first challenge of missing speed values by adding estimated average speed values to every road segment in the OSM road network. These added speed values enable routing applications to calculate fastest paths in road networks. The second challenge of misclassified roads is addressed by developing the **Error Search**. It identifies the most likely misclassifications, which can then be corrected by a human user. As the errors that lead to the largest detours in a high-level road network are detected with high ratings, these errors are the first to be corrected. Thus, it can be argued that after performing the error search and checking and correcting the identified errors with high ratings manually, the most significant road classification errors are eliminated. The main advantage of both modules is that they run intrinsically, as they can be applied without requiring other data besides the OSM road network.

As both modules can run independently, two independent OSM datasets are obtained as a result. These datasets are then combined into a single enhanced OSM dataset. For this thesis, the **Error Search** is performed before the **Fuzzy-FSE** because the road class is an input parameter for the **Fuzzy-FSE** and an incorrect classification falsifies

the average speed value. However, these few inaccuracies are mostly negligible compared to the overall accuracy of the **Fuzzy-FSE**.

The resulting enhanced OSM road network serves as database for Part II of this thesis and for the second part of **GRIND**. With the now improved routability, the OSM road data can be applied for the assessment of critical road infrastructure in a disaster context. The assessment of critical road infrastructure then benefits from the advantages of OSM data like the free and quick accessibility of data and its global coverage.

Part II

Assessment of Critical Road Infrastructure in a Disaster Context

Part II - Assessment of Critical Road Infrastructure in a Disaster Context uses the enhanced OSM dataset generated in Part I to realize the second part of GRIND. It consists of five modules to assess critical road infrastructure in a disaster context that partly rely on each other:

- a Core Module (CM), containing core routing functionalities used by the other modules,
- an Accessibility Index Calculation (AIC) module, implementing two accessibility indices,
- a Travel Demand Model (TDM) module, estimating average daily traffic between locations,
- a Disaster Impact Assessment (DIA) module, focusing on different kinds of natural disaster impacts on critical road infrastructure, and
- a Disaster Vulnerability Scan (DVS) module, evaluating the road network's vulnerability towards future disruptions during long-term disasters.

The CM employs the enhanced OSM dataset for routing tasks and is used by all other modules in the second part of GRIND. The other four modules provide different types of GRIND outputs. The AIC and TDM modules use the CM to obtain pre-disaster outputs and can be applied independently of each other. The DIA and DVS modules employ the AIC or the TDM module, or both, to consider various aspects of disaster consequences. The complete schema of GRIND is illustrated in Figure 4.13 and extends Figure 1.2 with a schema of the second part of GRIND.

This part begins with an introductory Chapter 5 on critical road infrastructure assessment in a disaster context, summarizing the related work in this research field. Chapter 5 then highlights major gaps in existing approaches and outlines GRIND's prerequisites following the identified gaps. The inner structure of the next three chapters follows the modular design of GRIND. Chapter 6 presents the methodologies of the modules in the second part of GRIND. In Chapter 7, case studies of wildfire scenarios in two different regions are performed, and the results are presented for each module. Finally, Chapter 8 discusses the methodology of the GRIND modules in detail.

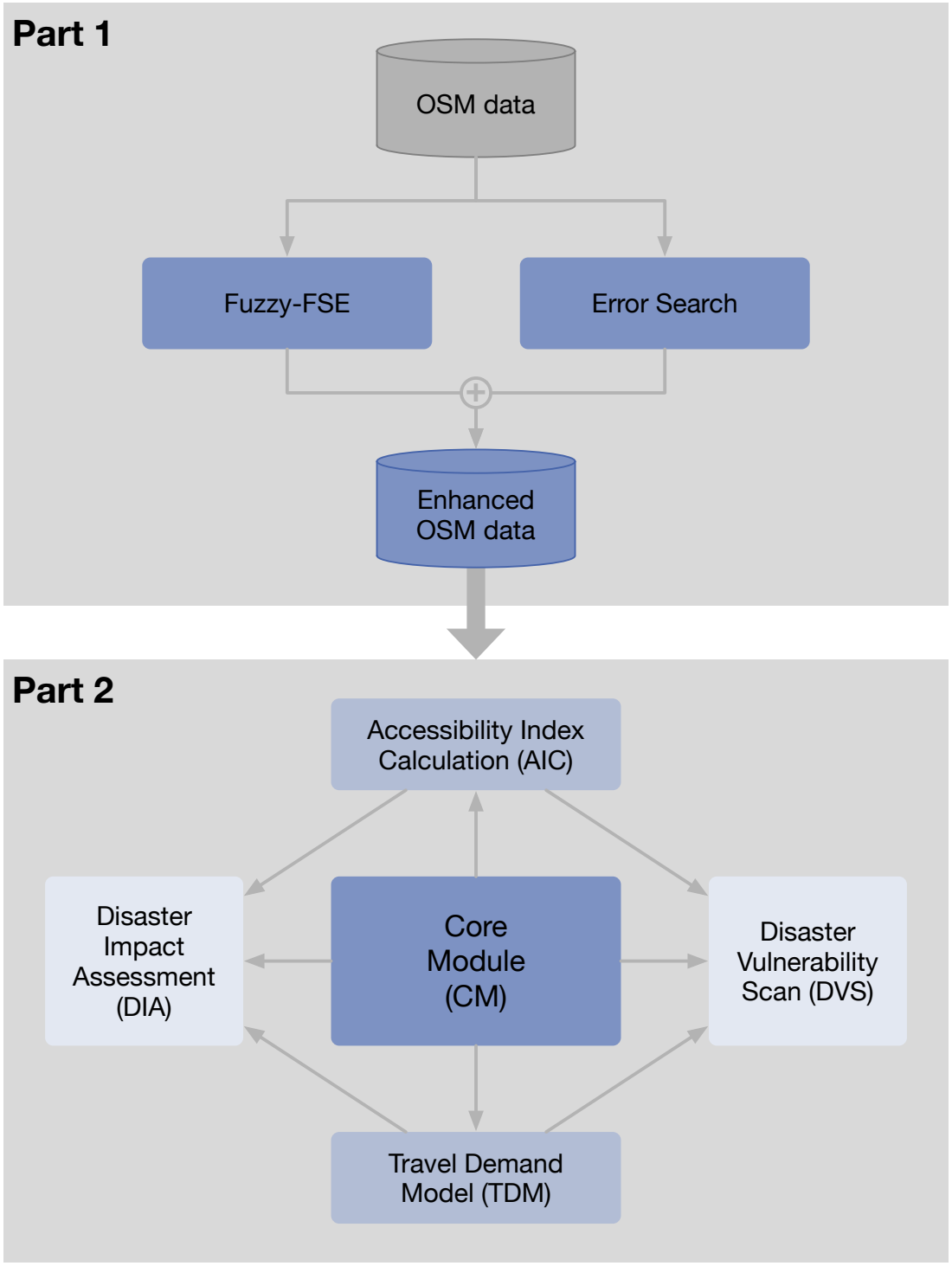

Figure 4.13: Complete schema of the generic concept for the assessment of critical road infrastructure in a disaster context (GRIND). The CM (dark blue) employs the enhanced OSM data. The other four modules of the second part provide different outputs. The AIC and TDM modules (light blue) focus on pre-disaster assessment and the DIA and DVS modules (very light blue) concentrate on post-disaster analyses.

5 Fundamentals on Critical Road Infrastructure Assessment in a Disaster Context

This chapter includes material from the journal article

Johanna Guth, Sven Wursthorn, Andreas Ch. Braun, and Sina Keller. "Development of a generic concept to analyze the accessibility of emergency facilities in critical road infrastructure for disaster scenarios: exemplary application for the 2017 wildfires in Chile and Portugal". In: *Natural Hazards* 97.3 (2019), pp. 979–999. It is cited as [65] and marked with a blue line.

This chapter also includes material from the author's unpublished master thesis:

Johanna Stötzer. "Development of a Generic Concept to Analyze the Accessibility of Emergency Facilities in Critical Road Infrastructure". Master's thesis. Institut of Photogrammetry and Remote Sensing, Karlsruhe Institute of Technology (unpublished). 2017. It is cited as [110] and marked with a dark green line.

Natural disasters happen unexpectedly all over the world and can cause immense damage to the road network and its functionality. Wildfires, for example, are an increasing threat as climate change furthers droughts and extreme temperatures in many countries. While they may often not directly destroy road infrastructure [111], the impact of wildfires on the road network's functionality can be severe. Road closures caused by the fires impact the road network and can cause considerable delays. These delays may last for a long time after a disaster, as the restoration of the road network's serviceability often takes a long time. In the wildfire example, all roads with the danger of fallen trees have to be checked by skilled workers before reopening [112]. Thus, it is essential to assess the performance of road infrastructure in the context of natural disasters.

Generally, sources of potential harm or situations with the potential to cause loss are called *hazards* [113]. A natural hazard is a geophysical process that involves the potential for damage or loss that exists in the presence of a vulnerable human community [114]. It is an unexpected or uncontrollable natural event of an unusual magnitude that might threaten people [113]. Natural hazards include, for example, wildfires, hurricanes, tsunamis, earthquakes, floods, and landslides. In regards to the term *disaster*, the definition of Faturechi

and Miller-Hooks [115] is used: a disaster is "an event in which such hazard has caused extensive physical damage; the event is nonrecurring and likely unanticipated, and its location, impact area, and severity cannot be predicted with certainty" [115, p. 2].

This chapter aims to set up the topic of critical road infrastructure in a natural disaster context and presents the fundamentals of GRIND. The topic of critical road infrastructure has been studied extensively in the scientific community. Section 5.1 presents concepts and studies which are related to the methodology of the AIC and DVS modules, as well as one part of the DIA module of GRIND (see Figure 4.13). Then, in Section 5.2, the literature on post-disaster impacts on road infrastructure is considered in detail as fundamentals for the TDM module and thus also for the other part of the DIA module of GRIND. Concluding from the preceding sections, Section 5.3 identifies the major gaps in existing studies. Based on the shortcomings in the related work, the prerequisites of GRIND are stated in Section 5.4.

5.1 Assessing the Functionality of Road Infrastructure in Disaster Scenarios

A variety of studies address the road infrastructure and aspects associated with disaster events involving road networks. Several concepts, methods, and performance measures exist that are used jointly. In general, a study assesses a specific concept (e. g., the concept of vulnerability), uses a particular method (e. g., a transport network analysis), and quantifies that concept by applying a performance measure (e. g., accessibility) [115]. This section aims at presenting selected studies to give an overview of the topic. A thorough review of the field and its development over time is presented by Berdica [116], Kröger and Zio [117], and Faturechi and Miller-Hooks [115].

Section 5.1.1 briefly presents seven general concepts and often-used methods. Then, selected studies are presented in Section 5.1.2, which are related to the methodologies used in GRIND. Finally, the related work on accessibility indices is presented as accessibility is used as a performance measure in the AIC module of GRIND (Section 5.1.3).

5.1.1 General Concepts and Methods

To assess road infrastructure performance in disasters, Faturechi and Miller-Hooks [115] distinguish seven interrelated concepts: risk, vulnerability, reliability, robustness, flexibility, survivability, and resilience. In the following, these concepts are described briefly. Furthermore, often-used methods to address these concepts are listed at the end of this subsection.

Risk is a concept used to characterize the threat of a disaster event with negative impact, considering its likelihood of occurrence and its consequences [115]. While risk may be a suitable measure when considering engineering failures it may be impractical for use in complex networks consisting of many components [118].

Vulnerability of a road transportation system is the susceptibility to incidents that can result in considerable reductions of the road networks serviceability [116]. Unlike risk, however, in the term vulnerability, the probability of a disaster event is not accounted for [119]. Studies assessing vulnerability are numerous. It has to be mentioned that, especially in the case of vulnerability, many alternate ways of understanding the term are found in the literature.

Reliability refers to the probability that a given element in a critical infrastructure system is functional at any given time. It is a probabilistic measure for elements in a critical infrastructure system and their ability not to fail or malfunction, given a series of established benchmarks or performance guidelines [120]. Reliability can be seen as the complement of vulnerability. While vulnerability identifies potential loss or degradation, reliability considers remaining functionality [121]. Concerning transportation networks, reliability can be characterized in three different aspects. The first is the reliability of connectivity, thus the overall possibility of reaching a chosen destination. The second is the reliability of travel time which refers to the probability of consistently arriving within a given time. The third is the capacity reliability meaning the probability of the network being invariable towards a higher traffic volume [116]. When probabilities of occurrence for failures may be significant and predictable (e. g., telecommunication networks, electric power grids,...), concepts of reliability are very common [115].

Robustness is often seen as synonymous with reliability. If they are to be distinguished, they differ in the aspect that reliability considers the probability of meeting a given level-of-service and robustness analyses the remaining functionality for a given event [115]. Originally used in computer technology [116], robustness concepts have been applied to transportation networks e. g., by Nagurney and Qiang [122] and Scott et al. [64].

Flexibility (also adaptability, agility) is defined as the ability to adapt and maintain satisfactory system performance in case of external disturbances [123]. Flexibility, as opposed to robustness, is the ability of a system to absorb changes with negative impact while robustness captures the ability to endure them [124].

Survivability is a term that is comparable to robustness. Morlok and Chang [123] define it using a supply-demand concept. They state that survivability is the fraction of the demand that can be satisfied after a disruption. The concept is mainly used in telecommunication networks [125] and needs adaptation for the use in transportation networks [126].

Resilience was initially introduced by Holling [127] as the capacity of a socio-ecological system to absorb the impact of disruptions while essentially maintaining its structure

and functions. It is often transferred to transportation infrastructures and can be measured by accounting for possible interventions that aid the system to nearly return to its pre-disaster state [115]. Numerous studies use the concept of resilience combined with other concepts [128, 129, 130].

Kröger and Zio [117] identify different methods to quantify these concepts depending on the type of the system, the available data, and the objective of analysis. Common methods are statistical analyses, which includes parametric and non-parametric models, regression analyses, hazard models, and accelerated lifetime models [e.g., 131, 132, 133, 134, 135, 136]. Additionally, probabilistic modeling like Markov chains, Petri nets, dynamic modeling, and Bayesian networks can often be found in studies [e.g., 20, 137, 138]. Probabilistic risk assessment, expert judgment, and tabular methods are all associated with the general term of risk analysis [e.g., 139]. Many studies perform simulations such as agent-based or Monte Carlo methods or use dynamic control system theory [e.g., 23, 24, 25, 140]. Finally, a wide variety of studies concentrate on complex network theory like graph theory and network flow theory [e.g., 29, 62, 64, 108, 141, 142, 143, 144, 145].

5.1.2 Exemplary Studies Organized by Performance Measure

As the concepts are too abstract to be quantified, different performance measures can be applied: travel time and distance, throughput and capacity, accessibility, topological measures, and economic measures. Performance measures can be found by considering the input and output of calculations performed in the studies. In the following, a few examples of studies using different concepts, methods and performance measures are presented and classified by performance measure. The combination of the three, characterizes a specific approach or framework.

Examples of using **travel time or distance** as a performance measure and complex network theory to model vulnerability are Jenelius et al. [119], Jenelius and Mattsson [146], and Knoop et al. [62]. While Jenelius et al. [119] and Knoop et al. [62] focus on link-level vulnerability indicators and single link failure, Jenelius and Mattsson [146] present an approach simulating area-covering disruptions. Al-Deek and Emam [135] apply a statistical analysis to road networks using the Weibull and the exponential distribution to compute travel time and capacity reliability. Also using travel time to asses reliability, Bell [147] presents a completely different two-player non-cooperative game theory approach: On the one hand, the network user tries to seek a path to minimize the expected trip cost, on the other hand, another entity chooses link degradation scenarios to maximize the expected trip cost. The effects of road closure on traffic flow patterns in New Zealand are assessed by Dalziell and Nicholson [137] to analyze the risk and impact of natural hazards on a road network. They use Monte

Carlo simulation to identify probability distributions for the costs of closure for each type of hazard and probability distributions for the benefit-cost ratios for each mitigation option.

Throughput or capacity are often used to model the concept of resilience. One example is Vugrin et al. [148] who perform a quantitative and qualitative resilience analysis of petrochemical supply chains in case of a hurricane. To describe how properties of a system can determine system resilience, three fundamental system capacities are used: absorptive capacity, adaptive capacity and restorative capacity. The framework of Vugrin et al. [148] can be used to choose different recovery strategies by comparing the resilience costs. Capacity performance measures can also assess reliability. Chen et al. [149] further develop their capacity reliability analysis by combining a reliability and uncertainty analysis, network equilibrium models and Monte Carlo methods to evaluate the performance of a degradable road network.

Murray-Tuite and Mahmassani [150], Scott et al. [64], Sullivan et al. [141] ,and Snelder et al. [136] use **topological measures** to estimate the performance of road networks [115]. Scott et al. [64] introduce the Network Robustness Index (NRI) by performing a complex network analysis to identify critical links in transportation networks. The NRI measures the criticality of a given link to the overall network and yields different highway planning solutions compared to the traditional volume-capacity ratio. The index is modified by Sullivan et al. [141] to employ a capacity-disruption level other than 100 %. Furthermore, the authors introduce the network trip robustness that can be used to compare different physical transportation networks regardless of scale, topology or level of connectivity. Snelder et al. [136] also investigate the concept of robustness and develop a framework for short term variations in supply by performing a statistical analysis. A conceptualization to model vulnerability with a game theory approach is done by Murray-Tuite and Mahmassani [150]. They look at the concept as a game between an evil entity and the traffic management agency. A key component is the vulnerability index derived from topological measures.

Finally, some studies employ **economic measures**. Tatano and Tsuchiya [151] present a framework for assessing the economic impact of seismic disruption in transportation. Economic equilibrium in the event of a disruption is calculated with a spatial computable general equilibrium model. The economic impact of major earthquakes at the New Madrid Seismic Zone in the center of the USA is described for three hypothetical scenarios in Ham et al. [26]. They use a model of inter-regional commodity flows and the corresponding transportation network flows. The results may be used to identify critical sections of the network and analyze post-event reconstruction strategies.

5.1.3 Accessibility in Critical Road Infrastructure

The introduction of accessibility indices as metrics of e.g vulnerability has been a substantial development in the research field of critical road infrastructure. Several standard measures

of accessibility exist [152, 153] that may be applied to evaluate the likely impacts of road network degradation. The advantage of employing accessibility-based metrics in such analyses is the consideration of the interaction between a degraded network and the overall travel behavior of network users [108]. A review of accessibility measures in the context of land-use and transport strategies is presented in Geurs and van Wee [154].

Accessibility analyses can provide valuable decision-aid tools for long-term network planning. Antunes et al. [155] present an accessibility-maximization approach for urban road networks. They calculate the accessibility of a center (city or region) as a sum of the spatial interactions between this center and all other centers, respectively, and analyze the transformation of the main road network of Portugal. Santos et al. [156] present a methodology to maximize accessibility in inter-urban road networks by combining accessibility and robustness objectives. Luathep et al. [142] develop an approach using a sensitivity analysis. They employ the Hansen Integral Accessibility Index [153] to assess network vulnerability based on travel time. Chen et al. [157] also propose accessibility-based performance measures but a) concentrate on the consequences of one or more link failures in terms of an increase in travel time and b) include user responses in a combined TDM. In a recent study, Weiss et al. [158] create a global map of travel time to cities to assess inequalities in accessibility in 2015 using the OSM and Google road network datasets.

Further studies consider disaster specific accessibility changes: Demirel et al. [159] demonstrate a framework to estimate the sensitivities of the European road network towards sea-level rise and storm surges by analyzing accessibility and connectivity indicators. Accessibility indicators are calculated based on travel time and traffic flow information. Lu and Peng [30] also analyze sea-level rise but focus on population and residence information along with travel time. They apply their model to the South Miami road network with two different sea-level rise scenarios. Another approach employs distance and traffic volume to derive an accessibility score to quantify the potential impact of flood damage on the transportation system [20]. Bono and Gutiérrez [160] present a network-based analysis of the impact of structural damage on urban accessibility following a disaster. They use OSM datasets to analyze the connectivity of the seismically damaged urban road network in Haiti after an earthquake of magnitude 7.0 and obtain a reduced accessibility map.

Studies that combine the concept of road network accessibility and emergency logistics planning are rare. Murawski and Church [161] aim at improving accessibility to rural health services by upgrading links of the transport network to all-weather roads. Novak and Sullivan [19] develop a new measure for evaluating accessibility to emergency services called the Critical Closeness Accessibility. They quantify the relative importance of each link in a roadway network with respect to its system-wide contribution to emergency service accessibility.

Accessibility indices are also often combined with network or vulnerability scans, which help identify critical locations in a network. The idea of vulnerability scans is to calculate

a vulnerability indicator (e.g., accessibility) in the original network and then degrading links in the network to find the links where a degradation has the largest impact on the vulnerability indicator. Taylor and Susilawati [108] perform a vulnerability scan of a road network in the south of Australia and use a remoteness and accessibility index to see the effect of link degradation for settlements. They find that the main issue with network scans is computational efficiency as degrading every link in a network and recalculating all pairs of shortest paths every time is very expensive computationally.

5.2 Post-Disaster Impact Assessment of Road Infrastructure

The reaction of humans to a disaster can be separated in different temporal phases. The mitigation and preparedness phase before a disaster as well as the response and recovery stage during and after an event. Disaster impacts can be considered before an event in the mitigation and preparedness phase as the impact of past or spatially distant disasters. Then, they serve as a learning experience for potential future events. In the post-disaster phase at the response and recovery stage, disaster impacts have to be assessed to develop a response strategy and estimate the damages and losses caused by the disaster. [162]

Disaster impacts are classified into two categories: direct and indirect impacts [163] or sometimes also damages and losses [164]. The impact of the destruction of social, environmental, or economic capital caused by a disaster event is summarized as direct impact [163] or damage [164]. Indirect impacts or losses [164] are secondary occurrences, induced by direct impacts, and often happen temporally and spatially distanced from the disaster event [163]. Focusing on the road infrastructure, direct impacts are tied to the value of investment required to replace the physical assets. Indirect impacts are connected to changes in transport flow due to the disaster and are mainly measured as an increase in travel time.

While most assessments contain an estimation of direct impact, indirect impacts are often ignored because they are more difficult to estimate after a disaster [165]. As an example, Post Disaster Needs Assessments (PDNAs) of different disasters worldwide can be considered. The indirect transport impacts account for less than 3 % of the total transport impacts for the earthquakes in Mexico (2003) and Peru (2011), the floods in Mexico (2012), and the hurricanes in Fiji (2016) and Jamaica (2010) [166, 167, 168, 169, 170]. This phenomenon can be observed in many PDNAs and is caused by a lack of data to assess indirect transport impacts with traditional methods [166, 167, 168, 169, 170].

Gajanayake et al. [163] categorize related studies in two categories: transport network analysis and transport modeling. They define transport network analysis as a branch of network theory that uses the road network's functionality to measure disaster impacts. In contrast, transport modeling employs transport models based on transport demand functions

to assess impacts [163]. These types of methods have typically been used separately [163] in past impact assessments. The related studies on post-disaster impact assessment generally apply the concepts, methods, and performance measures presented in Section 5.1.

The AIC module of GRIND features a transport network analysis while the TDM module uses transport modeling. In the DIA module, the AIC and TDM modules are used jointly. Thus, this section presents the fundamentals of both categories of studies. Section 5.2.1 lists selected transport network analysis studies and summarizes their advantages and disadvantages. The concept of transport modeling for impact assessments is described with exemplary studies and analyzed in Section 5.2.2.

5.2.1 Transport Network Analysis

Transport network analysis analyzes the transport network from a top-down, graph theory perspective as it considers the network as sets of links and nodes. A transport network's reduction in serviceability caused by a (natural) disaster is taken to measure the transport impact. Transport network analysis methods assume that the pre-disaster serviceability is the optimal level of service. The results of these approaches are often presented as a percentage or ratio of reduction in functionality. [163]

Transport network analysis approaches can be split in two categories [163]: topological and system-based approaches. Topological approaches are based on the number of links and nodes of a road network that are serviceable after a disaster. The approach by Bono and Gutiérrez [160], mentioned above in Section 5.1.3, is such a topological approach. Also, Muriel-Villegas et al. [171] present a topological approach analyzing connectivity reliability and the vulnerability of interurban transportation systems under network disruptions like flooding. As a result, a connectivity reliability index is obtained. Generally, topological approaches like [172, 173] rely on graph-based measures like centrality measures (e.g., betweenness centrality), connectivity measures (e.g., giant connected component), and network distances (e.g., network efficiency [174]). Graph-based evaluation is a powerful tool to detect, for example, critical nodes and vulnerable locations in a network [175]. However, the results of topological approaches are generally abstract performance measures like indices that lack comparability and require background knowledge to be interpreted.

System-based approaches allow for a greater variety of consequences to be measured and presented intuitively [130]. Impacts are often measured as average travel time or distance increases. For example, Chang and Nojima [176] use a system-based approach to measure the post-disaster transportation system performance with a case study of the Kobe earthquake in the year 1995. They propose three system performance measures that are based on accessibility. This is further developed into an accessibility index to assess the overall and distributional impacts of disasters [177]. In a different system-based approach, Utasse et al. [178] perform

a vulnerability assessment of alpine roads to a specific debris flow event. They measure accessibility as a travel time difference before and after the event to assess the impact.

One advantage of transport network analysis is that it generally allows for an impact-assessment of multiple disruptions, common in natural disaster scenarios. However, the focus of the method is to analyze the functionality of the road network. This focus renders the assignment of monetary costs to indirect impacts difficult. [163]

5.2.2 Transport Modeling

Transport modeling is a bottom-up approach to estimate the number of people using a particular mode of transport [163]. It can be used to model, for example, average daily traffic in road networks. Transport models are also used to assess the post-disaster impact on transport networks by accounting for commuter behavior changes after a disaster. Transport models typically follow four stages: Trip generation, trip distribution, modal split, and trip assignment (see Section 6.4.1) [179].

Researchers developing transport models either use basic equations to manually calculate the travel demand [e.g., 27, 28, 180] or use transport modeling software to set up the transport model [e.g., 21, 22, 181, 182, 183]. The objective of these studies is generally to assess the economic impact as the cost of delay for a specific disaster. For example, Negi et al. [27] perform a cost assessment of losses due to a landslide in India, and Wesemann et al. [28] assess the cost of delay for freeway closures due to an earthquake. Similarly, Winter et al. [183] and Pfurtscheller, Genovese, et al. [180] analyze the economic losses due to landslides in Scotland and Austria. Gajanayake et al. [163] find that different indicators are used to estimate the total cost of delay like an increase in individual travel time [e.g., 21, 27, 28, 183], additional fuel cost [e.g., 27, 28, 180], additional travel fare [e.g., 27, 180], additional emissions [e.g., 21, 183], and pavement maintenance and congestion costs [180, 21]. Most studies demonstrate that the cost for rerouting and delay accounts for the majority of total losses [e.g., 21, 27, 183].

Outside the scientific community, procedures exist which are in practice worldwide to assess direct and indirect impacts to road infrastructure after a disaster. A Post Disaster Needs Assessment (PDNA), which is generally performed after a natural disaster, aims at calculating the economic costs of disasters by assessing direct and indirect impacts. The United Nations - Economic Commission for Latin America and the Caribbean [164] and the Global Facility for Disaster Reduction and Recovery, together with the Worldbank [184], present guidelines for these PDNAs in the transport sector. Both methodologies require recent OD surveys in the affected area and operating costs for different vehicles [164, 184]. To estimate the total cost of indirect impacts, the cost of temporarily interrupted transport of cargo and persons and the value of temporary decline in toll receipts is considered [184].

Additionally, the Worldbank guidelines [184] account for the urgent expenditures made to reopen traffic and the higher cost in transportation due to the temporary utilization of alternative (longer and lower quality) roads. As part of the procedure, transport modeling is performed to estimate the total cost of delays.

In conclusion, transport models are widely used both in the scientific community and by governments worldwide to assess the indirect impact of disaster events. Their popularity stems from the possibility of presenting the results using a monetary value that is easier to interpret for practitioners. However, transport models require many input data. Origin and destination surveys and traffic flow data are often unavailable which hinders traditional transport modeling approaches. Furthermore, transport models are often built for cities or smaller regions and rarely consider entire countries [163]. Especially for country-scale disasters, these limitations hinder the post-disaster impact assessment.

5.3 Summary of the Major Gaps of Existing Approaches

The most relevant issue of related approaches is data availability on a global scale. Most studies of the above-quoted studies use commercial or administrative road network data, which is only applicable to the city, region, or town of interest and also often not freely available to the general public. Furthermore, many approaches rely on a combination of complex datasets, including traffic volume, capacity, OD surveys, and traffic flow [e.g., 19, 20, 26, 164]. These datasets increase the accuracy of, for example, impact assessments, but they are not available worldwide. Especially in regions with a relatively low GDP per capita and frequent natural disasters like Latin America and South-East Asia, this data is often not even available to local authorities for a PDNA [166, 167, 168, 169, 170]. Moreover, more complicated datasets increase both computing time and, more importantly, the time the study itself takes as the datasets have to be found and often preprocessed. In this thesis, only one study by Weiss et al. [158] is found that successfully applies OSM data on a global scale, but still in combination with other commercial data.

Considering the scale of different studies, most researchers focus on a local or regional scale and analyze one specific region or city [e.g., 26, 27, 28]. Few generic approaches exist [e.g., 158, 157]. Additionally, many researchers study critical road networks in urban environments [e.g., 29, 30, 172], but few focus on rural road networks. However, rural road networks have to be considered especially because large disparities prevail between rural and urban communities [185], for example in access to emergency facilities. A generic approach, which can be applied to different geographical scales, considers local road conditions, focuses predominantly on rural road networks, and includes the challenge of handling limited global data availability is not yet developed.

Gajanayake et al. [163] state that transport network analysis and transport modeling approaches have been used separately in the past. Studies combining these methods or using both of them to assess different aspects of post-disaster impacts do not yet exist. However, such an approach could be useful, especially for disaster management, who have to consider all aspects of post-disaster impacts to develop a response strategy.

Furthermore, most disaster-related studies focus on the impact of hurricanes [e.g., 148], flooding [e.g., 30, 159, 171], earthquakes [e.g., 26, 137, 151, 160], or landslides [e.g., 27, 178, 183]. Wildfires are rarely analyzed in related studies even though they often cause considerable damage to the road infrastructure [186]. Because of climate change, extreme temperatures and droughts occur more frequently than before and favor wildfires in many countries worldwide [65]. The recovery time of road networks after wildfires is often shorter than for other natural disasters [111]. Therefore, some studies focus on the evacuation of the affected population [187, 188]. However, the closure of roads during and after wildfires, for example, because of the danger of falling trees, or subsequent landslides, can cause massive indirect impacts that are rarely considered in the literature.

Finally, vulnerability scanning is widely used to identify network components where a failure or degradation has the largest impacts [e.g., 108, 119, 156, 189, 190, 191]. Studies use vulnerability scans to find vulnerable locations in the original network before disasters happen in the mitigation and preparedness phase. But, to this date, a vulnerability scan has not been performed during a long-lasting disaster such as wildfires to assess where a spread of such a disaster would be most critical.

5.4 Prerequisites for GRIND

Following the major gaps of existing approaches identified in Section 5.3, **GRIND** is designed, which uses the enhanced OSM data generated in Part I to perform pre- and post-disaster assessment of critical road infrastructure. Before developing the methodology, it is important to outline the prerequisites which are relevant to the generic approach. This approach is supposed to be applicable to a) a wide range of regions, b) heterogeneous data availability, c) different spatial scales d) analytical as well as prognostic studies [..., and e) various aspects of disaster impacts.] In order to fulfill these prerequisites, the following four conditions have to be met:

1. Data simplicity, due to the need to perform on relatively simple datasets like point and line vector data, which are widely available and readily applicable.

2. Data sparsity, in the sense that the concept does not depend on complex datasets such as traffic flow, [capacity,] or observations on travelers behavior. Such datasets, first of all, are not available worldwide and secondly, their behavior is hard to predict in

face of disasters. They could be used to produce analytical tasks but not to perform prognostic studies.

3. Adaptability to local road conditions, because in many regions, road quality differs significantly.
4. Flexibility towards disaster management requirements, because many different aspects of disaster consequences might have to be considered.

6 Methodology of the Critical Infrastructure Assessment

This section describes the methodology of the modules in the second part of GRIND (see Figure 4.13). It first presents the CM in Section 6.1 and introduces the methodology for creating a populated places dataset in Section 6.2. Then, the TDM module (see Section 6.4) and the AIC module (see Section 6.3) are described. The DIA and DVS modules are presented in Section 6.5 and Section 6.6.

6.1 Core Module

The CM uses the enhanced OSM data to calculate travel times between locations. It consists of selecting and preparing the OSM data for a study region, a workflow to integrate locations into the road network, and the shortest path calculation. All other modules of the second part of GRIND rely on the workflow in the CM. As input data, the CM requires the enhanced OSM data as well as origin and destination input locations.

In the first part of the CM, the OSM data for a respective region is selected using the boundary polygon (`boundary=administrative` see Section 2.3) or a bounding box to cut the input OSM data. The Fuzzy-FSE and the Error Search module, which are presented in Part I, preprocess the OSM road network in a routable graph, such that it consists of edges and nodes at every real intersection of edges. The spatial scale of the road network can be adapted by choosing the appropriate level of detail. For example, L1-L3 (see Table 2.1) could be chosen for a national analysis with an area of more than 100 000 km^2, and all levels could be selected for a local case study (area $<$ 5000 km^2). To avoid errors at the region's borders, roads, populated places, and facilities within a predefined perimeter percentage of the region area are included in the calculation.

The second step of the CM integrates origin and destination locations, represented as points, into the graph. A set of locations L, with $L \equiv l_1, l_2, ..., l_r$ is integrated into the network. For each location l_r, the nearest point on a road l_p is identified and the euclidean distance to the location l_r is calculated. Then, l_p is inserted into the network graph as a new node. The edge e_m, where l_p is located on, is split into two parts by l_p.

The third step of the CM implements the Dijkstra Algorithm [192] to calculate all shortest paths from all input origins to all input destinations. In the core module in our previous study, Guth et al. [65], we employ road distances multiplied by a weighting factor that depends on the road class. As a result, a region specific cost factor for the network is obtained. For this thesis, weighting factors are no longer necessary as the travel times calculated by the Fuzzy-FSE can be used. The speed values estimated with only OSM data are used to reduce the amount of data necessary for the concept. The road segments, created in the second step of the CM, between the input locations and the road network, are also assigned a speed value. The CM provides all travel times on the shortest paths from all input origins to all input destinations in the selected study region as an output.

6.2 The Populated Places Dataset

For some GRIND modules, settlements are required as point data that can later serve as origin or destination for routing applications. Additionally, for various GRIND modules, the population of each settlement is required. To obtain each settlement's population in OSM, we use the Global Human Settlement Population Grid (GHS-POP). In this section, the GHS-POP dataset is presented. Then, the workflow to derive the population of each settlement is described and evaluated.

6.2.1 The Global Human Settlement Population Grid

The GHS-POP [193] is a spatial raster dataset that depicts population distribution, expressed as the number of inhabitants per cell. The raster dataset has a maximal resolution of 250 m and features global coverage. The most recent GHS-POP raster, which is used in this thesis, was created in 2015. The dataset is part of the Global Human Settlement Layer project founded by the European Commission and the Geo Human Planet Initiative.

The generation of the GHS-POP data is described in detail in Freire et al. [194]. To obtain the GHS-POP raster, best-available population estimates for the years 1975, 1990, 2000 and 2015 are combined with best-available assessment of the spatial extent of human settlements as inferred from satellite imagery. Freire et al. [194] use population estimates from the CIESIN. The CIESIN data consists of country-based layers of the census and administrative polygons that contain the residential population for the target years. Population data are collected at the highest possible spatial resolution, which varies by country [194]. The spatial extent of human settlements is inferred from Landsat and Sentinel-1 data with a fully automatic supervised classification workflow [195]. The resulting dataset is called GHS-BUILT and achieves a R^2 of 89 % [195]. For the GHS-POP dataset, the GHS-BUILT

raster is combined with the CIESIN data based on raster-based asymmetric mapping (for details see [194]). This asymmetric mapping ensures that the total input population is preserved [194]. The GHS-POP dataset is validated against the official GEOSTAT 2011 resident population, and a correlation analysis yields an R^2 of 83 % [194].

6.2.2 From Gridded Population to Population per Settlement

OSM settlement data is combined with GHS-POP data to obtain a global dataset with settlements as points together with their population. This workflow consists of three steps, which are described in the following: 1. Extracting relevant settlement point data from OSM, 2. Creating Voronoi polygons from the point data, and 3. Intersecting the GHS-POP raster with the Voronoi polygons.

1. The first step to obtain settlements with their population is to extract OSM point data using the `place=*` tag, which is described in detail in Section 2.3. All settlements with the tags `place=city`, `place=town`, and `place=village` are selected and combined in a point layer. Settlements with the tag `place=hamlet` are not used because a visual assessment has shown that in OSM, the value `hamlet` is often wrongly assigned not to settlements but places of interest. The result is a global point dataset of populated places.

2. In a second step, Voronoi cells are created for these populated places. A Voronoi cell consists of every point in a Euclidean plane where the distance to the corresponding point is not greater than the distance to the other points in the plane. These Voronoi cells then form polygons. Voronoi polygons are calculated for each country separately to avoid problems with the ocean and with country borders, using the OSM state boundaries (see Section 2.3). The resulting Voronoi polygons for each country are then combined in a global polygon layer. Figure 6.1 shows exemplary Voronoi polygons for settlements in NSW in Australia.

3. In the last step, the GHS-POP data is combined with the Voronoi polygons. For that, a point layer from GHS-POP is created with centroids of each raster cell. The population values of all centroids intersecting with the respective Voronoi polygon are then added to obtain the corresponding settlement's population. The presented workflow preserves the total input population from the original census data GHS-POP is based on. The boundaries of exemplary Voronoi polygons and the GHS-POP raster data are displayed in Figure 6.1 (right) for settlements in NSW.

The resulting populated places dataset may contain large inaccuracies that stem from different sources. The first source of inaccuracies lies in the GHS-POP dataset. It is a product derived from built-up area and census data and may contain estimation errors

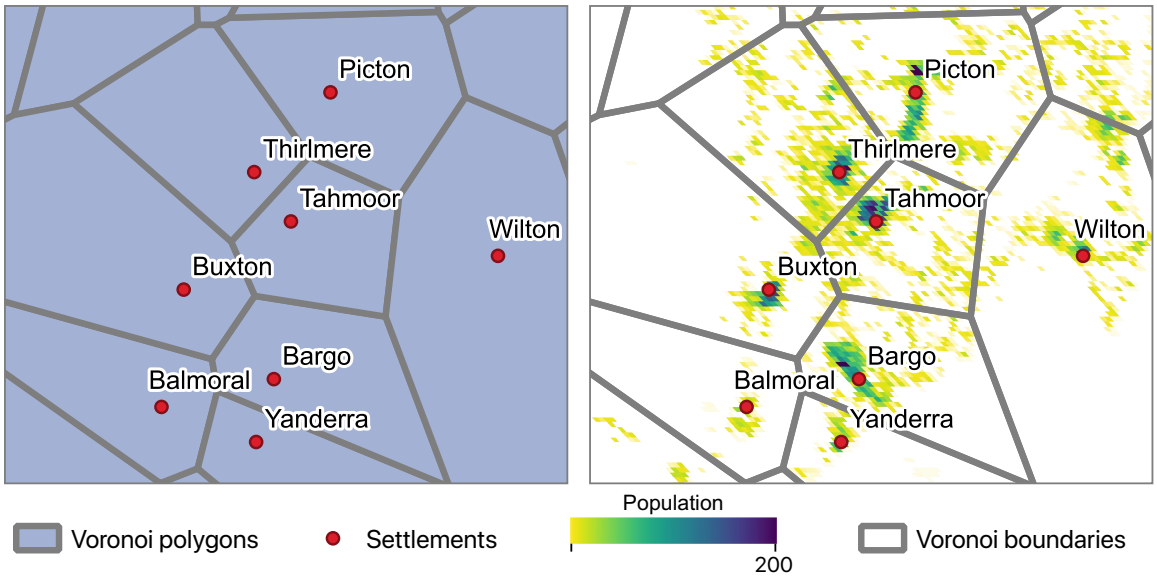

Figure 6.1: Exemplary Voronoi polygons for settlements in Australia (left). On the right, the same area with the gray boundaries of the Voronoi polygons is displayed together with the Global Human Settlement Population data. White raster cells are cells without population.

regarding the distribution of the population. Furthermore, as discussed in Section 2.4, the OSM data often contains errors such that settlements may be missing, or there may be extra settlements. For example, three settlements exist for Canberra: Canberra itself, North Canberra, and South Canberra.

Additionally, there are inaccuracies in the presented workflow to combine OSM and GHS-POP data. As the layout of settlements is often defined by natural boundaries or historical evolution, it does not always fit the form of the corresponding Voronoi polygon. Then, the population is wrongly assigned to the neighboring Voronoi polygon. A manual evaluation against 2016 census data from the Australian Bureau of Statistics [196] has shown that the workflow considerably underestimates larger settlements and slightly overestimates smaller towns. The estimation for smaller villages is relatively accurate as smaller villages are often further apart and thus fit into the Voronoi polygon. Differences between the estimation and the census data are also due to the OSM data, which often has multiple settlements close to each other, which census data only counts as one settlement. However, the total input population from the GHS-POP, which is constructed with census data, is preserved, such that inaccuracies might be present in the distribution of the population but not in the total amount of population.

This simple workflow allows the generation of a global populated places dataset using only freely-available, global data sources which accounts for conditions one and two in Section 5.4. To obtain origins and destinations for routing applications where the resulting population value can be a rough estimate, this dataset is sufficient, especially since the total population

is preserved. For other applications where a more accurate population value per settlement is necessary, the workflow might have to be improved.

6.3 Accessibility Index Calculation

GRIND enables the calculation of two different accessibility indices: the Accessibility and Remoteness Index of Australia (ARIA) [197] and the Emergency Facility Accessibility Index (EFAI) [65]. The AIC module requires input points of origins and destinations (emergency facilities and service centers) and the enhanced OSM road network to calculate both indices. Input points can be point data like the populated places dataset but also centroids of grid cells. The grid-based calculation enables the analysis of an entire area, as opposed to the point-based analysis where the indices are only calculated for single localities. Different grid resolutions, combined with different levels of detail in the road network, enable the calculation on multiple scales [65].

The ARIA and its calculation are presented in Section 6.3.1. In Section 6.3.2, the calculation of the EFAI is described. Both indices are adapted for this thesis to use the travel time calculated by the Fuzzy-FSE instead of road distances.

6.3.1 Accessibility and Remoteness Index of Australia

The ARIA was developed by the National Center for Social Applications of GIS as a joint project with the Australian Department of Health and Ageing in 1998 [197]. The ARIA is designed to be comprehensive, sufficiently detailed, as simple as possible, transparent, defensible, and stable over time. As it is supposed to be an unambiguously geographical approach to define remoteness, socio-economic and urban or rural factors are not incorporated in the measure [198].

The ARIA is a continuous index that is calculated initially based on road distance measurements from over 12 000 populated localities to the nearest service centers. For this thesis, the ARIA is adapted to use the travel time calculated by the Fuzzy-FSE instead of road distance. Travel time incorporates the road network hierarchy because vehicles can travel faster on high-level roads than on low-level roads. If road distance is used as a cost factor of the road network, all road classes are treated equally, resulting in paths that would normally not be traveled. Service centers are populated localities with a population greater than 1000 and are classified into five categories based on population size (Table 6.1). Each category offers distinct levels of public and private sector facility availability [108]. The populated places dataset (see Section 6.2) serves as input data for the service centers.

Table 6.1: ARIA service centre categories A-E [108].

Service center category	Population
A	$\geq$ 250 000
B	48 000 - 249 999
C	18 000 - 47 999
D	5000 - 17 999
E	1000 - 4999

The ARIA for GRIND is calculated with the travel time t_{iL} a person requires to travel along the road network from a locality i to the nearest service center in category L for L = A, B, C, D, E (as defined in Table 6.1). The ratio between t_{iL} and the mean travel time $\overline{t_L}$ of all localities to the nearest category L service center is calculated. To remove the effects of remaining extreme values, a threshold of three for the t_{iL} and $\overline{t_L}$ ratio is set. All t_{iL}, $\overline{t_L}$ ratios are summed up to obtain an ARIA value between 0 (high accessibility) and 15 (high remoteness). Equation (6.1) shows the calculation of the ARIA for locality i [108].

$$\mathrm{ARIA}_i = \sum_L \min\left\{3, \frac{t_{iL}}{\overline{t_L}}\right\} \tag{6.1}$$

The minimum travel time to larger centers are substituted for minimum travel times to smaller centers if the former is shorter than the latter. It is assumed that a higher category service center can provide the same services and more than a lower category service center.

The index's aim is to quantify accessibility in non-metropolitan Australia; thus, it does not consider intra-urban accessibility at all. However, customized ARIA versions have been developed, including the Metro ARIA that combines intra-urban accessibility to education, health, shopping, public transport and financial or post services [199].

6.3.2 Emergency Facility Accessibility Index

In Guth et al. [65], a new accessibility index, the EFAI, is designed based on the above-described ARIA. The EFAI is also a continuous index and considers access to facilities required in disaster cases: hospitals, police, and fire stations. The OSM tags `amenity=hospital`, `amenity=police`, and `amenity=fire_station` are used as facility locations (see Section 2.3). For GRIND, the EFAI for an origin i is defined as:

$$\mathrm{EFAI}_i = \sum_F \min\left\{3, \frac{t_{iF}}{\overline{t_F}}\right\}, \tag{6.2}$$

The factor t_{iF} represents the travel time from origin i to the nearest facility F. $\overline{t_F}$ is the mean travel time of all origins to the respective nearest facility F. The normalization enables the index to be relative to local road conditions of infrastructure development [65].

In contrast to Guth et al. [65], travel times are used instead of a class-dependent weighting factor for the road distance. For the previous study, no speed information was available, such that a weighting factor was used to account for different road hierarchy levels and qualities [65]. With the **Fuzzy-FSE**, a speed estimation is enabled, which already includes adaptations to local road conditions.

6.4 Travel Demand Model

The **TDM** module enables generating a simple Travel Demand Model (TDM) for intercity transport, solely based on OSM and population data. For that, the populated places dataset created in Section 6.2 and the OSM road network with travel times per road segment calculated in Chapter 3 is used. In this section, the classic four-stage TDM (Section 6.4.1) is introduced. This TDM is then adapted to enable the estimation of average daily trips from OSM and population data, only.

6.4.1 The Traditional Four-Stage Travel Demand Model

The development of TDMs to support transport planning is a vast and long-standing research area that is continually evolving. Travel demand models are usually used to estimate the number of people traveling in a network using a particular mode of transport from a bottom-up approach. Generally, models are a simplified representation of a part of the real world that focuses on certain elements considered important from a particular perspective [179]. The same is true for TDMs as they attempt to replicate the system of interest and its behavior. However, their value is limited to a specified range of problems under specific conditions [179]. The choice of a modeling approach is dependent, among other things, on the precision and accuracy required for the model, the level of detail required for the model, the availability of data, and the resources available for the study [179].

Years of experimentation and development in the field have resulted in a classic four-stage TDM: trip generation, trip distribution, mode choice, and trip assignment (see Figure 6.2). Ideally, the underlying data includes base-year levels of population of different types in each zone of the study area and levels of activities like employment, shopping space, educational and recreational facilities. Furthermore, OD surveys in the considered region serve as baseline for people's travel behavior. In the trip generation stage, this data is used to estimate the number of trips generated and attracted by each zone of the study area. The

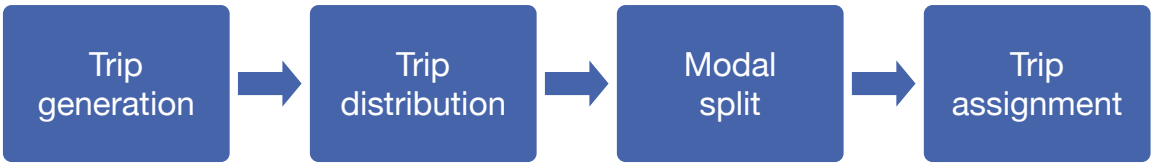

Figure 6.2: The traditional four-stage Travel Demand Model.

next stage, the trip distribution, follows with the allocation of these trips from origins to different destinations, which produces an OD matrix. In the modal split, trips in the matrix are allocated to different traffic modes (e.g., private vehicle, bus, tram) using a mode choice sub-model. Finally, the assignment of trips or route choice is the last stage of the classic TDM. In this stage, trips are assigned to their corresponding networks (public and private transport) by appointing them to paths in the network. [179]

As the road network is the focus of this thesis, only the road network and vehicle travel are considered for the TDM such that the modal split can be disregarded for this TDM. The trip generation sub-model usually estimates the number of trips produced and attracted by a zone or location by using household characteristics like the number of people and vehicles in a household, employment level, shopping space and educational and recreational facilities. However, the required data may differ depending on the level of detail of the model. For example, intracity travel behavior differs significantly from intercity travel behavior, where other factors have to be considered.

The trip distribution matches origins and destinations to develop an OD matrix as number of trips from every origin to every destination. The input values are the trips produced (G_i) and attracted (A_j) for each zone calculated in the first stage of the TDM. A trip distribution model follows two key principles: big producers attract more trips than small producers, and nearby zones attract more trips than far-away zones. A general model to distribute trips is given as:

$$T_{ij} = G_i \cdot \frac{A_j \cdot f(w_{ij})}{\sum_j A_j \cdot f(w_{ij})}, \tag{6.3}$$

where T_{ij} is the number of trips between origin i and destination j, G_i is the number of trips generated in origin i, A_j is the attractiveness of destination j and $f(w_{ij})$ is a resistance function. Two resistance functions that are frequently used are:

$$\text{(a)} \quad f(w_{ij}) = w_{ij}^{\alpha}, \qquad \text{(b)} \quad f(w_{ij}) = e^{\alpha \cdot w_{ij}}, \tag{6.4}$$

where α is a measure of cost decay, and w_{ij} is a cost factor in the network like network distance, travel time, or fuel consumption. Equation (6.3), in combination with the resistance function (a) in Equation (6.4), results in the classic gravity model. The combination of Equation (6.3), and the resistance function (b) in Equation (6.4) yields a utility maximization model that is based on a gravity model.

The last step is the trip assignment. It concerns the selection of paths between origins and destinations in the network. The specific path a trip travels is identified and the trips are then assigned to that path. The process involves a shortest path calculation for every OD pair. Ideally, the assigned trip volume is then compared to the capacity of the link. If the capacity of a link is exceeded, the travel time for the shortest paths changes and some trips might have to be reassigned. Thus, the trip assignment process is repeated several times until there is an equilibrium between travel demand and travel supply.

6.4.2 Development of a Travel Demand Model from OSM

The TDM is designed using only freely and globally available data accounting for conditions one and two in Section 5.4. The TDM is supposed to work with minimal data input and for intercity and rural transport. It is not intended to model transport within cities or large urban areas, as different input data is necessary for such a model. The OSM road network is used as a transport network, and the populated places dataset created in Section 6.2 is applied as origins and destinations. The network's cost factor is travel time, which is obtained by applying the Fuzzy-FSE (see Chapter 3). The population of each origin and destination serves as an estimate for the number of trips produced and attracted by a location or, in this case, populated place.

The TDM is similar to the TDM in Scott et al. [64] and is based on Equation (6.3). In the trip generation stage, the number of trips produced in a populated place per day is derived from the population like Scott et al. [64]. However, as multiplying the population by 1.5 in every populated place (like Scott et al. [64]) results in too many intercity trips for large cities, an exponential function depending on the population is employed. For the TDM, the number of trips per day generated in origin i (G_i) is calculated as the population of origin i (P_i) times the number of trips per person generated in origin i (g):

$$\begin{aligned} G_i &= P_i \cdot g \\ \text{with} \quad g &= g_{max} \cdot e^{-\alpha \cdot P_i}. \end{aligned} \tag{6.5}$$

The parameter α determines the slope of the function. For intercity transport, we hypothesize that α should be set such that small villages produce the maximum number of trips per day (g_{max}) as they probably have to travel for all basic necessities. We assume that large cities produce almost zero trips per day for intercity transport as most of their necessities can be met within the city. This assumption might have to be adapted to the cultural background of different study regions. Figure 6.3 shows Equation (6.5) with exemplary α values for $g_{max} = 1.5$.

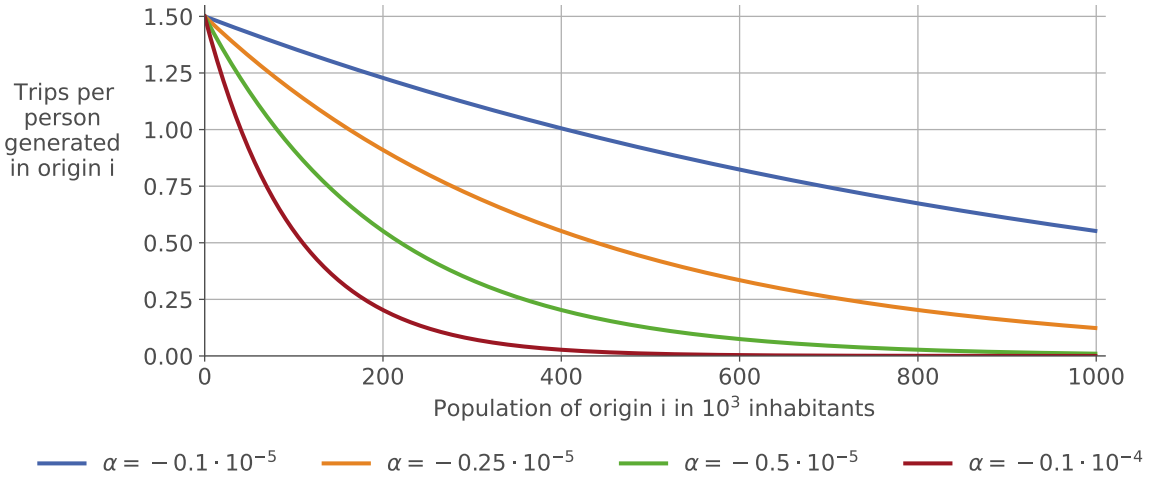

Figure 6.3: Exemplary measure of cost decay α values for Equation (6.5) with $g_{max} = 1.5$.

Then, the trip distribution sub-model is designed. The attraction of a destination j is also based on its population (P_j). As resistance function $f(w_{ij})$, a logit function is employed based on the cost decay factor β and the travel time from origin i to destination j C_{ij}:

$$f(w_{ij}) = e^{-\beta \cdot C_{ij}}. \tag{6.6}$$

A utility maximization model is chosen so that the resistance increase reflects the actual travel behavior more accurately than with the basic gravity model. The combination of both stages, trip generation, and trip distribution results in the following intercity TDM:

$$T_{ij} = P_i \cdot g_{max} \cdot e^{-\alpha \cdot P_i} \cdot \frac{P_j \cdot e^{-\beta \cdot C_{ij}}}{\sum_j P_j \cdot e^{-\beta \cdot C_{ij}}}. \tag{6.7}$$

In the trip assignment stage, trips are assigned to their paths by calculating the shortest path for every OD-pair. As capacity data is not available in OSM, the capacity of a link is not accounted for. Thus, a capacity overflow of a link is not considered and each trip is assigned to the shortest path.

Three parameters exist that have to be adapted for each study region to fit the TDM to local travel behavior. During the trip generation stage, the parameters g_{max} and α are set. In the trip distribution stage, the cost decay factor β is set. The parameters can either be adapted by employing expert knowledge about local travel behavior or using reference data of daily traffic volume in that region.

6.5 Disaster Impact Assessment

The assessment of disaster impacts on critical road infrastructure is a broad research field (see Section 5.2). In this thesis, two distinct approaches are presented to quantify the impact of a natural disaster on the road network with OSM data. On the one hand, a transport network analysis is performed, which measures the impact as a decrease of accessibility to the respective locations in the **AIC** module. On the other hand, the **TDM** module, developed in Section 6.4, is applied to account for the change in average daily travel time. These distinct approaches can highlight different aspects of natural disaster impacts on the road network, which might be helpful for disaster management.

The **DIA** module requires the information, which roads are impassable, for example, in a natural disaster. It degrades impassable roads by deleting them from the road network. The resulting road network is herein called a degraded network. Furthermore, the **DIA** module requires input data from the **AIC** module (see Section 6.3) and **TDM** module (see Section 6.4). It uses both of the modules mentioned above to calculate different aspects of natural disaster impacts on the road network. It has to be considered, that all aspects of natural disaster impacts can only be calculated for a connected network. Locations where the nearest road is a disconnected network component are considered completely disconnected.

This section presents both approaches to natural disaster impact assessment. The transport network analysis is described in Section 6.5.1. Section 6.5.2 describes the natural disaster impact assessment with a TDM.

6.5.1 Network Analysis Disaster Impact Assessment

The Network Analysis Disaster Impact Assessment (NADIA) measures the impact as a decrease of accessibility to (a) service centers and (b) emergency facilities. This enables the module to consider two different aspects of accessibility. The accessibility to service centers is essential for the impact on the every-day needs of the affected population. The impact on the accessibility to emergency facilities is relevant because these facilities are often required in emergencies. The module uses the **CM** and the **AIC** module of **GRIND**. The decrease of accessibility can be measured both as an absolute measure like a travel time difference and a relative measure like an index difference.

As an absolute measure of accessibility decrease, the travel time to (a) all service centers and (b) all emergency facilities is calculated in the original and degraded network for every input locality. Input localities can, for example, be settlements for a point-based analysis or centroids of grid cells for an area-based calculation. The difference in travel time between the original and degraded network serves as an absolute measure of accessibility decrease to emergency facilities or service centers.

The relative measure of accessibility decrease is the ARIA and EFAI index difference. The ARIA-Impact$_i$ for origin i can be calculated as:

$$\text{ARIA-Impact}_i = \sum_L \frac{t_{iL\ deg}}{\overline{t_L}} - \sum_L \frac{t_{iL}}{\overline{t_L}}, \tag{6.8}$$

with $t_{iL\ deg}$ being the travel time to the nearest service center L in the degraded network. Similarly, the EFAI-Impact$_i$ for origin i is calculated like in Guth et al. [65] but with travel time instead of road distance combined with a weighting factor:

$$\text{EFAI-Impact}_i = \sum_F \frac{t_{iF\ deg}}{\overline{t_F}} - \sum_F \frac{t_{iF}}{\overline{t_F}}. \tag{6.9}$$

$t_{iF\ deg}$ is the travel time to the nearest facility F in the degraded network. For both index impact calculations, no threshold is set. Like the absolute measure, it can also be calculated both point-based and area-based.

6.5.2 Travel Demand Model Disaster Impact Assessment

The Travel Demand Model Disaster Impact Assessment (TDMDIA) measures the impact of a natural disaster in travel time increase for average daily traffic. The module uses the **CM** to calculate travel times and the **TDM** module to obtain average daily trips for each location. In this case, the impact can only be calculated for populated places and not grid-based as the **TDM** module requires populated places as origins and destinations.

The travel time from all populated places to each other is calculated in the original and in the degraded network. The **TDM** provides the number of average daily trips for each combination. For this assessment the same number of average daily trips is assumed before and after the natural disaster scenario. The TM-Impact$_i$ is calculated by using the sum of the travel times of all daily trips from i to all j in the original and in the degraded network:

$$\text{TM-Impact}_i = (\sum_j t_{ij\ deg} \cdot T_{ij}) - (\sum_j t_{ij} \cdot T_{ij}), \tag{6.10}$$

with t_{ij} as the travel time from populated place i to populated place j in the original network, T_{ij} as the number of trips from i to j (calculated in the **TDM** module), and $t_{ij\ deg}$ as the travel time from populated place i to populated place j in the degraded network. As a result, the impact of a natural disaster as change in average daily travel time from i to all j is provided for each populated place. If the origin i and the destination j are disconnected from each other by the natural disaster, the impact is not calculated for this OD-pair. Like this, the TDMDIA is also able to assess the number of disconnected daily trips per populated place, which is an important information in a natural disaster scenario.

6.6 Disaster Vulnerability Scan

The DVS module is designed to identify the most vulnerable roads during a disaster scenario in case of a further spread of this scenario. In this case, it is developed for the application in wildfire scenarios. However, it can be used for other long-lasting natural disasters with a certain potential to grow like flooding events. The module uses the CM to calculate travel times as well as the AIC module and the TDM module to find vulnerable road segments. Furthermore, it requires a disaster footprint in the form of a polygon. For this thesis, the currently burning region of a wildfire scenario is used.

The DVS consists of five steps:

1. Creating different scenarios of disaster spread.
2. Calculating vulnerability indicators for the network, which is currently degraded by the natural disaster, herein called degraded network.
3. Degrading the network further by deleting additional roads, respectively, for each scenario of disaster spread. These networks are herein called double degraded networks.
4. Calculating vulnerability indicators for the double degraded network in each scenario of disaster spread.
5. Determining the resulting changes in the vulnerability indicators to identify the most critical roads in a scenario of disaster spread.

To simulate the disaster spread in case of a wildfire, the currently burning area polygon is used. The edge of the polygon is split into segments of a certain length. Listing 6.1 shows an exemplary implementation of a PL/Python procedural language function to cut a polygon into segments of a given length. Then, buffers around each segment are drawn to simulate the wildfire growth in the respective area. Each buffer represents one scenario of wildfire spread. These buffers overlap to include neighborhood effects. The probability of each scenario, which is based on many factors like wind direction, temperature, or availability of flammable material, is not considered. The scenario buffer generation is illustrated in Figure 6.4 (left).

```
CREATE OR REPLACE FUNCTION break_segments(
  result_tab text,
  poly_tab text,
  segment_length float
  ) RETURNS void
AS $$

## Create a table where the result of this query is inserted into
plpy.execute("DROP TABLE IF EXISTS " + result_tab + " CASCADE")
plpy.execute("CREATE TABLE " + result_tab +
  " (id SERIAL PRIMARY KEY, poly_id int, geom geometry) ")
```

```
## Selects all polygon-IDs into a list
ids = plpy.execute("SELECT path FROM " + poly_tab)
id_list= []
for i in ids:
  id_list.append(int(i['path']))

## Loop over every polygon
for poly_id in id_list:
  ## Create a new table only containing the exterior ring of that polygon
  plpy.execute("DROP TABLE IF EXISTS ring CASCADE")
  plpy.execute("CREATE TABLE ring AS
    (SELECT st_ExteriorRing(geom) as geom
      FROM " + poly_tab + "
      WHERE path = " + str(poly_id) + ")")

  ## Calculate length and no. of segments of the exterior ring
  length = float(plpy.execute("
    SELECT st_length(geom::geography) AS length
      FROM ring")[0]['length'])
  parts = length/segment_length

  ## If the polygon will be split in more than one segment
  if length >= segment_length + 0.5*segment_length:
    ## Calculate the fractions where the ring will be split into segments
    frac_list = [0.]
    frac_list.append(1/parts)
    for i in range(1,int(parts)):
      frac_list.append(frac_list[-1] + 1/parts)
    frac_list.append(1.)

    ## Split the ring and insert segments into the result table
    for i in range(len(frac_list)-1):
      plpy.execute("INSERT INTO " + result_tab + " (geom, poly_id)
        SELECT st_LineSubstring(geom, " + str(frac_list[i]) +
          "," + str(frac_list[i+1]) + "), " + str(poly_id) + "
          FROM ring")

  else:
    plpy.execute("INSERT INTO " + result_tab + " (geom, poly_id)
      SELECT geom, " + str(poly_id) + "
        FROM ring")

plpy.execute("DROP TABLE IF EXISTS ring CASCADE")

$$ LANGUAGE plpython3u;
```

Listing 6.1: Examplary implementation of a PL/Python function to cut a polygon into segments of a given length.

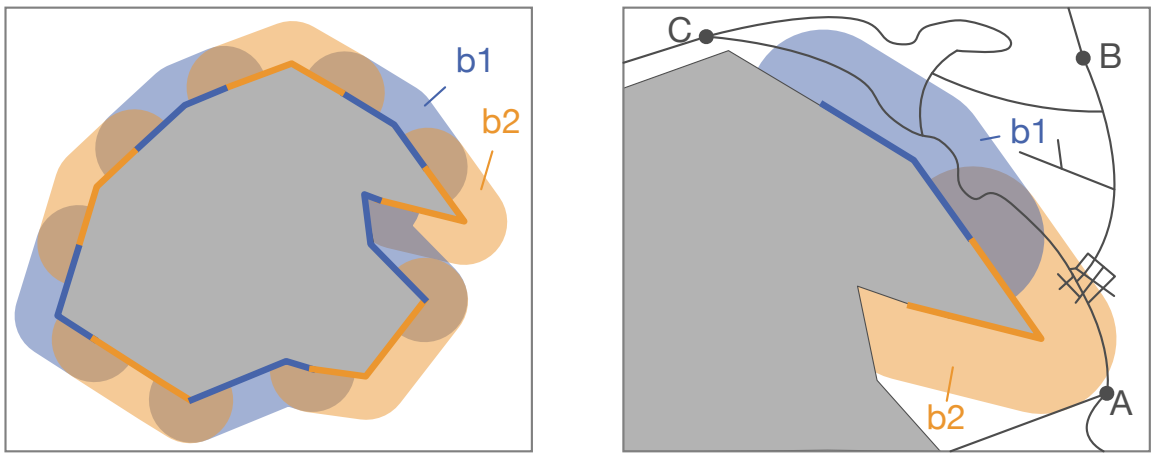

Figure 6.4: On the left, the scenario buffer generation for the wildfire spread is visualized. The currently burning area is colored gray, the segments on the edge of the burning area as well as the corresponding buffer scenarios are colored blue and orange alternately for better visualization. On the right, two buffers, b1 and b2, are displayed exemplarily with three points A, B, and C that serve as origins and destinations in the road network. The road network is illustrated with gray lines.

Network vulnerability scans are computationally expensive [108] because all pairs of shortest paths have to be calculated for each degradation scenario. For this scan, the computing time is reduced by only considering the relevant paths during the scan. When calculating the vulnerability indicators of the degraded network, all used shortest paths are stored in the database as sequences of road ids and with a unique path identifier. Then, each scenario buffer gets the information which paths use the roads intersecting with the respective scenario buffer by assigning path identifiers. Thus, only those paths are recalculated during the DVS, which use the roads intersecting with the respective scenario buffer.

The scenario in Figure 6.4 on the right can be considered as an example. During the DVS for scenario buffer b1, all roads intersecting with the blue buffer b1 are degraded. The shortest path from A to B does not intersect buffer b1 and is, therefore, not recalculated. The shortest paths from A to C and B to C go through buffer b1 and are recalculated during the scan. Similarly, during the scan for scenario buffer b2, the shortest paths from A to C and A to B have to be recalculated because they intersect with the orange buffer b2.

As a result, vulnerability indicator differences are obtained for each scenario buffer. From the CM, travel time differences are calculated. For facilities it calculates the average of the travel time from a location i to the nearest facilities hospital, fire station, and police before and after degrading the scenario buffer for all locations where the travel time is calculable in the double degraded network. Travel time is not calculable when there exists no shortest path between origin and destination because the networks are not connected. Then, the average of travel times from i to all facilities is added up for all locations before and after degrading the scenario buffer. The resulting vulnerability indicator is the difference of travel time average. The same is calculated for all locations i to all service centers.

From the AIC module the ARIA and EFAI differences are obtained. It calculates all ARIA and EFAI values before and after degrading the roads in the scenario buffer for all locations where the index is calculable in the double degraded network using Equation (6.8) and Equation (6.9). As for the DIA module, no threshold is set for ARIA and EFAI. Then, the average ARIA and EFAI before and after degrading the scenario buffer for the entire study region is calculated. The difference of average ARIA and EFAI serves as vulnerability indicator.

The TDM module calculates the average daily travel time difference for each scenario buffer. It calculates the travel time before and after degrading the scenario buffer for a location i to all destinations where the number of daily trips is larger than one and where the travel time in the degraded network can be calculated. The number of daily trips to every destination is assumed the same as before the event. Then, the sum of all daily travel times from all locations to all destinations before and after degrading the scenario buffer, respectively, is calculated. The total delay of daily trips is taken as a vulnerability indicator. Additionally, the sum of daily trips that get disconnected due to the degradation of the scenario buffer is calculated.

In summary, the following vulnerability indicators are calculated:

- CM: Travel time difference to facilities, travel time difference to service centers
- AIC: EFAI difference, ARIA difference
- TDM: Average daily travel time difference

These indicators highlight different aspects of vulnerability that are important for disaster management and can be considered separately or in combination. Scenario buffers where the vulnerability indicators show a big difference between the degraded and the double degraded networks are locations where a fire spread would be most critical for the functionality of the road network.

7 Case Studies and Transferability of GRIND

GRIND is applied exemplarily in two case study regions in Chile and Australia for two wildfire scenarios to test its potential and transferability. This chapter presents the case study results and regional analyses of these results. Some modules are applied in both study regions while others are tested only for the study region in Australia. Figure 7.1 visualizes which module is applied in which case study region. The TDM module is only applied in Australia because reference data or expert knowledge to tune the model is not available for the study region in Chile. Similarly, the DVS is not applied in Chile because of the missing TDM. Two case study regions are chosen that differ in their quality of OSM data and their stages of development to prove the generic and transferable design of GRIND.

		Chile	Australia
Core Module		✔	✔
Accessibility Index Calculation	ARIA	✔	✔
	EFAI	✔	✔
Travel Demand Model		✘	✔
Disaster Impact Assessment	AIC	✔	✔
	TDM	✘	✔
Disaster Vulnerability Scan		✘	✔

Figure 7.1: Application of GRIND modules in the case study regions in Chile and Australia.

This chapter begins with a presentation of both case study regions and wildfire scenarios in Section 7.1. Then, the results and a regional analysis of the CM and the AIC module are presented in Section 7.2. Section 7.3 demonstrates the application of the TDM module for the study region in Australia. The impact of two wildfire scenarios on the road network's functionality is analyzed in Section 7.4 with the DIA module. Finally, the DVS module is applied during a wildfire scenario in Section 7.5.

7.1 Case Study Regions and Scenarios

Two exemplary case studies are performed in geographically and economically different regions in Chile and Australia. The same three regions in central Chile as in Chapter 3 and Guth et al. [65] are considered: the BioBío, the Maule, and the Ñuble region. The Ñuble region is a new region that was created in 2018 by splitting the former BioBío region into two parts. In this thesis, the BioBío, Maule, and Ñuble regions are abbreviated as BM regions. In Australia, the south-eastern part of the state of New South Wales (SE-NSW) is considered. Both regions are chosen because they have recently had severe wildfires and because they differ in their state of development and quality of OSM data (see Section 2.2). The enhanced OSM data created in Part I is used for the road network in both case studies. Two exemplary wildfire scenarios are analyzed: one in the BM regions in Chile and one in SE-NSW in Australia.

Chile

A series of wildfires burned across Chile in January 2017. Until now, these wildfires are the largest in the country's history. The O'Higgins and BM regions were most affected. The wildfires destroyed 1644 houses, impacted 7157 people, and killed 11 persons [200]. The town of Santa Olga in the Maule region was destroyed, and a total area of 5182 km^2 was burned.

In this thesis, only the wildfires in the BM regions are considered, which amount to a total burnt area of 3807 km^2. The case study region is illustrated in Figure 7.2. The entire burnt area is taken as a footprint for the wildfire. In the BM regions, 1910 km of the road network (levels L1-L5 in Table 2.1) lie within the burnt area. Thereof, 105 km L1 roads, 133 km L2 roads, 78 km L3 roads, 1208 km L4 roads, and 386 km L5 roads intersect the burnt area. The total road network in the BM regions amounts to 30 278 km in L1-L5. The OSM dataset for the BM region contains 202 hospitals, 264 police stations, and 108 fire stations. In the populated places dataset, 323 settlements exist in the BM regions, thereof two service centers category A (Talca and Concepcíon), 12 service centers category B, 14 service centers category C, 66 service centers category D, and 144 service centers category E. To avoid errors at region borders, service centers, facilities, and roads that lie within 35 km (10 % of the regions' area) are included.

Australia

The 2019/2020 bushfire season was an unusually intense series of wildfires, mainly in NSW, Victoria, and South Australia. The fires burnt a total of 73 876 km^2, destroyed 3057 houses, and killed 33 people [201]. The mainly affected region was NSW with 55 957 km^2 burnt area, 2475 destroyed houses, and 25 deaths [201].

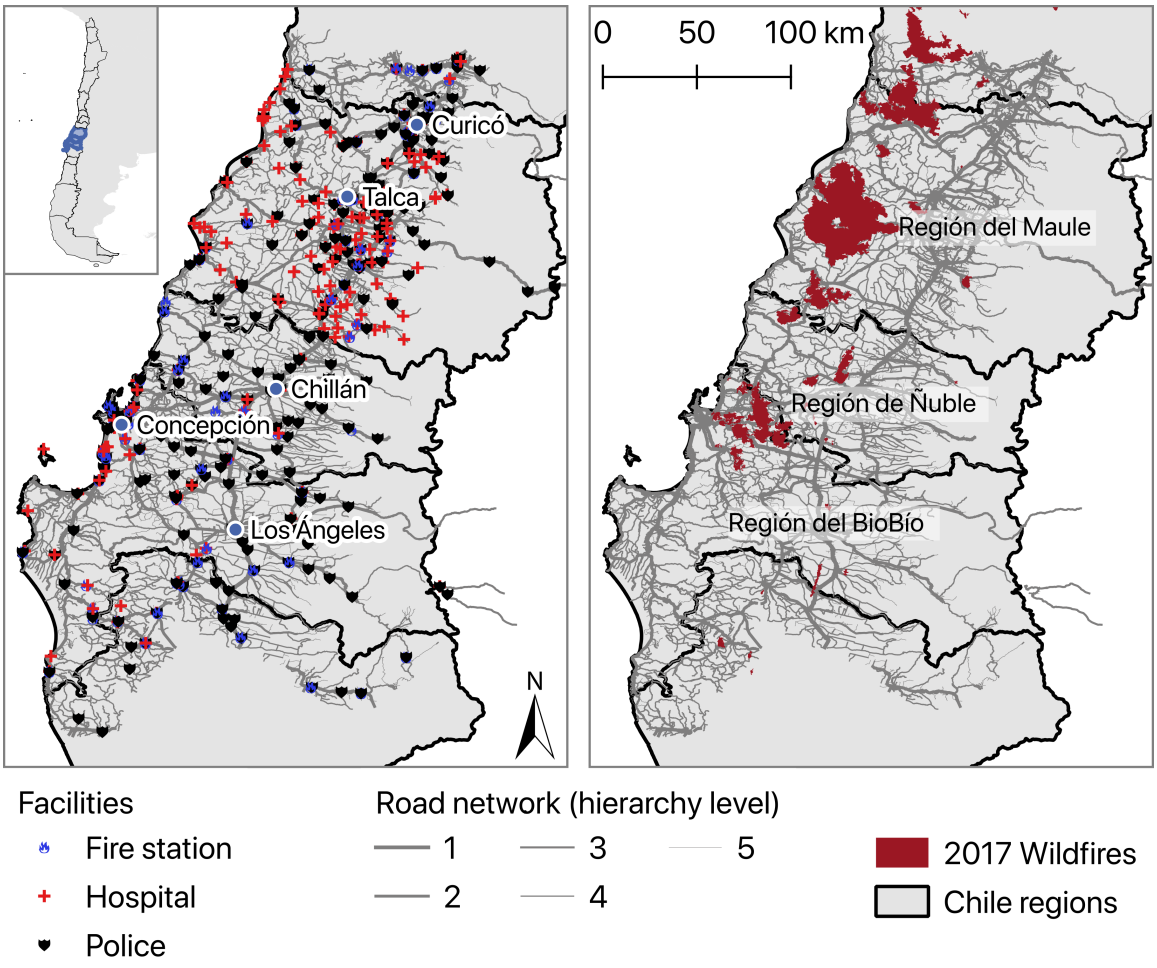

Figure 7.2: Case study region in Chile. On the left, the road network with the considered facilities and major settlements is illustrated. On the right, the burnt area of the 2017 wildfires is shown.

For the case study in this thesis, south-east New South Wales (SE-NSW) is considered with fires that are actively burning on 5th February 2020 (data source: [202]). This day is deliberately chosen to perform an example for a vulnerability scan during an ongoing natural disaster. An overview of the case study region is shown in Figure 7.3. The region SE-NSW for this thesis is defined as the area in NSW that is within 150 km around the wildfires. An additional buffer of 10 % of this area (circa 85 km buffer width) is included to avoid errors at the region borders (see Figure 7.3). The considered road network comprises 131 309 km of L1-L5 roads. 7818 km of road network lie within the wildfire area. Thereof, 278 km L1 roads, 349 km L2 roads, 1153 km L3 roads, 801 km L4 roads, and 5220 km L5 roads are within the wildfires. In total, there are 733 settlements in the considered region, thereof 4 service centers category A, 22 service centers category B, 29 service centers category C, 81 service centers category D, and 240 service centers category E. 85 hospitals, 219 police stations, and 373 fire stations exist in SE-NSW.

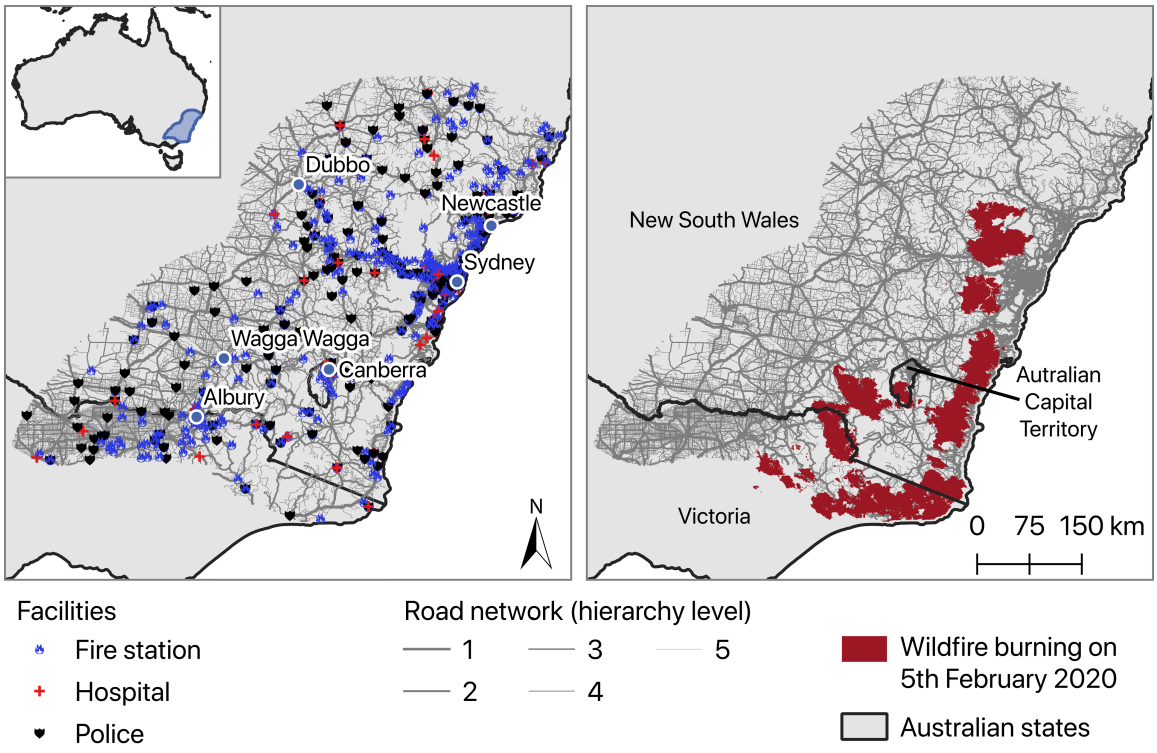

Figure 7.3: Case study region in Australia. On the left, the road network with the considered facilities and major settlements is illustrated. On the right, the active wildfires as of February 5th 2020 are shown.

7.2 Core Module and Accessibility Index Calculation

The CM calculates travel times to localities, in this case, facilities and service centers, for both study regions. A grid-based analysis is performed to enable an evaluation of the entire area. A grid resolution of one kilometer is chosen for the BM regions. The grid resolution in SE-NSW is two kilometers because of the bigger study area compared to the BM regions. Grid cells that are further away from a road than 5 km in Chile and 15 km in Australia are considered not accessible via the road network and are deleted. In Australia, the larger value of 15 km is chosen because of two reasons. First, Australia features more roads of the class Track than Chile (see Figure 2.2), which are not included in this analysis, such that there often exist tracks in the vicinity of higher-level roads to reach places further away. Second, the inner part of the Australian continent features a very low population density and is very rural compared to Chile, such that a wider radius around roads can be considered still accessible via the road network.

Figure 7.4 shows the travel time to the respective nearest hospitals and fire stations in the BM regions. Figure 7.5 illustrates the same for the study region in Australia. The travel time to hospitals and fire stations is displayed because these facilities are the most important ones in a wildfire scenario. However, the travel time to the nearest service

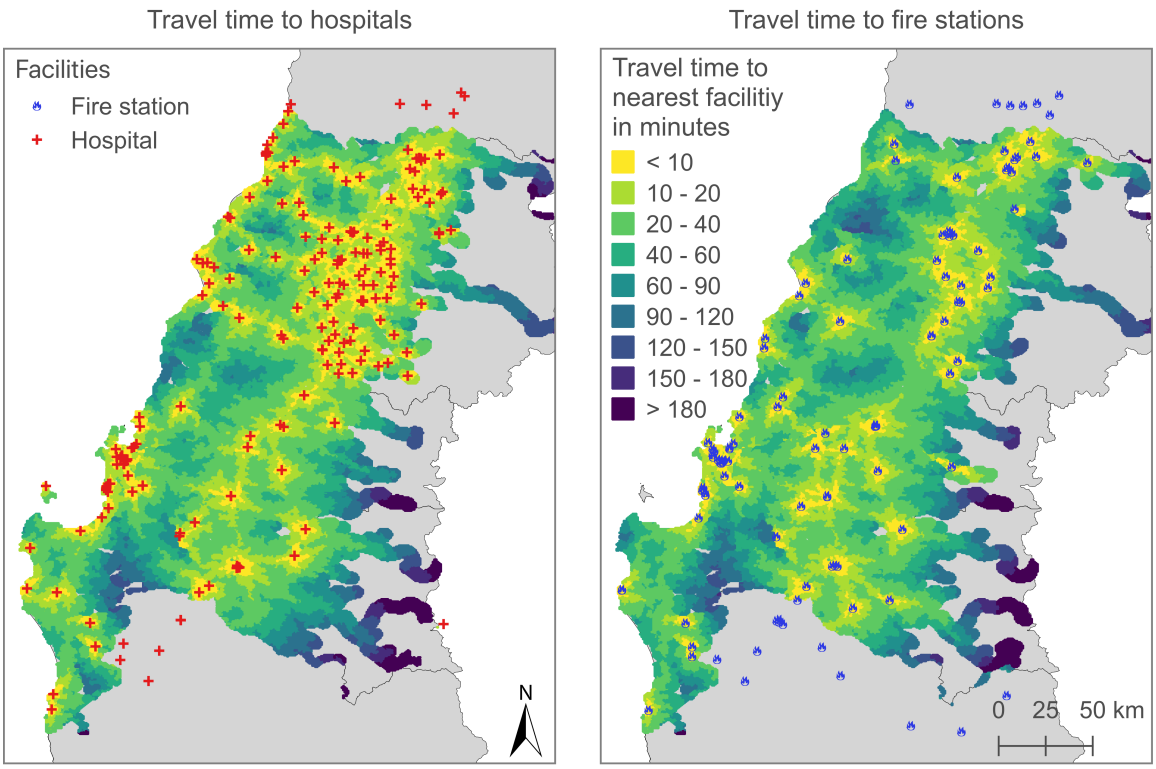

Figure 7.4: Travel time to the nearest hospitals (left) and fire stations (right) in the BM regions in Chile.

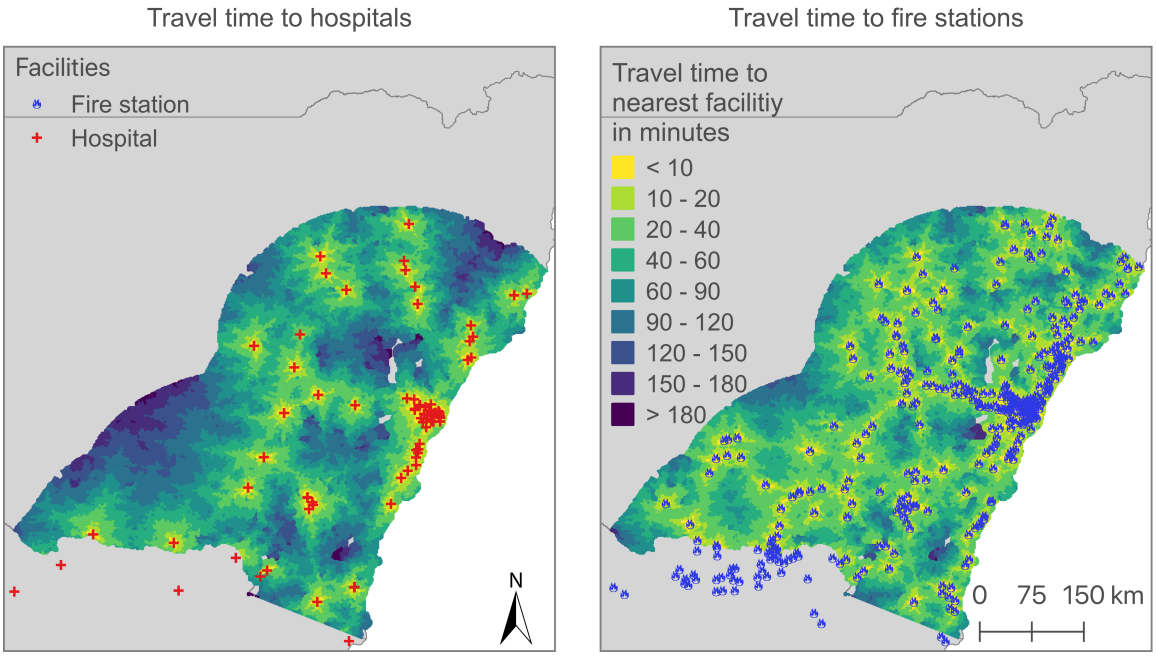

Figure 7.5: Travel time to the nearest hospitals (left) and fire stations (right) in SE-NSW in Australia.

Table 7.1: Mean, maximum, and SD of travel time in minutes from all grid cells to service centers and facilities in the two study regions.

		BM (Chile)			SE-NSW (Australia)		
		Mean	SD	Max	Mean	SD	Max
Service centers	A	101.9	54.4	595.5	232.6	89.2	552.2
	B	70.8	47.1	520.1	108.9	55.6	296.0
	C	54.4	42.5	501.4	75.4	41.4	268.6
	D	37.5	35.1	501.4	49.1	29.8	223.2
	E	31.0	33.7	501.4	32.5	21.4	177.2
Facilities	Hospital	39.2	40.8	505.2	63.4	34.7	214.0
	Police	28.8	27.7	216.1	36.8	22.9	178.7
	Fire station	42.4	34.9	262.4	36.8	23.4	171.6

center in each category and the travel time to the nearest police station is also calculated. Table 7.1 displays the mean and maximum travel times and the standard deviation to all service centers and facilities in both study regions.

In the results for the BM regions in Chile and SE-NSW in Australia in Figure 7.5, Figure 7.4, and Table 7.1, it can be seen that Australia is generally more remote than Chile. The average travel time to hospitals is almost twice as high in SE-NSW as in the BM regions. Furthermore, 49 % of the study region in Australia is located more than one hour away from a hospital. In Chile, only 17 % of the area is further away from hospitals than one hour. Interestingly, the maximum travel times to locations are much higher in the study regions in Chile than in SE-NSW, which hints at a few very remote places in the Andes.

The density of facilities and service centers is also generally higher in the BM regions than in SE-NSW. In SE-NSW, most facilities are mostly concentrated in the coastal regions where the majority of the population lives. It is noticeable that Australia has many more fire stations than hospitals, which are better distributed over the study region than hospitals. The high number of fire stations is probably caused by the frequent and severe wildfires the continent experiences regularly.

The **AIC** module calculates the ARIA and EFAI for both study regions, using the travel times calculated in the **CM**. Figure 7.6 shows both indices for the study region in Chile, and Figure 7.7 illustrates the ARIA and EFAI values for SE-NSW in Australia. If the shortest travel time cannot be calculated because one or more service center categories or facilities are not accessible via the road network, the entire index cannot be calculated, and the grid cell is deleted. This can be observed, for example, on the island in the South-West of the BM region, where a hospital is available, but a fire station is not (see Figure 7.4 and Figure 7.6).

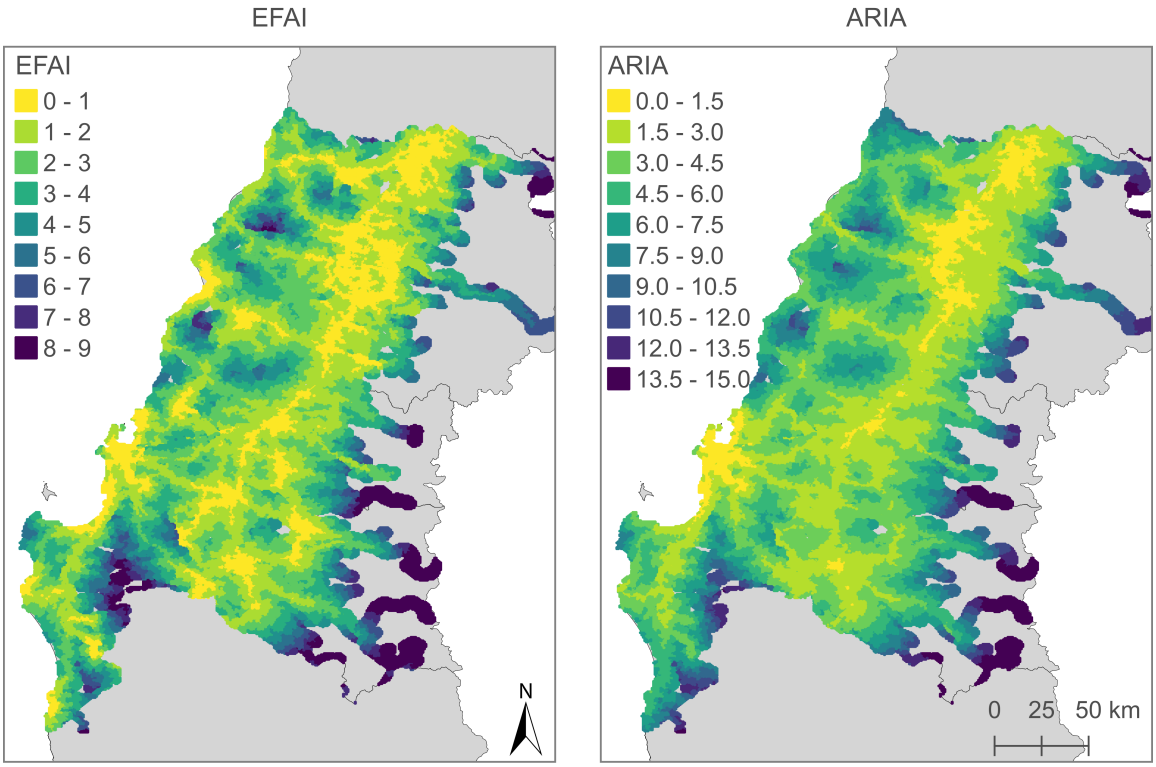

Figure 7.6: EFAI (left) and ARIA (right) values for the BM regions in Chile. Low index values (yellow and green) signify accessible grid cells, high index values (blue and lilac) visualize remote areas.

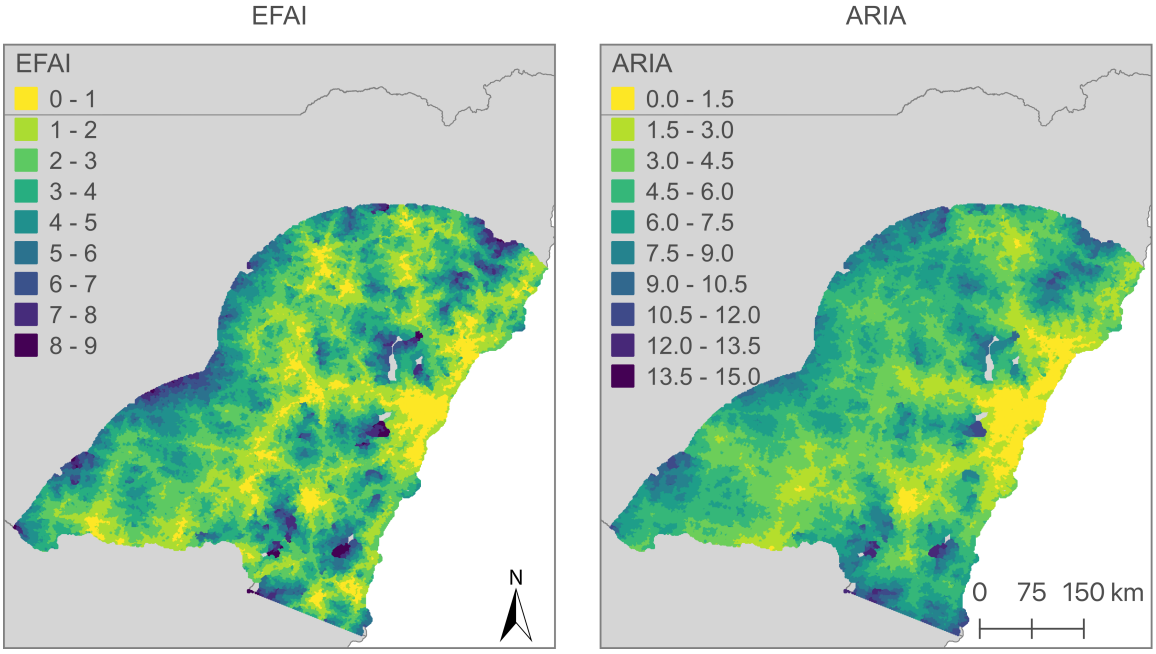

Figure 7.7: EFAI (left) and ARIA (right) values for the SE-NSW region in Australia. Low index values (yellow and green) signify accessible grid cells, high index values (blue and lilac) visualize remote areas.

The EFAI and ARIA in Figure 7.7 and Figure 7.6 demonstrate similar results. The EFAI in the BM regions shows good accessibility of emergency facilities on the coast and along the Ruta 5, the main south-north highway in the regions. Accessibility decreases a little for the coastal mountain ranges and a lot in the far east of the region where the Andes are located. The ARIA shows a similar picture but highlights the accessibility of service centers with low ARIA values near the category A service centers Talca and Concepcíon. The same is visible in SE-NSW as the ARIA clearly shows high accessibility of service centers in the greater vicinity of Sydney. The rest of SE-NSW features a lower ARIA while high EFAI values still occur in the middle and west of the study area.

7.3 Travel Demand Model

The TDM module is applied to the SE-NSW region. Data from the Traffic Volume Viewer [203] from the year 2019 is used as reference data. The Traffic Volume Viewer provides available traffic count data (volumes) of various stations in NSW. It differentiates between vehicle classes (light, heavy, or both), directions of traffic (east/westbound, south/northbound or both), and types of days or times of day (weekdays, weekends, AM peak hours, PM peak hours, off-peak hours, public holidays or all days average). Only stations with available data for both vehicle classes and all-days average are selected of all available data. Stations within big cities (mainly Sydney) are not considered reference data because the purpose of the model is to estimate intercity transport. As a result, 60 reference stations are obtained; thereof, 46 are located on `motorway` or `trunk`, 12 on `primary` roads, one on a `secondary` road, and one on a `tertiary` road.

The upper map in Figure 7.8 shows the study region with the hierarchical road network, and the populated places dataset generated in Section 6.2. The populated places serve as origins and destinations. The objective is to estimate the daily intercity trips between all origins and all destinations in the populated places dataset to obtain an OD-matrix. The maximum number of trips per person in a populated place g_{max}, is set to 1.5 like in Scott et al. [64].

The Traffic Volume Viewer reference data is used to fit the model parameters α and β in Equation (6.7) to the study region. The combination of $\alpha = 0.6 \cdot 10^{-5}$ and $\beta = 1.7 \cdot 10^{-3}$ performs best. Figure 7.9 shows a scatter plot of the estimated volumes and the reference volumes. The R^2 is 83.4 %, and the Root Mean Square Error (RSME) is 6199 vehicles per road segment. Without the two stations where the reference volume is greater than 50 000 (see Figure 7.9), the R^2 is significantly worse (63.1 %) with a slightly lower RSME of 6086 vehicles per road segment. The resulting volumes for every road segment and the model's error in relation to the reference values are shown in the lower map in Figure 7.8.

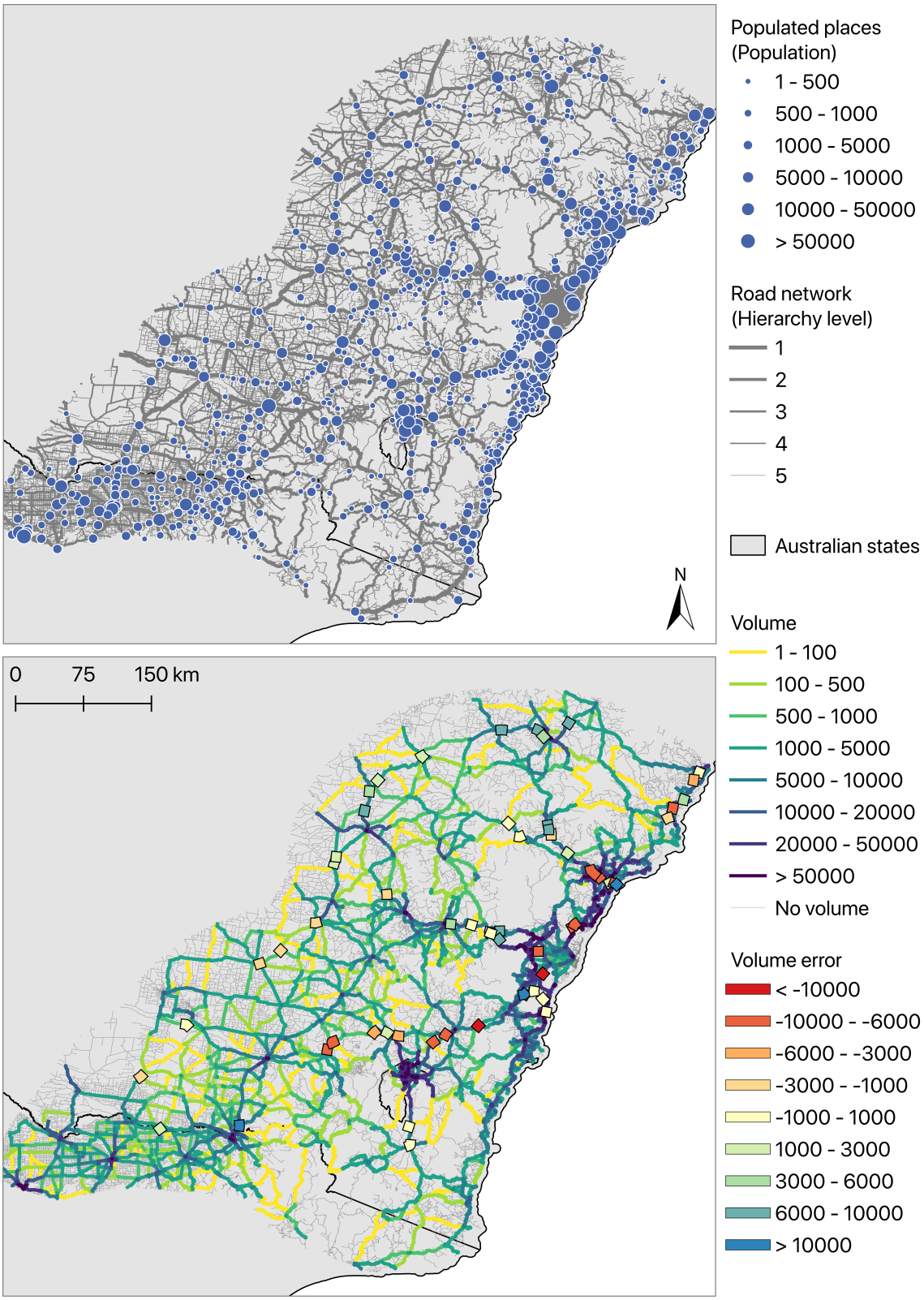

Figure 7.8: The upper map shows the road network (for hierarchy levels see Table 2.1) of the study area in New South Wales - Australia. Below, volumes of cars per day estimated by the developed TDM and the error in relation to the reference data (reference volume - estimated volume) is illustrated. Red road segments are underestimated, blue road segments are overestimated.

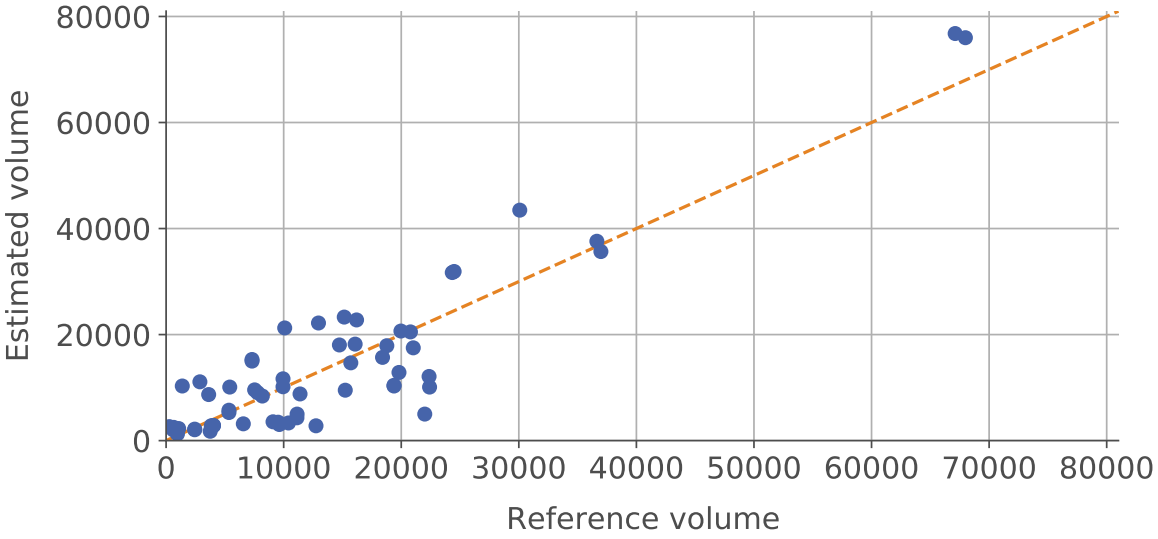

Figure 7.9: Scatter plot of the estimated volumes and the reference volumes in average vehicles per day. The closer the points are to the orange line, the better is the estimation.

Regarding the regional distribution of model errors, some patterns are noticeable in Figure 7.8. In the north-west of the region, the Newell and Oxley Highway are overestimated, while in the south-west, the Newell and other highways are slightly underestimated. The Hume Highway, which runs from east to west just north of Canberra, is significantly underestimated. The underestimation might stem from the fact that most traffic between Australia's largest cities Sydney and Melbourne, travels this route, and Melbourne is not included in this model. In the urban areas near the east coast, both over- and underestimation can be observed in close range. This phenomenon can be explained by the model not being able to estimate transport volume in urban areas as cities are represented as points in a network rather than polygons.

7.4 Disaster Impact Assessment

The DIA module is applied for both wildfire scenarios. In Section 7.4.1, a NADIA is conducted. The results for both study regions are presented and analyzed. Section 7.4.2 shows the results of the TDMDIA for SE-NSW in Australia.

7.4.1 Network Analysis Disaster Impact Assessment

The impact of a disaster scenario can be assessed as accessibility decrease in an absolute way using travel time or relatively with an index. In this subsection, the results for the two distinct approaches in both study regions are presented.

The travel time difference between the original and the degraded network from grid centroids to the nearest locations is calculated for the BM region and SE-NSW (see Section 6.5.1). In this case, locations are facilities (hospital, police, and fire station) or service centers in all categories. As a result, travel time differences as accessibility decrease due to the wildfires are obtained for each grid cell. The results are visualized exemplarily in Figure 7.10 for all facilities in the BM regions and Figure 7.11 for all service centers in SE-NSW. In some cases, the travel time can not be calculated because the wildfire disconnected an entire subnetwork. If there exists neither a service center nor a facility in this subnetwork, the grid cell is considered *disconnected*. A grid cell is also *disconnected* if it intersects but is not contained by the wildfires. Grid cells that are completely within wildfires are not counted in the analysis. If any facility or service center exists in the subnetwork,

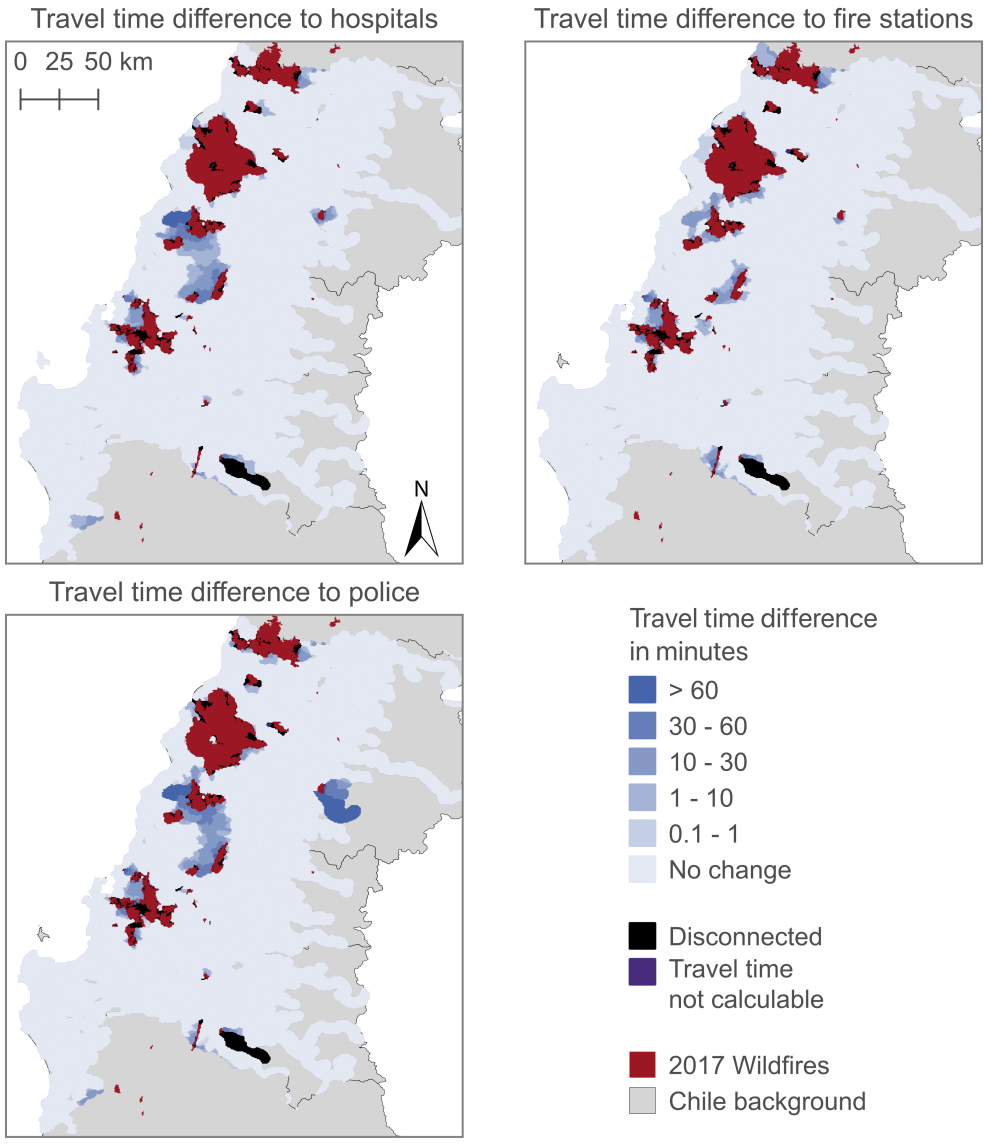

Figure 7.10: Impact of the 2017 wildfires as travel time to facilities difference before and after the event in the BM regions.

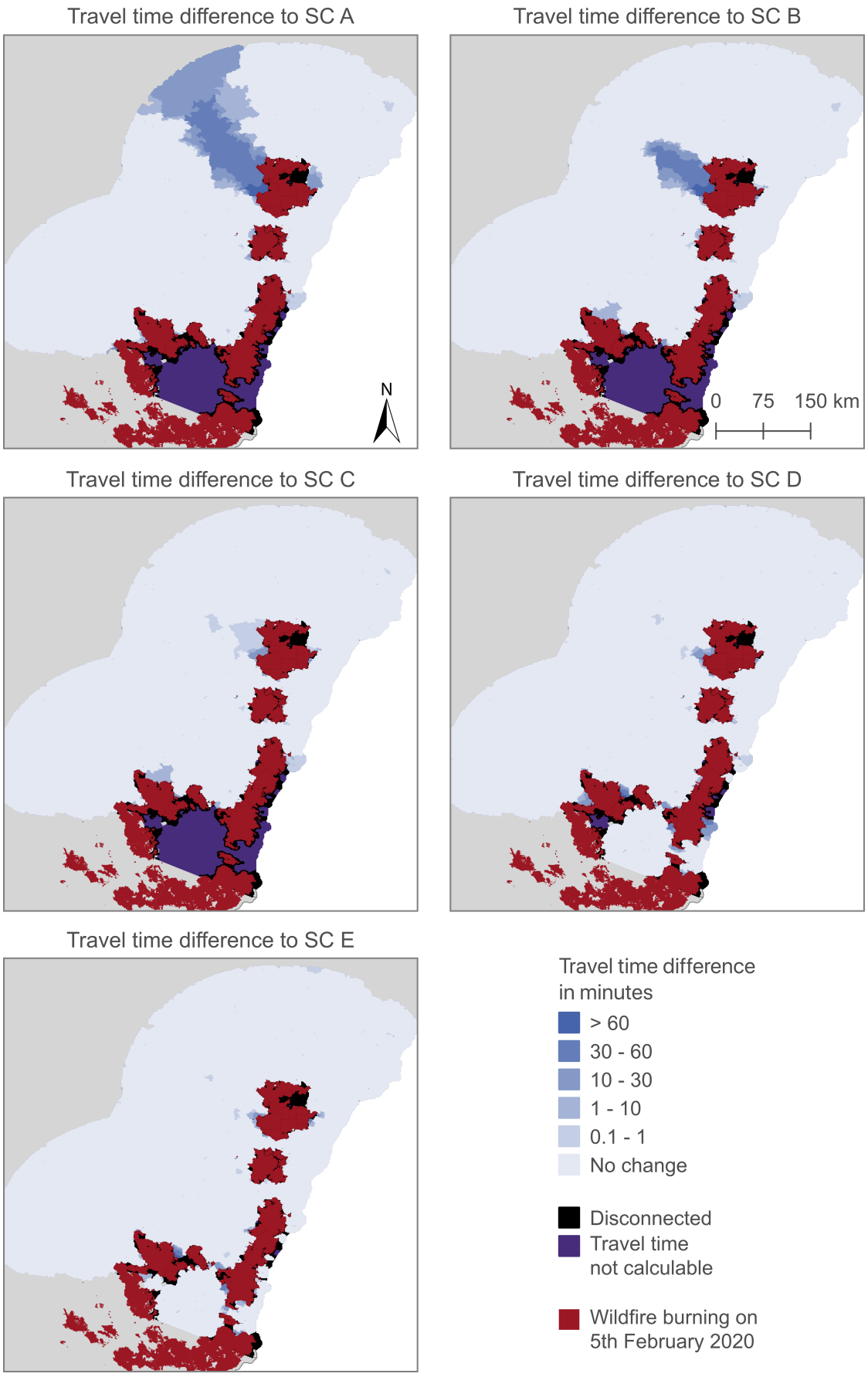

Figure 7.11: Impact of the wildfire burning on the 5th February 2020 as travel time to service center (SC) difference before and after the event in SE-NSW.

Table 7.2: Mean travel time (TT) in minutes from all grid cells to service centers and facilities for the original and the degraded network (NW) in the two study regions.

		BM - mean TT		SE-NSW - mean TT	
		Original NW	Degraded NW	Original NW	Degraded NW
Service centers	A	103.0	131.6	232.2	235.5
	B	69.8	74.9	105.9	107.2
	C	54.3	60.7	68.1	69.3
	D	37.3	39.7	47.0	47.5
	E	31.3	33.1	30.8	31.0
Facilities	Hospital	39.5	40.8	62.5	63.0
	Police	28.6	29.2	34.7	35.0
	Fire station	42.3	44.5	35.8	36.4

but the facility or service center that is being analyzed does not exist in the subnetwork, the grid cell is displayed as *travel time not calculable*.

Table 7.2 shows the mean values of all grid cells for the original and degraded network. Only grid cells are considered where the travel time in the degraded network can be calculated. The average travel time to high-level service centers is delayed for up to 28.6 min (BM) and 3.3 min (SE-NSW). In general, the average delay in the BM regions is higher than in the SE-NSW region.

The impact of wildfire scenarios is first analyzed for each facility and service center category separately, using travel time differences. Figure 7.10 and Figure 7.11 show that the accessibility decreases significantly, especially for the hospitals and fire stations in the BM regions and for service center categories A and B in SE-NSW. In SE-NSW, the travel time to service center categories A, B, and C is not calculable for a large area in the south of the region because the networks are disconnected. The average travel time to facilities and service centers increases slightly in both study regions, as visible in Table 7.2. The increase of average travel time is a little less in SE-NSW than in the BM regions, probably because the wildfires there hit more remote regions where the accessibility was already low before the event and where few roads exist. In the BM regions, the accessibility to high-level service centers is decreased significantly because the fires affected one of the major roads leading to Concepcíon.

The index impact as a relative measure of accessibility decrease is calculated according to Equation (6.9) and Equation (6.8) in Section 6.5.1. The EFAI-Impact and the ARIA-Impact are visualized for the BM regions in Figure 7.12 and SE-NSW in Figure 7.13. Note that the EFAI- and ARIA- Impact are not directly comparable because EFAI values range from zero to nine, and ARIA values range from zero to 15. The index impact can not be calculated if the travel time to one of the facilities (for the EFAI) or one of the service

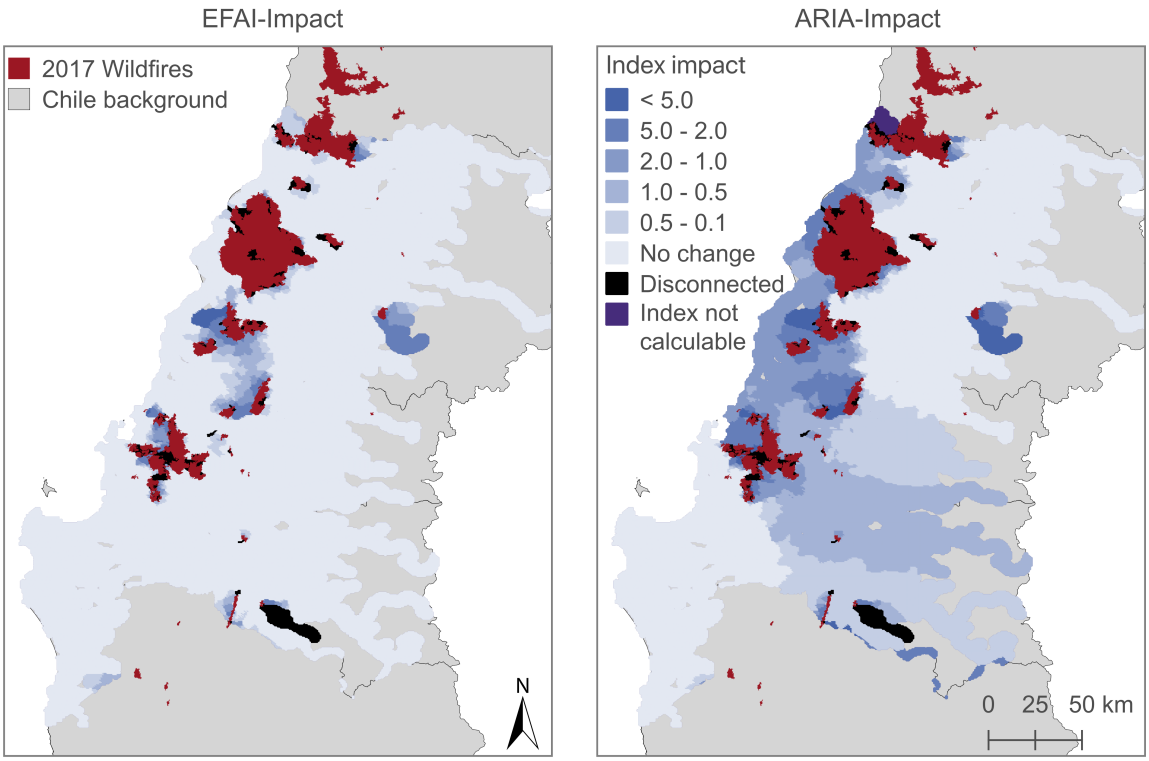

Figure 7.12: EFAI-Impact (left) and ARIA-Impact (right) values for the MB regions in Chile.

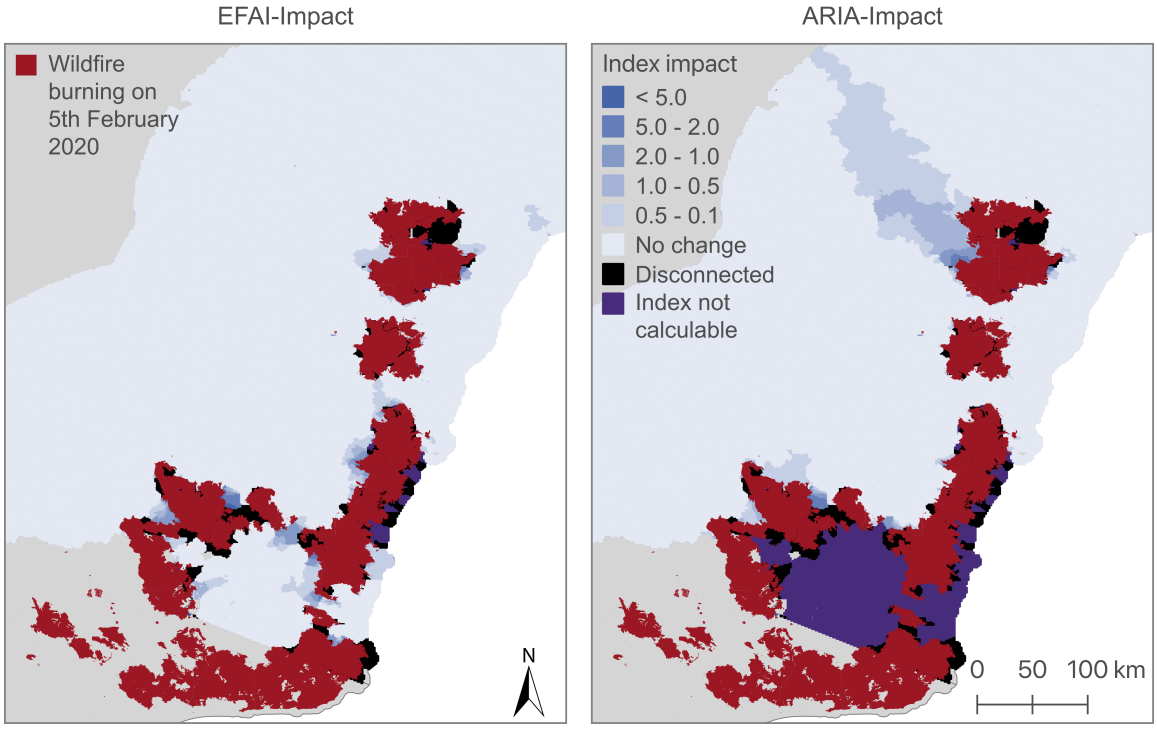

Figure 7.13: EFAI-Impact (left) and ARIA-Impact (right) values for SE-NSW in Australia.

centers (for the ARIA) can not be computed. Like for the travel time difference, grid cells are considered *disconnected* if there is neither a facility nor a service center in the subnetwork, or the grid cell intersects with the wildfires.

The EFAI-Impact in km^2 is visualized in Figure 7.14 for both study regions. In the BM region, when the EFAI-Impact is considered, 5505.49 km^2 are affected by the wildfires, which is 1.4 times the size of the wildfires (3807.17 km^2). Similarly, in SE-NSW, also looking at the EFAI-Impact, 27 209.03 km^2 are impacted by the wildfires (0.6 times the size of the wildfires). Figure 7.15 illustrates the ARIA-Impact in km^2. There, the affected area where accessibility to service centers decreases is 6.4 times the size of the wildfires with 24 380.19 km^2 in the BM regions and 1.6 times the size of the wildfires (42 144.43 km^2) in SE-NSW.

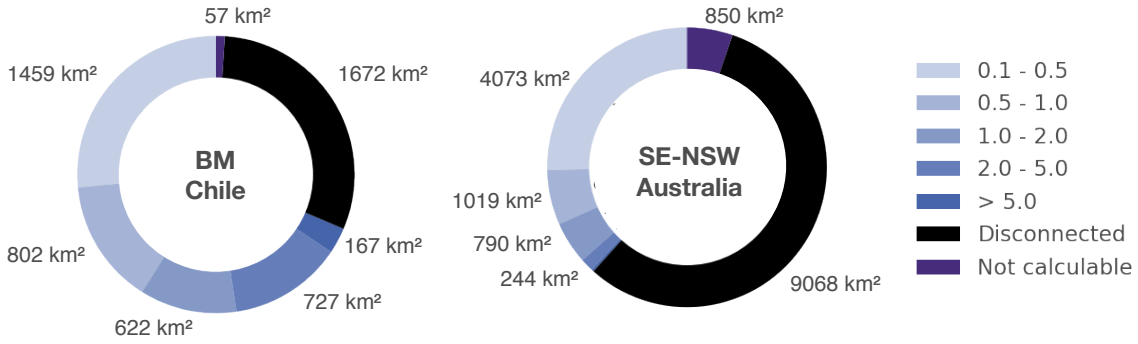

Figure 7.14: EFAI-Impact in square kilometer in both study regions.

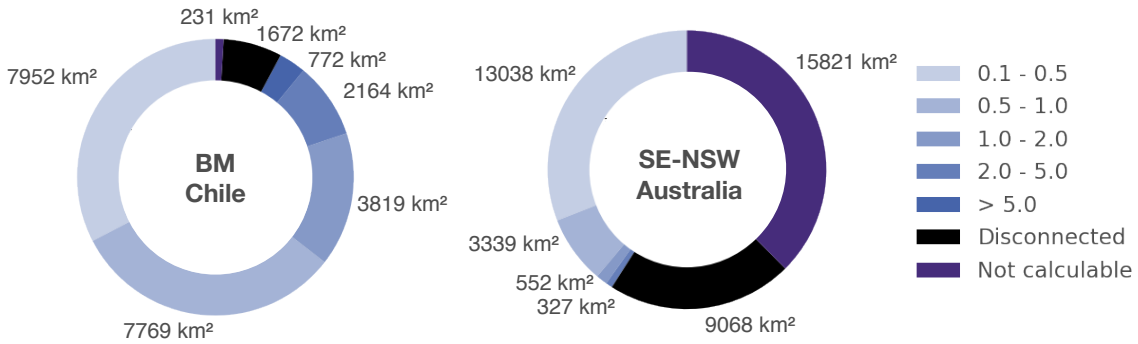

Figure 7.15: ARIA-Impact in square kilometer in both study regions.

The AIC allows for a combination of the facility and service center accessibility, respectively. Considering the EFAI-Impact, the accessibility to emergency facilities is decreased significantly for the center of the BM regions and slightly around the edges of the wildfires in SE-NSW. The ARIA impacts a larger area because only two service centers category A exist in Chile and four (thereof three at the coast) in Australia. Thus, for the ARIA, the travel time to these few service centers is calculated for all grid cells, and small fires might disconnect many shortest paths to find a longer alternative resulting in a large area of ARIA-Impact. Relatively, the BM regions are impacted more by the wildfires because more important roads have been blocked, while in SE-NSW, the fires occurred mainly in remote regions. In both

regions, significant parts of the study region get entirely disconnected. In regards to road infrastructure functionality, this is worse than an accessibility decrease because these areas are completely cut off. Especially in SE-NSW, very large areas on the south-east coast are completely disconnected by the wildfires. These areas can not access facilities like hospitals, and fire fighters can not reach the wildfires via the road network. The entire emergency logistics for this area would have to be provided by other means like ships or helicopters.

7.4.2 Travel Demand Model Disaster Impact Assessment

The TDM module can also be employed to assess a different aspect of the impact of a wildfire scenario, as described in Section 6.5.2. It is used to assess the total delay of daily trips for each settlement in SE-NSW in Australia. This subsection presents the TDMDIA results for the wildfires burning on 5th February 2020 in SE-NSW.

In the original network, 675 trips exist with travel time longer than two hours, in the degraded network 15 432 daily trips are longer than two hours. The mean duration of daily trips is 20.42 min in the original network and 20.67 min in the degraded network for all daily trips that are not disconnected in the degraded network. Table 7.3 displays the number of trips from all origins to all destinations in the degraded network per delay in minutes in relation to the original network.

Table 7.3: Number of trips per delay in minutes from all origins to all destinations.

Delay in minutes	Number of trips
No delay	4 320 696
< 1	40 435
1 - 5	29 379
5 - 10	19 134
10 - 20	5370
20 - 40	2132
40 - 60	11 975
> 60	1982

The upper map in Figure 7.16 shows the total delay per settlement in hours in SE-NSW in Australia. The total delay is calculated with Equation (6.10) as the sum of the delay of all daily trips from a settlement to all other settlements. In total, 171 out of 608 settlements experience no delay in daily trips due to the wildfires. The daily trips of six settlements to all other settlements are delayed more than 100 h with a maximum delay of 6528 h for trips starting in the town of Windsor. The total delay of daily trips caused by the wildfires as a sum of the delay for all settlements is over 18 314 h.

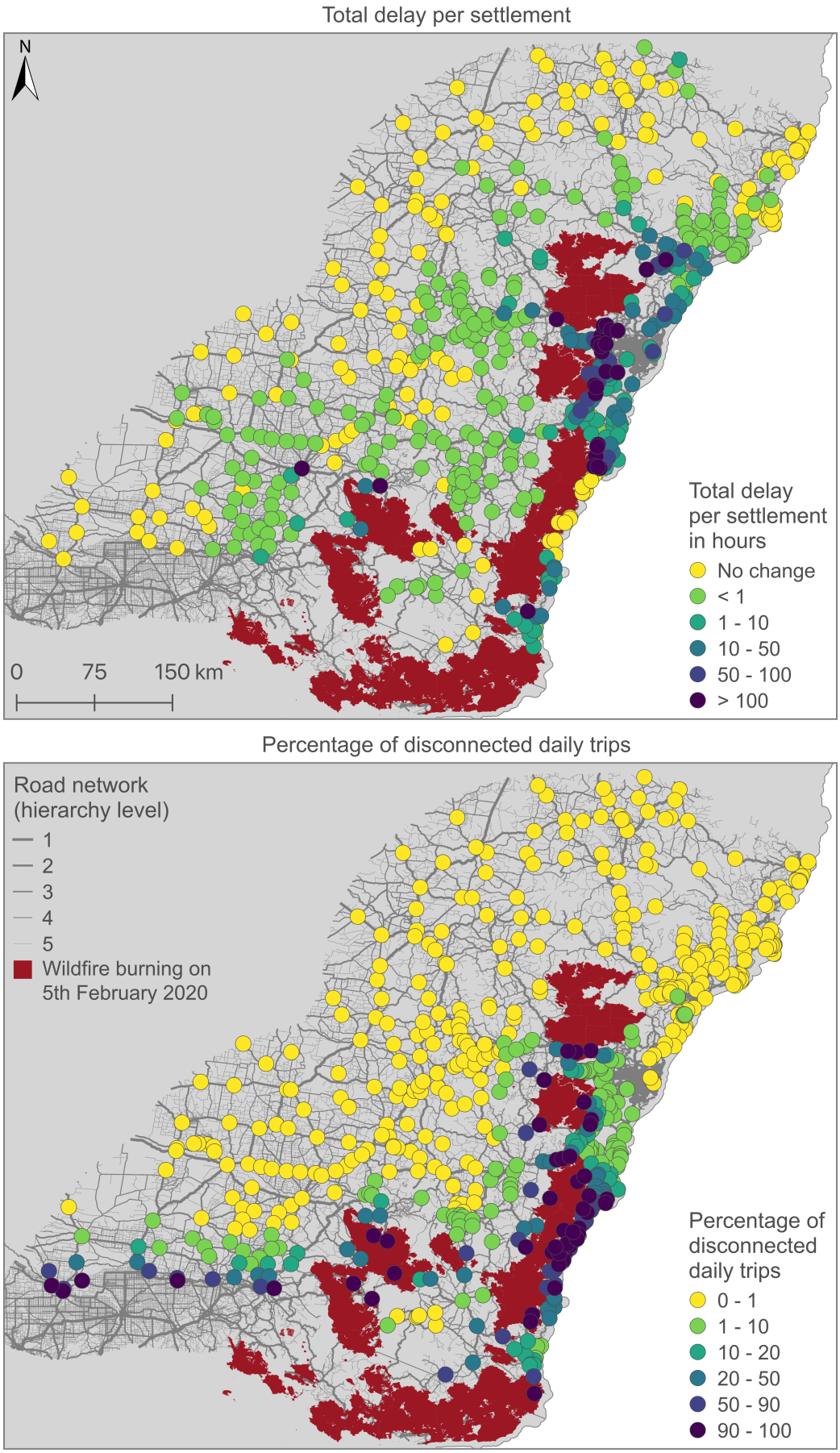

Figure 7.16: Impact of the wildfires burning on the 5th February 2020 as total delay in daily trips in hours (above) and as percentage of disconnected daily trips (below) in SE-NSW.

The percentage of disconnected daily trips per settlement is illustrated in the lower map in Figure 7.16. Forty-six settlements are entirely disconnected from the main network as all daily trips are not calculable. In total, 75 settlements have more than 50 % of daily trips disconnected.

The TDM in the DIA module assesses demand specific impacts of the wildfire scenario in SE-NSW. The wildfires delay daily traffic in SE-NSW significantly. The largest impact in form of delay can be observed close to the wildfires around Sydney where many people live and therefor a lot of traffic exists. The TDM shows that a delay of under one hour occurs also for settlements which are up to 100 km away from the wildfires. Hence, the impact of the wildfires is felt also much further away than the ARIA- and EFAI-Impact would suggest. Also, in the south-east of the region, where wildfires disconnected a significant amount of daily trips, a long delay can be observed. Regarding the disconnections, most daily trips for the settlements on the south-east coast are disconnected. This underlines the results of the EFAI- and ARIA-Impact and highlights the difficult situation on the south-east coast at this time.

7.5 Disaster Vulnerability Scan

The DVS is performed for SE-NSW using travel time to service centers and facilities (CM), the ARIA and EFAI (AIC module), and average daily traffic (TDM module) as vulnerability indicators for the wildfires burning on 5th February 2020. The methodology of the DVS is described in Section 6.6.

To generate the scenario buffers, the edges of the wildfire polygons are split into segments of 2 km length. Because the edge of the wildfire polygons are rarely of a length exactly dividable by 2 km one segment in each polygon is of different length. It is either up to 1 km longer, if the rest of dividing the total length by 2 km is smaller than 1 km, or up to 1 km shorter, if the rest is longer than 1 km. An exemplary 3 km-buffer is chosen to simulate a wildfire spread of 3 km. In total, 5152 scenario buffers are created; thereof, 3304 intersect with a road and 423 intersect with a shortest path.

Figure 7.17 illustrates the results of the DVS using the difference of travel time sum to facilities and service centers. For 8 scenario buffers, the sum of average travel time from all locations to facilities is longer than 300 min. For service centers, 36 scenario buffers cause a travel time rise more than 300 min. A fire spread near the roads close to Sydney would generally have the biggest impact on road network functionality.

The EFAI- and ARIA-Impact of each scenario buffer is shown in Figure 7.18. Note the different scales of the indices, as they are not directly comparable. The EFAI-Impact is, in general, higher than the ARIA-Impact. A fire spread east of the long wildfire in

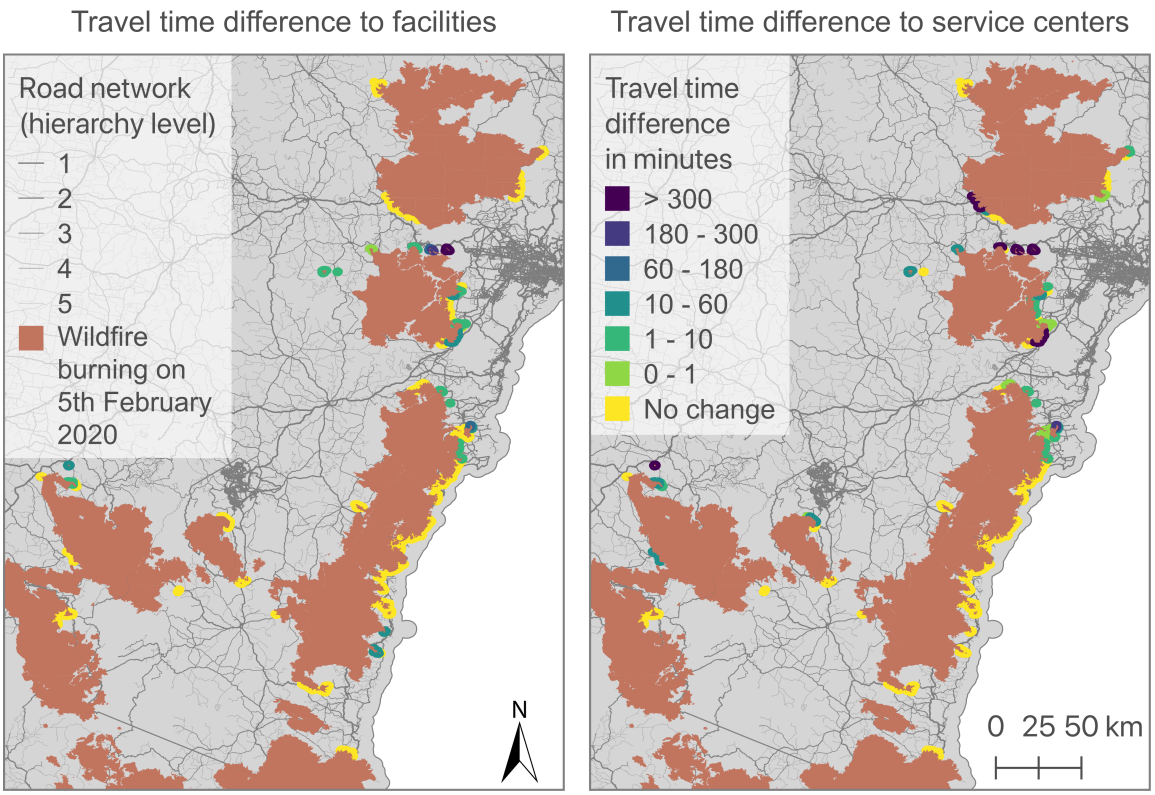

Figure 7.17: DVS with travel time sums to facilities (left) and service centers (right) in SE-NSW.

the south-east of the region would have very little impact because it has already been mostly disconnected (see Figure 7.16 below).

Figure 7.19 visualizes the results of the DVS using the TDM as vulnerability indicator. Two aspects are illustrated: on the left, the scenario buffers are colored according to how many daily trips are disconnected if the fire spreads there, on the right, the total daily delay for the entire network is visualized. As a reference, the degraded network has a total daily travel time (as sum of all daily trips from all locations to all locations) of circa 1 050 000 h.

The region close to the wildfires around Sydney is the most vulnerable to a wildfire spread, as demonstrated by all vulnerability indicators. Especially the Barrier Highway, going through the Blue Mountains (west of Sydney), and the Hume Highway (south-west of Sydney) are vulnerable towards a fire spread. These highways are two of the most commonly traveled roads in this region. Especially a fire spread that affects the Barrier Highway would reduce the accessibility of emergency facilities and service centers significantly (see Figure 7.17 and Figure 7.18).

In the south of SE-NSW, a fire spread would have smaller impacts. The accessibility of service centers is almost not affected, and the accessibility of facilities is only affected by three wildfire spread scenarios on the south-east coast. However, the situation in this region is already severe before a potential further spread of the wildfires. As illustrated

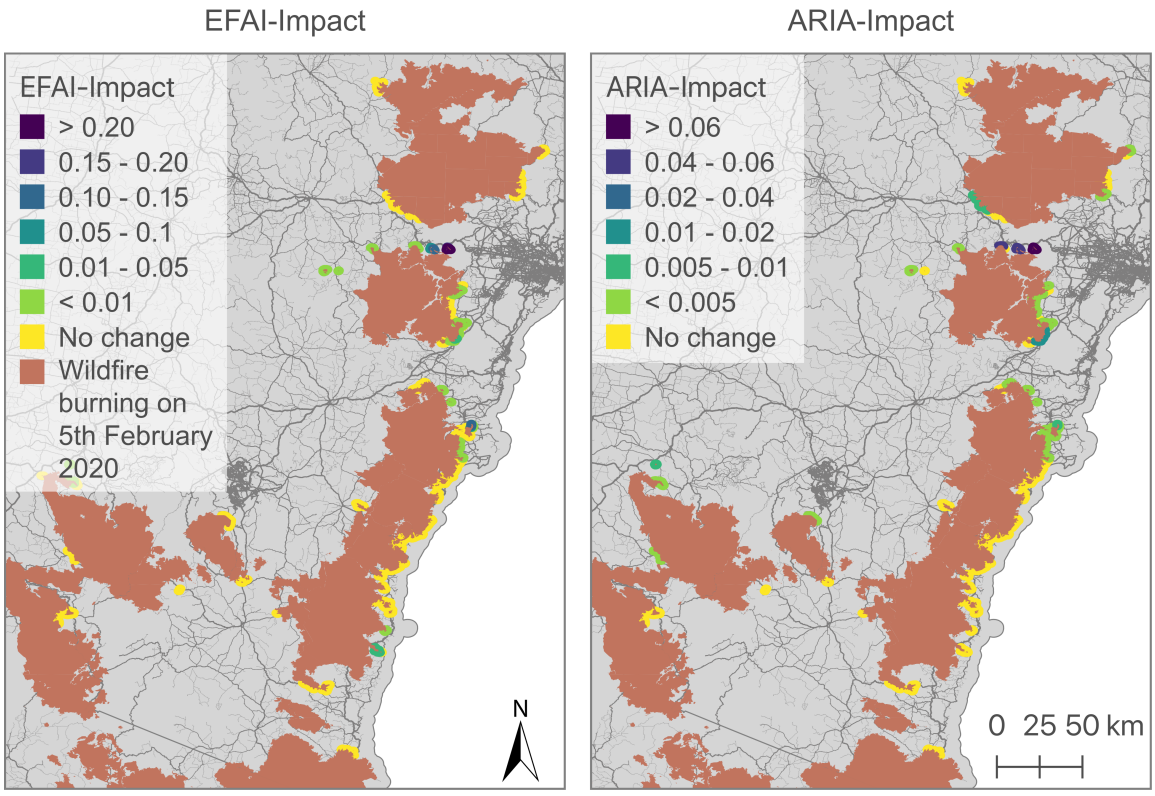

Figure 7.18: DVS with index impacts of the EFAI (left) and ARIA (right) in SE-NSW.

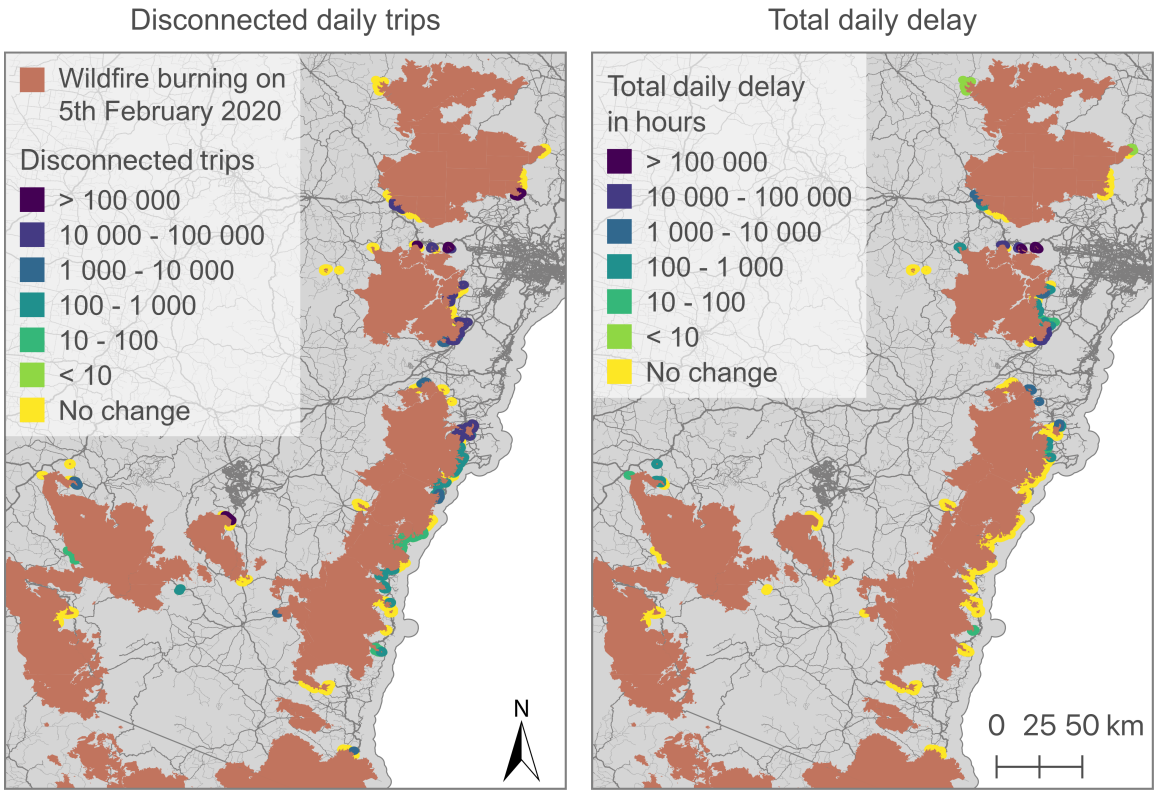

Figure 7.19: DVS with the TDM in SE-NSW. On the left, the number of disconnected daily trips is illustrated for each scenario buffer. On the right, the total daily delay is visualized.

in Figure 7.13 and Figure 7.16, almost the entire south-east coast is already at least partly disconnected from the rest of the road network. Because travel times can not be calculated for disconnected parts of the network, the DVS cannot detect further impacts of a wildfire spread on the road network's functionality. A vulnerability towards further disconnections due to wildfire spread can be observed in Figure 7.19 for the entire south-east coast.

In summary, this chapter presents the results of applying GRIND for two wildfire scenarios in different case study regions. As such, it proves the transferability of GRIND. In the next chapter, the strengths and limitations of each GRIND module seperately, and of the concept as a whole are discussed in detail.

8 Methodological Discussion of the Assessment of Critical Road Infrastructure in GRIND

This chapter discusses the case study results, demonstrated in Chapter 7, for each module of GRIND. A brief regional analysis and comparison of the specific results of both case study regions is performed in Section 7.1. This discussion's focus is the applicability of GRIND for the assessment of critical road infrastructure in the disaster context. The advantages and limitations of each GRIND module are analyzed in detail, and their application potential for disaster management is highlighted.

This chapter starts by analyzing the effect of applying the Fuzzy-FSE and Error Search in Part I. Then, the results of the CM and AIC module (Section 8.2), the TDM module (Section 8.3), the DIA module (Section 8.4), and the DVS module (Section 8.5) are discussed. Finally, the limitations of GRIND are presented in Section 8.6.

8.1 Fuzzy-FSE and Error Search in GRIND

In Part I of this thesis, Chapter 2 demonstrates that the quality of the OSM road network is often not sufficient, especially for routing applications. Two major challenges are identified: the often missing speed information and the frequently low attribute accuracy regarding the road classification. Two modules are developed to address these challenges: the Fuzzy-FSE (see Chapter 3), which estimates speed values, and the Error Search (see Chapter 4), which searches for road classification errors. In GRIND, these modules are applied to the OSM road network data to obtain an enhanced OSM road network dataset, which can then be used for part II of GRIND.

In the following, the applications of these modules are discussed with respect to the assessment of critical road infrastructure in GRIND. First, the benefit of using the Fuzzy-FSE to estimate travel times is analyzed. Then, the advantages of the Fuzzy-FSE for the generic concept are discussed.

Fuzzy-FSE

Travel Times versus Network Distance The Fuzzy-FSE estimates average speed values for every road segment, which can then be used to calculate travel times. The simplest alternative for routing applications is to use network distance if speed information is not available. However, the use of network distance completely disregards road hierarchy and thus road quality. There is a difference in speed between high-level roads like `motorways` and low-level roads like `tertiary` roads in every country worldwide. The same distance on a high-level road can be traveled much faster than on a low-level road. For example, the road distance from Sydney to Newcastle in NSW in Australia is 125 km, and it takes 74 min without traffic to travel this route (calculated by the GD-API). A similar road distance from the small town of Towong to Jindabyne in the South-West of NSW of 137 km has a travel time of 132 min (calculated by the GD-API). The difference is that the route from Sydney to Newcastle travels the Pacific highway and the route from Towong to Jindabyne follows a low-level road. This phenomenon highlights the importance of accounting for the average speed on a road.

The original ARIA [197] only considers network distances. This might not lead to large errors when considering only the highway network like Taylor and Susilawati [108], but, as soon as more road classes are included, the road quality has to be taken into account. Network distance overestimates the accessibility of remote regions because these regions are often only connected with low-level roads. Thus, the region might seem more accessible using network distance because the bad road quality limits the driving speed. Using travel time as a cost factor resolves this issue.

Travel Times versus Weighting Factors In our previous study in [65], we employ weighting factors to account for different road qualities. These weighting factors are adaptable to different study regions and are an acceptable approximation if speed values are not available. However, travel times are easier to interpret than weighted road distances which renders the impact assessment more intuitive. Furthermore, the application of weighting factors, like the application of fixed speed profiles per road class, is characterized by jumps at class borders. The Fuzzy-FSE resolves this issue as it relies not only on the road class to estimate average speed but also on the road surface, the road length, and the curviness of a road. These parameters are then combined with Fuzzy Control using expert knowledge.

Advantages and Limitations of the Fuzzy-FSE The advantages and limitations of the Fuzzy-FSE, in general, are discussed in detail in Section 3.8. Regarding the application in the generic concept, the main advantages are the adaptability to local road conditions and the possibility to estimate speed values from only OSM data. The Fuzzy-FSE reaches an acceptable accuracy of around 70 % for both study regions (see Section 3.7). Nevertheless, it has to be considered that the accuracy is highly dependent on the applied expert knowledge and that the Fuzzy-FSE is not designed for urban regions.

Error Search

The Error Search presented in Chapter 4 consists of two independent parts: the search for disconnected network components and the gap search. Both are applied in GRIND to obtain the enhanced OSM dataset.

Search for Disconnected Network Components The search for disconnected network components is applied for the road network consisting of L1-L5 roads in the BM regions and NSW. Consequently, disconnected network components are either connected to the main network, if the connection was in the wrong road class, or deleted, if the component itself was assigned the wrong road class. If these disconnected network components are not detected, in the generic concept, grid cells close to the roads of the disconnected network component are assigned to these roads (see Section 6.1). Because the component is not connected to the rest of the road network, the shortest paths to facilities and service centers for all grid cells assigned to the roads of the disconnected network component can not be calculated. This behavior results in large areas where travel times and the indices can not be calculated.

Before applying the search for disconnected network components, travel times are not calculable for 397.1 km^2 of grid cells in the BM regions. Similarly, travel times are not calculable for 16 611.9 km^2 (2.15 % or the area) of the entire state of NSW in Australia without the treatment of disconnected network components. Thus, a relatively simple search for disconnected network components can have a big effect on the assessment of critical road infrastructure in the generic concept.

Gap Search The second part of the Error Search is the gap search. As demonstrated in Chapter 4, the gap search identifies gap candidates first where the shortest path in a subnetwork is significantly longer than in the complete network. During the case study in Section 4.5, the 50 errors with the longest detour in subnetwork S5 feature a detour from 70.97 km to 294.14 km if the error is not corrected. This can lead to wrong accessibility indicators if the route to the next facility or service center lies on that path. A location is then deemed much more remote than it is because of road classification errors.

To further elaborate on this issue, the S3 of NSW (all L1-L3 roads in NSW) is considered before and after correcting the errors identified in Chapter 4. The travel times from all settlements in NSW (857 settlements) to their nearest service center in each category are calculated in the network with and without errors. For most settlements, the travel time to the nearest service center remains unchanged as the shortest paths do not pass over the roads with classification errors. However, for some settlements, the travel time to service centers increases significantly when the errors are not corrected (see Table 8.1). The total increase is higher if the travel time to low-level service centers is considered because then, low-level roads, which contain more errors, are used more frequently.

Table 8.1: Travel time (TT) increase in minutes in all settlements and number of settlements where the travel time to the nearest service center changes if road class errors are not corrected.

	TT OSM - TT Enhanced OSM	Changed settlements
SC A	162.9	9
SC B	45.65	6
SC C	226.3	24
SC D	219.3	14
SC E	200.8	16

In conclusion, the influence of the error detection by gap search on the results of the critical infrastructure assessment depends on the location of the errors. If the errors lie on many shortest paths to facilities or service centers, the correction of these errors improves the results significantly. Furthermore, suppose access to a region is blocked during the impact assessment. In that case, undetected road classification errors in the only alternative route to this region may lead to the false assumption that the region is not accessible.

8.2 Core Module and Accessibility Index Calculation

The CM calculates the travel time from all grid cells to the nearest facilities and service centers. The AIC module uses the CM to calculate the EFAI and ARIA. In the following, the methodological aspects of these modules are discussed. The strengths and limitations of the different approaches are summarized in Table 8.2.

Travel Time versus Index With the generic concept, both travel times as absolute values and indices as relative indicators of accessibility can be calculated. Both approaches feature different advantages and limitations. Absolute values of travel times are generally easier to calculate and very intuitive to interpret. A regional planner or disaster manager can directly see where a region is, for example, further away from a hospital than one hour and can act accordingly. However, the combination of travel time in a single measure is difficult. Considering the example of SE-NSW, the mean travel time to hospitals is almost double the mean travel time to fire stations (see Table 7.1). A simple sum or average of all facilities or service centers is then inconclusive and might skew the results in favor of one facility or service center. The EFAI and ARIA account for that by converting each travel time to a ratio of travel times such that each facility or service center travel time is standardized and can be summed up. Thus, a single measure for facility or service center accessibility can be constructed. The downside of indices is that the values are not intuitive and require background knowledge to be interpreted. Regarding the comparison of results, travel times can be compared directly and unambiguously. However, sometimes

different regions are not directly comparable because one region features much more rural areas than the other, much like the analyzed study regions in Chile and Australia. A relative index like the ARIA or EFAI furthers a comparison by taking into account the different stages of development or urban-rural distribution.

ARIA versus EFAI The ARIA and EFAI index consider two different aspects of accessibility. The focus of the ARIA is the accessibility to everyday needs, which are located in service centers. The higher the service center category, the more specialized needs like special medical care or necessities can be provided. Considering the application in disaster scenarios, this is especially important for long-lasting disasters as the population requires food in low-level service centers and other specialized equipment in high-level service centers. However, it could be argued that the accessibility to category A and B service centers is more important for everyday needs than for emergency scenarios as special necessities can often be postponed. The EFAI, on the other hand, only considers access to or from emergency facilities required in a disaster scenario. This information is especially important for the short time reaction where people might be hurt or wildfires need to be stopped. The EFAI and ARIA are based on the same principle but have different value ranges such that their values are not directly comparable. As the ARIA is a tested and elaborated method [108], both indices are validated methods that are relatively simple and data-sparse.

Accuracy of the Indices In the context of this generic concept, the accuracy of the ARIA depends on the accuracy of the populated places dataset, which is itself dependent on the OSM settlement data quality. However, large settlements in OSM are often wrongly mapped as several suburbs (for example, Canberra in Australia). For the populated places dataset, the population is then distributed over multiple settlements. A classification in service centers might categorize these multiple settlements in a lower class than the higher-order settlement. This issue has to be considered when calculating the ARIA with the generic concept. The EFAI, on the other hand, is dependent on the classification quality of OSM facilities.

Grid-Based and Multi-Scale Approach The CM and AIC module include the possibility of a grid-based analysis. This grid-based analysis is not population-based but considers accessibility also for uninhabited or sparsely inhabited areas. Especially in disaster scenarios, this is valuable because disasters may happen in very remote regions but still threaten the few people living there. On the downside, a grid-based analysis requires more computing time than a point-based approach and might include some small errors because of the centroid's location. Both a point-based and a grid-based analysis are possible in the generic concept. GRIND includes the possibility to consider multiple scales by using different grid resolutions and levels of road network. Examples of two case studies on two spatial scales are shown in Guth et al. [65]. They perform a regional-scale analysis of the 2017 wildfires in Chile and a local scale analysis of the 2017 wildfires in Portugal. Guth et al. [65] demonstrate that on a local scale, regional planners can analyze the importance of the minor-level road network such as residential streets and paths.

Table 8.2: Summary of strengths and limitations of the calculation of travel times, the ARIA, and the EFAI in the CM and AIC module.

	Strengths	Limitations
Travel times	• Absolute measure of accessibility • Intuitive interpretation • Directly and unambiguously comparable • Simple and data sparse	• Combination into single measure for all facilities or service centers difficult • Not relative to local road conditions and urban-rural distribution
ARIA	• Relative to local road conditions • Accessibility to everyday needs • Combined measure for service centers • Simple and data sparse	• Requires background knowledge for interpretation • Values of indices not directly comparable • Accessibility to service center categories A and B may be irrelevant in a disaster context • Accuracy depends on populated places dataset
EFAI	• Relative to local road conditions • Accessibility to emergency facilities • Combined measure for facilities • Simple and data sparse	• Requires background knowledge for interpretation • Values of indices not directly comparable

Application The CM and AIC module can be applied before disaster scenarios. In the mitigation and preparedness phase, places with poor accessibility can be identified which can support regional planners' decisions. Three strategies are possible to improve accessibility: road quality can be enhanced to obtain shorter travel times, shorter or more direct roads can be constructed, or new facilities or service centers can be built. Furthermore, both modules can be applied in the DIA and DVS module.

8.3 Travel Demand Model

The results for the TDM module, applied for SE-NSW in Australia, are shown in Section 6.4. The following section discusses the limitations and strengths of the model and its applicability to GRIND and summarizes them in Table 8.3.

Limitations Compared to state-of-the-art, detailed TDMs, this model performs rather poorly, especially considering the RSME of over 6000 vehicles per day. This is mainly because of the prerequisite that only globally-available, free data sources should be used. The combination of OSM settlement points and population estimates is not enough to model such a complex

Table 8.3: Summary of strengths and limitations of the TDM module.

	Strengths	Limitations
Travel demand model (TDM)	• Easy and fast to calculate • Intuitive interpretation • Estimation based on purely OSM data • Adaptable to different regions worldwide	• Low accuracy • Capacity of roads not considered • Accuracy dependent on populated places dataset and travel times

system like an intercity TDM in all its detail. For this model, populated places are given as points, which leads to false results near large settlements as they consist of a separate TDM themselves. Furthermore, the capacity of roads is not considered in the trip distribution phase as capacity data is not available in OSM. This furthers the model to overuse roads that would normally not be used because it would exceed road's capacity. Additional uncertainty is caused by the use of population estimates (Section 6.2) and speed estimates (Chapter 3), which both have estimation errors. Furthermore, an evaluation of the model is only possible for high-level roads like `motorway` and `trunk`, as no reference data exists for lower-level roads. Ideally, more data and more accurate data could be combined to establish a more accurate intercity TDM. Such a model could include a road network with capacity information, a detailed population estimate, economic data like the GDP of a location, the tourist flows, and other data collected with questionnaires about intercity travel behavior.

Strengths However, the prerequisites for this study have to be considered (see Section 5.4), especially considering data simplicity and data sparsity. The objective is not to produce an accurate, detailed TDM as this is not possible with this little data. For GRIND, a rough estimate of daily trips per OD pair, based on pure population and OSM data is intended. This model should be easy to use, fast to calculate, and easy to adapt to different regions worldwide. Considering these limitations, the developed TDM is adequate as it provides an idea about average daily trips, which can later be used in the DIA and DVS modules in GRIND.

8.4 Disaster Impact Assessment

As described in Section 6.5, the DIA module employs both network analysis and transport modelling. The results of the DIA of two exemplary wildfire scenarios are presented in Section 7.4. This section discusses the impact assessment results regarding its methodological aspects. The strengths and limitations of the different approaches are summarized in Table 8.4.

Travel Times versus Indices The DIA module enables an impact assessment both with travel time and with the ARIA and EFAI. The strengths and limitations of both methods, which have already been mentioned in Section 8.2, also prevail for the impact calculation.

Individual travel times are easier to interpret but difficult to stack into a single measure. The largest disadvantage of both indices is that they cannot be calculated as soon as one facility or one service center is disconnected. In SE-NSW, this amounts to a total area of 15 821 km^2 where the ARIA can not be calculated, mainly in the south of SE-NSW, because the service centers A-C are not accessible (see Figure 7.11 and Figure 7.13). Furthermore, the impact of the wildfires on the accessibility to service center category A is much higher than for other service center categories. This impact makes up most of the area of the ARIA-Impact in both regions. Arguably, the accessibility to service centers of category A or B might not be essential in a disaster scenario and could be excluded from the index to avoid unrealistic impacts. Concerning the EFAI, some facilities might be more important than others. For example, the accessibility of fire stations is of major importance in a wildfire scenario, while police stations might not be essential. Therefore the individual travel time impact might be more interesting for emergency management than the EFAI.

Disconnected Network Components Generally, disconnections are an issue. A disconnection is usually much worse than a travel time increase because it means that a region is rendered completely inaccessible. The NADIA can quantify impact, either as travel time or as index difference, if the shortest path can be found. However, if a road connection does not exist, it can not quantify the impact but only states that it is disconnected. Ideally, a quantifiable impact of disconnections would also be included in the impact calculation. The TDMDIA can provide a little more information on disconnected settlements because it can provide a percentage of disconnected daily trips. A settlement with all daily trips disconnected probably experiences a more significant impact of wildfires than a settlement with only 50 % of daily trips disconnected. In the case of half of all daily trips disconnected, it can be expected that at least some minimal help is accessible in a disaster scenario.

Travel Demand Model The accuracy of the TDMDIA results highly depends on the accuracy of the TDM. In this case, the TDM can be considered a rough estimate of daily trips, as mentioned in Section 8.3. Therefore, the results of the TDMDIA have to be analyzed rather relatively than absolutely. The TDM does not account for a change of travel behavior after the event as it aims at analyzing the impact on daily traffic. Evacuation behavior is very hard to predict in disaster scenarios. It depends on many different and often not tangible factors. For example, the cultural background and the experience of past events highly influence evacuation behavior and compliance with official recommendations [204]. These factors are not calculable or predictable using only OSM data and, therefore, not in the scope of this thesis.

Network Analysis versus Transport Modelling Both types of impact assessment methods, the network analysis and transport modeling have their merits (see also Section 5.2). Network analysis with the CM and AIC module has the advantage of being easy to calculate with very little data. It considers thematic accessibility rather than demand-based accessibility and focuses on the functionality of the road network. The exact implications are often more difficult to interpret because of the missing demand aspect. On the other hand, the

Table 8.4: Summary of strengths and limitations of the application of the CM, AIC module, and TDM module for a post-disaster impact assessment with the DIA module.

	Strengths	Limitations
Travel times (CM)	• Intuitive interpretation • Possibility to analyze each facility or service center accessibility separately • Simple and data sparse • Thematic accessibility	• Combination into single measure for all facilities or service centers difficult • Impact of disconnections not quantifiable
Indices (AIC)	• Combined measures for facilities or service centers • Simple and data sparse • Thematic accessibility	• Requires background knowledge for interpretation • Impact of disconnections not quantifiable • Values of index impacts not directly comparable • Impact not calculable if one facility or service center is disconnected
Travel demand model (TDM)	• Intuitive interpretation • Delays in daily travel time • Provides percentage of disconnected daily trips • Translatable to monetary values • Demand-based accessibility	• Low accuracy of the TDM • Capacity of roads not considered • Does not account for evacuation or change in travel behavior after event

TDM module requires more and more complicated data or suffers uncertainty of the model. Nevertheless, it can estimate demand-based impacts of wildfires as delays in daily travel time, which is easy to interpret for disaster management. Furthermore, the results of a TDMDIA can be translated to monetary values, which is useful for PDNAs (see Section 5.2.2).

Application The advantage of the impact assessment in GRIND is that these approaches are used jointly. This enables disaster management to consider different aspects of impacts:

- the absolute accessibility decrease to specific facilities or service centers in travel time,
- the relative index difference as a combination of facility or service center accessibility,
- and the absolute impact on daily traffic.

In disaster scenarios, all these aspects can be crucial, and their combined examination can help decision-makers.

8.5 Disaster Vulnerability Scan

The results of the DVS, described in Section 6.6, are presented in Section 7.5. In this section, these methodological aspects of the DVS are discussed. Its strengths and limitations are summarized in Table 8.5.

Scenario Buffers For the DVS, the wildfire spread is simulated in overlapping buffers. Another common alternative for a vulnerability scan is the degradation of single links. The advantage of overlapping buffers is that neighboring effects are included in the analysis. If the wildfire affects one road, the neighboring road is most likely also affected. A single link degradation is not able to capture these effects. However, the buffer method is a simplification of the real world with the assumption that wildfire spread is equal in all directions. This assumption does not consider the actual potential of fire spread, which depends on many factors like fuel availability, temperature, and wind direction. In these case studies, an exemplary buffer width of 3 km is chosen, but other values are possible. A multi-buffer analysis could also be performed to simulate multiple scenarios of fire spread Such a multi-buffer analysis could employ different buffer widths (for example, 1 km, 3 km, and 5 km) to account for variable speeds of fire spread.

Travel Times versus Indices The vulnerability indicators are calculated using the CM, the AIC module, and the TDM module. As in the DIA module, the vulnerability indicators focus on different aspects of vulnerability and have their strengths and limitations. The travel time difference is easy to interpret, but one facility or service center may be overweighted. For example, the travel time to service center category A is generally longer than the travel time to a service center category E. Thus, by taking the average of all travel times to service centers, the category A service center is overrepresented. The relative index eliminates this issue but leads to hard-to-interpret values. Furthermore, the range of values is very small because the area of the fire spread is so small compared to the total area that it causes little effects.

Travel Demand Model The TDM module provides a daily delay in hours, which is easy to interpret. However, it is highly dependent on the accuracy of the underlying model. Regarding the computing time, the TDM is calculated faster than the travel time to the nearest facility or service center. For the nearest facility or service center, the closest facility or service center has to be recalculated every time because a different facility or service center could now be the closest one. For the TDM, fewer paths have to be recalculated, and then a simple sum calculates the total delay.

Disconnected Network Components The fact that disconnections can not be measured as impact remains an issue for the DVS (see also Section 8.4). Therefore, the resulting vulnerability indicators have to be considered in combination with the number of disconnected trips. Furthermore, the situation in the degraded network has to be taken

Table 8.5: Summary of strengths and limitations of the DVS module. The strengths and limitations of the CM, AIC module, and TDM module for the DVS module are the same as in Table 8.4.

	Strengths	Limitations
Disaster Vulnerability Scan (DVS)	• Ability to include neighboring effects by overlapping scenario buffers • Index impacts as combined measure of accessibility decrease to service centers or facilities • Fast calculation of TDM • Provides number of disconnected daily trips	• Probability of disaster spread not accounted for • Range of index impact values very small • Slower calculation for Travel time or index impact than for daily delay • Impact of disconnections unrepresentable

into account when looking at the results of the DVS. Wildfire spreads in already disconnected regions cause no apparent change during the DVS. However, in reality, they have the potential to threaten already vulnerable communities further. Ideally, this phenomenon could also be displayed by the DVS.

Application The DVS offers a wide range of applications. It can be used to find locations where a fire spread would be most critical for the functionality of the road network. The vulnerability is considered in three different aspects: accessibility to emergency facilities, accessibility to service centers, and daily traffic. Disaster management can then prioritize fire fighting, and efforts to extinguish fires near critical roads can be reinforced.

8.6 Limitations of GRIND

Uncertainties of GRIND The results of GRIND are subject to some uncertainties that result from the underlying data and the developed methodologies. On the one hand, errors may be introduced by low-quality OSM data. Although the Error Search mostly detects road classification errors, there might be other errors in the OSM data like roads missing or false classification of facilities. Furthermore, the travel times calculated by the Fuzzy-FSE might deviate from the true value with a RMSE of around 13 km/h (BM) and 15 km/h (NSW). The limitations of the Fuzzy-FSE are described in detail in Section 3.8. For the ARIA calculation and the TDM module, population data is required. This population data may contain misestimations from the underlying GHS-POP dataset and the methodology to assign population data to settlements (see Section 6.2). Finally, the TDM is also based on expert knowledge and delivers only a rough estimate of daily traffic rather than exact values.

These uncertainties largely stem from the prerequisite of using only free, worldwide available data (see Section 5.4). In a disaster scenario, the quick availability of data is often more important than exact results to provide a rapid post-disaster impact assessment. Therefore,

Table 8.6: Summary of strengths and limitations of GRIND.

	Strengths	Limitations
GRIND	• Data sparse (requires only worldwide available data) • Fast to calculate after disaster • Modular and flexible towards requirements of disaster management • Enables grid-based and multi-scale analysis • Considers different aspects of accessibility	• Contains uncertainties caused by underlying data • Contains uncertainties caused by the developed methodologies • Does not account for behavior change of network users after a disaster • Not applicable for entirely urban regions • Requires expert knowledge about regional specifics (road quality, daily transport)

this thesis' objective is not to provide a 100 % accurate result, but a generic concept that can generate results quickly using OSM without having to search for regional data sources.

Application Constraints Some application constraints exist for GRIND. First, it does not account for a behavior change of network users after a disaster. Thus, evacuation behavior is not included in the model. People react differently to disasters, and predicting evacuation behavior is a different task that is a vast research field itself as many factors have to be considered. Secondly, GRIND is not applicable to entirely urban regions. As discussed in Chapter 3, the estimation of travel time in urban regions requires different input parameters and is much more subject to temporal changes than rural travel time. Because the accuracy of GRIND results depends heavily on the accuracy of the travel times, GRIND's performance is poor if the travel times are false.

The strengths and limitations of GRIND are summarized in Table 8.6.

Part III

Synopsis

9 Conclusions and Outlook

The third and last part of this thesis recapitulates the research goals towards the main objective and summarizes the major contributions. The potential of GRIND and its limitations are highlighted in a comprehensive conclusion (see Section 9.1). Section 9.2 focuses on possible optimizations and points out future research directions.

9.1 Synoptical Discussion and Conclusions

This thesis's main objective is to develop a generic, multi-scale concept to assess critical road infrastructure in a disaster context using OSM data. Based on the observation that OSM data is not directly usable for routing applications, two consecutive research goals were established to fulfill the main objective.

The first research goal, addressed in Part I of this thesis, is to improve the routability of OSM data. Part I can stand autonomously of Part II of this thesis and proves valuable for all kinds of routing applications. Therefore, Section 9.1.1 concludes Part I independently of GRIND. The second research goal of assessing critical road infrastructure in a disaster context is addressed in Part II using the enhanced OSM dataset generated in Part I. GRIND results from a combination of both parts and is concluded in Section 9.1.2. Finally, the application potential of GRIND for disaster management is presented in Section 9.1.3.

9.1.1 Synoptical Discussion and Conclusion of Part I

Part I of this thesis concentrates on OSM road network data. In the following, the main contributions of Part I are briefly discussed and concluded.

Quality Analysis A global quality analysis of OSM road network data regarding attribute completeness of tags, which might be relevant for routing applications, is performed. Also, the related work on OSM road network data quality is summarized concerning six widely known data quality elements for geographic data. In conclusion, the OSM road network can nowadays be considered relatively complete and accurate as feature completeness and positional accuracy are sufficiently high. OSM even surpasses authoritative data in some regions. However, considering OSM data in routing applications, the attribute completeness and accuracy are still lacking. The most relevant shortcomings of OSM data for routing

applications and especially for the analysis of critical infrastructure, are identified as the often missing speed information and frequent road classification errors.

Fuzzy-FSE A multi-parameter Fuzzy Framework for estimating average speed information in rural road networks is developed. It combines the parameters road class, road slope, road surface, and link length. These parameters can all be extracted or calculated from OSM. The **Fuzzy-FSE** is applied successfully in two case study regions that differ in their state of development and their OSM data quality. The implementation and the datasets of the **Fuzzy-FSE** are published on GitHub. A major advantage of the **Fuzzy-FSE** is the worldwide applicability in rural regions. For urban regions, the methodology has to be extended as other factors influence average speed in urban compared to rural regions. The **Fuzzy-FSE** offers the advantages of Fuzzy Control as it allows for fuzzy input parameters and contains the reasoning process of a human operator. In contrast to machine learning approaches, training data is not required because the **Fuzzy-FSE** is based on expert knowledge. The downside of expert knowledge is that the **Fuzzy-FSE** is much more susceptible to false assumptions than, for example, a machine learning model would be. The most significant advantage of the **Fuzzy-FSE** is its ability to estimate average speed with only OSM data as input.

Error Search A novel approach to detect, rate, and categorize potential road classification errors in OSM is designed. It bases on the assumption that both disconnected parts and gaps of subnetworks in the OSM road network are indicators for road classification errors if the disconnection or the gap can be resolved in the complete network. The **Error Search** searches independently for disconnected parts and gaps in subnetworks. For the **Error Search** at gaps, different parameters are identified that indicate gaps that are then combined in a rating system to obtain an error probability. Identified errors can then be checked and corrected by a human user. A detailed and efficient implementation of the developed methodology is published on GitHub. In conclusion, the **Error Search** finds fewer road classification errors at disconnected parts than at gaps. A gap search finds a significant number of misclassifications and can additionally provide an error probability based on the developed rating system. Some limitations have to be considered. On the one hand, the underlying assumption is not true in all cases because roads may rarely turn into lower-quality roads for a certain distance and then turn back to the original road class. On the other hand, the **Error Search** is not able, but also not designed to find all classification errors. Instead, only the errors potentially leading to long detours if only a high-level network is considered are identified. Because of these limitations, a human user has to check the identified errors. The **Error Search** is intrinsic such that no additional data besides the OSM road network is required.

Enhancement of OSM for Routing Applications The **Fuzzy-FSE** and the **Error Search**, developed in Part I require only OSM data as input data. This fact renders them valuable tools for all kinds of routing applications working with OSM data to improve their underlying data and find potential errors. Applications for these modules can be found in all areas where

routing is necessary, like transport of goods, car travel, and network planning. Especially for the assessment of critical infrastructure in a disaster context, speed information in rural road networks and a correctly classified high-level road network prove to be essential. The free and open-source publication of the implementation on GitHub enables other users to reproduce the results and transfer the methodology to other regions if needed.

9.1.2 Synoptical Discussion and Conclusion of GRIND

This thesis develops **GRIND**, a generic, multi-scale concept for the assessment of critical road infrastructure in a disaster context using OSM data. **GRIND** consists of two parts, which correspond to the structure of this thesis. The first part of **GRIND** enhances the OSM road network data used in the second part of **GRIND**. In the following, the main contributions of **GRIND** towards the main objective are briefly discussed and concluded.

Application of Enhanced OSM Data The application of OSM data in general benefits **GRIND** in many ways. OSM is available worldwide, featuring a continuously improving data quality, which allows for a global application of **GRIND**. Furthermore, OSM data is free-to-use and saves valuable time for disaster management by not searching for local data sources in a disaster case. However, its application for routing purposes proves challenging without preprocessing the road network data. Therefore, the first part of **GRIND** is necessary to assess critical road infrastructure with OSM data. The travel times calculated by the **Fuzzy-FSE** are required as a cost factor for the road network. The **Fuzzy-FSE** can estimate travel times only based on OSM data and simultaneously allows for adaptations depending on local road conditions. The **Fuzzy-FSE** reaches an acceptable accuracy of around 70 % for both study regions. Road classification errors are inconvenient for routing applications in general. For multi-scale approaches like **GRIND** that only consider a high-level road network, road classification errors are even worse as they can lead to large detours and disconnected subnetworks. For **GRIND**, the developed **Error Search**, and a subsequent correction of errors, proves to be essential to ensure the correctness of the results.

Absolute and Relative Measures of Accessibility **GRIND** enables the calculation of absolute and relative accessibility measures using the **CM** and **AIC** module for an entire region (grid-based) or individual locations (point-based). Travel time to service centers and facilities is provided as an absolute measure of accessibility and features the main advantage of being easy to interpret. But, the combination of travel time to service centers or facilities in a single measure by sum or average might skew the results in favor of one service center or facility. Therefore, **GRIND** can also calculate relative accessibility measures, namely the ARIA and EFAI, which each consider different aspects of accessibility. The ARIA accounts for accessibility to service centers and focuses on the accessibility to everyday needs. The EFAI indicates accessibility to emergency facilities and therefore specializes in the application in a disaster context. Both indices are validated methods that are relatively simple and data-sparse.

Travel Demand Model The TDM module of GRIND estimates intercity daily traffic based on purely OSM and worldwide available population data. The developed model is easy to use, fast to calculate, and adaptable to different regions worldwide. Compared to state-of-the-art detailed travel demand models, it performs inferior and contains many inaccuracies due to estimation errors of input data and the model itself. However, considering the prerequisites of GRIND about data simplicity and data sparsity, the model proves adequate for GRIND as it provides an idea about daily trips. The main benefit of the TDM module is its application in the DIA and DVS module. The TDM features a lot of potential for future enhancements.

Disaster Impact Assessment The DIA module of GRIND assesses the impact of natural disasters on road networks in three different aspects: the absolute accessibility decrease to specific facilities or service centers in travel time, the relative index difference as a combination of facility or service center accessibility, and the absolute impact on daily traffic. The main advantage of the DIA in GRIND is that these different approaches are used jointly. In disaster scenarios, their combined examination can help decision-makers. With the TDM, a translation to monetary values of impacts is also possible by assigning a cost of delay. Disconnected road network parts remain an issue for the DIA module because their impact is not quantifiable. But, the TDM is able to deliver a percentage of disconnected daily trips for each settlement, which provides some information about the impact of disconnections.

Disaster Vulnerability Scan The DVS is a novel application of the commonly used network scan during a disaster scenario. It uses the AIC and TDM modules of GRIND to identify areas where a disaster spread would have the most significant impact on the functionality of the road infrastructure. The application of overlapping buffers to simulate a disaster spread instead of single link failures allows GRIND to include neighboring effects. The probability of a disaster spread at a certain location is not accounted for. Like in the DIA module, the different aspects of impacts estimated during the vulnerability scan enable a differentiated consideration of disaster impacts.

GRIND Summary and Limitations The combination of these contributions results in GRIND. For the application of GRIND, its limitations have to be considered. It is not applicable to urban regions, and evacuation behavior is not included in the modules. Furthermore, GRIND is subject to uncertainties that result from the underlying data and the developed methodologies. However, in a disaster scenario, the quick availability of data and simple but fast models are often more important than exact results. GRIND provides such a comprehensive, modular, and multi-scale concept that is readily applicable for disaster scenarios worldwide and overcomes the often-overlooked challenge of limited data availability.

9.1.3 Application of GRIND for Disaster Management

GRIND assesses critical road infrastructure in different phases of the disaster management cycle. The GRIND modules in the context of the disaster management cycle are visualized in Figure 9.1.

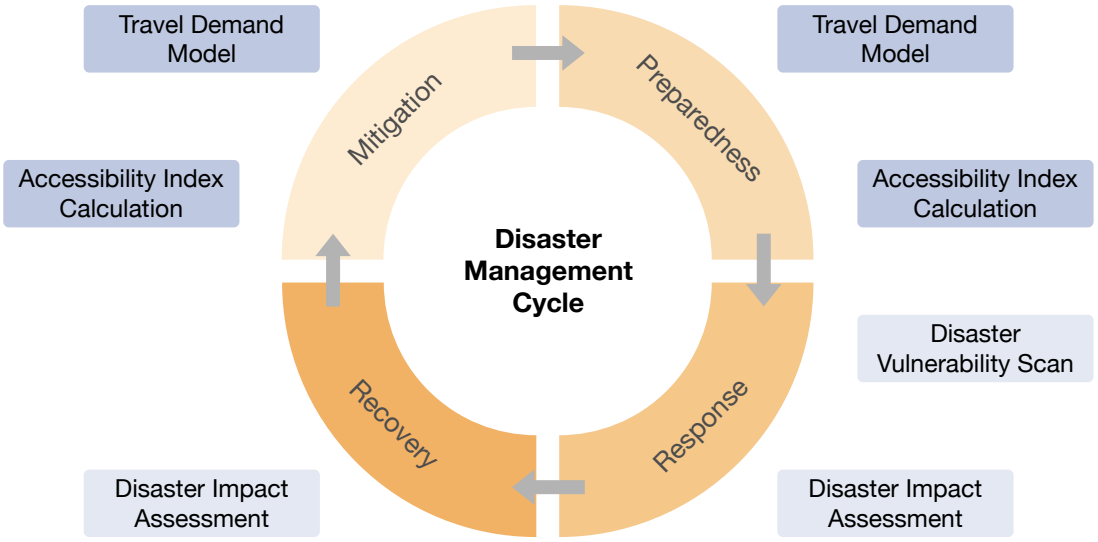

Figure 9.1: The modules of the generic concept in the context of the disaster management cycle.

The AIC and TDM modules can be used in the mitigation and preparedness phase to identify places with poor accessibility or locate frequently traveled roads. The DIA module can be employed in the response phase to find regions with decreased accessibility or places where daily traffic is significantly delayed. During a disaster in the immediate response phase, the DVS module can be applied to detect regions where a disaster spread would be most critical. Finally, in the recovery phase, the DIA module can help develop recovery strategies by quantifying the impact of a disaster. GRIND can also be employed to develop a preliminary PDNA until more accurate data is available.

GRIND is a comprehensive concept for the assessment of critical road infrastructure. Using OSM data, GRIND can provide disaster impact assessments relatively fast, even if no other data besides OSM is available. For regional planners and disaster management, it is a valuable and flexible tool that can be applied globally and includes country- or region-specific adaptations.

9.2 Potential Advances and Outlook

The modules developed in this thesis offer many possibilities for future enhancements. In the following, these potential advances are presented regarding the **Fuzzy-FSE**, the **Error Search**, and the assessment of critical road infrastructure.

Extension of the Fuzzy-FSE As demonstrated in Keller et al. [86], data-driven machine learning models can improve the estimation of average speed, but also require an additional data source for reference data. The combination of Machine Learning and Fuzzy Control could be a promising direction for future research. The **Fuzzy-FSE** itself could benefit from the inclusion of data from additional data sources to produce more accurate results. Furthermore, it could be investigated if an adaptation of the **Fuzzy-FSE** to urban circumstances is possible. This would require different input parameters and possibly also other data sources. The implementation of the **Fuzzy-FSE** is freely available on GitHub, such that the entire community can easily extend it.

Enhancement of the Error Search The **Error Search** could benefit from analyzing available tags of gap candidates and their connecting roads for continuity. The effect of strokes on the error probability could be analyzed. The rating system, as a multi-criteria decision system, could be extended, for example, by weighting the input parameters. Furthermore, remote sensing methods could be applied to track the road at gap candidates if a shape change indicates a class change. Ideally, further case studies are performed in different study regions worldwide with different qualities of OSM data to enable a detailed sensitivity analysis. The efficiency of the **Error Search** could be tested with real-world OSM contributors. The **Error Search** implementation is also available on GitHub, which enables everyone to extend it.

Optimization of the Critical Infrastructure Assessment The critical infrastructure assessment presented in Part II of this thesis can be easily extended because of its modular structure. One limitation, the inability to quantify the impact of disconnections, could be resolved by calculating indices that do not depend on a connected road network like the Critical Closeness Accessibility of Novak and Sullivan [19]. Additional data sources might have to be considered to calculate further indices. The developed travel demand model offers many possibilities for future optimizations. Following the prerequisite of only using worldwide available data, other OSM data could be included to estimate a location's attractiveness. For example, building densities, land use, and points of interest, like schools or shopping opportunities, could provide information about how certain areas are used. Additionally, a global data source with the GDP of subregions might also help the model to estimate attractiveness. During the trip assignment stage, capacity data would be most beneficial to avoid an unrealistic overflow on some roads. A capacity estimation of OSM roads using the road class and lanes information could prove a promising future research direction.

The disaster impact assessment could benefit from a more accurate travel demand model. An additional module could be implemented to transform the output of the TDM into actual economic losses by calculating the total cost of delay. Such a module would have to differentiate between the transport of goods and people and consider other factors like the temporary decline in toll receipts. Regarding the DVS module, the vulnerability scan could be performed with multiple buffers to simulate different speeds of disaster spread. Furthermore, the probability of a disaster spread could be considered. For example, in a wildfire scenario, the wind direction, temperature, and availability of flammable material could be included in a simulation of disaster spread.

Bibliography

[1] Vinod Thomas and Ramón López. “Global increase in climate-related disasters”. In: *Asian Development Bank Economics Working Paper Series* 466 (2015) (cit. on p. 1).

[2] Christopher Field, Vicente Barros, Thomas Stocker, and Qin Dahe. *Managing the risks of extreme events and disasters to advance climate change adaptation: special report of the intergovernmental panel on climate change*. Cambridge University Press, 2012 (cit. on p. 1).

[3] Matteo Coronese, Francesco Lamperti, Klaus Keller, Francesca Chiaromonte, and Andrea Roventini. “Evidence for Sharp Increase in the Economic Damages of Extreme Natural Disasters”. In: *Proceedings of the National Academy of Sciences* 116.43 (2019), pp. 21450–21455 (cit. on p. 1).

[4] Benjamin Wisner, Piers M. Blaikie, Piers Blaikie, Terry Cannon, and Ian Davis. *At Risk: Natural Hazards, People’s Vulnerability and Disasters*. Psychology Press, 2004 (cit. on p. 1).

[5] Karnjana Songwathana. “The Relationship between Natural Disaster and Economic Development: A Panel Data Analysis”. In: *Procedia Engineering* 212 (2018), pp. 1068–1074 (cit. on p. 1).

[6] Wolfgang Kröger. “Critical Infrastructures at Risk: A Need for a New Conceptual Approach and Extended Analytical Tools”. In: *Reliability Engineering & System Safety* 93.12 (2008), pp. 1781–1787 (cit. on p. 1).

[7] Andreas Atzl and Sina Keller. “A Systemic Approach for the Analysis of Infrastructure-Specific Social Vulnerability”. In: *From Social Vulnerability to Resilience: Measuring Progress towards Disaster Risk Reduction* 17 (2013), pp. 27–43 (cit. on p. 1).

[8] Blazej Cipeluch, Ricky Jacob, Adam Winstanley, and Peter Mooney. “Comparison of the accuracy of OpenStreetMap for Ireland with Google Maps and Bing Maps”. In: *In Proceedings of the Ninth International Symposium on Spatial Accuracy Assessment in Natural Resuorces and Enviromental Sciences*. Leicester, UK: University of Leicester, 2010, p. 4 (cit. on pp. 2, 22, 24, 28, 37).

[9] Christopher Barrington-Leigh and Adam Millard-Ball. “The world’s user-generated road map is more than 80% complete”. In: *PLOS ONE* 12.8 (2017), pp. 1–20 (cit. on pp. 2, 10, 11, 23, 24).

[10] Juliane Mondzech and Monika Sester. “Quality Analysis of OpenStreetMap Data Based on Application Needs”. In: *Cartographica: The International Journal for Geographic Information and Geovisualization* 46.2 (2011), pp. 115–125 (cit. on pp. 2, 22, 28).

[11] Sukhjit Singh Sehra, Jaiteg Singh, and Hardeep Singh Rai. “Analysing OpenStreetMap data for topological errors”. In: *International Journal of Spatial, Temporal and Multimedia Information Systems* 1.1 (2016), pp. 87–101 (cit. on pp. 2, 23, 27, 28).

[12] Sukhjit Sehra, Jaiteg Singh, and Hardeep Rai. “Assessing OpenStreetMap Data Using Intrinsic Quality Indicators: An Extension to the QGIS Processing Toolbox”. In: *Future Internet* 9.2 (2017), pp. 1–15 (cit. on pp. 2, 23, 26, 28, 55).

[13] Jesús Almendros-Jiménez and Antonio Becerra-Terón. “Analyzing the Tagging Quality of the Spanish OpenStreetMap”. In: *ISPRS International Journal of Geo-Information* 7.8 (2018), pp. 1–26 (cit. on pp. 2, 23, 25, 26, 28, 77).

[14] Rade Stanojevic, Sofiane Abbar, and Mohamed Mokbel. “W-edge: weighing the edges of the road network”. In: *Proceedings of the 26th ACM SIGSPATIAL International Conference on Advances in Geographic Information Systems - SIGSPATIAL ’18*. Seattle, Washington: ACM Press, 2018, pp. 424–427 (cit. on pp. 2, 30, 32).

[15] Enrico Steiger, Maksim Rylov, and Alexander Zipf. “Echtzeitverkehrslage basierend auf OSM-Daten im OpenRouteService.” In: *AGIT Journal* 2 (2016), pp. 264–267 (cit. on pp. 2, 32).

[16] Maximilian Leodolter, Hannes Koller, and Markus Straub. “Estimating Travel Times from Static Map Attributes”. In: *2015 International Conference on Models and Technologies for Intelligent Transportation Systems (MT-ITS)*. Budapest, Hungary: IEEE, 2015, pp. 121–126 (cit. on p. 2).

[17] Amin Mobasheri. “A Rule-Based Spatial Reasoning Approach for OpenStreetMap Data Quality Enrichment; Case Study of Routing and Navigation”. In: *Sensors* 17.11 (2017), pp. 1–18 (cit. on p. 2).

[18] Stefan Keller. “ReMAPTCHA: A map-based anti-spam method that helps to correct OpenStreetMap”. In: *GI_Forum 2014 – Geospatial Innovation for Society*. Salzburg: Austrian Academy of Sciences Press, 2015, pp. 40–44 (cit. on pp. 2, 55).

[19] David C. Novak and James L. Sullivan. “A Link-Focused Methodology for Evaluating Accessibility to Emergency Services”. In: *Decision Support Systems* 57 (2014), pp. 309–319 (cit. on pp. 3, 90, 94, 152).

[20] Jungyul Sohn. “Evaluating the Significance of Highway Network Links under the Flood Damage: An Accessibility Approach”. In: *Transportation Research Part A: Policy and Practice* 40.6 (2006), pp. 491–506 (cit. on pp. 3, 88, 90, 94).

[21] Yi Wen, Li Zhang, Zhitong Huang, and Mingzhou Jin. “Incorporating Transportation Network Modeling Tools within Transportation Economic Impact Studies of Disasters”. In: *Journal of Traffic and Transportation Engineering (English Edition)* 1.4 (2014), pp. 247–260 (cit. on pp. 3, 93).

[22] G. Shen and S. G. Aydin. “Highway Freight Transportation Disruptions under an Extreme Environmental Event: The Case of Hurricane Katrina”. In: *International Journal of Environmental Science and Technology* 11.8 (2014), pp. 2387–2402 (cit. on pp. 3, 93).

[23] Victor Knoop, Serge Hoogendoorn, and Henk van Zuylen. “Approach to critical link analysis of robustness for dynamical road networks”. In: *Traffic and granular flow’05*. Springer, 2007, pp. 393–402 (cit. on pp. 3, 88).

[24] Victor Knoop, Henk van Zuylen, and Serge Hoogendoorn. “The influence of spillback modelling when assessing consequences of blockings in a road network”. In: *European Journal of Transport and Infrastructure Research* 8.4 (2008) (cit. on pp. 3, 88).

[25] Wolfgang Burgholzer, Gerhard Bauer, Martin Posset, and Werner Jammernegg. “Analysing the Impact of Disruptions in Intermodal Transport Networks: A Micro Simulation-Based Model”. In: *Decision Support Systems* 54.4 (2013), pp. 1580–1586 (cit. on pp. 3, 88).

[26] Heejoo Ham, Tschangho John Kim, and David Boyce. “Assessment of Economic Impacts from Unexpected Events with an Interregional Commodity Flow and Multimodal Transportation Network Model”. In: *Transportation Research Part A: Policy and Practice* 39.10 (2005), pp. 849–860 (cit. on pp. 3, 89, 94, 95).

[27] Indervir S. Negi, Kishor Kumar, Anil Kathait, and P. S. Prasad. “Cost Assessment of Losses Due to Recent Reactivation of Kaliasaur Landslide on National Highway 58 in Garhwal Himalaya”. In: *Natural Hazards* 68.2 (2013), pp. 901–914 (cit. on pp. 3, 93–95).

[28] Larry Wesemann, Tijana Hamilton, Steve Tabaie, and Gerald Bare. “Cost-of-Delay Studies for Freeway Closures Caused by Northridge Earthquake”. In: *Transportation Research Record* (1996), pp. 1–9 (cit. on pp. 3, 93, 94).

[29] Rawia Ahmed El-Rashidy and Susan M. Grant-Muller. “An Assessment Method for Highway Network Vulnerability”. In: *Journal of Transport Geography* 34 (2014), pp. 34–43 (cit. on pp. 3, 88, 94).

[30] Qing-Chang Lu and Zhong-Ren Peng. “Vulnerability Analysis of Transportation Network under Scenarios of Sea Level Rise”. In: *Transportation Research Record: Journal of the Transportation Research Board* 2263 (2011), pp. 174–181 (cit. on pp. 3, 90, 94, 95).

[34] Linda See, Peter Mooney, Giles Foody, et al. “Crowdsourcing, Citizen Science or Volunteered Geographic Information? The Current State of Crowdsourced Geographic Information”. In: *ISPRS International Journal of Geo-Information* 5.5 (2016), pp. 1–23 (cit. on p. 8).

[35] Lívia Castro Degrossi, João Porto de Albuquerque, Roberto dos Santos Rocha, and Alexander Zipf. “A taxonomy of quality assessment methods for volunteered and crowdsourced geographic information”. In: *Transactions in GIS* 22.2 (2018), pp. 542–560 (cit. on p. 8).

[36] Michael F. Goodchild. “Citizens as sensors: the world of volunteered geography”. In: *GeoJournal* 69.4 (2007), pp. 211–221 (cit. on p. 8).

[38] Hansi Senaratne, Amin Mobasheri, Ahmed Loai Ali, Cristina Capineri, and Mordechai (Muki) Haklay. “A review of volunteered geographic information quality assessment methods”. In: *International Journal of Geographical Information Science* 31.1 (2017), pp. 139–167 (cit. on p. 8).

[40] ODC. *Open Database License (ODbL) v1.0*. 2009 (cit. on p. 8).

[42] Johanna Guth, Sven Wursthorn, and Sina Keller. “Multi-Parameter Estimation of Average Speed in Road Networks Using Fuzzy Control”. In: *ISPRS International Journal of Geo-Information* 9.1 (2020), pp. 1–18 (cit. on pp. 13, 30, 38, 39, 41–45, 177).

[43] ISO. *ISO 19157:2013, Geographic information - Data quality (ISO_19157:2013)*. Geneva, Switzerland: International Organization for Standardization, 2013 (cit. on p. 20).

[44] Cidalia Costa Fonte, Vyron Antoniou, Lucy Bastin, et al. “Assessing VGI Data Quality”. In: *Mapping and the Citizen Sensor*. London: Ubiquity Press, 2017, pp. 137–163 (cit. on pp. 21, 27).

[45] Jean-Francois Girres and Guillaume Touya. “Quality Assessment of the French OpenStreetMap Dataset: Quality Assessment of the French OpenStreetMap Dataset”. In: *Transactions in GIS* 14.4 (2010), pp. 435–459 (cit. on pp. 22, 25–27).

[46] Mordechai Haklay. “How Good is Volunteered Geographical Information? A Comparative Study of OpenStreetMap and Ordnance Survey Datasets”. In: *Environment and Planning B: Planning and Design* 37.4 (2010), pp. 682–703 (cit. on pp. 22, 24, 26).

[47] Ina Ludwig, Angi Voss, and Maike Krause-Traudes. “A Comparison of the Street Networks of Navteq and OSM in Germany”. In: *Advancing Geoinformation Science for a Changing World*. Berlin, Heidelberg: Springer, 2011, pp. 65–84 (cit. on pp. 22, 24–26).

[48] Pascal Neis, Dennis Zielstra, and Alexander Zipf. “The Street Network Evolution of Crowdsourced Maps: OpenStreetMap in Germany 2007-2011”. In: *Future Internet* 4.1 (2011), pp. 1–21 (cit. on pp. 22, 24, 25, 27, 28).

[49] Ming Wang, Qingquan Li, Qingwu Hu, and Meng Zhou. “Quality Analysis of Open Street Map Data”. In: *ISPRS - International Archives of the Photogrammetry, Remote Sensing and Spatial Information Sciences* XL-2/W1 (2013), pp. 155–158 (cit. on pp. 22, 24–26).

[50] Dennis Zielstra, Hartwig H. Hochmair, and Pascal Neis. “Assessing the Effect of Data Imports on the Completeness of OpenStreetMap - A United States Case Study”. In: *Transactions in GIS* 17.3 (2013), pp. 315–334 (cit. on pp. 22, 24).

[51] Christopher Barron, Pascal Neis, and Alexander Zipf. “A Comprehensive Framework for Intrinsic OpenStreetMap Quality Analysis: A Comprehensive Framework for Intrinsic OpenStreetMap Quality Analysis”. In: *Transactions in GIS* 18.6 (2014), pp. 877–895 (cit. on pp. 23, 24, 26).

[52] Anita Graser, Markus Straub, and Melitta Dragaschnig. “Towards an Open Source Analysis Toolbox for Street Network Comparison: Indicators, Tools and Results of a Comparison of OSM and the Official Austrian Reference Graph: Towards an Open Source Analysis Toolbox for Street Network Comparison”. In: *Transactions in GIS* 18.4 (2014), pp. 510–526 (cit. on pp. 23–26).

[53] Silvana Philippi Camboim, João Vitor Meza Bravo, and Claudia Robbi Sluter. “An Investigation into the Completeness of, and the Updates to, OpenStreetMap Data in a Heterogeneous Area in Brazil”. In: *ISPRS International Journal of Geo-Information* 4.3 (2015), pp. 1366–1388 (cit. on pp. 23–25, 27).

[54] Nikola Davidovic, Peter Mooney, Leonid Stoimenov, and Marco Minghini. “Tagging in Volunteered Geographic Information: An Analysis of Tagging Practices for Cities and Urban Regions in OpenStreetMap”. In: *ISPRS International Journal of Geo-Information* 5.12 (2016) (cit. on pp. 23, 26, 27, 77).

[55] Demetris Demetriou. “Uncertainty of OpenStreetMap data for the road network in Cyprus”. In: *Fourth International Conference on Remote Sensing and Geoinformation of the Environment*. Ed. by Kyriacos Themistocleous, Diofantos G. Hadjimitsis, Silas Michaelides, and Giorgos Papadavid. 2016 (cit. on pp. 23, 25–27).

[56] Maria Antonia Brovelli, Marco Minghini, Monia Molinari, and Peter Mooney. “Towards an Automated Comparison of OpenStreetMap with Authoritative Road Datasets”. In: *Transactions in GIS* 21.2 (2017), pp. 191–206 (cit. on pp. 23, 24).

[57] Ron Mahabir, Anthony Stefanidis, Arie Croitoru, Andrew Crooks, and Peggy Agouris. "Authoritative and Volunteered Geographical Information in a Developing Country: A Comparative Case Study of Road Datasets in Nairobi, Kenya". In: *ISPRS International Journal of Geo-Information* 6.1 (2017), pp. 1–24 (cit. on pp. 23, 24).

[58] Hongyu Zhang and Jacek Malczewski. "Accuracy Evaluation of the Canadian OpenStreetMap Road Networks". In: *International Journal of Geospatial and Environmental Research* 5.2 (2018), pp. 1–16 (cit. on pp. 24–26).

[59] Kent T. Jacobs and Scott W. Mitchell. "OpenStreetMap Quality Assessment Using Unsupervised Machine Learning Methods". In: *Transactions in GIS* 24 (2020), pp. 1280–1298 (cit. on p. 24).

[60] Ran Goldblatt, Nicholas Jones, and Jenny Mannix. "Assessing OpenStreetMap Completeness for Management of Natural Disaster by Means of Remote Sensing: A Case Study of Three Small Island States (Haiti, Dominica and St. Lucia)". In: *Remote Sensing* 12.1 (2020), pp. 1–25 (cit. on p. 24).

[61] Johanna Stötzer, Sven Wursthorn, and Sina Keller. "Fuzzy Estimation of Link Travel Time from a Digital Elevation Model and Road Hierarchy Level:" in: *Proceedings of the 5th International Conference on Geographical Information Systems Theory, Applications and Management*. Heraklion, Crete, Greece: SCITEPRESS - Science and Technology Publications, 2019, pp. 15–25 (cit. on pp. 30, 37, 42, 48, 49, 178).

[62] Victor L. Knoop, Maaike Snelder, Henk J. van Zuylen, and Serge P. Hoogendoorn. "Link-level vulnerability indicators for real-world networks". In: *Transportation Research Part A: Policy and Practice* 46.5 (2012), pp. 843–854 (cit. on pp. 30, 88).

[63] Xueping Li, Zhaoxia Zhao, Xiaoyan Zhu, and Tami Wyatt. "Covering models and optimization techniques for emergency response facility location and planning: a review". In: *Mathematical Methods of Operations Research* 74.3 (2011), pp. 281–310 (cit. on p. 30).

[64] Darren M. Scott, David C. Novak, Lisa Aultman-Hall, and Feng Guo. "Network Robustness Index: A new method for identifying critical links and evaluating the performance of transportation networks". In: *Journal of Transport Geography* 14.3 (2006), pp. 215–227 (cit. on pp. 30, 87–89, 105, 120).

[65] Johanna Guth, Sven Wursthorn, Andreas Ch. Braun, and Sina Keller. "Development of a generic concept to analyze the accessibility of emergency facilities in critical road infrastructure for disaster scenarios: exemplary application for the 2017 wildfires in Chile and Portugal". In: *Natural Hazards* 97.3 (2019), pp. 979–999 (cit. on pp. 30, 79, 85, 95, 98, 101–103, 108, 114, 135, 138, 177).

[66] Walter Collischonn and Jorge Victor Pilar. "A direction dependent least-cost-path algorithm for roads and canals". In: *International Journal of Geographical Information Science* 14.4 (2000), pp. 397–406 (cit. on p. 31).

[69] Dennis Luxen and Christian Vetter. "Real-time routing with OpenStreetMap data". In: *Proceedings of the 19th ACM SIGSPATIAL International Conference on Advances in Geographic Information Systems - GIS '11*. Chicago, Illinois: ACM Press, 2011, p. 513 (cit. on p. 32).

[72] Subrata Kumar Behera. "Connecting India's North East with Bangladesh: a study of transport linkages". PhD thesis. Scholl of International Studies, Jawaharlal Nehru University, India, 2008, p. 233 (cit. on pp. 32, 39).

[73] Lars Brabyn and Chris Skelly. “Geographical Access to Services, Health (GASH): Modelling Population Access to New Zealand Public Hospitals”. In: *The 13 th Annual Colloquium of the Spatial Information Research Centre*. Dunedin, New Zealand, 2001, p. 11 (cit. on p. 32).

[74] Ebrahim H Mamdani and Sedrak Assilian. “An experiment in linguistic synthesis with a fuzzy logic controller”. In: *International Journal of Man-Machine Studies* 7.1 (1975), pp. 1–13 (cit. on pp. 33, 34).

[75] Magdi S. Mahmoud. *Fuzzy Control, Estimation and Diagnosis*. Cham: Saudi Arabia: Springer International Publishing, 2018 (cit. on pp. 34, 35).

[76] X. J. Wang, R. H. Zhao, and Y. W. Hao. “Flood Control Operations Based on the Theory of Variable Fuzzy Sets”. In: *Water Resources Management* 25.3 (2011), pp. 777–792 (cit. on p. 35).

[77] Aaron K. Shackelford and Curt H. Davis. “A combined fuzzy pixel-based and object-based approach for classification of high-resolution multispectral data over urban areas”. In: *IEEE Transactions on Geoscience and Remote Sensing* 41.10 (2003), pp. 2354–2364 (cit. on p. 35).

[78] Xinming Tang, Yu Fang, and Wolfgang Kainz. “Fuzzy topological relations between fuzzy spatial objects”. In: *Fuzzy systems and knowledge discovery*. Ed. by Lipo Wang, Licheng Jiao, Guanming Shi, Xue Li, and Jing Liu. Berlin, Heidelberg: Springer Berlin Heidelberg, 2006, pp. 324–333 (cit. on p. 35).

[79] Gordon Hayward and Valerie Davidson. “Fuzzy logic applications”. In: *Analyst* 128 (2003), pp. 1–3 (cit. on p. 35).

[80] Rahul Deb Das and Stephan Winter. “A fuzzy logic based transport mode detection framework in urban environment”. In: *Journal of Intelligent Transportation Systems* (2018), pp. 1–12 (cit. on p. 35).

[81] Jan Jantzen. *Foundations of Fuzzy Control*. Chichester, UK: John Wiley & Sons, Ltd, 2007 (cit. on p. 35).

[82] David Douglas and Thomas Peucker. “Algorithms for the reduction of the number of points required to represent a digitized line or its caricature”. In: *Cartographica: the international journal for geographic information and geovisualization* 10.2 (1973), pp. 112–122 (cit. on p. 36).

[83] NASA and USGS. *Shuttle Radar Topography Mission. 1 Arc second void-filled.* `https://earthexplorer.usgs.gov`. Downloaded 25 May 2018. 2013 (cit. on p. 36).

[84] B.K.P. Horn. “Hill shading and the reflectance map”. In: *Proceedings of the IEEE* 69.1 (1981), pp. 14–47 (cit. on p. 37).

[85] Xinqiang Chen, Zhibin Li, Yinhai Wang, et al. “Evaluating the impacts of grades on vehicular speeds on interstate highways”. In: *PLOS ONE* 12.9 (2017). Ed. by Xiaolei Ma (cit. on p. 39).

[86] Sina Keller, Raoul Gabriel, and Johanna Guth. “Machine Learning Framework for the Estimation of Average Speed in Rural Road Networks with OpenStreetMap Data”. In: *ISPRS International Journal of Geo-Information* 9.11 (Oct. 2020), pp. 1–26 (cit. on pp. 49, 50, 152, 177).

[87] Johanna Guth, Sina Keller, Stefan Hinz, and Stephan Winter. “Towards detecting, characterizing, and rating of road classification errors in crowd-sourced road network databases”. In: *Journal of Spatial Information Science* 22 (2020), pp. 1–30 (cit. on pp. 52, 58, 60, 62–73, 77, 78, 177).

[88] Michael W. Hancock and Bud Wright. *A policy on geometric design of highways and streets*. 7th ed. Washington, DC, USA: American Association of State Highway and Transportation Officials, 2013 (cit. on p. 52).

[89] Sabine Timpf and Andrew Frank. “Using hierarchical spatial data structures for hierarchical spatial reasoning”. In: *International Conference on Spatial Information Theory*. Springer. 1997, pp. 69–83 (cit. on p. 52).

[90] Bing Liu. “Route finding by using knowledge about the road network”. In: *IEEE Transactions on Systems, Man, and Cybernetics - Part A: Systems and Humans* 27.4 (1997), pp. 436–448 (cit. on p. 53).

[92] Nikos Karagiannakis, Giorgos Giannopoulos, Dimitrios Skoutas, and Spiros Athanasiou. “OSMRec tool for automatic recommendation of categories on spatial entities in OpenStreetMap”. In: *Proceedings of the 9th ACM Conference on Recommender Systems*. RecSys 15. Vienna, Austria: Association for Computing Machinery, 2015, pp. 337–338 (cit. on p. 54).

[93] Arnaud Vandecasteele and Rodolphe Devillers. “Improving volunteered geographic information quality using a tag recommender system: the case of OpenStreetMap”. In: *Openstreetmap in GIScience*. Springer, 2015, pp. 59–80 (cit. on p. 55).

[94] Ivan Majic, Stephan Winter, and Martin Tomko. “Finding equivalent keys in OpenStreetMap: Semantic similarity computation based on extensional definitions”. In: *Proceedings of the 1st Workshop on Artificial Intelligence and Deep Learning for Geographic Knowledge Discovery - GeoAI ’17*. Los Angeles, California: ACM Press, 2017, pp. 24–32 (cit. on p. 55).

[95] Ivan Majic, Elham Naghizade, Stephan Winter, and Martin Tomko. “Discovery of topological constraints on spatial object classes using an extended topological model”. In: *Journal of Spatial Information Science* 2019.18 (2019), pp. 1–30 (cit. on p. 55).

[96] Linus Röman and Simon Finnman. “Algorithmic approach to error correction in map datasets using conflation techniques”. In: *Department of Computer Science, Faculty of Engineering, Lund University* Master’s thesis (2018) (cit. on p. 55).

[97] Hampus Londögård and Hannah Lindblad. “Improving the OpenStreetMap data set using deep learning”. In: *Department of Computer Science, Faculty of Engineering, Lund University* Master’s thesis (2018), pp. 1–73 (cit. on p. 55).

[98] Michael Stypa and Hannes Sandberg. “Improving the semantic accuracy and consistency of OpenStreetMap using machine learning techniques”. In: *Department of Computer Science, Faculty of Engineering, Lund University* Master’s thesis (2018) (cit. on pp. 55, 56).

[99] Musfira Jilani, Padraig Corcoran, and Michela Bertolotto. “Multi-granular street network representation towards quality assessment of OpenStreetMap data”. In: *Proceedings of the Sixth ACM SIGSPATIAL International Workshop on Computational Transportation Science - IWCTS ’13*. Orlando, FL, USA: ACM Press, 2013, pp. 19–24 (cit. on p. 55).

[100] Musfira Jilani, Padraig Corcoran, and Michela Bertolotto. “Automated highway tag assessment of OpenStreetMap road networks”. In: *Proceedings of the 22nd ACM SIGSPATIAL International Conference on Advances in Geographic Information Systems - SIGSPATIAL ’14*. Dallas, Texas: ACM Press, 2014, pp. 449–452 (cit. on pp. 55, 56).

[101] Padraig Corcoran, Peter Mooney, and Michela Bertolotto. “Inferring semantics from geometry: the case of street networks”. In: *Proceedings of the 23rd SIGSPATIAL International Conference on Advances in Geographic Information Systems - GIS ’15*. Bellevue, Washington: ACM Press, 2015, pp. 1–10 (cit. on pp. 55, 56).

[103] John Adrian Bondy and Uppaluri Siva Ramachandra Murty. *Graph Theory with Applications*. Vol. 290. Macmillan London, 1976 (cit. on p. 57).

[105] PSMA Australia. *Transport and topography - data product description*. Tech. rep. Sydney (Australia), 2019, pp. 1–89 (cit. on pp. 66, 67).

[107] Ina Ludwig, Angi Voss, and Maike Krause-Traudes. “A Comparison of the Street Networks of Navteq and OSM in Germany”. In: *Advancing Geoinformation Science for a Changing World*. Berlin, Heidelberg: Springer, 2011, pp. 65–84 (cit. on p. 77).

[108] Michael A.P. Taylor and Susilawati Susilawati. “Remoteness and Accessibility in the Vulnerability Analysis of Regional Road Networks”. In: *Transportation Research Part A: Policy and Practice* 46.5 (2012), pp. 761–771 (cit. on pp. 79, 88, 90, 91, 95, 101, 102, 111, 135, 138).

[109] Robert C. Thomson. “The’ Stroke’ Concept in Geographic Network Generalization and Analysis”. In: *Progress in Spatial Data Handling: 12th International Symposium on Spatial Data Handling*. Ed. by Andreas Riedl, Wolfgang Kainz, and Gregory A. Elmes. Berlin, Heidelberg: Springer Berlin Heidelberg, 2006, pp. 681–697 (cit. on p. 80).

[110] Johanna Stötzer. “Development of a Generic Concept to Analyze the Accessibility of Emergency Facilities in Critical Road Infrastructure”. Master’s thesis. Institut of Photogrammetry and Remote Sensing, Karlsruhe Institute of Technology (unpublished). 2017 (cit. on p. 85).

[111] Mohammad Mojtahedi, Sidney Newton, and Jason Von Meding. “Predicting the Resilience of Transport Infrastructure to a Natural Disaster Using Cox’s Proportional Hazards Regression Model”. In: *Natural Hazards* 85.2 (2017), pp. 1119–1133 (cit. on pp. 85, 95).

[113] Peter T. Bobrowsky, ed. *Encyclopedia of Natural Hazards*. Encyclopedia of Earth Sciences Series. Dordrecht: Springer Netherlands, 2013 (cit. on p. 85).

[114] Daniel Stillwell. “Natural hazards and disasters in Latin America”. In: *Natural Hazards* 6.2 (1992), pp. 131–159 (cit. on p. 85).

[115] Reza Faturechi and Elise Miller-Hooks. “Measuring the Performance of Transportation Infrastructure Systems in Disasters: A Comprehensive Review”. In: *Journal of infrastructure systems* 21.1 (2014), pp. 1–15 (cit. on pp. 85–89).

[116] Katja Berdica. “An Introduction to Road Vulnerability: What Has Been Done, Is Done and Should Be Done”. In: *Transport Policy* 9 (2002), pp. 117–127 (cit. on pp. 86, 87).

[117] Wolfgang Kröger and Enrico Zio. *Vulnerable Systems*. London: Springer Science & Business Media, 2011 (cit. on pp. 86, 88).

[118] Michael A. P. Taylor, Somenahalli V. C. Sekhar, and Glen M. D’Este. “Application of Accessibility Based Methods for Vulnerability Analysis of Strategic Road Networks”. In: *Networks and Spatial Economics* 6.3-4 (2006), pp. 267–291 (cit. on p. 87).

[119] Erik Jenelius, Tom Petersen, and Lars-Göran Mattsson. “Importance and Exposure in Road Network Vulnerability Analysis”. In: *Transportation Research Part A: Policy and Practice* 40.7 (2006), pp. 537–560 (cit. on pp. 87, 88, 95).

[120] Daniel A. Griffith. *Spatial Autocorrelation and Spatial Filtering: Gaining Understanding through Theory and Scientific Visualization*. Advances in spatial science. Berlin ; New York: Springer, 2003 (cit. on p. 87).

[121] Glen M. D’Este and Michael A. P. Taylor. “Modelling Network Vulnerability at the Level of the National Strategic Transport Network”. In: *Journal of the Eastern Asia Society for transportation studies* 4.2 (2001), pp. 1–14 (cit. on p. 87).

[122] Anna Nagurney and Qiang Qiang. “Robustness of Transportation Networks Subject to Degradable Links”. In: *Europhysics Letters (EPL)* 80.6 (2007), pp. 1–7 (cit. on p. 87).

[123] Edward K. Morlok and David J. Chang. “Measuring Capacity Flexibility of a Transportation System”. In: *Transportation Research Part A: Policy and Practice* 38.6 (2004), pp. 405–420 (cit. on p. 87).

[124] Reza Faturechi and Elise Miller-Hooks. “A Mathematical Framework for Quantifying and Optimizing Protective Actions for Civil Infrastructure Systems: A Mathematical Framework for Civil Infrastructure Protection”. In: *Computer-Aided Civil and Infrastructure Engineering* (2013) (cit. on p. 87).

[125] Tony H. Grubesic and Alan T. Murray. “Vital Nodes, Interconnected Infrastructures, and the Geographies of Network Survivability”. In: *Annals of the Association of American Geographers* 96.1 (2006), pp. 64–83 (cit. on p. 87).

[126] Ahmed Abdel-Rahim, Paul Oman, Brian Johnson, et al. “Modeling Urban Surface Transportation Network Dependability and Security”. In: *Final Rep. No. KLK238* 07 (2007), pp. 1–77 (cit. on p. 87).

[127] Crawford S. Holling. “Resilience and Stability of Ecological Systems”. In: *Annual review of ecology and systematics* 4.1 (1973), pp. 1–23 (cit. on p. 87).

[128] Aura Reggiani, Peter Nijkamp, and Diego Lanzi. “Transport Resilience and Vulnerability: The Role of Connectivity”. In: *Transportation Research Part A: Policy and Practice* 81 (2015), pp. 4–15 (cit. on p. 88).

[129] Susan Cutter, ed. *From Social Vulnerability to Resilience: Measuring Progress toward Disaster Risk Reduction Outcomes of the 7th UNU-EHS Summer Academy of the Munich Re Foundation Chair on Social Vulnerability, 1 - 7 July 2012, Hohenkammer, Germany*. Bonn: UNU-EHS (cit. on p. 88).

[130] Lars-Göran Mattsson and Erik Jenelius. “Vulnerability and Resilience of Transport Systems – A Discussion of Recent Research”. In: *Transportation Research Part A: Policy and Practice* 81 (2015), pp. 16–34 (cit. on pp. 88, 92).

[131] Mahdi Arezoumandi. “Estimation of Travel Time Reliability for Freeways Using Mean and Standard Deviation of Travel Time”. In: *Journal of Transportation Systems Engineering and Information Technology* 11.6 (2011), pp. 74–84 (cit. on p. 88).

[132] Abishai Polus. “A Study of Travel Time and Reliability on Arterial Routes”. In: *Transportation* 8.2 (1979), pp. 141–151 (cit. on p. 88).

[133] Susilawati Susilawati, Michael A. P. Taylor, and Sekhar V. C. Somenahalli. “Distributions of Travel Time Variability on Urban Roads”. In: *Journal of Advanced Transportation* 47.8 (2013), pp. 720–736 (cit. on p. 88).

[134] Michael.A.P. Taylor and Susilawati. “Modelling Travel Time Reliability with the Burr Distribution”. In: *Procedia - Social and Behavioral Sciences* 54 (2012), pp. 75–83 (cit. on p. 88).

[135] Haitham Al-Deek and Emam Emam. “New Methodology for Estimating Reliability in Transportation Networks with Degraded Link Capacities”. In: *Journal of Intelligent Transportation Systems: Technology, Planning, and Operations* 10.3 (2006), pp. 117–129 (cit. on p. 88).

[136] Maaike Snelder, Henk J. van Zuylen, and Lambertus H. Immers. “A Framework for Robustness Analysis of Road Networks for Short Term Variations in Supply”. In: *Transportation Research Part A: Policy and Practice* 46.5 (2012), pp. 828–842 (cit. on pp. 88, 89).

[137] Erica Dalziell and Alan Nicholson. “Risk and Impact of Natural Hazards on a Road Network”. In: *Journal of Transportation Engineering* 127.2 (2001), pp. 159–166 (cit. on pp. 88, 95).

[138] Mauricio Sánchez-Silva, M. Daniels, G. Lleras, and D. Patiño. “A Transport Network Reliability Model for the Efficient Assignment of Resources”. In: *Transportation Research Part B: Methodological* 39.1 (2005), pp. 47–63 (cit. on p. 88).

[139] Huizhao Tu, Hao Li, Hans Van Lint, and Henk van Zuylen. “Modeling travel time reliability of freeways using risk assessment techniques”. In: *Transportation Research Part A: Policy and Practice* 46.10 (2012), pp. 1528–1540 (cit. on p. 88).

[140] Ryuhei Kondo, Yasuhiro Shiomi, and Nobuhiro Uno. “Network evaluation based on connectivity reliability and accessibility”. In: *Network reliability in practice*. Springer, 2012, pp. 131–149 (cit. on p. 88).

[141] James L. Sullivan, David C. Novak, Lisa Aultman-Hall, and Darren M. Scott. “Identifying Critical Road Segments and Measuring System-Wide Robustness in Transportation Networks with Isolating Links: A Link-Based Capacity-Reduction Approach”. In: *Transportation Research Part A: Policy and Practice* 44.5 (2010), pp. 323–336 (cit. on pp. 88, 89).

[142] Paramet Luathep, Agachai Sumalee, H. W. Ho, and Fumitaka Kurauchi. “Large-Scale Road Network Vulnerability Analysis: A Sensitivity Analysis Based Approach”. In: *Transportation* 38.5 (2011), pp. 799–817 (cit. on pp. 88, 90).

[143] Fumitaka Kurauchi, Nobuhiro Uno, Agachai Sumalee, and Yumiko Seto. “Network Evaluation Based on Connectivity Vulnerability”. In: *Transportation and Traffic Theory 2009: Golden Jubilee*. Ed. by William H. K. Lam, S. C. Wong, and Hong K. Lo. Boston, MA: Springer US, 2009, pp. 637–649 (cit. on p. 88).

[144] Lorenzo Masiero and Rico Maggi. “Estimation of Indirect Cost and Evaluation of Protective Measures for Infrastructure Vulnerability: A Case Study on the Transalpine Transport Corridor”. In: *Transport Policy* 20 (2012), pp. 13–21 (cit. on p. 88).

[145] Hong-ying Yin and Li-qun Xu. “Measuring the Structural Vulnerability of Road Network: A Network Efficiency Perspective”. In: *Journal of Shanghai Jiaotong University (Science)* 15.6 (2010), pp. 736–742 (cit. on p. 88).

[146] Erik Jenelius and Lars-Göran Mattsson. “Road Network Vulnerability Analysis of Area-Covering Disruptions: A Grid-Based Approach with Case Study”. In: *Transportation Research Part A: Policy and Practice* 46.5 (2012), pp. 746–760 (cit. on p. 88).

[147] Michael G.H Bell. “A Game Theory Approach to Measuring the Performance Reliability of Transport Networks”. In: *Transportation Research Part B: Methodological* 34.6 (2000), pp. 533–545 (cit. on p. 88).

[148] Eric D. Vugrin, Drake E. Warren, and Mark A. Ehlen. “A Resilience Assessment Framework for Infrastructure and Economic Systems: Quantitative and Qualitative Resilience Analysis of Petrochemical Supply Chains to a Hurricane”. In: *Process Safety Progress* 30.3 (2011), pp. 280–290 (cit. on pp. 89, 95).

[149] Anthony Chen, Hai Yang, Hong K. Lo, and Wilson H. Tang. “Capacity Reliability of a Road Network: An Assessment Methodology and Numerical Results”. In: *Transportation Research Part B: Methodological* 36.3 (2002), pp. 225–252 (cit. on p. 89).

[150] Pamela Murray-Tuite and Hani Mahmassani. “Methodology for Determining Vulnerable Links in a Transportation Network”. In: *Transportation Research Record: Journal of the Transportation Research Board* 1882 (2004), pp. 88–96 (cit. on p. 89).

[151] Hirokazu Tatano and Satoshi Tsuchiya. “A Framework for Economic Loss Estimation Due to Seismic Transportation Network Disruption: A Spatial Computable General Equilibrium Approach”. In: *Natural Hazards* 44.2 (2008), pp. 253–265 (cit. on pp. 89, 95).

[152] Debbie A. Niemeier. “Accessibility: An Evaluation Using Consumer Welfare”. In: *Transportation* 24.4 (1997), pp. 377–396 (cit. on p. 90).

[153] Walter G. Hansen. “How Accessibility Shapes Land Use”. In: *Journal of the American Institute of Planners* 25.2 (1959), pp. 73–76 (cit. on p. 90).

[154] Karst T. Geurs and Bert van Wee. “Accessibility Evaluation of Land-Use and Transport Strategies: Review and Research Directions”. In: *Journal of Transport Geography* 12.2 (2004), pp. 127–140 (cit. on p. 90).

[155] Antonio Antunes, Alvaro Seco, and Nuno Pinto. “An Accessibility–Maximization Approach to Road Network Planning”. In: *Computer-Aided Civil and Infrastructure Engineering* 18.3 (2003), pp. 224–240 (cit. on p. 90).

[156] Bruno F. Santos, António P. Antunes, and Eric J. Miller. “Interurban Road Network Planning Model with Accessibility and Robustness Objectives”. In: *Transportation Planning and Technology* 33.3 (2010), pp. 297–313 (cit. on pp. 90, 95).

[157] Anthony Chen, Chao Yang, Sirisak Kongsomsaksakul, and Ming Lee. “Network-Based Accessibility Measures for Vulnerability Analysis of Degradable Transportation Networks”. In: *Networks and Spatial Economics* 7.3 (2007), pp. 241–256 (cit. on pp. 90, 94).

[158] Daniel J. Weiss, Andi Nelson, Harry S. Gibson, et al. “A Global Map of Travel Time to Cities to Assess Inequalities in Accessibility in 2015”. In: *Nature* 553 (2018), pp. 333–336 (cit. on pp. 90, 94).

[159] Hande Demirel, Mert Kompil, and Françoise Nemry. “A Framework to Analyze the Vulnerability of European Road Networks Due to Sea-Level Rise (SLR) and Sea Storm Surges”. In: *Transportation Research Part A: Policy and Practice* 81 (2015), pp. 62–76 (cit. on pp. 90, 95).

[160] Flavio Bono and Eugenio Gutiérrez. “A Network-Based Analysis of the Impact of Structural Damage on Urban Accessibility Following a Disaster: The Case of the Seismically Damaged Port Au Prince and Carrefour Urban Road Networks”. In: *Journal of Transport Geography* 19.6 (2011), pp. 1443–1455 (cit. on pp. 90, 92, 95).

[161] Lisa Murawski and Richard L. Church. “Improving Accessibility to Rural Health Services: The Maximal Covering Network Improvement Problem”. In: *Socio-Economic Planning Sciences* 43.2 (2009), pp. 102–110 (cit. on p. 90).

[162] Ulrich Ranke. *Natural Disaster Risk Management : Geosciences and Social Responsibility*. 1st ed. 2016. SpringerLinkSpringer eBook Collection. Cham: Springer, 2016 (cit. on p. 91).

[163] Akvan Gajanayake, Guomin Zhang, Tehmina Khan, and Hessam Mohseni. “Postdisaster Impact Assessment of Road Infrastructure: State-of-the-Art Review”. In: *Natural Hazards Review* 21.1 (2020), pp. 1–14 (cit. on pp. 91–95).

[164] Omar Bello, Laura Ortíz, Liudmila Ortega, et al. *Handbook for Disaster Assessment*. Tech. rep. Chile: United Nations - Economic Commission for Latin America and the Caribbean (UN-ECLAC), 2014 (cit. on pp. 91, 93, 94).

[165] Bureau of Transport Economics Australia. *Economic Costs of Natural Disasters in Australia*. Canberra: Bureau of Transport Economics, 2001 (cit. on p. 91).

[166] Alberto Eduardo Bisbal Sanz, María Mercedes de Guadalupe Masana García, Marycruz Flores Vila, et al. *Impacto Socioeconòmico y Ambiental Des Sismo Del 15 de Agosto de 2007*. Tech. rep. 1. Lima, Perú: Instituto Nacional de Defensa Civil, 2011 (cit. on pp. 91, 94).

[167] CEPAL, Sede subregional en México and México CENAPRED. *Impacto Socioeconómico de Las Inundaciones Registradas En El Estado de Tabsco de Septiembre A Noviembre de 2011*. Tech. rep. 2012 (cit. on pp. 91, 94).

[168] Simone Eseler, Leila Mead, and Sailesh Kumar Sen. *Fiji, Post-Disaster Needs Assessment - Tropical Cyclone Winston, February 20, 2016*. Tech. rep. Government of Fiji, 2016, p. 160 (cit. on pp. 91, 94).

[169] Planning Institute of Jamaica. *Jamaica Macro Socio-Economic and Environmental Assessment of the Damage and Loss Caused by Tropical Depression No. 16/ Tropical Storm Nicole*. Tech. rep. 2010, p. 109 (cit. on pp. 91, 94).

[170] Secretarìa de Gobernacìon, CEPAL, Sede subregional en México, and México CENAPRED. *Impacto Socioeconómico Del Sismo Ocurrido El 21 de Enero de 2003 En El Estado de Colima México*. Tech. rep. 2003 (cit. on pp. 91, 94).

[171] Juan E. Muriel-Villegas, Karla C. Alvarez-Uribe, Carmen E. Patiño-Rodriguez, and Juan G. Villegas. “Analysis of Transportation Networks Subject to Natural Hazards – Insights from a Colombian Case”. In: *Reliability Engineering & System Safety* 152 (2016), pp. 151–165 (cit. on pp. 92, 95).

[172] Nazli Yonca Aydin, H. Sebnem Duzgun, Friedemann Wenzel, and Hans Rudolf Heinimann. “Integration of Stress Testing with Graph Theory to Assess the Resilience of Urban Road Networks under Seismic Hazards”. In: *Natural Hazards* 91.1 (2018), pp. 37–68 (cit. on pp. 92, 94).

[173] Michal Bíl, Rostislav Vodák, Jan Kubeček, Martina Bílová, and Jiří Sedoník. “Evaluating Road Network Damage Caused by Natural Disasters in the Czech Republic between 1997 and 2010”. In: *Transportation Research Part A: Policy and Practice* 80 (2015), pp. 90–103 (cit. on p. 92).

[174] Vito Latora and Massimo Marchiori. “Vulnerability and protection of infrastructure networks”. In: *Physical Review E* 71.1 (2005) (cit. on p. 92).

[175] Irene Eusgeld, Wolfgang Kröger, Giovanni Sansavini, Markus Schläpfer, and Enrico Zio. "The role of network theory and object-oriented modeling within a framework for the vulnerability analysis of critical infrastructures". In: *Reliability Engineering & System Safety* 94.5 (2009), pp. 954–963 (cit. on p. 92).

[176] Stephanie Chang and Nobuoto Nojima. "Measuring Post-Disaster Transportation System Performance: The 1995 Kobe Earthquake in Comparative Perspective". In: *Transportation Research Part A: Policy and Practice* 35.6 (2001), pp. 475–494 (cit. on p. 92).

[177] Stephanie Chang. "Transportation Planning for Disasters: An Accessibility Approach". In: *Environment and Planning A: Economy and Space* 35.6 (2003), pp. 1051–1072 (cit. on p. 92).

[178] Marina Utasse, Vincent Jomelli, Delphine Grancher, et al. "Territorial Accessibility and Decision-Making Structure Related to Debris Flow Impacts on Roads in the French Alps". In: *International Journal of Disaster Risk Science* 7.2 (2016), pp. 186–197 (cit. on pp. 92, 95).

[179] Juan de Dios Ortuzar and Luis G. Willumsen, eds. *Modelling Transport*. 4th ed. Oxford: Wiley-Blackwell, 2011 (cit. on pp. 93, 103, 104).

[180] Clemens Pfurtscheller, Elisabetta Genovese, et al. "The Felbertauern landslide of 2013: impact on transport networks, effects on regional economy and policy decisions". In: *Sustainability environmental economics and dynamics studies* (2018) (cit. on p. 93).

[181] Evangelos Mitsakis, Iraklis Stamos, Michalis Diakakis, and Joseph M. Salanova Grau. "Impacts of High-Intensity Storms on Urban Transportation: Applying Traffic Flow Control Methodologies for Quantifying the Effects". In: *International Journal of Environmental Science and Technology* 11.8 (2014), pp. 2145–2154 (cit. on p. 93).

[182] Feng Xie and David Levinson. "Evaluating the Effects of the I-35W Bridge Collapse on Road-Users in the Twin Cities Metropolitan Region". In: *Transportation Planning and Technology* 34.7 (2011), pp. 691–703 (cit. on p. 93).

[183] M. G. Winter, B. Shearer, D. Palmer, et al. "The economic impact of landslides affecting the Scottish road network". In: *Landslides and engineered slopes. Experience, Theory and Practice*. CRC Press, 2018, pp. 2059–2064 (cit. on pp. 93, 95).

[184] GFDRR, UN-ECLAC, World Bank, et al. *PDNA Guidelines Volume B - Transport (Infrastructure Sector)*. Tech. rep. 2015 (cit. on pp. 93, 94).

[185] Sunarin Chanta, Maria E. Mayorga, and Laura A. McLay. "Improving Emergency Service in Rural Areas: A Bi-Objective Covering Location Model for EMS Systems". In: *Annals of Operations Research* 221.1 (2014), pp. 133–159 (cit. on p. 94).

[186] John M Diaz. "Economic Impacts of Wildfire". In: *Southern Fire Exchange, SFE Fact Sheets* 7 (2012), pp. 1–4 (cit. on p. 95).

[187] Pallab Mozumder, Nejem Raheem, John Talberth, and Robert P. Berrens. "Investigating Intended Evacuation from Wildfires in the Wildland–Urban Interface: Application of a Bivariate Probit Model". In: *Forest Policy and Economics* 10.6 (2008), pp. 415–423 (cit. on p. 95).

[188] Thomas J. Cova, David M. Theobald, John B. Norman, and Laura K. Siebeneck. "Mapping Wildfire Evacuation Vulnerability in the Western US: The Limits of Infrastructure". In: *GeoJournal* 78.2 (2013), pp. 273–285 (cit. on p. 95).

[189] Bi Yu Chen, William H.K. Lam, Agachai Sumalee, Qingquan Li, and Zhi-Chun Li. "Vulnerability Analysis for Large-Scale and Congested Road Networks with Demand Uncertainty". In: *Transportation Research Part A: Policy and Practice* 46.3 (2012), pp. 501–516 (cit. on p. 95).

[190] Erik Jenelius, Tom Petersen, and Lars-Göran Mattsson. "Importance and Exposure in Road Network Vulnerability Analysis". In: *Transportation Research Part A: Policy and Practice* 40.7 (2006), pp. 537–560 (cit. on p. 95).

[191] Susana Freiria, Alexandre O. Tavares, and Rui Pedro Julião. "The Multiscale Importance of Road Segments in a Network Disruption Scenario: A Risk-Based Approach: Road Segments in a Network Disruption Scenario". In: *Risk Analysis* 35.3 (2015), pp. 484–500 (cit. on p. 95).

[192] Edsger W. Dijkstra. "A Note on Two Problems in Connexion with Graphs". In: *Numerische mathematik* 1.1 (1959), pp. 269–271 (cit. on p. 98).

[193] Marcello Schiavina, Sergio Freire, and Kytt MacManus. *GHS-POP R2019A - GHS Population Grid Multitemporal (1975-1990-2000-2015)*. http://doi.org/10.2905/0C6B9751-A71F-4062-830B-43C9F432370F. 2019 (cit. on p. 98).

[194] Sergio Freire, Erin Doxsey-Whitfield, Kytt MacManus, Jane Mills, and Martino Pesaresi. "Development of New Open and Free Multi-Temporal Global Population Grids at 250 m Resolution". In: *Geospatial Data in a Changing World; Association of Geographic Information Laboratories in Europe (AGILE). AGILE 2016.* (2016), pp. 1–6 (cit. on pp. 98, 99).

[195] Christina Corbane, Martino Pesaresi, Thomas Kemper, et al. "Automated Global Delineation of Human Settlements from 40 Years of Landsat Satellite Data Archives". In: *Big Earth Data* 3.2 (2019), pp. 140–169 (cit. on p. 98).

[197] DHAC. *Measuring Remoteness: Accessibility/Remoteness Index of Australia (ARIA)*. Canberra, ACT: Commonwealth Dept. of Health and Aged Care, 2001 (cit. on pp. 101, 135).

[198] John Glover, Sarah Tennant, Public Health Information Development Unit (Australia), Australia, and Department of Health and Ageing. *Remote Areas Statistical Geography in Australia: Notes on the Accessibility/Remoteness Index for Australia (ARIA+ Version)*. Adelaide: Public Health Information Development Unit [for the] Commonwealth Department of Health and Ageing, 2003 (cit. on p. 101).

[199] Jarrod Lange and Danielle Taylor. "A Metropolitan Accessibility Index for Australian Capital Cities-Metro ARIA". In: *Proceedings of the 8th International Conference on Population Geographies: The Spatial Dimensions of Population (ICPG2015)* (2015) (cit. on p. 102).

[201] Alexander I. Filkov, Tuan Ngo, Stuart Matthews, Simeon Telfer, and Trent D. Penman. "Impact of Australia's Catastrophic 2019/20 Bushfire Season on Communities and Environment. Retrospective Analysis and Current Trends". In: *Journal of Safety Science and Resilience* 1.1 (2020), pp. 44–56 (cit. on p. 114).

[204] Susanne Kubisch, Johanna Guth, Sina Keller, et al. "The Contribution of Tsunami Evacuation Analysis to Evacuation Planning in Chile: Applying a Multi-Perspective Research Design". In: *International Journal of Disaster Risk Reduction* 45 (May 2020), pp. 1–14 (cit. on pp. 141, 177).

[205] Andreas Braun, Johanna Stötzer, Susanne Kubisch, and Sina Keller. "Critical Infrastructure Analysis (CRITIS) in Developing Regions – Designing an Approach to Analyse Peripheral Remoteness, Risks of Accessibility Loss, and Isolation Due to Road Network Insufficiencies in Chile". In: *GI_Forum* 1 (2018), pp. 302–321 (cit. on p. 177).

[206] Andreas Braun, Johanna Stötzer, Susanne Kubisch, André Dittrich, and Sina Keller. “A Vulnerability Index and Analysis for the Road Network of Rural Chile”. In: *Natural Hazard Impacts on Technological Systems and Infrastructures – European Geosciences Union General Assembly, Vienna, Austria, 23–28 April 2017*. 2017 (cit. on p. 178).

[207] S. Keller, F. M. Riese, J. Stötzer, P. M. Maier, and S. Hinz. “Developing a Machine Learning Framework for Estimating Soil Moisture with VNIR Hyperspectral Data”. In: *ISPRS Annals of Photogrammetry, Remote Sensing and Spatial Information Sciences* IV-1 (Sept. 2018), pp. 101–108 (cit. on p. 178).

[208] Susanne Kubisch, Johanna Stötzer, Sina Keller, María T Bull, and Andreas Braun. “Combining a Social Science Approach and GIS-Based Simulation to Analyse Evacuation in Natural Disasters: A Case Study in the Chilean Community of Talcahuano”. In: *Proceedings of the 16th ISCRAM Conference – València, Spain, May 2019*. 2019, pp. 1–19 (cit. on p. 178).

Online Resources

[31] PostgreSQL Global Development Group. *PostgreSQL: The World’s Most Advanced Open Source Database*. 2020. URL: `https://www.postgresql.org/` (visited on Jan. 23, 2020) (cit. on p. 3).

[32] PostGIS Developers. *PostGIS — Spatial and Geographic Objects for PostgreSQL*. 2020. URL: `http://postgis.net/` (visited on Jan. 23, 2020) (cit. on p. 3).

[33] pgRouting Contributors. *pgRouting Project — Open Source Routing Library*. 2020. URL: `http://pgrouting.org/` (visited on Jan. 23, 2020) (cit. on p. 3).

[37] OSM Contributors. *OpenStreetMap*. 2020. URL: `https://www.openstreetmap.org` (visited on Sept. 5, 2020) (cit. on p. 8).

[39] OSM Wiki. *Using OpenStreetMap: OpenStreetMap Wiki*. 2020. URL: `http://wiki.openstreetmap.org/` (visited on Oct. 25, 2020) (cit. on pp. 8–12, 14, 16–20, 26, 27, 32, 36, 56).

[41] ESRI. *ESRI GIS Dictionary*. 2020. URL: `http://webhelp.esri.com/arcgisserver/9.3/java/geodatabases/definition_frame.htm` (visited on Sept. 17, 2020) (cit. on p. 9).

[67] Johanna Guth. *johannaguth/Fuzzy-Framework-for-Speed-Estimation: First Release, v0.1*. Version v0.1. Nov. 2019. URL: `https://doi.org/10.5281/zenodo.3530687` (cit. on pp. 31, 40, 42, 43, 178).

[68] ORS. *OpenRouteService: The spatial services API with plenty of features*. 2018. URL: `https://openrouteservice.org/` (visited on Nov. 30, 2018) (cit. on p. 32).

[70] OTP. *OpenTripPlanner – Multimodal Trip Planning*. 2018. URL: `http://www.opentripplanner.org/` (visited on Nov. 30, 2018) (cit. on p. 32).

[71] YOURS. *YourNavigation - Worldwide routing on OpenStreetMap data*. 2018. URL: `http://yournavigation.org` (visited on Nov. 30, 2018) (cit. on p. 32).

[91] Johanna Guth. *johannaguth/OSM-errorsearch-road-class: First release of the OSM road class error search - tested for the regions New South Wales (Australia) and Bio-Bio and Maule (Chile)*. Version v1.0. July 2020. URL: https://doi.org/10.5281/zenodo.3957386 (cit. on pp. 53, 54, 64, 79, 178).

[102] Osmose Contributors. *Osmose - backend*. 2020. URL: https://github.com/osm-fr/osmose-backend (visited on June 30, 2020) (cit. on p. 56).

[104] Daniel Wendt, Anton Patrushev, Adrien Pavie, et al. *Osm2pgrouting - Import Tool for OpenStreetMap Data to pgRouting Database*. 2018. URL: https://github.com/pgRouting/osm2pgrouting (visited on Jan. 23, 2020) (cit. on p. 61).

[106] Academic. *List of Gaps in Interstate Highways*. 2020. URL: https://enacademic.com/dic.nsf/enwiki/422412 (visited on Nov. 5, 2020) (cit. on p. 76).

[112] Ben Knight. *On Fire-Damaged Roads in Victoria, Army Crews Face the Daunting Job of Removing 'killer' Trees*. 2020. URL: https://www.abc.net.au/news/2020-01-12/fire-hit-roads-have-army-crews-remove-killer-trees-in-victoria/11860638 (visited on Sept. 25, 2020) (cit. on p. 85).

[196] Australian Bureau of Statistics. *Census New South Wales, Population by State/UCLs*. 2016. URL: https://guest.censusdata.abs.gov.au/webapi/jsf/tableView/tableView.xhtml (visited on Sept. 10, 2020) (cit. on p. 100).

[200] UNS. *Chile: Incendios Forestales - Enero 2017. Reporte de Situaciòn No. 02 (Al 07 de Febrero de 2017). United Nations System*. 2017. URL: https://reliefweb.int/report/chile/chile-forest-fires-january-2017-situation-report-no-01-31-january-2017 (visited on June 26, 2018) (cit. on p. 114).

[202] National Bushfire Recovery Agency. *2020 National Operational Bushfire Boundaries*. 2020. URL: https://data.gov.au/data/dataset/2020-operational-bushfire-boundaries (visited on Aug. 8, 2020) (cit. on p. 115).

[203] NSW Government - Transport for NSW. *Traffic Volume Viewer*. 2019. URL: https://www.rms.nsw.gov.au/about/corporate-publications/statistics/traffic-volumes/aadt-map/index.html (visited on Sept. 15, 2020) (cit. on p. 120).

List of Abbreviations

AIC	Accessibility Index Calculation
ARIA	Accessibility and Remoteness Index of Australia
BM	BioBío and Maule
CIESIN	Center for International Earth Science Information Network
CM	Core Module of Generic Concept for the Assessment of Critical Road Infrastructure in a Disaster Context (GRIND)
DEM	Digital Elevation Model
DIA	Disaster Impact Assessment
DVS	Disaster Vulnerability Scan
EFAI	Emergency Facility Accessibility Index
FCS	Fuzzy Control System
Fuzzy-FSE	Fuzzy Framework for Speed Estimation
GD-API	Google Directions API
GHS-POP	Global Human Settlement Population Grid
GIS	Geographic Information System
GNSS	Global Navigation Satellite System
GRIND	Generic Concept for the Assessment of Critical Road Infrastructure in a Disaster Context
GDP	Gross Domestic Product
ISO	International Organization for Standardization
MF	Membership Function
NADIA	Network Analysis Disaster Impact Assessment
NASA	National Aeronautics and Space Administration
NNSW	North New South Wales

NRI	Network Robustness Index
NSW	New South Wales
OD	origin-destination
OSM	OpenStreetMap
PDNA	Post Disaster Needs Assessment
Q1	25^{th} percentile
Q3	75^{th} percentile
IQR	Interquartile Range
R^2	Coefficient of Determination
RMSE	Root Mean Squared Error
SD	Standard Deviation
SE-NSW	south-east New South Wales
TDM	Travel Demand Model
TDMDIA	Travel Demand Model Disaster Impact Assessment
SRTM	Shuttle Radar Topography Mission
USA	United States of America
VGI	Volunteered Geographic Information

List of Figures

List of Tables

List of Publications

A

In the following, the publications are listed, which have been published by or with the author of this thesis, Johanna Guth (former Stötzer), within the time period 2017-2020. The ideas and developments presented in this thesis have party been published in these publications and clearly marked in this thesis.

Main Publications:

- Johanna Guth, Sven Wursthorn, Andreas Ch. Braun, and Sina Keller. "Development of a generic concept to analyze the accessibility of emergency facilities in critical road infrastructure for disaster scenarios: exemplary application for the 2017 wildfires in Chile and Portugal". In: *Natural Hazards* 97.3 (2019), pp. 979–999. **Peer-reviewed**, cited as [65] and marked in blue.
- Johanna Guth, Sven Wursthorn, and Sina Keller. "Multi-Parameter Estimation of Average Speed in Road Networks Using Fuzzy Control". In: *ISPRS International Journal of Geo-Information* 9.1 (2020), pp. 1–18. **Peer-reviewed**, cited as [42] and marked in orange.
- Johanna Guth, Sina Keller, Stefan Hinz, and Stephan Winter. "Towards detecting, characterizing, and rating of road classification errors in crowd-sourced road network databases". In: *Journal of Spatial Information Science* 22 (2020), pp. 1–30. **Submitted and undergone first round of peer-review**, cited as [87] and marked in green.

Further Publications – Journal Articles:

- Andreas Braun, Johanna Stötzer, Susanne Kubisch, and Sina Keller. "Critical Infrastructure Analysis (CRITIS) in Developing Regions – Designing an Approach to Analyse Peripheral Remoteness, Risks of Accessibility Loss, and Isolation Due to Road Network Insufficiencies in Chile". In: *GI_Forum* 1 (2018), pp. 302–321. **Peer-reviewed**.
- Susanne Kubisch, Johanna Guth, Sina Keller, María T. Bull, Lars Keller, and Andreas Ch. Braun. "The Contribution of Tsunami Evacuation Analysis to Evacuation Planning in Chile: Applying a Multi-Perspective Research Design". In: *International Journal of Disaster Risk Reduction* 45 (May 2020), pp. 1–14. **Peer-reviewed**, cited as [204].
- Sina Keller, Raoul Gabriel, and Johanna Guth. "Machine Learning Framework for the Estimation of Average Speed in Rural Road Networks with OpenStreetMap Data". In: *ISPRS International Journal of Geo-Information* 9.11 (Oct. 2020), pp. 1–26. **Peer-reviewed**, cited as [86].

Further Publications – Conferences:

- Andreas Braun, Johanna Stötzer, Susanne Kubisch, André Dittrich, and Sina Keller. "A Vulnerability Index and Analysis for the Road Network of Rural Chile". In: *Natural Hazard Impacts on Technological Systems and Infrastructures – European Geosciences Union General Assembly, Vienna, Austria, 23–28 April 2017*. 2017.
- S. Keller, F. M. Riese, J. Stötzer, P. M. Maier, and S. Hinz. "Developing a Machine Learning Framework for Estimating Soil Moisture with VNIR Hyperspectral Data". In: *ISPRS Annals of Photogrammetry, Remote Sensing and Spatial Information Sciences* IV-1 (Sept. 2018), pp. 101–108. **Peer-reviewed**.
- Johanna Stötzer, Sven Wursthorn, and Sina Keller. "Fuzzy Estimation of Link Travel Time from a Digital Elevation Model and Road Hierarchy Level:" in: *Proceedings of the 5th International Conference on Geographical Information Systems Theory, Applications and Management*. Heraklion, Crete, Greece: SCITEPRESS - Science and Technology Publications, 2019, pp. 15–25. **Peer-reviewed**, cited as [61] and marked in red.
- Susanne Kubisch, Johanna Stötzer, Sina Keller, María T Bull, and Andreas Braun. "Combining a Social Science Approach and GIS-Based Simulation to Analyse Evacuation in Natural Disasters: A Case Study in the Chilean Community of Talcahuano". In: *Proceedings of the 16th ISCRAM Conference – València, Spain, May 2019*. 2019, pp. 1–19. **Peer-reviewed**.

Published Open-Source Software:

- Johanna Guth. *johannaguth/Fuzzy-Framework-for-Speed-Estimation: First Release, v0.1*. Version v0.1. Nov. 2019. URL: `https://doi.org/10.5281/zenodo.3530687`. cited as [67].
- Johanna Guth. *johannaguth/OSM-errorsearch-road-class: First release of the OSM road class error search - tested for the regions New South Wales (Australia) and Bio-Bio and Maule (Chile)*. Version v1.0. July 2020. URL: `https://doi.org/10.5281/zenodo.3957386`. cited as [91].

Colophon

This thesis was typeset with LaTeX 2_ε. It uses the *Clean Thesis* style developed by Ricardo Langner. The design of the *Clean Thesis* style is inspired by user guide documents from Apple Inc.

Download the *Clean Thesis* style at `http://cleanthesis.der-ric.de/`.